CELLULAR MECHANISMS OF ACUTE HYPOXIC PULMONARY VASOCONSTRICTION IN INTRAPULMONARY VEINS

CIPRIAN DOSPINESCU

A thesis submitted in partial fulfilment of
the requirements of
The Robert Gordon University
for the degree of Doctor of Philosophy

March 2009

DECLARATION

This thesis in candidature for the degree of Doctor of Philosophy has been composed entirely by myself. The work which is documented was carried out by myself. All sources of information contained within which have not arisen from the results generated have been specifically acknowledged.

Ciprian Dospinescu

To my father

CONTENTS

LIST OF FIGURES

LIST OF TABLES

ACKNOWLEDGMENTS

I would like to thank the following people, who have contributed in various ways to the succession of events that brought me here today.

Firstly, to my principal supervisor, Dr. Stuart F. Cruickshank, for his patience and for being a permanent source of enthusiasm and fresh ideas, and introducing me into the world of smooth muscle research. I would also like to thank the other members of my supervisory team, Prof. Cherry L. Wainwright for always being available to answer my questions and offer guidance and Dr. Dorothy McCaig for all her help and guidance.

To all the staff in the School of Pharmacy, in particular to Mrs. Margaret Brown for always being available to provide invaluable technical help.

To The Robert Gordon University for the RDI studentship, the Overseas Research Student Award Scheme and the Ratiu Foundation UK for complementing the financial support which made my studies possible. Also, to the Ratiu Foundation UK and Mrs. Ramona Mitrica in particular, the Boehringer Ingelheim Foundation and The Physiological Society for further funding for training purposes.

To Dr. Iain Rowe from the Centre for Integrative Physiology at the University of Edinburgh, for providing me with access to equipment and helping with control experiments for monitoring oxygen saturation.

To my family, my father who I know would have been very proud, my mother for her love and immense efforts to which I owe everything, my brother for always being there for me and my dearest wife Paula for her love, encouragement and understanding throughout my interminable student career.

To my dear friends Lili, James, Ellie and Elvis, for the lovely evenings with witty debates in the Howff and elsewhere and for the introduction into the world of ales and Scottish food.

To Iulia, Razvan & Cristina, Sebi & Sorana, Costel & Andreia and Vasi for being such wonderful and supportive friends throughout the years.

Not lastly, I thank Sarah, Karen and Emma, for putting a smile on my face during the long days in the lab, and to all other past and present PhD student colleagues in PD1 and PC27, including Tim, Ben, Colin, Anita, Julie, Nicola, Pramod, Ray, Simon, Noelle, Barbara and Clare.

PUBLICATIONS

Dospinescu, C. & Cruickshank, S. F. *$[Cl^-]_o$ and $[Ca^{2+}]_o$ affect hypoxia-induced contractions differently in porcine intrapulmonary arteries and veins* (September 2006) (Abstracts, The Physiological Society workshop on Cardiopulmonary Function in Health and Disease, Prague, The Czech Republic)

Dospinescu, C. & Cruickshank, S. F. *Cl^- channel blocker NFA inhibits $PGF_{2\alpha}$ and hypoxia-induced contractions in porcine intrapulmonary veins but not in arteries*. (August 2006) (Abstracts, FASEB Summer Research Conference, Smooth Muscle, Snowmass Village, Colorado, USA)

Dospinescu, C., McCaig, D., Wainwright, C. L. & Cruickshank, S. F. *Different role for $[Cl^-]_o$ in hypoxia induced contractions of small intrapulmonary arteries and veins*. (2006) J Mol Cell Cardiol 40(6):1015 (Abstracts, The 26th Annual Scientific Meeting of the European Section of the International Society for Heart Research in Manchester, UK)

Dospinescu, C., Yamawaki, N., McCaig, D., Wainwright, C. L. & Cruickshank, S. F. *Low chloride potentiation of hypoxic pulmonary vasoconstriction*. (2005) J Physiol 568P:PC44 (Abstracts, The Physiological Society Focused Meeting on Ion channels, genes and regulation in smooth muscle, University of Oxford, UK)

ABSTRACT

In the pulmonary circulation, alveolar hypoxia contributes to blood flow regulation. Hypoxic pulmonary vasoconstriction (HPV) involves both pulmonary arteries and veins, but little is known of the contractile mechanisms specific to the veins. The aim of these studies was to examine the hypoxic response in small porcine intrapulmonary veins in relation to the arterial response, and investigate the effects of hypoxia on ion conductances in single myocytes from intrapulmonary veins.

In wire myography experiments, intrapulmonary veins contracted more than size-matched arteries in response to hypoxia and agonists KCl and $PGF_{2\alpha}$. Venous contractions were inhibited by removal of extracellular Ca^{2+} or in the presence of Cl^- channel blocker NFA, effects not seen in the arteries. To examine the mechanisms of venous contraction at cellular level, single pulmonary vein smooth muscle cells (PVSMC) were freshly isolated and characterised morphologically and electrophysiologically for the first time. In patch-clamp studies, hypoxia reversibly inhibited a whole-cell outward current in the presence of BK_{Ca} channel antagonist Penitrem A. By subtracting currents recorded in normoxia and hypoxia, a novel hypoxia-sensitive K^+ current ($I_{K(H)}$) was revealed in PVSMC. $I_{K(H)}$ was a rapidly activating, partially inactivating current and was sensitive to K_V channel blocker 4-AP. The biophysical properties of $I_{K(H)}$ revealed the voltage window of current availability with a peak near the resting membrane potential of PVSMC.

In conclusion, these findings highlight differences between the contractile properties of veins and arteries and reveal a significant contribution of Ca^{2+} influx and an NFA-sensitive conductance during venous contraction to agonists and hypoxia. Furthermore, the results suggest that a novel hypoxia-sensitive K_V current contributes to membrane potential under resting conditions in PVSMC and its inhibition by hypoxia may contribute to the initiation of HPV in porcine intrapulmonary veins.

ABBREVIATIONS

4-AP	4-aminopyridine
5-HT	5-hydroxytryptamine (serotonin)
ACh	acetylcholine
ALI	acute lung injury
ARDS	adult respiratory distress syndrome
BAPTA	1,2-bis(2)aminophenoxy]ethane-N,N,N',N'-tetraacetic acid
BK_{Ca}	large-conductance calcium-activated potassium channels
$[Ca^{2+}]_i$	intracellular free calcium concentration
C_m	membrane capacitance
cADPR	cyclic ADP-ribose
CCE	capacitative calcium entry
Cl_{Ca}	calcium-activated chloride channels
CM	cardiomyocytes
CPA	cyclopiazonic acid
CV	coefficient of variation
DMSO	dimethyl sulfoxide
EC_{50}	half-maximal effective concentration
EGTA	Ethylene glycol-bis(2-aminoethylether)-N,N,N',N'-tetraacetic acid
EDNO	endothelium-derived nitric oxide
ET_A	endothelin receptor type A
ET_B	endothelin receptor type B
ET-1	endothelin-1
HAPO	high altitude pulmonary oedema
HBS	HEPES-based bath solution
$HBS_{Low\text{-}Cl}$	low-Cl^- HEPES-based bath solution
$HBS_{Ca\text{-}free}$	Ca^{2+} free HEPES-based bath solution
HEPES	4-(2-Hydroxyethyl)piperazine-1-ethanesulfonic acid
HPV	hypoxic pulmonary vasoconstriction

$I_{K(H)}$	hypoxia-sensitive potassium current
$I_{K(Pen)}$	Penitrem A-insensitive current
$I_{K(V)}$	voltage-activated potassium current
I_{out}	voltage-activated outward current
IP_3-R	inositol-1,4,5-triphosphate receptors
K_{ATP}	ATP-sensitive potassium channels
K_{Ca}	calcium-activated potassium channels
K_V	voltage-gated potassium channels
KCl	potassium chloride
LTC_4	leukotriene C_4
MAP	mitogen-activated protein kinase
MLC	myosin light chain
MLCK	myosin light chain kinase
MLCP	myosin light chain phosphatase
n	number of replicates
NFA	niflumic acid
NO	nitric oxide
NPPB	5-Nitro-2-(3-phenylpropylamino) benzoic acid
OD	outer diameter
Po_2	partial pressure of oxygen
PA	pulmonary artery
PAF	platelet-activating factor
PAF-R	platelet-activating factor receptor
PASMC	pulmonary artery smooth muscle cells
$PGF_{2\alpha}$	prostaglandin $F_{2\alpha}$
PGI_2	prostacyclin
PHT	pulmonary hypertension
PKC	protein kinase C
PPH	primary pulmonary hypertension
PPHN	persistent pulmonary hypertension of the neonate

PTK	protein tyrosine kinase
PV	pulmonary vein
PVCM	pulmonary vein cardiomyocytes
PVOD	pulmonary veno-occlusive disease
PVR	pulmonary vascular resistance
PVSMC	pulmonary vein smooth muscle cells
R_s	series resistance
RMP	resting membrane potential
ROK	Rho kinase
ROS	reactive oxygen species
RyR	ryanodine receptors
SD	standard deviation
SEM	standard error of the mean
SMC	smooth muscle cells
SOCC	store-operated calcium channels
STOC	spontaneous transient outward current
TEA	tetraethylammonium chloride
TxA_2	thromboxane A_2
τ_{act}	time constant of current activation
$V_{½}$	membrane potential at half-maximal inactivation
VGCC	voltage-gated Ca^{2+} channels
VSM	vascular smooth muscle

Chapter 1.
General Introduction

The pulmonary circulation is a vascular bed adapted structurally and functionally to contribute to the lung's primary function of respiratory gas exchange. Optimal blood oxygenation requires that, irrespective of cardiac output, capillary blood flow is delivered at an appropriate rate and that it also adequately matches the ventilation of each respiratory unit (alveolus).

The process of gas exchange takes place by diffusion of O_2 and CO_2 through the alveolar-capillary membrane across concentration gradients. The alveoli are surrounded by a high density network of thin-walled capillaries – nearly 1000 pulmonary capillaries per alveolus – which has been likened to a "sheet of blood". This enables a vast contact surface between the alveolar and capillary membranes of approximately 50 to 100 m^2 (Levitzky, 2002b) providing a very high capacity for gas diffusion.

All segments of the pulmonary circulation – the arteries, the capillary network and the veins – function as a low-pressure and low-resistance circulatory system. The larger pulmonary vessels are thinner walled and have less smooth muscle than systemic vessels, making them less resistant to flow. Haemodynamically, this is reflected in blood pressure values in the pulmonary circulation that are approximately six times less than systemic values (Dembinski *et al.*, 2004). Collapsed pulmonary capillaries have the ability to open in response to increased flow, contributing to decreased vascular resistance (Dembinski et al., 2004) and to

the prevention of stress damage on the very thin alveolar-endothelial membrane (Levick, 2003). The low vascular resistance and high compliance are particularly important during situations when raised metabolism (e.g. during exercise) increases cardiac output and, as a result, the pulmonary circulation must be able to accommodate large fluctuations in blood flow, ranging from resting values of 4-6 l/min (adult human) to values of 20-25 l/min (maximum flow, non-athlete) (Levick, 2003).

Equally important for efficient gas exchange is the need for blood flow in each area of the lungs to correspond to the degree of ventilation. When regional alveolar oxygen saturation is low, the adjacent pulmonary vessels constrict and blood is diverted to other, better ventilated, areas of the lungs. This physiological mechanism that achieves the optimisation of the ventilation-perfusion ratio is termed hypoxic pulmonary vasoconstriction (HPV).

1.1. The pulmonary veins

1.1.1. Anatomy

The role of the pulmonary veins (PV) is to carry oxygenated blood from the pulmonary capillaries to the left atrium. The pulmonary venous network (shown in Figure 1.1) is the last segment of the pulmonary circulation and its vessels form a vascular tree comprising 15 branching orders (Hughes and Morrell, 2001). The first segment is formed by post-capillary venules, which collect the blood from the capillary bed. These join together and eventually form one vein for each lobule, followed by one for each segment, which in turn form trunks for each lobe (i.e. three for the right lung and two for the left lung). In humans, the veins take a course along the edges of the pulmonary lobules and segments in the interlobular septa, separate from the arteries that follow the bronchi in a centro-lobular position (Kay, 1983). The right middle and upper lobar veins normally unite and therefore two main pulmonary veins emerge from each lung (Gray, 1918). These four main

extrapulmonary veins pass through the fibrous layer of the pericardium and open separately into the superior and posterior walls of the left atrium and are named: *right superior*, *right inferior*, *left superior*, and *left inferior* pulmonary veins (see Figure 1.2).

Occasionally, anatomical variations from this standard morphological position may occur. A frequent possibility is that the two main veins – superior and inferior – on either side open in a single ostium in the left atrium (Ho *et al.*, 2001). Another, less common, alternative is that the right middle lobar vein does not join the upper one and opens through a fifth separate ostium in the wall of the left atrium (Wittkampf *et al.*, 2003).

1.1.2. Morphology

1.1.2.1. Ultrastructure of the venous wall

As in the systemic circulation, veins in the pulmonary vasculature have an endothelium, smooth muscle and adventitia and have less abundant smooth muscle than similar sized pulmonary arteries (PA) (Hughes and Morrell, 2001).

In human pulmonary veins larger than 100 μm, the venous intima consists of an internal elastic lamina lined by the endothelium, the media is a disorganized arrangement of smooth muscle with collagen and elastic fibrils and there is no clearly demarcated adventitia (Kay, 1983). Post-capillary veins that have only occasional smooth muscle fibres have been termed ‘partially muscular veins’, while larger ones have a continuous muscle layer, but no external elastic lamina (Hislop and Reid, 1973). In small veins with an external diameter of less than 300 μm, the wall thickness expressed as a percentage of the vessel diameter was found to be significantly increased compared to larger veins (Hislop and Reid, 1973).

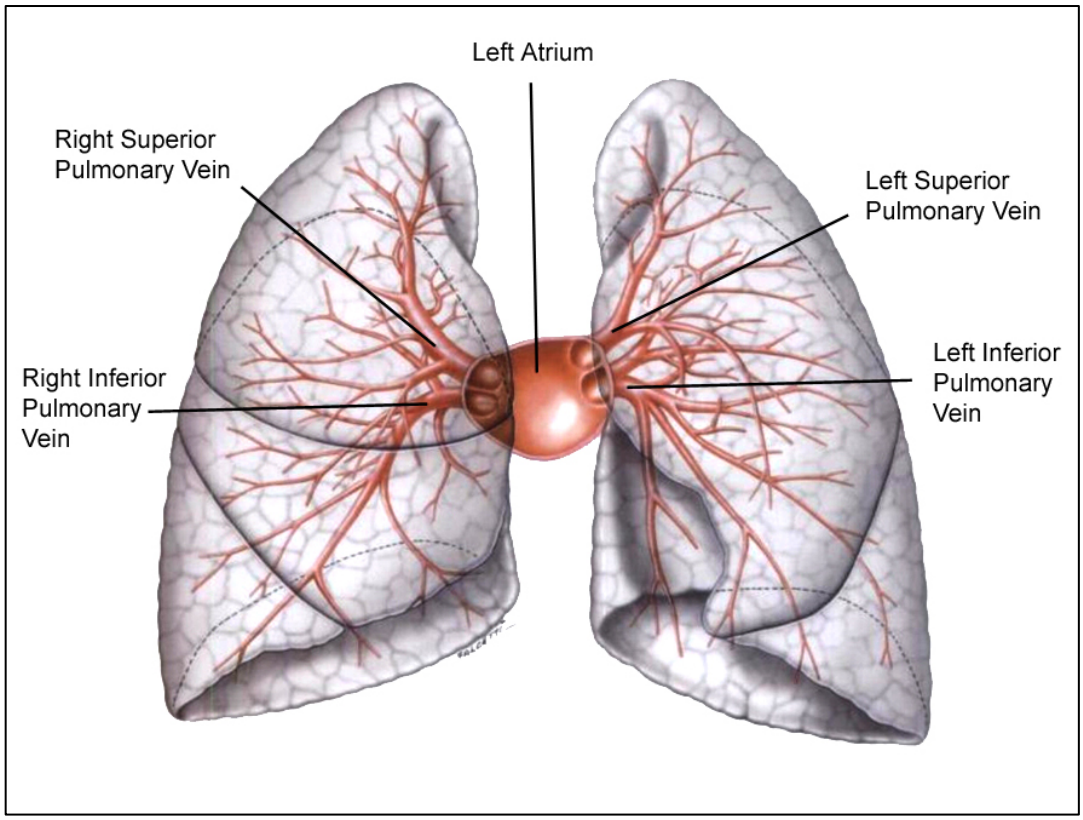

Figure 1.1. Schematic drawing of the pulmonary venous network. Anterior view of the lungs, venous network and the left atrium (used with permission from Uflacker, 2006 p. 271).

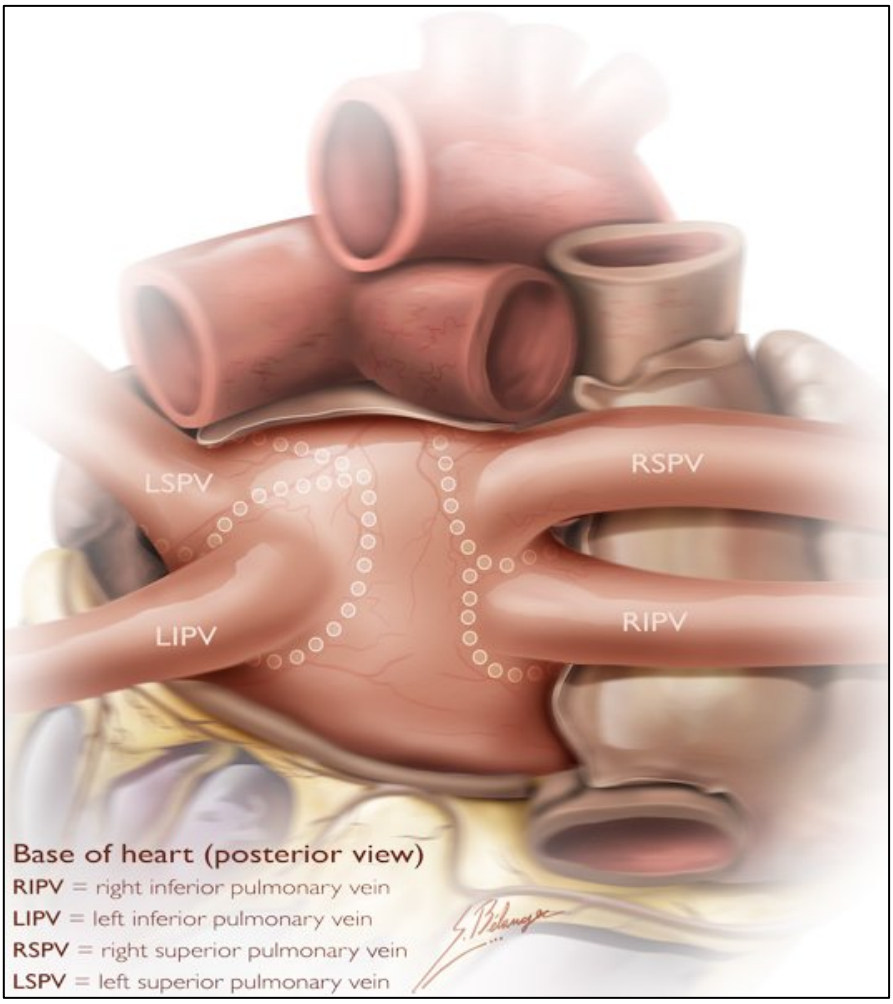

Figure 1.2. The main pulmonary veins. Macroscopic dorsal view of the base of the heart and main vessels with the main four pulmonary veins opening in the left atrium (used with permission from O'Riordan, 2005).

In the rat, veins lack an internal elastic lamina between the endothelial and smooth muscle layers and the smooth muscle is discontinuous, often only present in the form of "muscular pads" (Dingemans and Wagenvoort, 1978). The smooth muscle cells are surrounded by a matrix substance that also contains collagen fibrils and elastic lamellae and the external margin of the smooth muscle wall is delineated by attenuated fibroblasts (Ludatscher, 1968). Smooth muscle is present even in the smallest of veins, although the layer has a thickness of only one or two cells. The ultrastructure of venules was found to be very similar to arterioles, although they had even less smooth muscle and lacked the isolated patches of elastin that were present between the endothelium and media of arterioles.

Kay (1983) carried out a comparative study on the morphology of the pulmonary vasculature in mammals and found marked variation in the structure of the pulmonary veins between species. Pulmonary veins with fibrous content such as in humans were also found in the cat, civet, dog, ferret, fox, goat, horse, monkey and rabbit. On the contrary, in the cow, guinea pig, llama, pig and rat, the pulmonary venous walls were muscular.

1.1.2.2. The myocardial layer

The architecture of the pulmonary venous wall differs from arteries in one other respect. In addition to the typical layers that form the wall of any blood vessel, the pulmonary veins have an external muscular layer of cells which resemble the cardiac myocytes in the atrial myocardium (Ludatscher, 1968). This feature of the pulmonary venous wall was confirmed in all species examined (Nathan and Gloobe, 1970). The cardiac-like cells are arranged in a mesh-like pattern forming a "myocardial sleeve" around the pulmonary vein's smooth muscle layer (Masani, 1986). These pulmonary vein cardiomyocytes have the ability to initiate spontaneous electrical activity and induce atrial arrhythmias (Chen *et al.*, 2000) and are thought to be involved alongside pulmonary vein smooth muscle cells (PVSMC) in modulating pulmonary venous tone in rats (Michelakis *et al.*, 2001). Although speculations have

been made about a possible sphincter-like role for this myocardium (Burch and Romney, 1954, Nathan and Gloobe, 1970), no definitive evidence on the role it plays *in vivo* has emerged.

However, in most large mammals including humans, the myocardial layer is limited to extrapulmonary sites (Nathan and Gloobe, 1970, Roux *et al.*, 2004) and, therefore, the only type of muscle present in the wall of intrapulmonary veins is smooth muscle.

1.1.3. Regulation of venous tone

Within the pulmonary circulation, the veins have been traditionally regarded as passive conduits without significant haemodynamical influence in blood flow regulation or contribution to total vascular resistance. As a consequence, the pulmonary veins have historically received relatively little interest from researchers outside their role in cardiac arrhythmias. This is despite many studies that have shown significant vasoactivity of the pulmonary veins (reviewed below) and, in some cases, higher contractions than in similar sized arteries. For example, in guinea-pig lung explants, histamine and 5-HT induced greater contractions in the veins compared to the arteries (Shi *et al.*, 1998). The same was shown for contractions by U46619 in piglets (Arrigoni *et al.*, 1999) and by hypoxia in the rat (Zhao *et al.*, 1993), while PAF contracted pulmonary veins while relaxing arteries in the ferret (Gao *et al.*, 1995b).

Such reports contradict existing dogma and represent important evidence that the pulmonary veins are capable of active vasomotion, suggesting a significant role for the vein in the regulation of pulmonary blood flow.

1.1.3.1. Contribution to total pulmonary vascular resistance

The relative contributions of each vascular segment to total vascular resistance differ between the systemic and pulmonary circulation. While in the systemic circulation arteries account for approximately 70% of total vascular resistance, pulmonary resistance is distributed roughly equally between arteries, capillaries and veins (Levitzky, 2002a). As vascular resistance is a determinant of blood flow, the implication is that, in the pulmonary circulation, the veins are playing a relatively more important role in blood flow regulation (Fung and Huang, 2004).

Existing studies looking at the relative contributions of each longitudinal segment – arteries, microcirculation and veins – to total vascular resistance in the pulmonary circulation were reviewed by Gao and Raj (2005b). There was some variation in the findings of the studies considered and this was attributed to the differences in measuring techniques, experimental conditions, as well as age and species of the animals being studied. However, the overall evidence suggested that the veins contribute significantly to vascular resistance in the lungs. Zhuang *et al*. (1983) attributed as much as 49% of total vascular resistance to the pulmonary veins, while Kadowitz *et al*. (1975) found that approximately 50% of the total increase in resistance caused by sympathetic nerve stimulation under conditions of steady flow was due to venoconstriction. Increased vascular tone in the pulmonary veins contributes to increased total pulmonary vascular resistance (Raj and Chen, 1986) and this can have implications during oedema formation when post-capillary venoconstriction raises upstream microvascular hydrostatic pressures and fluid filtration (Dauber and Weil, 1983).

1.1.3.2. Neurotransmitters

Kadowitz *et al.* (1975) studied the contribution of intrapulmonary lobar veins to the rise in vascular resistance induced by sympathetic nerve stimulation in pentobarbital-anesthetised dogs. Under conditions of controlled blood flow, stimulation of the stellate ganglia at 3, 10, and 30 cycles/s increased the resistance to flow by

constricting pulmonary veins and vessels upstream to the small veins, and at each applied frequency venoconstriction contributed approximately 50% to total increase in vascular resistance. Furthermore, injected norepinephrine (10 μg) induced a pressure fall in the left atrium and large veins, while the pressure in the small lobar intrapulmonary veins increased (in both the apex and left lower lobe).

Vasoactive neurotransmitters were also shown to induce contractions of isolated canine pulmonary veins in isometric tension experiments using organ baths. The contractions of canine intrapulmonary lobar veins in response to norepinephrine were blocked by phentolamine (Joiner *et al.*, 1975a). Both selective adrenergic agonists ciralozine (α_1) and B-HT 933 (α_2) induced concentration-dependent vasoconstrictions suggesting that both subtypes of α-adrenergic receptors coexist and mediate contraction of pulmonary veins (Ohlstein *et al.*, 1989). The application of ACh (0.1 to 10 μM) elicited contractile responses in third generation intralobar veins (1-2 mm internal diameter) mediated primarily through M_3 muscarinic receptors (Ding and Murray, 2005b).

1.1.3.3. Humoral substances

Various circulating mediators and hormones induce vasoactive effects on pulmonary veins by acting on specific receptors (see Table 1.1).

Histamine and 5-HT induced robust contractions in pulmonary veins (~ 300 μm external diameter) of guinea pigs which were greater than in the arteries (Shi *et al.*, 1998). Venous contractions to 5-HT were markedly inhibited by the 5-HT_2 receptor antagonist ketanserin. The H_1 receptor antagonist clorpheniramine abolished, while the H_2 receptor antagonist cimetidine enhanced both the sensitivity and the maximal responses of venous responses to histamine.

Metabolites of the cyclooxygenase pathway were also shown to mediate pulmonary venous contractions. In isolated lamb lungs perfused with low venous intraluminal pressures and moderate basal vasomotor tone, the thromboxane A_2 (TxA_2) analogue

U46619 given in a 5 μg/kg bolus followed by a steady infusion of 1 μg/kg/min induced a more than twofold rise in venous resistance (Raj and Anderson, 1990). In organ bath experiments, the same agonist (U46619, 0.1 μM) induced contractions of isolated rings of small intrapulmonary veins (1-2 mm inner diameter) from dogs (Ding and Murray, 2005a). Prostaglandin $F_{2\alpha}$ ($PGF_{2\alpha}$) induced contractions of canine, sheep and human pulmonary venous strips (Joiner *et al.*, 1975b) and the prostanoid receptor agonists sulprostone, 17-phenyl-PGE_2 and iloprost contracted human PV rings (Walch *et al.*, 2001).

The potent inflammatory mediator platelet-activating factor (PAF) contracted pulmonary veins and relaxed arteries in the ferret (Gao *et al.*, 1995b) and contractions induced by the parathyroid hormone-related protein were greater in the pulmonary veins compared to the arteries of the newborn lamb (Gao and Raj, 2005a).

1.1.3.4. Endothelium-derived factors

In both the pulmonary and systemic vasculature, the endothelium plays a critical role in the regulation of vascular tone (Barnes and Liu, 1995). Endothelial cells have the ability to release a range of constrictor and dilator mediators with profound impact on vasomotion.

The potent vasoactive peptide ET-1 contracted veins with a greater sensitivity than in arteries and venoconstriction contributed to oedema induced by ET-1 in lungs perfused with physiological salt solution (Rodman *et al.*, 1992). The same observation on the sensitivity of veins to ET-1 was made on third-generation intrapulmonary vessels from sheep of all age groups (Toga *et al.*, 1992). In the pig, venous contractions induced by ET-1 were mediated through both ET_A and ET_B receptors (Zellers *et al.*, 1994).

Small pulmonary veins were also shown to be more responsive than arteries to vasodilator stimuli. In very small concentrations (1-100 pM), ET-1 caused endothelium-dependent relaxations in the veins and arteries, which were also larger in the veins (Zellers *et al.*, 1994). In the same study, it was reported that the release of vasodilators from the endothelium, such as endothelium-derived nitric oxide (EDNO) and prostacyclin, was higher in the veins.

Elsewhere, Gao *et al.* (1995a) reported similar findings in newborn lambs and suggested that the enhanced role of EDNO in modulation of vascular reactivity in the veins may be linked to varied levels of activity of soluble guanylate cyclase in vascular smooth muscle.

1.1.3.5. Hypoxia

Hypoxic pulmonary vasoconstriction, which is primarily thought to occur in small pulmonary arteries, was also demonstrated in the veins (for an extended review, see section 1.2). Using myography experiments, Tracey *et al.* (1989) showed that pulmonary venules (~1 mm diameter) from guinea pigs contracted in response to hypoxia and anoxia. In isolated perfused lungs, alveolar hypoxia induced a 40% rise in pulmonary venous pressure (10 to 60 μm diameter) of newborn pigs (Fike and Kaplowitz, 1992) and significantly increased the venous resistance in subpleural 20- to 50-μm-diameter venules of adult and 3- to 5-week old ferrets (Raj *et al.*, 1990) and 20- to 80-μm-diameter venules of newborn lambs (Raj and Chen, 1986).

Table 1.1. Receptors mediating vasomotion in the pulmonary veins.

Receptor	Subtype	Action	Reference
5-HT	5-HT_2	Contraction	(Shi *et al.*, 1998)
Adrenergic	α_1, α_2	Contraction	(Ohlstein *et al.*, 1989)
Endothelin	ET_A	Contraction	(Zellers *et al.*, 1994)
	ET_B	Contraction (smooth muscle mediated) Vasodilation (endothelium mediated)	
Histamine	H_1	Contraction	(Shi *et al.*, 1998)
	H_2	Vasodilation	
Muscarinic	M_3	Contraction	(Ding and Murray, 2005b)
PAF-R		Contraction	(Gao *et al.*, 1995b)
Prostanoid	TP, EP_1	Contraction	(Walch *et al.*, 2001)
	DP, IP	Vasodilation	(Walch *et al.*, 1999)

1.2. Hypoxic pulmonary vasoconstriction

The constriction of vessels in response to hypoxia is a typical feature of the pulmonary circulation, as systemic vessels relax in response to decreasing oxygen saturation in the blood. Hypoxic pulmonary vasoconstriction (HPV) is a physiological reaction to *regional* alveolar hypoxia that helps the organism maintain the essential high oxygen levels in arterial blood, but which can also have a detrimental impact by contributing to pulmonary disease during acute and chronic *global* alveolar hypoxia.

1.2.1. Initial reports

Early published observations of hypoxic pulmonary vasoconstriction were made in 1876 with the work of Lichtheim (cited by Bradford and Dean, 1894). He described an asphyxia-induced rise in pulmonary artery pressure without an accompanying rise in systemic pressure and concluded that this was due to vasomotor fibres in the pulmonary vessels.

In 1894, Bradford and Dean induced asphyxia in curarised animals by discontinuing artificial respiration and observed a gradual, but considerable rise in pulmonary artery pressure. They also reported that "a greater effect is obtained on the pulmonary circulation by asphyxia than by any other mode of excitation" (Bradford and Dean, 1894 p. 75).

However, the first ones to make a systematic assessment and propose a physiological mechanism for this response were von Euler and Liljestrand in 1946. In anaesthetised cats ventilated with 10.5% oxygen, they observed an acute rise in pulmonary artery pressure (see Figure 1.3) which was not affected by vagotomy or ablation of the stellate ganglia (von Euler and Liljestrand, 1946).

Following their observations, they hypothesized that this acute physiological response was a local regulatory mechanism, which acts to optimise the distribution of pulmonary blood flow through direct constricting action of hypoxia on pulmonary arterioles, independent of the autonomic nervous system. They postulated the following (von Euler and Liljestrand, 1946 p. 318):

> *"oxygen want and carbon dioxide accumulation [...] call forth a contraction of the lung vessels, thereby increasing the blood flow to better aerated lung areas, which leads to improved conditions for the utilization of the alveolar air"*

One year later, Motley *et al.* (1947) reported hypoxic pulmonary vasoconstriction for the first time in humans. Five conscious spontaneously-breathing male subjects were given a low oxygen gas mixture (10 per cent O_2 in N_2) to breathe for short periods of approximately 10 minutes. Hypoxic breathing induced a significant degree of transient pulmonary hypertension, with a recorded rise in mean pulmonary artery pressure from 13.1 to 23 mm Hg and an almost twofold increase in pulmonary vascular resistance.

These initial reports set the context for further research on HPV with later studies focused on elucidating the mechanism(s) responsible for sensing and initiating the pressor response to acute hypoxia and locating the exact site of action of hypoxia on pulmonary vessels (Fishman, 1976).

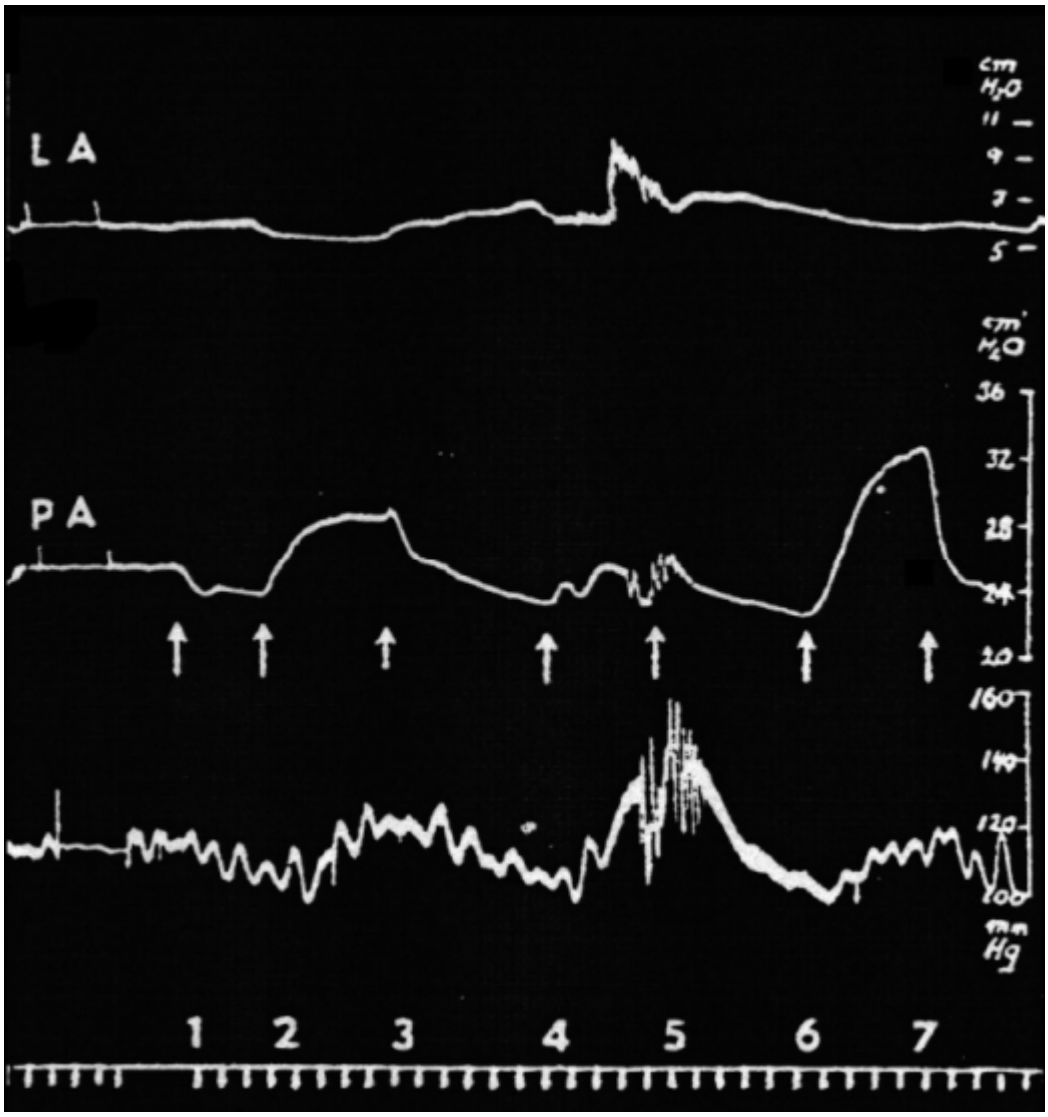

Figure 1.3. The first recording of hypoxic pulmonary vasoconstriction.
Cat anesthetized with chloralose, 3.9 kg, kept on artificial ventilation, open thorax. LA, left atrium; PA, pulmonary artery. Bottom trace, systemic blood pressure. 1 = O_2 (from air); 2 = 6.5% CO_2 in O_2; 5 = O_2; 6 = 10.5% O_2 in N_2; 7 = O_2; t = 30 s. (used with permission from von Euler and Liljestrand, 1946).

1.2.2. The HPV response

1.2.2.1. Physiological and pathological relevance

Alveolar oxygen is an important regulator of vascular tone in the pulmonary circulation. When some of the alveoli are ventilated with a gas mixture lower in oxygen content than atmospheric air, blood flow in the surrounding capillaries is reduced through the contraction of nearby pulmonary vessels. As a result, local perfusion is adjusted to match alveolar ventilation and the ventilation/perfusion ratio is maintained close to its optimal value of 0.8 (Levick, 2003). Hence, by causing blood to be diverted away to the better oxygenated areas of the lungs, HPV helps improve gas exchange and keeps the blood supply to the systemic circulation highly saturated in oxygen.

The level of alveolar oxygen tension required to trigger a hypoxic constriction in humans and adult animals is reportedly below 60 mm Hg (Hales, 2004). Harris and Heath (cited in Dumas *et al.*, 1999) found that when the partial pressure of oxygen (Po_2) in the alveolar air decreases below 50 mm Hg in humans, the pulmonary vascular resistance increases by 50% as a response. However, the recorded values may depend on the experimental model and technique used, as milder hypoxic conditions (70 mm Hg) have been reported to induce HPV in rabbit lungs (Weissmann *et al.*, 1995). In addition, the level of hypoxia required to trigger maximal hypoxic contractions varies in different species investigated (Peake *et al.*, 1981).

The HPV mechanism functions as a physiological shunt (Traber and Traber, 2002), with most blood flow by-passing the regions with hypoxic alveolar ventilation. One important consequence of this property of HPV is that it is more effective on a reduced scale. The smaller the region affected by hypoxia is, the greater the proportion of blood being diverted away will be as a result of HPV (Marshall *et al.*, 1981).

However, if hypoxia is generalised to one or both lungs, this response may become detrimental due to resulting the global hypoxic vasoconstriction. The vasoconstricting response that occurs during acute hypoxia is partially responsible for the development of high altitude pulmonary oedema (Hultgren *et al.*, 1971). Prolonged generalised exposure to hypoxia can contribute to vascular remodelling and pathological states such as hypoxic pulmonary hypertension (Weitzenblum and Chaouat, 2001).

1.2.2.2. Site(s) of hypoxic pulmonary vasoconstriction

The site of action of hypoxia in the pulmonary circulation has been the subject of considerable debate. Finding out where hypoxia acts in the lungs has been a central objective in HPV research, as it would help explain the other important question of how hypoxia acts (Fishman, 1976). The main obstacle was represented by the difficulty of accessing the pulmonary circulation, especially pulmonary microvessels, for direct measurements of haemodynamic pressures. The interpretation and understanding of available evidence has developed over time, largely influenced by experimental techniques available.

During the early years of work in the field of HPV, different investigators attributed the main role in turn to each segment of the pulmonary vasculature: the arteries (von Euler and Liljestrand, 1946, Lloyd, 1964), capillaries (Duke, 1954) and the veins (Rivera-Estrada *et al.*, 1958).

The first reports of HPV measured significant rises in pulmonary artery pressure during hypoxia (von Euler and Liljestrand, 1946, Motley *et al.*, 1947). Coupled with the known fact that small resistance arteries are primarily responsible for vascular resistance in the systemic circulation, this lead investigators to assume that the hypoxic pressor effect takes place through vasoconstriction of precapillary vessels (Kuida *et al.*, 1962, Lloyd, 1964). Others, however, reported a significant fall in pulmonary arterial blood volume concomitant with the hypoxia-induced increase in vascular resistance, which, they thought, could not be accounted for solely by the

reduction of volume in the arteriolar segment (Sackner *et al.*, 1966). They interpreted these observations as evidence that hypoxic vasoconstriction occurred throughout the entire pulmonary arterial tree.

A different proposition was put forward by Nisell (1951), who argued that the hypoxic constriction occurs on the venous side. Working with isolated perfused cat lungs, he observed a decrease in the pulmonary vascular resistance during perfusion with hypoxic or hypercapnic blood. He suggested that hypoxia acts by venous constriction and arterial vasodilation. Results from *in vivo* haemodynamic studies in anesthetised dogs (Hall and Hall, 1953) agreed with the findings of Nisell. When pulmonary lobes were perfused *in situ* with oxygenated blood from the carotid arteries, hypoxic ventilation caused an increase in vascular resistance, thought to be due to vasoconstriction distal to pulmonary arterioles.

Further evidence to support hypoxic post-capillary vasoconstriction came from Rivera-Estrada *et al*. (Rivera-Estrada *et al.*, 1958). Anesthetised dogs were exposed to 5 and 10 per cent oxygen, while pressures were measured in the pulmonary artery, left atrium and the pulmonary capillary wedge position, which was verified to be a good reflection of venous pressure both before and after hypoxia. Hypoxia increased both the capillary wedge pressure and the pulmonary arterial pressure, while only a minimal change was seen in left atrial pressure. More importantly, the gradient between the venous and the left atrial pressures rose significantly in the absence of left ventricular failure, which was interpreted to be due to hypoxia-induced venoconstriction.

In the subsequent years, the theory that alveolar hypoxia affects primarily post-capillary vessels gained some acceptance and the venous contribution to HPV was emphasised (reviewed in Fishman, 1961).

Others agreed that HPV may take place distal to the pulmonary arterioles, but believed that pulmonary capillaries and not veins were the most important segment. Research by Duke (1954) on isolated cat lungs perfused with heparinised own blood

showed that hypoxic ventilation of alveoli cannot be replaced by hypoxic perfusion as a trigger of HPV. Her experiments found that perfusing air-ventilated lungs with partially de-oxygenated blood failed to induce a rise in pulmonary artery pressure, whereas ventilation with N_2 during the same perfusion conditions did elicit a hypoxic pressor response. These findings suggested that the relevant HPV location is probably at or downstream of the site where gas exchange takes place. After further back-perfusion experiments gave a similar response to those in which perfusion was made through the pulmonary artery, Duke concluded that capillaries were most likely to be the site sensitive to low oxygen. This interpretation, however, did not receive a large amount of support, the main concern about it being the fact that the capillaries were known to lack smooth muscle and were not believed to contribute actively to the increase in pulmonary resistance (Fishman, 1961).

A new turning point emerged when further research highlighted that small arteries are directly susceptible to alveolar hypoxia, since alveolar O_2 content affects the oxygenation of blood in distal arteries (Sobol *et al.*, 1963, Jameson, 1964). This previously missing link attracted more support for the role of arterioles as the main site of HPV (reviewed in Fishman, 1976).

More compelling evidence to confirm the role of arteries was brought by the use of new techniques. Kato and Staub (1966) induced hypoxic constriction in anaesthetised cats and then rapidly froze the lower lung lobes at end inspiration with liquid propane. They then sectioned the tissue, measured internal diameters of distal muscular arteries (~ 100-200 μm) and found active constriction of arteries accompanying the terminal respiratory units, reflected in a 32 per cent decrease in their average internal diameter during hypoxia. Hirschman and Boucek (1963) used angiography to assess the vasomotor responses of dog distal pulmonary arteries (as small as 0.2 - 0.3 mm) by injecting a contrast substance directly into a branch of the pulmonary artery via a non-wedging catheter. Hypoxia induced a twofold rise in pulmonary artery pressure with corresponding angiographic changes in small

arteries. These consisted of collars of constriction appearing at sites of bifurcation, beading and spiralling of previously straight small arteries.

More recent research indicates that the microcirculation, including both pre- and post-capillary small vessels, is predominantly responsible for the increase in tone during HPV. Shirai *et al.* (1986) used an X-ray TV system and contrast angiography to assess hypoxia-induced changes in volume and flow velocity and internal diameters of small vessels from the cat lungs. They found that hypoxia acted primarily on small arteries with an internal diameter of 200-300 μm, but small veins also constricted. Similarly, measurements of pressure gradients partitioned across the segments of the pulmonary circulation using occlusion techniques indicated that hypoxia constricted pre-capillary and, to a lesser extent, post-capillary vessels in canine lungs (Hakim, 1988). Hillier *et al.* (1997) used a videomicroscope to make direct and accurate measurements of the diameter of subpleural microvessels in isolated dog lungs. During hypoxia, the overall average diameter of 30- to 70-μm microvessels decreased by approximately 25 per cent and the reduction occurred in both arterioles and venules by a relatively similar amount. However, in some species, hypoxia only constricted 20- to 30-μm arterioles and not venules (rat, Yamaguchi *et al.*, 1998).

Finally, although – beginning with the first report by Nisell (1951) – veins have been repeatedly highlighted as an active participant in HPV and recent studies have brought new evidence to support this (Raj and Chen, 1986, Tracey *et al.*, 1989, Raj *et al.*, 1990, Hasebe *et al.*, 1992, Zhao *et al.*, 1993, Feletou *et al.*, 1995, Uzun and Demiryurek, 2003), most current reviews choose to overlook their contribution and focus solely on the arterial side (Ward and Aaronson, 1999, Dumas *et al.*, 1999, Sylvester, 2001, Moudgil *et al.*, 2005, Weissmann *et al.*, 2006), with few others emphasising the venous involvement (Gao and Raj, 2005b, Bonnet and Archer, 2007).

1.2.2.3. Time course of HPV responses

The profile of the hypoxia-induced response in the pulmonary vasculature depends to a large extent on the experimental model. In general, responses are monophasic *in vivo*, in intact lungs and isolated pulmonary veins, while in isolated pulmonary arteries hypoxia induces a biphasic increase in tone (Ward and Aaronson, 1999, Zhao *et al.*, 1993).

In humans, following the onset of hypoxic breathing, the pressure in the pulmonary vasculature begins to rise rapidly and reaches a maximum value after 2 to 4 minutes (Motley *et al.*, 1947). The pressure remains raised during brief hypoxic breathing episodes (15 to 20 minutes) and returns promptly to normal values after switching to breathing ambient air. In calves exposed to low oxygen gas mixtures, Kuida *et al.* (1962) observed the pressure increasing within 15 to 30 seconds and reaching a plateau in the first 3 minutes, while in dogs the mean pulmonary artery pressure rose in the first 4 minutes and then stabilised for the duration of the hypoxic period (Rivera-Estrada *et al.*, 1958, Malik and Kidd, 1973).

Usually, in the isolated perfused lung preparation, HPV responses are similar to those seen under *in vivo* conditions (Madden and Gordon, 2004). In cat lungs, the rise in pulmonary arterial pressure occurs after 20-30 seconds, reaches its maximum value in approximately 2 to 4 minutes and remains raised until the lungs are again ventilated with air (Duke, 1954). Similarly, in rabbit lungs the HPV response is apparent after 28 seconds and achieves its half maximal value after approximately 2 minutes (Weissmann *et al.*, 1995).

When isolated pulmonary arteries are challenged with hypoxia, they respond by eliciting isometric tension in a biphasic manner (Bennie *et al.*, 1991). The first phase consists of a transient contraction within the initial 2 to 4 minutes and is followed by a partial relaxation towards baseline (Leach *et al.*, 1994). The second phase usually involves a lesser amplitude sustained increase in tension, which develops gradually

over long periods of as much as 40 minutes (Leach *et al.*, 1994) to 1 hour (Zhao *et al.*, 1993).

The distinction between the two phases of HPV in the arteries appears to be important, as they have been shown to have different underlying mechanisms. The two contractile phases are differently affected by endothelium modulation (Hoshino *et al.*, 1994) and degree of stretch (Ozaki *et al.*, 1998) and are seemingly reliant on distinct sources of intracellular free calcium (Salvaterra and Goldman, 1993). More importantly, the first phase is thought, due to its transient nature, to be less physiologically relevant than the sustained second phase (Ward and Aaronson, 1999).

In contrast, the contraction induced by hypoxia in rat pulmonary veins is monophasic and its magnitude is greater than either phase of the response of size-matched arteries (Zhao *et al.*, 1993). The venous contraction peaks after approximately 10 minutes and is followed by a relaxation, which however does not reach initial baseline tone even after 1 hour of hypoxia.

1.2.3. HPV in different experimental models (*in vivo* & *in vitro*)

The initial observations and the postulation of the physiological role of HPV were formulated following *in vivo* studies, but the understanding of HPV mechanisms has been advanced more recently through the use of reductive *in vitro* experimental models, such as isolated vessels contractile studies and single cell techniques (reviewed by Madden and Gordon, 2004).

The large variety in findings and interpretations, sometime conflicting, reported on the effects of hypoxia on the pulmonary vasculature has to be attributed in a large part to the diversity of experimental setups and conditions used during investigations of HPV. In addition, the hypoxic response may be influenced by other factors such as species (Peake *et al.*, 1981), age (Owen-Thomas and Reeves, 1969) and gender (Wetzel and Sylvester, 1983), making the overall picture a complex one.

1.2.3.1. In vivo models

Hypoxic pulmonary vasoconstriction was first described under *in vivo* experimental conditions (Bradford and Dean, 1894, von Euler and Liljestrand, 1946). Subsequently, the exploration of the effects of hypoxic ventilation on the pulmonary circulation was also undertaken using *in vivo* models such as anaesthetised open-chested mechanically-ventilated animals (e.g. dogs, Rivera-Estrada *et al.*, 1958, Peters and Roos, 1952), awake spontaneously breathing animals (e.g. calves, Kuida *et al.*, 1962, dogs, Thilenius *et al.*, 1964, lambs, Frostell *et al.*, 1991) and, occasionally, humans (Motley *et al.*, 1947).

In such studies, the pulmonary haemodynamic changes in response to hypoxia were monitored and interpreted. Some or all of the following parameters were usually obtained during experiments. The pressures in the pulmonary artery, left atrium or pulmonary artery wedge position (illustrative of left atrial pressure) and sometimes pulmonary veins were recorded using intravascular catheters (Rivera-Estrada *et al.*, 1958, Aviado, 1960, Forrest and Fargas-Babjak, 1978). Measurements were made of oxygen consumption and oxygen content in the arterial and mixed venous blood, and these helped calculate total pulmonary blood flow (cardiac output) using the Fick principle (Peters and Roos, 1952). Alternatively, cardiac output was measured using the dye-dilution (Kuida *et al.*, 1962, Thilenius *et al.*, 1964) or thermodilution methods (Forrest and Fargas-Babjak, 1978). Pulmonary vascular resistance was indirectly determined by dividing the pressure gradient between the pulmonary artery and the left atrium to pulmonary blood flow (Sackner *et al.*, 1966).

These techniques helped assess the changes induced by hypoxia in the context of haemodynamic systemic influences. The hypoxic pressor response was found to occur independent of an increase in blood flow or backward pressure from the left atrium (Cournand, 1950) and was therefore believed to be due to increased tone in the pulmonary vessels.

The main disadvantage of the *in vivo* approach lies in the difficulty of completely separating the HPV response within the lungs from systemic factors. Another concern is that in intact animal studies, investigators normally assess the effects of global alveolar hypoxia, while HPV achieves its physiological purpose best during localised hypoxia (Marshall *et al.*, 1981). There have been, however, some attempts to take this into account, by ventilating with low oxygen gas mixtures only a single lobe (Hall and Hall, 1953, Shirai *et al.*, 1986) or different combinations of lobes (Marshall *et al.*, 1981) in order to assess the effects of regional hypoxia.

1.2.3.2. The isolated perfused lung

The ability to elicit HPV in the isolated perfused whole-lung helped establish the fact that the hypoxic pressor response occurs within the lungs independent of any systemic influences. The technique also facilitated the study of the mechanisms of HPV under conditions of isolation from any potentially interfering neural, humoral and haemodynamic systemic factors.

Duke and Killick (1952) used isolated cat lungs which were perfused at a constant rate of flow through the pulmonary artery with the heparinised blood of the animal and ventilated with intermittent positive pressure. Ventilation with N_2 induced a prompt monophasic rise in pulmonary artery pressure, which was similar to the response observed in the intact animal. The response was still present, albeit sometimes in a reduced amount, when blood was partially or completely replaced with Ringer Locke solution or with Dextran, suggesting that no blood constituents are required to initiate HPV.

The same experimental approach was used to propose or verify various mechanistic theories, such as: the role of various putative chemical mediators that would be synthesised and released within the lung (reviewed in Fishman, 1976), the involvement of K^+ channels (Post *et al.*, 1992) and the redox theory (Archer *et al.*, 1993).

Another important study using isolated lung experiments highlighted marked differences in the responses induced by hypoxia between species (Peake *et al.*, 1981). It reported the largest vasoconstrictor response in lungs from the pig and the ferret and smaller responses in cat and rabbit lungs.

1.2.3.3. Contractile studies using isolated vessels

The contractile properties of isolated pulmonary vessels under conditions of hypoxia have been extensively investigated using *in vitro* techniques such as tissue baths and myography for smaller vessels. This approach afforded more flexibility in the manipulation of extracellular conditions and made it possible to accurately correlate the tension response with the size of the vessel studied.

Dissected segments of pulmonary vessels from various species mounted in tissue baths and attached to force transducers allowed researchers to measure the isometric tension elicited by the vascular wall under the influence of hypoxia (e.g. rabbit PA strips, Lloyd, 1968, Detar and Gellai, 1971, porcine PA strips, Holden and McCall, 1984, human PA strips, Hoshino *et al.*, 1988, rat PA rings, Rodman *et al.*, 1989, rat PV and PA rings, Zhao *et al.*, 1993, porcine PV and PA rings, Feletou *et al.*, 1995). The reactivity of isolated vessels to hypoxia was sometimes investigated with different techniques, such as plethysmography (Smith and Coxe, 1951). Relatively large segments (~ several mm external diameter) from proximal pulmonary vessels were normally used in these experiments and the results were found to be inconsistent (Madden and Gordon, 2004).

With the emergence of small vessel myography, it was possible to study the effect of hypoxia on small intrapulmonary vessels (below 1 mm external diameter), which are believed to contribute the greatest proportion to hypoxia-induced vasoconstriction (for discussion, see section 1.2.2). Madden *et al.* (1985) were able to show consistent and reproducible hypoxia-induced contractions in small (< 300 μm diameter) pulmonary arteries of the cat. Myography facilitated the characterisation of hypoxic contractions (Lee and Kim, 1999) and the investigation of HPV mechanisms,

including the involvement of extracellular Ca^{2+} influx (Harder *et al.*, 1985a), Ca^{2+} release from intracellular stores (Dipp *et al.*, 2001, Du *et al.*, 2005) and reactive oxygen species (Thompson *et al.*, 1998). Furthermore, it was also used to elicit HPV in pulmonary venules of guinea pigs and to demonstrate that the parenchyma surrounding the vessel wall is not required for the full expression of hypoxic contractions (Tracey *et al.*, 1989).

Myography was sometimes used in more complex setups in conjunction with other techniques, such as Ca^{2+} measurements with Ca^{2+}-sensitive fluorophores, providing an excellent tool to monitor contractile force and levels of cytoplasmic free Ca^{2+} simultaneously (Robertson *et al.*, 2003).

1.2.3.4. Role of pretone in isolated vessel experiments

In most preparations of isolated pulmonary arteries, a minimal level of agonist-induced contraction normally precedes the application of hypoxia in order to achieve a hypoxic vasoconstrictor response (Aaronson *et al.*, 2002). The role of pretone is to enhance, but not qualitatively affect the responses obtained (Dipp *et al.*, 2001). In pulmonary arteries from various species, hypoxic pressor responses were found to be more robust after preconstriction, although responses were also seen without agonist-induced pretone (e.g. cat, Madden *et al.*, 1985, sheep, Demiryurek *et al.*, 1991a, man, Demiryurek *et al.*, 1993, rabbit, Dipp *et al.*, 2001). However, when preconstriction was not used with rat tissue, pulmonary artery rings at passive resting tension contracted insignificantly or did not contract at all to hypoxia (Bennie *et al.*, 1991). The same was seen by Leach *et al.* (1994), who observed very small responses to hypoxia in rat distal pulmonary arteries in the absence of pretone.

With isolated pulmonary veins, however, significant responses to hypoxia can be evoked even in the absence of agonist-induced preconstriction (e.g. pig, Miller *et al.*, 1989, sheep, Uzun and Demiryurek, 2003).

The role of the agonist preconstrictor is the achievement of a small level of active tension and priming of vascular tissue for the hypoxic response. This could be physiologically relevant as it is thought to emulate the resting tone pulmonary vessels are subject to *in vivo* (Aaronson *et al.*, 2006). However, the exact underlying mechanisms by which pretone enhances or makes HPV possible is not entirely understood (Ward and Aaronson, 1999, Aaronson *et al.*, 2006), but may be linked to depolarisation (Turner and Kozlowski, 1997) or release of Ca^{2+} from intracellular stores (Gelband and Gelband, 1997).

One of the agonists most commonly used to induce preconstriction is $PGF_{2\alpha}$ in concentrations of 1 μM (Dipp *et al.*, 2001), 3 μM (Robertson *et al.*, 1995, Robertson *et al.*, 2001), 5 μM (Thompson *et al.*, 1998) or as much as 10 μM (Leach *et al.*, 1994, Rogers *et al.*, 1997). Ozaki *et al.* (1998) assessed systematically the dependence of the hypoxic response on pretone in pulmonary arteries isolated from rat lungs. They found the largest hypoxic contractions when pretone was induced using EC_{25} and EC_{50} of $PGF_{2\alpha}$ (for small pulmonary arteries, these were 0.27 and 1.01 μM respectively).

Other types of agonists that have been used with success include α-adrenoreceptor agonists, high extracellular $[K^+]$ induced depolarisation, angiotensin II, thromboxane analogues and 5-HT (Rodman *et al.*, 1989, Bennie *et al.*, 1991, Demiryurek *et al.*, 1991a, Uzun *et al.*, 1998, Karamsetty *et al.*, 2002).

1.2.3.5. Studies on smooth muscle cells

Murray *et al.* (1990) showed for the first time that hypoxia contracts pulmonary vascular smooth muscle directly. They cultured smooth muscle cells from foetal bovine pulmonary arteries on a flexible growth surface and found that exposing the cells to hypoxia (Po_2 ~ 25 mm Hg) caused wrinkles and distortions to appear on the growth surface. The contractions were confirmed by detecting an increase of 45% in the level of phosphorylated MLC in response to hypoxia.

Non-dedifferentiated smooth muscle cells isolated from small intrapulmonary arteries of the cat were also shown to contract significantly to hypoxia (Madden *et al.*, 1992). The greatest proportion of shortening was found in smooth muscle cells from arteries with diameters between 200 and 600 μm. In equivalent cells that were primary cultured, the level of cytoplasmic free Ca^{2+} increased by 64% during hypoxia (Vadula *et al.*, 1993).

These experiments demonstrated undeniably that pulmonary vascular smooth muscle cells are not only the effector in hypoxic pulmonary vasoconstriction, but are also able to sense low O_2 and initiate HPV without the need for any intermediary mediator.

In further studies on smooth muscle cells, the effects of lowering Po_2 on membrane potential and whole cell currents were studied using patch-clamping techniques. Hypoxia was found to block potassium currents and significantly depolarise the membrane potential of fresh enzymatically dispersed canine pulmonary artery smooth muscle cells (PASMC) (Post *et al.*, 1992) and of primary cultured PASMC from the rat (Yuan *et al.*, 1993a).

Through the use of selective pharmacological agents in patch-clamping studies and backing by immunohistochemistry, the susceptibility to low O_2 was attributed to particular subtypes of voltage-gated K^+ channels (K_V) channels in rat PASMC (Patel *et al.*, 1997, Archer *et al.*, 1998).

1.2.3.6. Other experimental models

A number of other experimental approaches arose from the need to measure *in vivo* hypoxic constrictions in small pulmonary vessels that are difficult to reach via intraluminal catheterisation. The opportunity to achieve this was provided by imaging techniques such as standard contrast angiography (Hirschman and Boucek, 1963, Shirai *et al.*, 1986), videomicroscopy coupled to a computerized image-

enhancement system (Hillier *et al.*, 1997) or real-time confocal laser scanning luminescence microscopy (Yamaguchi *et al.*, 1998).

Another innovative technique was used by Kato and Staub (1966) who froze cat lungs during expression of HPV, which they sectioned in order to measure the diameters of distal pulmonary arteries. Similarly, Glazier and Murray (1971) used frozen dog lungs to evaluate changes in vascular tone by measuring the pulmonary capillary red blood cell concentration.

More recently, HPV mechanisms were studied using transgenic animal models. Archer *et al.* (2001) employed gene targeting to create functional knockout mice for a subtype of K_V channels and showed blunted hypoxic responses in the engineered animals.

1.3. Effector mechanisms of acute HPV

Since HPV was first reported, the link between the decrease of alveolar Po_2 and the development of tension in the pulmonary vascular wall has been much investigated (reviewed in Dumas *et al.*, 1999, Archer and Michelakis, 2002, Moudgil *et al.*, 2005, Aaronson *et al.*, 2006) and the substantial evidence accumulated has led to a significant overall increase in the understanding of HPV mechanisms.

The hypotheses that HPV could be mediated through the autonomic nervous system or through a systemically-released circulating vasoactive substance were disproved relatively early. Since HPV was demonstrated in isolated lungs and vessels, any theory involving systemic factors could be safely ruled out (Fishman, 1976). The subsequent efforts to uncover the mechanisms of HPV were thus focused on two main directions, illustrated by the question raised more than 30 years ago (Fishman, 1976) of whether the hypoxic pressor response develops through chemical mediators released or activated in the lung or through direct action of hypoxia on the vascular smooth muscle in the pulmonary circulation.

Multiple pathways have been identified to induce contraction by contributing to the rise of intracellular levels of free Ca^{2+} during the hypoxic response (McMurtry et al., 1976, Gelband and Gelband, 1997, Wang et al., 2005a) and additional contractile mechanisms not requiring an increase of cytosolic Ca^{2+} have been found to play a role during sustained HPV (Robertson *et al.*, 1995). Despite these advances, HPV still remains an incompletely elucidated physiological mechanism. Moreover, although a significant proportion of the overall HPV response occurs in the pulmonary veins (Gao and Raj, 2005b), relatively little is known about venous specific mechanisms during HPV.

1.3.1. Mediators in HPV

If a chemical mediator was central to HPV, it would have to be synthesised and released, or merely activated, in the lungs in response to hypoxia and then act to constrict vascular smooth muscle (Fishman, 1976). Such a mechanism would provide a simple explanation to the dilemma of opposing vasoactive actions of hypoxia on pulmonary and systemic vessels.

The search for a mediator that could be responsible for inducing HPV focused on several vasoactive substances (Dumas *et al.*, 1999). The main potential source of release of such mediators was thought to be represented by the endothelial cells (Holden and McCall, 1984, Kovitz *et al.*, 1993), but cells in the lung parenchyma were also considered for this role (Lloyd, 1968).

1.3.1.1. Role of endothelium

The endothelium is an important source of vasoactive factors in blood vessels. Endothelium-derived vasoconstrictors and vasodilators contribute to vascular tone regulation and affect vascular resistance in the pulmonary circulation.

Investigations into the role of the endothelium in HPV have generated contradictory results. Isolated smooth muscle cells and isolated vessels without endothelium

contract when exposed to low O_2 (Madden *et al.*, 1992, Marshall and Marshall, 1992), suggesting the endothelium is not required for the expression of HPV. However, Ward and Aaronson (1999) made the case that, in these experiments, very short exposures to hypoxia were used, and the observations made only account for the transient hypoxic response and not for the longer, more physiologically relevant, phase. In studies which looked at sustained hypoxic vasoconstriction (> 20 minutes), the evidence suggests the presence of the endothelium is required for the development of full hypoxic vasoconstriction in pulmonary arteries from several species (e.g. man, Demiryurek *et al.*, 1993, dog, Hoshino *et al.*, 1994, rabbit, Dipp *et al.*, 2001). In the pulmonary veins, the dependence of hypoxic responses on the endothelium was found to be less than in arteries (Feletou *et al.*, 1995).

1.3.1.2. Endothelin-1

The endothelium-derived vasoconstrictor peptide endothelin-1 has been linked to the role of HPV mediator, but the evidence remains inconclusive. The hypoxic response of porcine PA was blocked by endothelial denudation, and restored when the vessels were primed with 0.1 nM ET-1 (Liu *et al.*, 2001), suggesting a basal level of ET-1 was required for the full expression of HPV. However, acute hypoxia increased (Oparil *et al.*, 1995), did not change (Willette *et al.*, 1997) or decreased (Medbo *et al.*, 1998) ET-1 levels. Even in studies where a rise in ET-1 was detected during hypoxia, the increase occurred at a very slow rate suggesting ET-1 may participate, but not hold a primary role in HPV (Takeda *et al.*, 1997). Selective ET_A receptor and non-selective ET_A/ET_B receptor blockade inhibited HPV, but this effect was prevented by the addition of angiotensin II as a costimulator (Sato *et al.*, 2000). These findings suggest that the effect of ET-1 on HPV is a generic priming role, the same as seen with other agonists (Aaronson *et al.*, 2002).

1.3.1.3. Nitric oxide

Alternatively, the hypoxic constrictor response could also develop through decreased release of vasodilator agents from the endothelium. EDNO is the most potent endothelium-derived relaxing factor, with an important role in the regulation of vessel tone and vascular resistance. In the pulmonary circulation, synthesis of EDNO is reduced during hypoxia (Le Cras and McMurtry, 2001) and it has been suggested that this could be the underlying mechanism of HPV (Rodman *et al.*, 1990). However, suppression of NO synthesis does not mimic the HPV response (Shirai *et al.*, 1997) and NO does not contribute significantly to pulmonary vascular resistance (PVR) during normoxia as would be expected if its inhibition was involved in the hypoxic response (Hasunuma *et al.*, 1991, Leach *et al.*, 1994). These and other inconsistent findings (reviewed in Aaronson *et al.*, 2002) imply that EDNO is improbable to have a central role in HPV.

1.3.1.4. Cyclooxygenase and lipooxygenase products

The vasoactive products of the cyclooxygenase pathway have also been considered as possible HPV mediators. In canine isolated pulmonary arteries, HPV was inhibited by cyclooxygenase inhibitor indomethacin and a thromboxane A_2/prostaglandin H_2 receptor antagonist (Hoshino *et al.*, 1994) suggesting an involvement of vasoconstricting prostanoids, but these findings failed to find support in other studies (Leach *et al.*, 1994, Liu *et al.*, 2001). A different mechanism, involving hypoxia-induced inhibition of the release of vasodilator prostacyclin (PGI_2), was also suggested. Experiments with sheep and human pulmonary arteries, indicated that HPV was, at least in part, due to the inhibition of a vasodilator prostanoid (Demiryurek *et al.*, 1991b, Demiryurek *et al.*, 1993). Conversely, as most other studies did not find that inhibition of the cyclooxygenase pathway abolishes HPV (Aaronson *et al.*, 2002), prostanoids are believed to be only modulators of the hypoxic response.

A role for leukotrienes in HPV was suggested in the rat, as leukotriene C_4 (LTC_4) induced a pressor response and leukotriene blockers inhibited HPV (Morganroth *et al.*, 1984). Other studies did not confirm this proposition, LTC_4 was rejected as an HPV mediator in the ferret (Tseng *et al.*, 1990) and rat (Davidson *et al.*, 1990) and the participation of the lipooxygenase pathway was also excluded in rabbit lungs (Weissmann *et al.*, 1998).

1.3.1.5. Other mediators

Other vasoactive substances that have been put forward as HPV mediators include angiotensin II (Berkov, 1974), adenosine (Thomas and Marshall, 1993), histamine, 5-HT and PAF (Wadsworth, 1994). Whilst these vasoactive agents modulate vascular tone and resistance in the lungs, there is not enough current evidence to support their role as HPV chemical mediators according to the criteria set by Fishman (1976).

1.3.2. Intrinsic mechanisms

With the observation of hypoxia-induced contractions in isolated pulmonary arterial smooth muscle cells from cows and cats (Murray *et al.*, 1990, Madden *et al.*, 1992), the balance of evidence tipped in favour of the concept that hypoxic pulmonary vasoconstriction is fundamentally an intrinsic property of smooth muscle cells. Thus, any locally synthesised or circulating vasoactive substance that may be influencing HPV is now considered merely a modulator, its role being not to initiate, but rather to shape the hypoxic response (Douglas *et al.*, 1993, Dumas *et al.*, 1999).

In the pulmonary artery, hypoxia causes membrane depolarisation, raises the level of cytosolic free Ca^{2+} and induces an increase in vascular tone. Harder *et al.* (1985b) used electrophysiological recordings with glass microelectrodes to show hypoxia-induced membrane depolarisation and generation of action potentials in small pulmonary arteries from the cat and suggested that reduced Po_2 directly affected ion

conductances in the plasma membrane of smooth muscle cells. In cultured PASMC from foetal lambs (Cornfield *et al.*, 1993) and rats (Salvaterra and Goldman, 1993), acute hypoxia induced a reversible rise in the intracellular concentration of Ca^{2+}, which was partially dependent on both release of Ca^{2+} from SR stores and entry of extracellular Ca^{2+}.

Most investigators currently agree that the full expression of HPV requires the added participation of multiple interconnected cellular mechanisms (see Figure 1.4), however the identity of the initial event still raises much debate (Ward and Aaronson, 1999, Moudgil *et al.*, 2005, Aaronson *et al.*, 2006). Post *et al*. (1992) and Yuan *et al*. (1993a) found strong evidence that hypoxia causes direct inhibition of K^+ channels in the plasma membrane of smooth muscle cells and proposed that this is the primary key event of the hypoxic response. Other studies support an initial role for Ca^{2+} release from intracellular stores (Jabr *et al.*, 1997, Liu *et al.*, 2001, Dipp *et al.*, 2001) with subsequent activation of capacitative Ca^{2+} entry (CCE). During prolonged hypoxia, other mechanisms intervene, such as Ca^{2+} sensitisation of the contractile apparatus, which permits an increase in contractile force without a concomitant rise in the intracellular free calcium concentration ($[Ca^{2+}]_i$) (Robertson *et al.*, 1995, Robertson *et al.*, 2003).

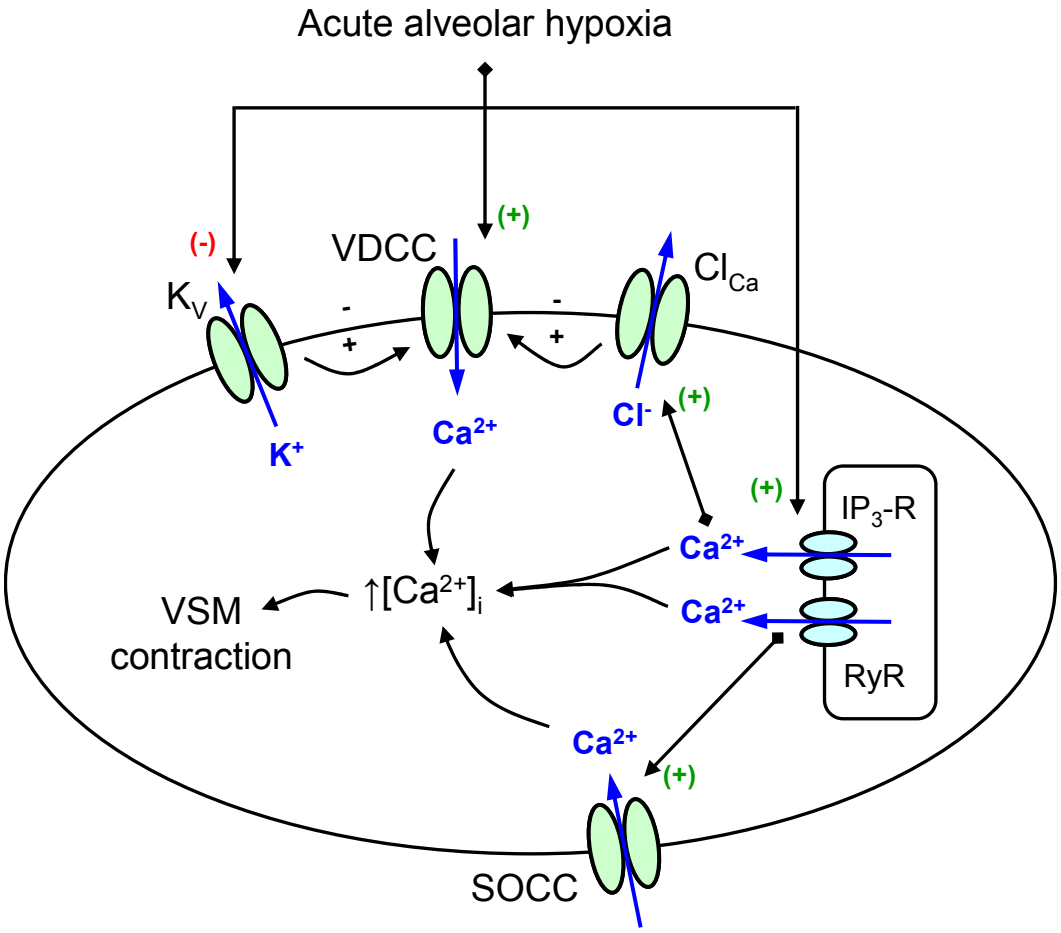

Figure 1.4. Role of ion channels in HPV signalling in PASMC.

Multiple ion channels participate in the signalling pathways involved in the hypoxic response in pulmonary arteries, the mechanisms are discussed in the text.

K_V, voltage-activated K^+ channels, VGCC, voltage-activated Ca^{2+} channels, Cl_{Ca}, Ca^{2+}-activated Cl^- channels; IP_3-R, inositol-1,4,5-triphosphate receptors, RyR, ryanodine receptors, SOCC, store-operated Ca^{2+} channels.

1.3.3. Hypoxic inhibition of K^+ channels

The most established hypothesis for the initiation of HPV involves the hypoxic inhibition of O_2-sensitive K_V channels in the plasma membrane of pulmonary vascular smooth muscle cells (Archer and Michelakis, 2002, Moudgil *et al.*, 2005). This primary event is thought to trigger an activation cascade with subsequent membrane depolarisation and rise of cytoplasmic Ca^{2+} by way of Ca^{2+} influx through voltage-gated Ca^{2+} channels (VGCC).

1.3.3.1. Effect of hypoxia on $I_{K(V)}$

The first direct evidence that hypoxia reduces whole-cell K^+ currents was provided by Post *et al*. (1992) in canine pulmonary artery smooth muscle cells. Using fresh smooth muscle cells enzymatically dispersed from second and third branches of pulmonary arteries of dogs, they showed that lowering the Po_2 from 130 mm Hg to 40 mm Hg depolarised the membrane and inhibited outward K^+ currents elicited through voltage step and ramp depolarisations. The Ca^{2+} channel antagonist nisoldipine, as well as chelation of $[Ca^{2+}]_i$ with BAPTA abolished the hypoxic inhibition of K^+ currents, which was interpreted as indirect evidence that the hypoxia sensitive current was carried through Ca^{2+}-activated K^+ (K_{Ca}) channels. In the same study, hypoxic responses in isolated lung preparations and isolated vessels were mimicked by blockers of K^+ channels. Finally, the inhibitory effect of hypoxia on K^+ channels was not present in myocytes isolated from canine renal artery, showing it is probably unique to smooth muscle cells (SMC) in the pulmonary vasculature, as is HPV itself.

The hypoxic inhibition of K^+ channels was confirmed shortly thereafter in cultured rat pulmonary arterial smooth muscle cells (Yuan *et al.*, 1993a), but the new evidence implied that specifically voltage-gated K^+ channels (K_V) and not K_{Ca} are the type of K^+ channels that is sensitive to hypoxia. Under experimental conditions preventing K_{Ca} activation (i.e. Ca^{2+} free media and Ca^{2+} chelator EGTA present both in the intracellular and extracellular solutions), hypoxia (average Po_2 = 44 Torr)

inhibited the outward voltage-activated K^+ ($I_{K(V)}$) current by approximately 60%. The activation potential of the O_2-sensitive steady-state current was -52 mV, while the resting membrane potential (RMP) was -41 mV, suggesting a proportion of the respective channels were contributing to RMP and their inhibition by hypoxia could trigger hypoxia-induced depolarisation. The role of K_V channels in HPV was confirmed in further studies (Post et al., 1995, Archer et al., 1996).

The O_2-sensitive $I_{K(V)}$ current has been described as slowly inactivating, carried through a delayed rectifier channel (Post *et al.*, 1995, Archer *et al.*, 2000). Pharmacologically, it was found to be sensitive to voltage-activated potassium channel blocker 4-AP, but not to the Ca^{2+}-activated K^+ antagonist charybdotoxin (Archer et al., 2000).

1.3.3.2. Molecular identity of O_2-sensitive K_V channels

The search for the molecular identity of the K_V channel acting as a hypoxic sensor resulted in several subtypes of K_V channels being proposed as candidates for the role of O_2-sensitive K_V in PASMC.

Archer *et al.* (1998) investigated hypoxia sensitive channels in rat pulmonary arteries. Based on the previously reported pharmacological and electrophysiological properties of O_2-sensitive K_V, they selected the Kv2.1 and Kv1.5 channel subtypes as potential candidates. Using specific antibodies, they showed that these channels are expressed in rat PASMC and contribute to the whole-cell potassium current. Moreover, anti-Kv2.1 induced depolarisation and contraction of PA rings, while anti-Kv1.5 inhibited the increase in $[Ca^{2+}]_i$ and contraction during hypoxia. These findings prompted the authors to suggest an involvement of these subtypes in a two step mechanism of HPV initiation, whereby hypoxia initially inhibits only Kv2.1, the resulting depolarisation activates Kv1.5 which is then further inhibited by hypoxia augmenting the HPV response.

More evidence to support the involvement of these two subtypes in HPV emerged later. Using a functional knockout mouse model, Archer *et al.* (2001) demonstrated diminished hypoxic vasoconstriction in Kv1.5 deficient animals. In rat PASMC, Patel *et al.* (1997) described a novel hypoxia-sensitive heteromer composed of the Kv2.1 α-subunit and the Kv9.3 β regulatory subunit. The Kv2.1/Kv9.3 channel is a delayed rectifier active at resting membrane potential, making it a suitable O_2-sensitive K_V channel candidate. In another study, hypoxia inhibited Kv1.2 and Kv2.1, but not Kv1.5 homomers transfected into a mouse L-cell line (Hulme *et al.*, 1999). However, co-expression of Kv1.2/Kv1.5 resulted in a hypoxia-sensitive channel active at resting membrane potential, as was the Kv2.1/Kv9.3 heteromer. Furthermore, in native rat PASMC, ablation of the Kv2.1 subtype with anti-Kv2.1 antibody prevented the inhibition of $I_{K(V)}$ by hypoxia (Hogg *et al.*, 2002) and in a heterogeneous population of rat PASMC the expression of the Kv1.5 subtype was correlated with the hypoxia sensitivity of the cells (Platoshyn *et al.*, 2007).

1.3.4. Ca^{2+} in HPV

As in all types of muscle cells, the cytoplasmic concentration of free Ca^{2+} is the main determinant of smooth muscle contraction. At any time, the level of $[Ca^{2+}]_i$ is achieved through the dynamic equilibrium of Ca^{2+} movement between the cytoplasmic compartment and the extracellular environment and intracellular Ca^{2+} stores, respectively (Karaki *et al.*, 1997).

In the pulmonary arterial smooth muscle, hypoxia induces a rise in intracellular free Ca^{2+} (Vadula *et al.*, 1993), which is due to both influx of extracellular Ca^{2+} (Cornfield et al., 1994) and release from intracellular Ca^{2+} stores (Gelband and Gelband, 1997).

1.3.4.1. Ca^{2+} entry

In smooth muscle cells, voltage-gated Ca^{2+} channels (VGCC) provide the main path for Ca^{2+} entry through the predominant subgroup of L-type Ca^{2+} channels. They are activated by depolarisation, blocked by dihydropyridines and are present in a lesser density in the veins compared to the arteries (Walker, 1995).

During HPV, Ca^{2+} enters smooth muscle cells through VGCC. The hypoxic response in rat lungs was inhibited by VGCC blocker verapamil (McMurtry et al., 1976) and enhanced by VGCC agonist BAY K 8644 (McMurtry, 1985).

In other studies, VGCC block resulted only in a decrease of HPV, suggesting influx through VGCC is not the only source of cytoplasmic Ca^{2+}. The hypoxic responses of human pulmonary arterial strips were attenuated, but not abolished by VGCC antagonists nifedipinde, nicardipine and by the removal of extracellular Ca^{2+} (Hoshino *et al.*, 1988). HPV was also only partial inhibited by verapamil in human pulmonary arteries (Ohe *et al.*, 1992).

However, in sheep pulmonary artery rings, verapamil had no effect on the HPV response with or without preconstriction (Demiryurek *et al.*, 1993). Similarly, in rat intrapulmonary arteries, VGCC antagonists did not affect the sustained phase of HPV and partially inhibited the transient phase (Robertson et al., 2000b), suggesting depolarisation-mediated Ca^{2+} entry is not prevalent and an alternative, voltage independent Ca^{2+} influx pathway may contribute to HPV.

In addition, there is evidence that hypoxia promotes Ca^{2+} channel activity not only indirectly through depolarisation-induced activation of VGCC. In rabbit PASMC isolated from distal arteries, Franco-Obregon and Lopez-Barneo (1996a) observed hypoxia-induced potentiation of the amplitude of Ca^{2+} currents. In PASMC from larger, conduit arteries the effect was opposite, and there were also differences in Ca^{2+} channel density between the two types of cell.

1.3.4.2. Ca^{2+} release and capacitive entry

In human pulmonary arterial strips, an alternative source for the rise in $[Ca^{2+}]_i$ that occurs during HPV is the release of Ca^{2+} from intracellular stores into the cytoplasm (Hoshino et al., 1988). By depleting intracellular Ca^{2+} stores, the hypoxic pressor response in canine pulmonary arteries was significantly inhibited (Jabr et al., 1997). Ryanodine receptor (RyR) (Morio and McMurtry, 2002) and inositol 1,4,5-trisphosphate receptor (IP_3-R) (Mauban *et al.*, 2005) sensitive Ca^{2+} stores have been suggested to contribute to this mechanism, although there is some disagreement about the latter (Jin *et al.*, 1993).

Post *et al.* (1995) made a series of observations examining the role of $[Ca^{2+}]_i$ in the hypoxic inhibition of K^+ currents in canine PASMC. Hypoxia (induced with sodium dithionite) reduced K^+ currents, but this was prevented by intracellular buffering of Ca^{2+} and mimicked by caffeine. Using simultaneous measurements of $[Ca^{2+}]_i$ and membrane potential, they observed that in response to the application of hypoxia the rise in $[Ca^{2+}]_i$ preceded membrane depolarisation. The authors suggested that K^+ channel inhibition depends on Ca^{2+} release and proposed a mechanism whereby the release of Ca^{2+} from internal stores is an early event in HPV which causes inhibition of K^+ channels, membrane depolarisation and subsequent Ca^{2+} entry through voltage-gated channels.

Gelband and Gelband (1997) brought more evidence in support of this theory. In the presence of thapsigargin, cyclopiazonic acid (CPA) and ryanodine (used to deplete intracellular Ca^{2+} stores) hypoxia did not elicit any significant change in tone, $[Ca^{2+}]_i$ or membrane potential.

Furthermore, Dipp and Evans (2001) investigated the role of cyclic ADP-ribose (cADPR) in the hypoxic response in rat lungs. Their findings suggested that the release of Ca^{2+} from ryanodine-sensitive stores during sustained HPV takes place through build up of cADPR and proposed that this event may represent a primary trigger in HPV.

However, the possibility that the initial Ca^{2+} release activates a different pathway, not involving voltage-gated channels, has also been raised. Capacitative Ca^{2+} entry (CCE), which is activated by depletion of SR Ca^{2+} stores (Putney *et al.*, 2001) was considered a candidate. In a series of experiments on canine PASMC, Ng *et al.* (2005) showed that dihydropyridine insensitive influx of Ca^{2+}, probably CCE, plays a role in HPV. In rat PASMC, store-operated Ca^{2+} channels (SOCC) mediate CCE during acute hypoxia (Wang *et al.*, 2005a). CCE was also shown to be present in canine PVSMC and changes in CCE induced by intravenous anaesthetics were mediated by tyrosine kinase (Shimizu *et al.*, 2006).

1.3.4.3. Ca^{2+}-activated Cl^- channels

An alternative mechanism that promotes vasoconstriction in vascular smooth muscle involves Ca^{2+}-activated Cl^- channels (Cl_{Ca}) (Large and Wang, 1996). As the name suggests, Cl_{Ca} channels are activated by an increase in $[Ca^{2+}]_i$. Subsequently, the movement of Cl^- ions follows the electrical gradient, and opposes the concentration gradient, resulting in a net efflux which induces membrane depolarisation and thus amplifies the increase in $[Ca^{2+}]_i$ by activating VGCC.

In rat aorta, Cl^- currents contribute significantly to the contractile response to norepinephrine (Lamb and Barna, 1998). Cl_{Ca} were also shown to be present in smooth muscle cells from rat pulmonary arteries (Yuan, 1997). In this study, inward Ca^{2+}-activated Cl^- currents ($I_{Cl(Ca)}$) in PASMC were activated by Ca^{2+} released from IP_3-sensitive stores by CPA, as well as by depolarisation-induced Ca^{2+} entry. These findings suggest that Cl_{Ca} channels contribute to agonist-induced vasoconstriction in pulmonary arteries, and may also be activated by the increase in cytoplasmic free Ca^{2+} induced by acute hypoxia.

Furthermore, during chronic hypoxia, a positive feedback mechanism involving Cl_{Ca} channels contributes to increased levels of cytosolic Ca^{2+} in the development of pulmonary hypertension (Yang *et al.*, 2006). Moreover, Cl_{Ca} channel blockers were

found to reduce the proliferation of rat PASMC under conditions of chronic hypoxia (Yang *et al.*, 2008).

1.3.5. Role of sensitisation

Agonists contract vascular smooth muscle by rising free cytoplasmic Ca^{2+}, as well as through increasing the sensitivity of contractile myofilaments to Ca^{2+} (Himpens *et al.*, 1988). While the former acts to induce contraction through Ca^{2+}/calmodulin activation of myosin light chain kinase (MLCK) and phosphorylation of MLC, the latter involves reducing myosin light chain phosphatase (MLCP) activity and thus diminishing its inhibitory role on VSM contraction (Somlyo and Somlyo, 1993).

The relation between $[Ca^{2+}]_i$ and hypoxia-induced contractile force was investigated for the first time in an HPV study, in which recording of isometric tension in a small vessel myograph was made concomitant to fluorescence measurements using ratiometric intracellular Ca^{2+} indicators. Robertson *et al.* (1995) used this technique on isolated intrapulmonary arteries of the rat. During the first transient phase of HPV, the increase in contractile force was accompanied by a simultaneous rise in $[Ca^{2+}]_i$. However, the second phase was different, in that the sustained increase in tension was not matched by an elevation of $[Ca^{2+}]_i$, which remained constant throughout. These observations showed that Ca^{2+} sensitisation is involved in the HPV response.

Several regulatory intracellular protein kinases have been suggested to participate in the sensitisation process during hypoxic contractions of pulmonary vessels (reviewed in Ward et al., 2004), but some of the reported findings are difficult to interpret due to the non-specificity of pharmacological agents used (Robertson and McMurtry, 2004).

1.3.5.1. Protein kinase C

In rat pulmonary arteries (Jin *et al.*, 1992) and isolated perfused rat (Orton et al., 1990), rabbit (Weissmann et al., 1999) and dog lungs (Barman, 2001), the sustained hypoxic vasoconstriction was dependent on activation of protein kinase C (PKC). Conversely, in other studies Ca^{2+} sensitisation during hypoxia in rat pulmonary arteries was shown to be PKC-independent (Robertson *et al.*, 1995). However, the presumed PKC inhibitors used in these studies have been shown not to be selective blockers of PKC (Davies et al., 2000).

The emergence of more targeted approaches has resulted in new relevant evidence in this field. Knockout mice with a deletion of the gene for the PKC-ε isoform had blunted hypoxic responses compared to wild type mice (Littler *et al.*, 2003). Using novel specific inhibitors and gene deletion, Rathore *et al.* (2006, 2008) demonstrated the involvement of PKC-ε in the hypoxia-triggered signalling cascade leading to the rise of $[Ca^{2+}]_i$ and contraction in mouse PASMC. However, the inhibition of classical PKC isoforms (α and β1) failed to affect the hypoxic response in rat pulmonary artery rings (Tsai et al., 2007).

1.3.5.2. Protein tyrosine kinases

Protein tyrosine kinases (PTK), reported to modulate Ca^{2+} sensitivity in smooth muscle (Steusloff et al., 1995), were also found to be involved in HPV. In the presence of PTK inhibitors genistein and tyrphostin, pulmonary artery rings did not contract to hypoxia, but contracted to 5-HT (Uzun *et al.*, 1998).

Similarly, pulmonary venous hypoxic responses, with or without preconstriction, were inhibited by genistein and tyrphostin and enhanced by the PTK activator sodium orthovanadate (Uzun and Demiryurek, 2003).

1.3.5.3. Rho-kinase

In vascular smooth muscle, Rho-kinases (ROK) have been recognized to contribute to agonist-induced Ca^{2+} sensitisation (Somlyo and Somlyo, 2000). Once activated by the GTP-bound RhoA, ROK phosphorylates MLCP thereby inactivating it.

The ROK blocker Y-27632 caused a concentration-dependent inhibition of sustained hypoxic responses in rat intrapulmonary arteries and isolated perfused lungs (Robertson et al., 2000a).

Following exposure to hypoxia, ROK activity and MLC phosphorylation were increased in cultured PASMC (Wang et al., 2001). Y-27632, C3 (specific Rho inhibitor) and toxin B (inhibitor of Rho proteins) reduced MLC phosphorylation during hypoxia, while ROK activation by hypoxia was diminished by C3 and toxin B. These findings strongly suggest a role for the Rho/Rho-kinase pathway in Ca^{2+} sensitisation during sustained HPV.

1.3.5.4. p38 mitogen-activated kinase

Mitogen-activated protein (MAP) kinases are another family of kinases expressed in smooth muscle cells, that participate in the regulation of cellular differentiation, proliferation and contraction (Robertson and McMurtry, 2004).

A member of this family, p38 MAP kinase, has been reported to be involved in sustained HPV in rat pulmonary arteries (Karamsetty et al., 2002). In this study, acute hypoxia enhanced the phosphorylation of p38 MAP kinase. Inhibition of p38 MAP kinase with SB-202190 abolished only the sustained phase of HPV, while activating p38 MAP kinase with anisomycin potentiated both phases of the hypoxic response.

1.4. Role of veins in pulmonary disease

1.4.1. Pulmonary oedema

Acute pulmonary oedema is a clinical emergency which involves the extravasation of fluid from the pulmonary capillaries into the interstitial space and the alveoli. The main known mechanisms that contribute to oedema formation are (i) reversal of physiological Starling forces through elevated capillary hydrostatic pressure or low plasma oncotic pressure, (ii) damage to the alveolar-capillary barrier and (iii) insufficiency of the lymphatic drainage system (Sovari, 2008).

During oedema formation, post-capillary venoconstriction by raising upstream microvascular hydrostatic pressures may contribute to fluid filtration and increased extravascular lung water (Dauber and Weil, 1983). Pulmonary venous constriction has been implicated in pulmonary oedema due to congestive heart failure (Burkhoff and Tyberg, 1993), neurogenic causes (Smith and Matthay, 1997), narcotic abuse (Hakim *et al.*, 1992), high-altitude (Maggiorini *et al.*, 2001), endotoxins (Pearl *et al.*, 1992), anaphylaxis (Shibamoto *et al.*, 1992), lung injury (Dauber and Weil, 1983), as well as in oedema induced experimentally by administration of thromboxane (Yoshimura et al., 1989) and ET-1 (Rodman et al., 1992).

1.4.1.1. High altitude pulmonary oedema

One particular type of oedema that affects non-acclimatised healthy individuals in the first days after rapid ascents to altitudes above 3,000 m is high altitude pulmonary oedema (HAPO) (Bartsch *et al.*, 2005). Although some early reports excluded contributions of the veins in HAPO (Hultgren *et al.*, 1964), others speculated that increased vasomotor activity in the small veins could play a central role (Fred *et al.*, 1962). Wagenvoort and Wagenvoort (1982) later provided morphological evidence in support of this theory by showing venous hypertrophy in high-altitude residents, which they presumed to be due to chronic hypoxic

venoconstriction. More recently, it was shown that the causes of HAPO are non-cardiogenic (Bartsch *et al.*, 2005) and not due to inflammation-induced increased permeability in the pulmonary capillaries (Kleger *et al.*, 1996, Swenson *et al.*, 2002). The underlying mechanism appears to be entirely hydrostatic through increased pulmonary capillary pressure, with a contribution from hypoxic constriction of small pulmonary vessels including venules (Maggiorini *et al.*, 2001).

1.4.1.2. Lung injury oedema

Increased pulmonary microvascular pressure contributes to the formation of oedema during acute lung injury (ALI)/adult respiratory distress syndrome (ARDS) (Matthay and Zimmerman, 2005).

In chloralose-anesthetized dogs, Dauber and Weil (1983) induced lung injury pulmonary oedema using oleic acid. They reported an increase in the pressure in small pulmonary veins from 9.8 to 12.6 mm Hg which increased upstream microvascular hydrostatic pressures and fluid filtration. Venoconstriction was also the main contributor to the increase in capillary pressure during oedema due to anaphylaxis induced by an intra-arterial injection of *Ascaris suum* antigen in isolated canine lungs (Shibamoto *et al.*, 1992). In isolated perfused rat lungs, oedema formation induced by protamine (a cationic protein associated with pulmonary endothelial injury) was enhanced by PAF receptor dependent venoconstriction and mechanically increased pulmonary venous pressure (Chen *et al.*, 1990).

The administration of endotoxin from Escherichia coli in cats and dogs (intact animals and isolated perfused lungs) induced pulmonary vasoconstriction predominantly in the small veins and/or venules (Kuida *et al.*, 1958). In anaesthetized sheep, venous resistance rose more than arterial resistance during the early stages of acute pulmonary hypertension induced by infusion of E. coli endotoxin (Pearl *et al.*, 1992).

The role of ET-1 in endotoxemic pulmonary hypertension was studied in pigs in both *in vitro* and *in vivo* conditions (Rossi *et al.*, 2008). In myography experiments, ET-1 constricted veins slightly more than arteries, while the ET_B receptor agonist sarafotoxin was a potent constrictor of veins but caused only small contractions in arteries. *In vivo* administration of endotoxin induced predominantly downstream haemodynamic changes. In this ALI experimental model, the dual ET-1 receptor antagonist tezosentan reversed the increases in pulmonary capillary pressure and venous resistance caused by infusion of endotoxin. It was concluded that the endothelin system plays an important part in endotoxin-induced PHT, possibly through the involvement of the ET_B receptor.

1.4.1.3. Other types of experimentally induced oedema

The haemodynamics of oedema formation have been studied by inducing oedema in experimental settings using various potent vasoconstrictors. In rat lungs perfused with physiological salt solution, the oedemagenic effect of ET-1 was mediated through venoconstriction (Rodman *et al.*, 1992). Venoconstriction was also shown to be the primary factor in pulmonary oedema induced by a thromboxane A_2 analogue in lambs (Yoshimura et al., 1989).

Researching the association between narcotic abuse and pulmonary oedema, Hakim *et al.* (1992) found that the administration of morphine in lungs of cats and dogs induced an increase in PVR mainly through pulmonary venoconstriction. This effect appeared to be mediated by the release of histamine in the lungs.

1.4.2. Hypoxic pulmonary hypertension

Chronic pulmonary hypertension (PHT) is a life-threatening condition which occurs most often secondary to chronic respiratory or cardiovascular disease. The aetiology of secondary PHT is usually multifactorial, with long-standing hypoxic pulmonary

vasoconstriction due to chronically impaired alveolar ventilation being commonly one of the contributors (Blythe et al., 1998).

Prolonged hypoxia induces structural changes in the pulmonary vasculature that may lead to PHT (Smith and Heath, 1977). Morphological studies showed that the structural changes taking place in the pulmonary vasculature during chronic hypoxia occur in both veins and arteries. In studies on human subjects affected by chronic hypoxia – either because of living at high altitude or pulmonary disease – chronic lesions of the pulmonary vasculature were found not only in arteries, as expected, but also in the veins (Wagenvoort and Wagenvoort, 1976, Wagenvoort and Wagenvoort, 1982). These changes consisted of medial hypertrophy, arterialisation and the development of longitudinal bundles of smooth muscle cells within the intima of small intrapulmonary veins. Similar observations were made in a study on hypoxic rats (Dingemans and Wagenvoort, 1978). In small intrapulmonary veins (125 - 300 μm diameter) of patients suffering from chronic bronchitis and emphysema, the proportion of wholly muscular veins was significantly increased compared to controls (Shelton et al., 1977).

The involvement of pulmonary veins is apparent from the early stages of chronic hypoxia. Sheehan *et al.* (1992) ventilated the right apical lobe of sheep with 100% N_2 for 20 hours. Following the exposure, small pulmonary veins and arteries (0.5 to 2 mm diameter) were dissected from the hypoxic lobe and another control lobe and used in contractile studies. PV rings contracted to acute hypoxia while arteries did not, and the responses in hypoxia-exposed PV were much larger than in control PV. Moreover, the sensitivity to the TxA_2 agonist U46619 increased significantly in the veins exposed to hypoxia. These findings suggest that the veins are the first to undergo changes during exposure to hypoxia, making them more responsive to contractile agonists and more likely to contribute early to potentially developing PHT.

1.4.2.1. Involvement of K^+ channels

During chronic hypoxia, vascular remodelling contributes to the progression of pulmonary hypertension. In PASMC from chronically hypoxic rats, K^+ currents were reduced by 40-50% compared to normoxic controls (Smirnov et al., 1994).

Episodes of 24-72 h of hypoxia affected the expression of specific α-subunits of K_V channels in primary cultured rat PASMC (Wang et al., 1997). The amount of mRNA and protein levels of Kv1.2 and Kv1.5 was reduced significantly, suggesting the reduced overall K_V currents may be a contributing factor in chronic hypoxic vasoconstriction.

These findings were consistent with the results of a later study by Platoshyn *et al.* (2001). Aside from decreased K_V expression, they also reported impaired K_V channel function with a reduced whole-cell K_V current, depolarised membrane potential and increased $[Ca^{2+}]_i$ in rat hypoxic PASMC. These features were not observed in mesenteric artery smooth muscle cells exposed to the same conditions. Moreover, dysfunctional K_V channels have been identified in PASMC from patients with pulmonary hypertension and are thought to play a key role in the vascular remodelling that contributes to the progression of pulmonary hypertension (Yuan et al., 1998a).

Wang *et al.* (2005b) exposed rats to hypoxia (10% O_2) for 3 weeks. Several α-subunits (Kv1.1, Kv1.5, Kv1.6, Kv2.1, and Kv4.3) were found to be downregulated in the hypoxic rats. However, there was no effect on expression of the regulatory β-subunits, which are known to confer faster inactivation properties when they associate with α-subunits (Rettig *et al.*, 1994). This finding could explain the more rapidly inactivating K_V currents seen in chronically hypoxic PASMC (Shimoda *et al.*, 1999).

Overall, these data indicate that changes in the pulmonary vasculature during hypoxia involve the altered expression and/or function of voltage-gated K^+ channels, which contribute to the development of hypoxic pulmonary hypertension.

1.4.2.2. Other mechanisms

Endothelin, which has been reported to be a more potent contractile agonist in the PV compared to the PA (Rodman et al., 1992, Toga et al., 1992), may also play a role in the development of PHT due to prolonged hypoxia. In rat lungs exposed to hypoxia for 7 or 14 days, immunohistochemical examination revealed that hypoxia upregulated the ET precursor peptide, ET-converting enzyme and ET receptors in distal pulmonary veins (Takahashi et al., 2001). These changes in the pulmonary veins are probably part of the vascular remodelling process leading to chronic hypoxic pulmonary hypertension.

During high altitude hypoxia, upregulation of PAF-R protein expression and PAF synthesis contribute to vascular remodelling in the lungs of foetal lambs and the same mechanism may participate in the development of persistent pulmonary hypertension of the neonate (PPHN) (Bixby et al., 2007). Veins are known to be more reactive to PAF than arteries. In the ferret, PAF contracted third-order pulmonary venous rings while relaxing arteries (Gao *et al.*, 1995b). Furthermore, in ovine foetal pulmonary vascular smooth muscle, PAF and hypoxia induced a higher rate of proliferation in PVSMC compared to PASMC, suggesting that, in the low oxygen environment of foetal life, increased PAF modulates PV development and the lack of down-regulation of PAF after birth may contribute to PPHN (Ibe *et al.*, 2008).

1.4.3. Non-hypoxic pulmonary hypertension

1.4.3.1. Primary pulmonary hypertension

Primary pulmonary hypertension (PPH) is an infrequent idiopathic disease, which inherently makes it a diagnosis of exclusion.

The pulmonary vasculature of 19 patients with PPH was quantitatively examined by light microscopy (Chazova et al., 1995). The small pulmonary veins (< 250 μm external diameter) of more than half of the patients had an increase in intimal and adventitial thickness (averaged at approximately twofold), although the changes were less in magnitude and frequency than in arteries.

The arterial occlusion technique was used in a study on patients with PPH with the aim of identifying the site of increased pulmonary vascular resistance (Fesler et al., 2003). The findings revealed a raised pulmonary capillary pressure, with a normal longitudinal distribution of vascular resistance, which the authors suggested could be explained by a significant contribution of veins to total increase in vascular resistance.

1.4.3.2. Pulmonary veno-occlusive disease

Approximately 5 to 25% of patients diagnosed with PPH present with extensive and diffuse occlusion of venules and small pulmonary veins, in the form of pulmonary veno-occlusive disease (PVOD) (Mandel et al., 2000). This condition can only be diagnosed definitely by surgical lung biopsy. The aetiology of PVOD is still unresolved, but it has been linked to a variety of risk factors such as infection with the human immunodeficiency virus (HIV), the Epstein-Barr virus or cytomegalovirus. Genetic factors, toxic exposures and autoimmune disorders have also been implicated. Although an uncommon condition, PVOD is important to recognise due to its poor prognosis, inefficiency of treatment with vasodilators and requirement for lung transplantation.

1.4.4. Electrical activity and role in atrial fibrillation

As early as 1876, Brunton & Fayrer published their observations that the pulmonary veins of rabbits and cats were exhibiting pulsations after all cardiac activity had stopped (Brunton and Fayrer, 1876). The independent pace-making activity in the pulmonary veins was confirmed in the 1980s by Cheung (1981a, 1981b), who was the first to use electrophysiological techniques to record action potentials in cardiomyocytes from guinea pig pulmonary veins.

The electrophysiological properties of these pulmonary vein cardiomyocytes (PVCM), although not fully characterised, are most probably distinct from those of atrial myocytes (Honjo et al., 2003, Ehrlich et al., 2003). The key distinctive feature of these cells is their ability to initiate spontaneous electrical activity and act as pacemakers to induce atrial arrhythmias (Chen et al., 1999, 2000). Moreover, the spontaneous $[Ca^{2+}]_i$ oscillations in the PVCM are affected by hypoxic conditions (Cruickshank and Drummond, 2003). These cells share the feature of lower density of inward rectifier K^+ current with the pace-making cells from the sino-atrial node (Honjo et al., 2003).

With the help of multielectrode catheter mapping, the pulmonary veins were clinically confirmed to be a major site of origin for ectopic beats that induce paroxysms of atrial fibrillation (Haissaguerre et al., 1998), and were also reported to be involved in chronic pacing-induced sustained atrial fibrillation (Wu et al., 2001). The anatomical distribution of the triggering foci as found by Haissaguerre *et al*. (1998) correlated to the histological findings that showed more extensive myocardial sleeves in the superior pulmonary veins (Chen et al., 1999, Ho et al., 2001), which possibly suggests that cells from the myocardial sleeves of the pulmonary veins are latent pacemakers, normally suppressed by sinus rhythm. Furthermore, successful treatment with radio-frequency ablation of ectopic foci in the pulmonary veins in patients with frequent and drug-resistant paroxysmal atrial fibrillation (Haissaguerre et al., 1998) supports these findings.

It has now become increasingly accepted that the pulmonary veins are an important source of arrhythmogenic activity in atrial fibrillation and that the myocardial sleeves are central to this activity (Khan, 2004, Fynn and Kalman, 2004, Melnyk et al., 2005).

Whether the PV myocardium exerts any physiologically relevant contractile activity is currently unknown. While speculations have been made about such a role in the rat (Michelakis *et al.*, 2001), the fact that in humans and most large mammals myocardial sleeves extend only to extrapulmonary sites (Nathan and Gloobe, 1970) makes a contribution of PVCM to venous tone improbable.

1.5. Aims and objectives

As reviewed in the previous sections of this chapter, considerable evidence exists that veins participate in all stages of HPV, acute and chronic. The venous response to acute hypoxia contributes to the regulation of blood flow (Gao and Raj, 2005b) and has been implicated in the progression of disease states such as pulmonary oedema (Maggiorini *et al.*, 2001). During chronic hypoxia, remodelling in the pulmonary veins contributes to pulmonary hypoxic hypertension (Wagenvoort and Wagenvoort, 1982, Sheehan *et al.*, 1992).

However, recent research in the field of HPV has largely focused on elucidating the underlying mechanisms of the arterial response to hypoxia. While some reports investigating the contractility of isolated veins exist (discussed above), studies examining the effects of hypoxia in venous smooth muscle at cellular level are not available in the literature.

The aim of the studies presented here was to investigate the contractile mechanisms of acute hypoxic vasoconstriction in porcine intrapulmonary veins. Contractile studies – using the wire myography technique – and single cell electrophysiology studies were carried out pursuing the following objectives:

- to verify whether isolated segments of small intrapulmonary veins from the pig contract in response to hypoxia, in the presence and absence of preconstriction;
- to characterise the potential venous contractile responses in relation to the responses of size-matched intrapulmonary arteries, and examine the role of specific ions during hypoxic contractions;
- to develop a cell isolation protocol in order to obtain fresh physiologically viable smooth muscle cells from small intrapulmonary veins and to examine their morphometric and passive electrical properties;

- to examine the effect of hypoxia on ion conductances in single smooth muscle cells from porcine intrapulmonary veins.

Chapter 2.
General Methods

2.1. Animal tissue

All experimental procedures were in accordance with UK legislation. Porcine tissue was used in all experiments – wire myography and cell electrophysiology studies –, having been previously reported to exhibit vigorous pulmonary vasoconstrictor responses to hypoxia (Mitzner and Sylvester, 1981, Sylvester *et al.*, 1983).

Fresh tissue was obtained daily from a local abattoir (Scotch Premier Meat Ltd, Inverurie, Aberdeenshire). Usually the heart and lungs, removed *en bloc* from adult pigs (as seen in Figure 2.1A), were delivered within 1-2 hours from kill.

Dissection was carried out immediately after receiving the tissue. Vessels were normally dissected from either the left middle or cranial pulmonary lobes (marked B and A respectively, in Figure 2.1B), as their anatomical characteristics allowed easier access to the intrapulmonary venous tree. The respective lobe was separated, placed on a dissection dish and fixed with pins (as seen in Figure 2.2, top). The pulmonary venous tree was dissected under a binocular microscope. During dissection, to maintain the viability of vessels, the tissue was regularly irrigated with cold Ca^{2+}-free dissection solution (composition in mM: 119 NaCl, 4.7 KCl, 1.18 KH_2PO_4, 1.17 $MgSO_4$, 25 $NaHCO_3$, 10 HEPES, 5.5 Glucose; pH adjusted to 7.4 with NaOH).

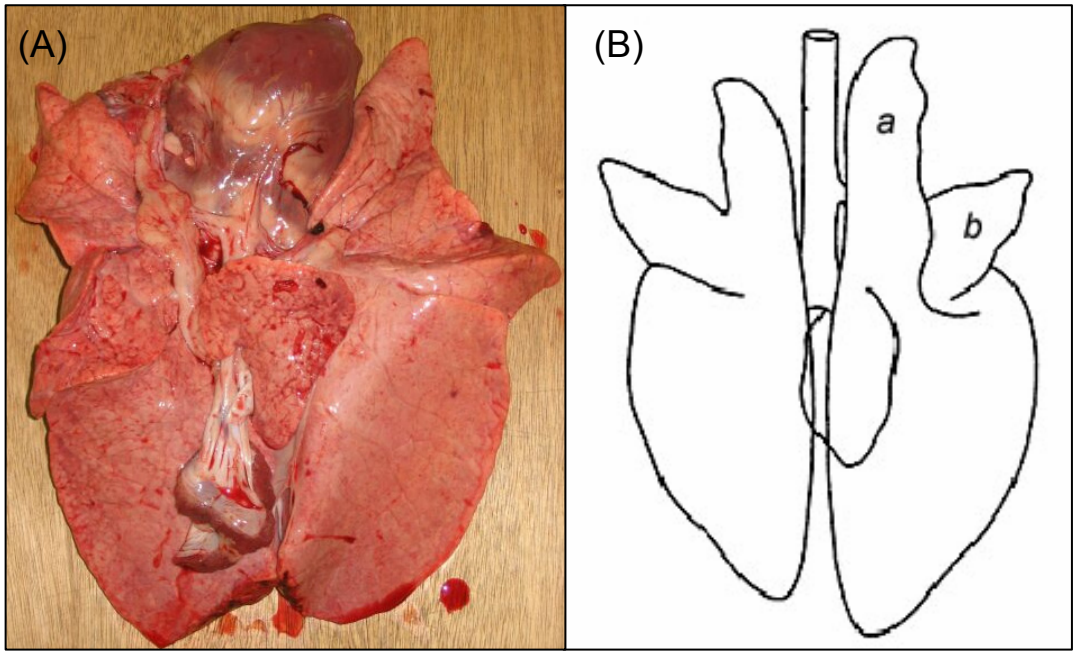

Figure 2.1. Anatomy of porcine lungs. (A) Macroscopic ventral view of porcine lungs and heart *en bloc*. (B) Drawing showing the lobes of porcine lungs, *a* and *b* indicate the left cranial and middle lobes respectively, which were usually used in experiments.

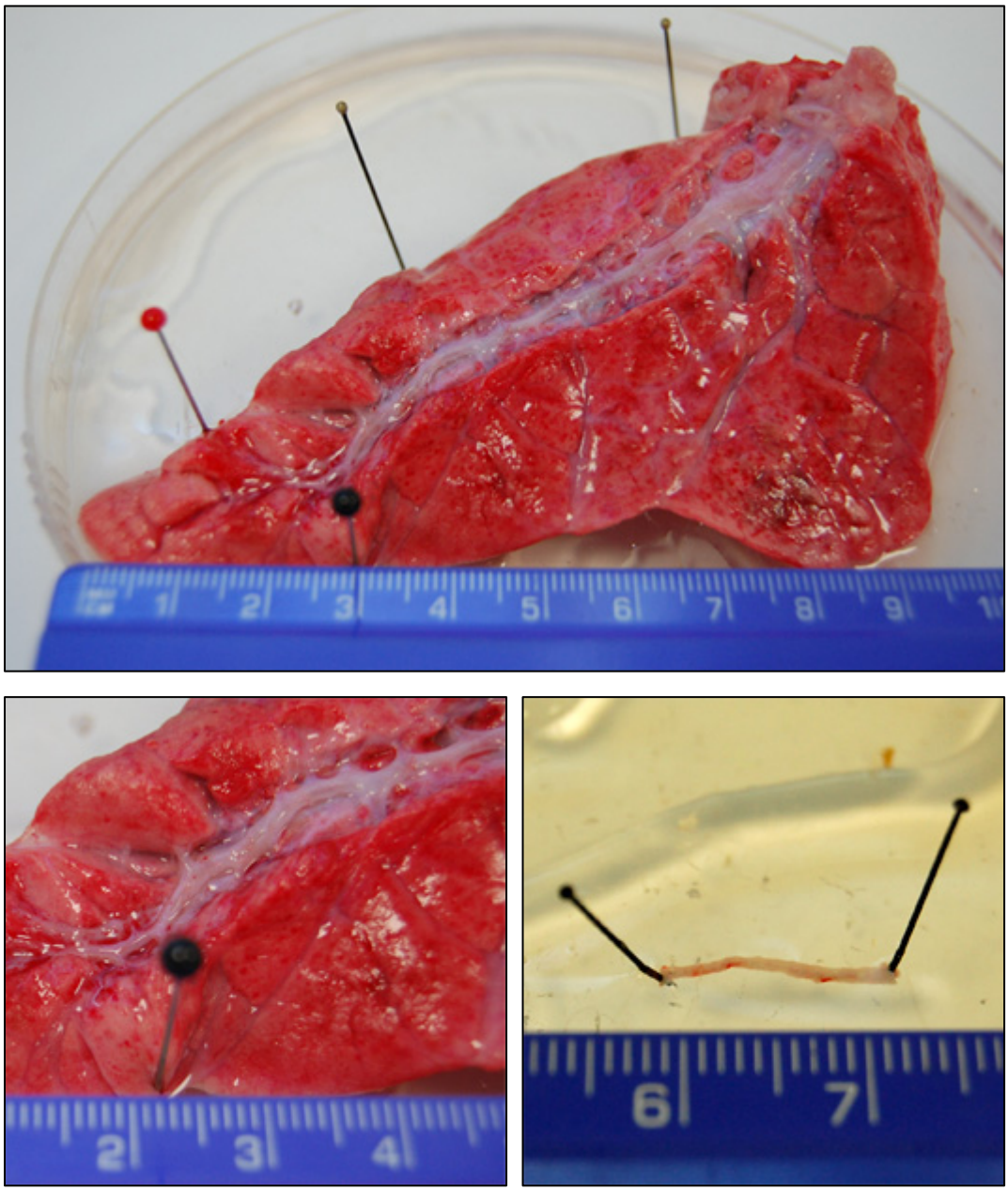

Figure 2.2. Dissection of intrapulmonary veins. (*top*) Macroscopic view of left middle pulmonary lobe. (*bottom left*) Dissection of the distal part of the intrapulmonary venous tree. (*bottom right*) Isolated segment of 7th order intrapulmonary vein; numbers on ruler represent centimetres.

Segments of the 5th to 7th order intrapulmonary vessels were dissected out and either used immediately in experiments or placed in ice-cold dissection solution for 1/2-1 hours. The outer diameter of the vessels was measured with the help of a graticule fitted into the eyepiece of the microscope.

2.2. Wire myography

Wire myography is an *in vitro* experimental technique designed by Mulvany and Halpern (1977) to investigate the contractile properties of isolated small vessels and other tubular structures with very small diameters (between approximately 60 μm and 3 mm). The technique is, in principle, similar to other methods used in contractile studies, such as the organ bath technique. It involves the measurement of isometric tension elicited by the vascular wall under fixed strain in response to various stimuli and is therefore a valuable tool for investigating the underlying mechanisms of vascular contraction.

2.2.1. Tissue preparation

Following dissection, isolated pulmonary vessels with outer diameters ranging from 300 μm to 1000 μm (mean ± SD of 610.4 ± 142.6 μm, n = 134) were cut in segments with a length of 1.5 ± 0.35 mm (mean ± SD, n = 134) and used immediately or kept in ice-cold dissection solution for 30-60 minutes.

Depending on the experimental protocol, either two venous rings or one arterial and one venous ring were mounted in the chamber of a 410A Dual Wire Myograph System (Danish Myo Technology, Aarhus, Denmark), which was connected to a PC through a PowerLab 4/25 unit (ADInstruments, UK).

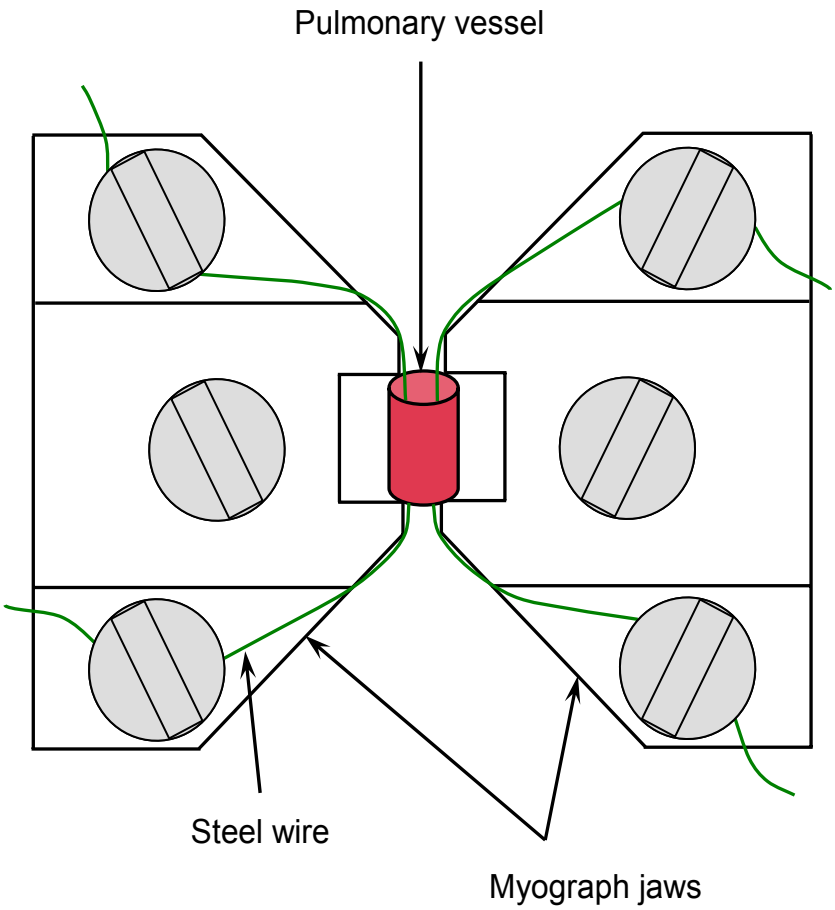

Figure 2.3. Mounting of vessels on the 410A myograph system.
Schematic drawing showing a vessel segment mounted between the jaws of the myograph using 40 µm diameter stainless steel wire. The 410 system is a dual myograph and has two such pairs of jaws.

The chamber of the myograph was temperature-controlled and was filled with HEPES-based bath solution (HBS) of the following composition: 150 mM NaCl, 5.4 mM KCl, 1.2 mM $MgCl_2$, 1.8 mM $CaCl_2$, 10 mM HEPES, 10 mM glucose (pH adjusted to 7.4 with NaOH) and gassed with air. Following the heating of the myograph bath to 37°C and calibration, the rings of pulmonary vessels were immersed in bath solution in the myograph chamber. Using fine forceps, two 40 μm diameter stainless steel wires were threaded through the lumen of each vessel and attached to the myograph jaws (see Figure 2.3).

2.2.2. Resting tone optimisation and normalisation

In order to achieve an identical passive pressure in all vessels, normalisation was performed with the help of the DMT Normalization Module integrated in the Chart software (procedure described in detail in section 3.2.1). Alternatively, in some experiments the resting tension of 2 mN (equivalent to 0.204 grams force; optimal resting tension in preliminary experiments) was used.

To account for the biological variability of responses, the tension values were expressed as percentages of the control response to 80 mM KCl of the same vessel.

2.2.3. Hypoxic challenges in myography experiments

Hypoxia (< 25 mm Hg) was achieved by gassing the bath solution directly in the myograph chamber with N_2 gas. Each hypoxic challenge lasted for 30 minutes and after every period of hypoxia the vessels were allowed to recover for at least 30 minutes in normoxia.

2.2.3.1. Monitoring O_2 saturation

During experiments, the partial pressure of O_2 (Po_2) in the bath solution was monitored continuously with the aid of a 1302 Microcathode Oxygen Electrode coupled to a 782 Oxygen Meter (Strathkelvin Instruments, Glasgow, UK). The

electrode was immersed in the bath solution through a close-fitting hole in the plastic cover of the myograph chamber.

Po_2 values were recorded with the 782 System's own software (version 3.0, Strathkelvin Instruments, Glasgow, UK) at the sampling rate of 1 Hz. Following completion of each wire myography experiment, the O_2 data readings were exported and appended offline to the corresponding Chart file as a separate trace alongside the force readings.

2.3. Isolation of pulmonary vein smooth muscle cells

For the purpose of carrying out single cell electrophysiology studies on smooth muscle cells from the pulmonary veins, the alternatives were to use either cultured or freshly isolated myocytes. During cell culture, the phenotype of vascular smooth muscle cells changes from contractile to proliferative. The cells lose their ability to contract due to structural reorganisation with loss of myofilaments (Chamley-Campbell *et al.*, 1979, Thyberg, 1996), and resting membrane potential and potassium channel activity may also be affected during proliferation (Platoshyn *et al.*, 2000). Thus, the approach of using freshly dispersed cells was chosen as the more likely to produce physiologically relevant results. This is supported further by recent evidence which suggests that the effect of hypoxia on Ca^{2+} entry pathways in PASMC can be altered by cell culture (Ng *et al.*, 2008).

An appropriate cell isolation protocol was developed and adjusted to yield cells suitable for patch-clamping experiments. The aim was to obtain physiologically viable myocytes, with intact cellular membranes, preferably in a relaxed elongated state and in sufficient numbers (ideally 10-20 cells per field at 20x magnification) to allow patch clamping experiments for 4-6 hours.

2.3.1. Development of a cell isolation protocol

Following a literature search, several protocols used previously with success for the isolation of smooth muscle cells from pulmonary vessels were considered (Cruickshank *et al.*, 2003, Michelakis *et al.*, 2001, Piper and Large, 2003, Clapp and Gurney, 1991). However, none of these protocols had been specifically used for the species and type of vessel required (i.e. porcine pulmonary vein); therefore a modified protocol was developed for the purpose of this project.

Two alternatives of cell isolation were attempted: *same day protocol* – completing the dissociation shortly after dissecting the vessels (within 1-2 h) – and *overnight protocol* – storing the tissue with the enzymes in a refrigerator overnight (for 15-17 h) to allow for better penetration of the enzymes and finishing the protocol the next day. Although sometimes it resulted in a low yield of cells (with most fields at 20x magnification containing fewer than 5 cells), the "same day" protocol provided more satisfactory results with respect to the viability of the cells and suitability for longer recordings during patch-clamp protocols.

By changing incubation times and type and quantities of enzymes, the protocols were adjusted and optimised. In every dissociation experiment, the result was evaluated by recording the yield of cells in the suspension (from 0 = "no cells" to 5 = "very many cells"), as well as a qualitative remark for the overall morphological appearance of the majority of the cells (especially considering cellular membranes). Adjustments were made to the protocol in the attempt to achieve the best compromise between either obtaining insufficient numbers of myocytes or having most cells inadequate to use for patch-clamping experiments (contracted and/or with blebs of cellular membrane; see Figure 2.4 for examples of such cells).

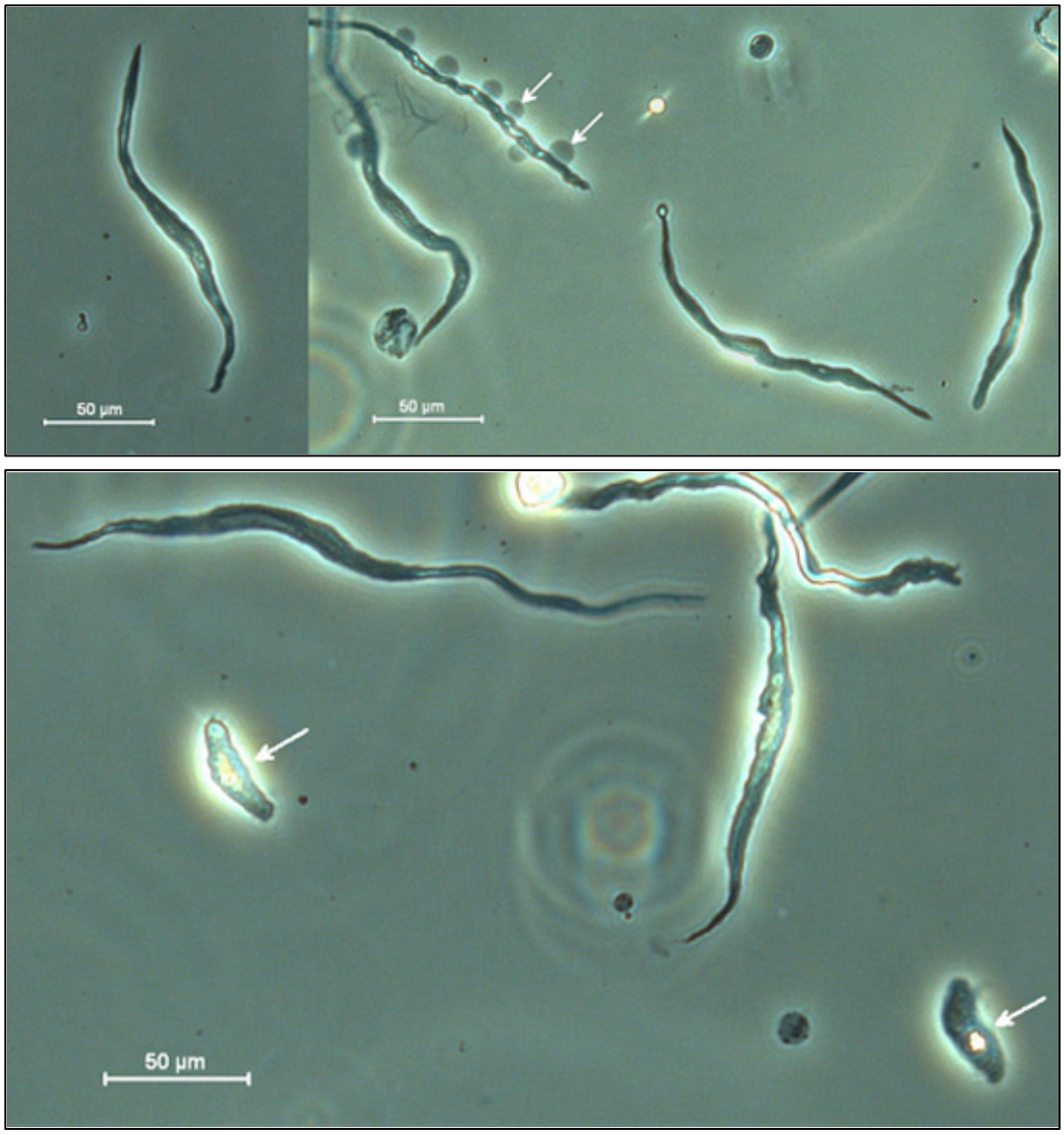

Figure 2.4. Various states of freshly isolated cells (phase contrast microscopy). (*top left*) Relaxed elongated single cell with intact membrane appearing physiologically viable. (*top right*) PVSMC with blebs of membrane (white arrows). (*bottom*) Contracted PVSMC (white arrows).

In previous studies, it was reported that enzymatic dissociation could benefit from the addition of bovine serum albumin (BSA), which served as a cell nutrient and to dilute the proteolytic action of the enzymes (Michelakis *et al.*, 2001, Clapp and Gurney, 1991). When the protocol was adjusted to include BSA (2 mg/ml) during papain digestion, no significant beneficial effect was noted.

2.3.2. Cell isolation protocol

The best results were obtained using a modified version of a protocol previously described by Cruickshank *et al.* (2003). Single smooth muscle cells enzymatically isolated from porcine pulmonary vein were most suitable for patch-clamping studies when the protocol detailed below was used.

2.3.2.1. Tissue preparation

Intrapulmonary venous segments – of 5^{th} to 7^{th} order branch, with an outer diameter of 910 ± 114 μm (mean ± SD, n = 144) and length of ~ 5 mm – were dissected from the left middle or cranial lobe as described above. Occasionally, if the above mentioned lobes were missing or damaged during removal of heart and lungs at the abattoir, vessels were taken from other pulmonary lobes, without any noticeable difference in experimental results.

The vessels were then placed in dissection solution in a separate dissecting dish and fixed with pins (as seen in Figure 2.2, bottom right). Under a dissecting microscope, the adventitial tissue was carefully removed using a pair of forceps and spring scissors and the vessel was cut open longitudinally.

2.3.2.2. Dispersion of smooth muscle cells

The tissue prepared as described above was placed in a microtube containing iced HEPES-based dissociation solution (composition in mM: 128 NaCl, 5.4 KCl, 0.95 KH_2PO_4, 0.35 Na_2HPO_4, 4.16 $NaHCO_3$, 10 HEPES, 10 Glucose, 2.9 Sucrose; pH adjusted to 7.3 with NaOH) supplemented with 1.5 mg/ml Papain from Papaya latex (Sigma Aldrich, UK) and 0.75 mg/ml DL-dithiothreitol.

Venous segments were then stored on ice for 1-2 hrs followed by incubation in a water bath at 37 °C for 8-10 minutes. Thereafter, the tissue was washed at least three times using enzyme-free fresh dissociation solution and transferred to dissociation solution with 1.5 mg/ml collagenase for a further 8-10 minutes at 37°C.

Finally, after rinsing in enzyme-free fresh dissociation solution, gentle trituration with a fire polished wide-bore Pasteur pipette yielded a suspension of freshly dispersed pulmonary vein smooth muscle cells (as shown in Figure 2.5) that were viable and contractile (in response to 80 mM KCl). The cells were stored at 4°C and were used for cell electrophysiology studies. Cells remained viable for at least 5-6 hours.

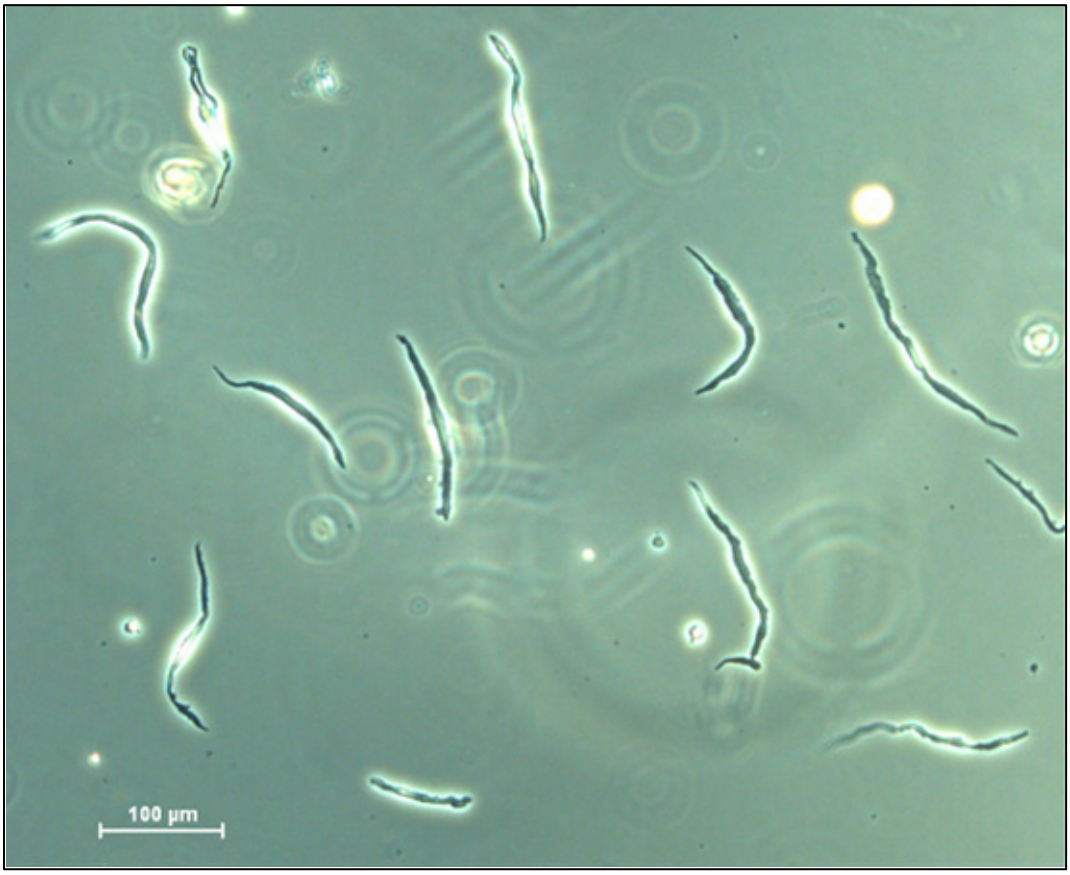

Figure 2.5. Freshly dispersed relaxed smooth muscle cells from porcine intrapulmonary veins. A bright halo present around the cells was considered an indication of intact cellular membranes.

2.4. Whole-cell patch clamping

The whole-cell configuration of the patch-clamping technique was used to investigate changes in whole-cell voltage-activated currents (in voltage clamp mode) under hypoxic conditions in freshly dispersed single porcine pulmonary vein smooth muscle cells.

2.4.1. Tissue preparation

All experiments were performed at room temperature. Approximately 80-100 µl of the cell suspension were transferred on the glass coverslip bottom of a low profile large bath recording chamber (RC-26GPL, Harvard Apparatus, Kent, UK) and left to settle for approximately 10 to 15 minutes. The perfusion chamber was mounted on the stage of a Nikon Eclipse TS100 inverted microscope with the aid of a platform (PH-1, Harvard Apparatus, Kent, UK) and a stage adapter (SA-TS100, Harvard Apparatus, Kent, UK). After the cells settled and adhered to the bottom coverslip, the chamber was filled with bath solution of the following composition (in mM): 150 NaCl, 5.4 KCl, 1.2 $MgCl_2$, 1.8 $CaCl_2$, 10 HEPES, 10 Glucose (pH adjusted to 7.4 with 10 M NaOH).

2.4.2. Preparation of patch pipettes

Pipettes were fabricated from thin-wall borosilicate glass capillaries (1.5 mm O.D. x 1.17 mm I.D.; Clark Electromedical Instruments, Reading, UK) on a two-stage micropipette vertical puller (PP-830, Narishige, Tokyo, Japan). The micropipettes were then heat-polished using a microforge (MF-830, Narishige, Tokyo, Japan) to a final resistance of approximately 3-4 MΩ when filled with standard intracellular solution with a composition of (mM): 110 KCl, 2.5 $MgCl_2$, 10 HEPES, 3.6 ATP (pH adjusted to 7.2 with KOH).

The pipettes were made in small batches of 4-6 immediately prior to being used throughout each experimental day, as this approach resulted in a reduced number of blocked pipette tips.

2.4.3. Making the giga-seal

An appropriate target cell was chosen based on the intact cell membrane and preferably elongated and smooth appearance. This was done before lowering the pipette in the solution to reduce the time until the pipette tip touched the cell membrane and therefore minimise the chances of contaminating the tip of the pipette.

After the pipette was filled with intracellular solution, it was mounted in the pipette holder and lowered into the bath solution with the help of the controls of a coarse mechanical manipulator. The "Pipette Seal Test / Signal Monitor" facility of the WinWCP software was used to monitor the progress through the steps towards achieving the whole-cell configuration.

With the amplifier in voltage clamp mode, the initial holding voltage was set at 0 mV and a small test pulse with duration of 50 ms and amplitude of 10 mV was applied to enable calculation of pipette resistance and monitor seal formation. The tip was then brought in focus and moved closer to the cell chosen as target, using a three-axes hydraulic, remotely controlled micromanipulator (MHW-3, Narishige, Tokyo, Japan). The pipette resistance was recorded in the log file and had an average value of 3.6 ± 0.8 MΩ (mean ± SD, n = 920). The offset control of the amplifier was used to adjust the pipette offset current to zero. Pipette capacitance was compensated electronically, but series resistance was normally not compensated.

With the pipette in the proximity of the target cell, the tip was carefully moved closer until it gently touched the cell membrane. To form a giga-seal, gradually increasing suction was applied while monitoring resistance and aiming to obtain a seal resistance higher than 1 GΩ (*cell-attached configuration*). Immediately after

obtaining the giga-seal, the holding voltage was changed to -80 mV, a value negative to the resting membrane potential of smooth muscle cells. This was done to stabilise the giga-seal and avoid depolarising the cell membrane during the next step of achieving the whole-cell configuration (Molleman, 2003).

As soon as the seal stabilised, the resistance was recorded – average seal resistance was 5.3 ± 3.7 GΩ (mean ± SD, n = 688) – and breakthrough to the whole-cell configuration was attempted. If, however, the formation of the giga-seal failed through a seal or patch break, the micropipette was considered contaminated and discarded and a new attempt was made on a new target cell.

2.4.4. The whole-cell configuration

To achieve the desired *whole-cell configuration*, the patch under the pipette tip has to be ruptured in order to establish communication between the intracellular environment and the pipette solution. This can be done in two ways: through *suction* – the application of negative pressure to the inside of the pipette – or *zapping* – the application of a large current pulse of short duration which can be varied.

The zapping function was available through the Axopatch 200B amplifier. Zapping with a single +1.3V pulse at the minimum duration of 0.5 ms resulted most often in the break of the seal, therefore suction was used in the majority of experiments to achieve the whole-cell configuration.

Suction was applied through the side arm of the pipette holder which was connected to a 1 ml syringe through a length of thin tubing (1 mm I.D. 2 mm O.D.) which ran outside the Faraday cage.

Successful breakthrough was indicated by the rapid increase in size of the capacitive transients visible on the current trace at the beginning and the end of the voltage step (due to membrane capacitance). The test pulse was then removed and the holding voltage was kept at -80 mV. After the whole-cell configuration was established,

approximately 5 minutes were allowed for diffusion of ions between the cytoplasm and the pipette solution. Thereafter, preset voltage step protocols were run to record voltage activated whole-cell currents. Leakage currents were subtracted offline using standard protocols contained within the software suite.

2.4.5. Liquid junction potentials

A liquid junction potential (LJP) arises at the unstirred interface between two solutions with different ion compositions due to difference in electrochemical potentials and mobilities of ions (Kenyon, 2002). The resulting voltage introduces a difference between the measured potential and the actual membrane potential of the cell.

LJPs were calculated with the aid of an Excel sheet developed by Kenyon and downloaded from http://www.physio.unr.edu/Faculty/kenyon/Junction_Potentials/jp.xls [Accessed 26 January 2007] using the specific ionic concentrations and the experimental temperature converted in degrees Kelvin, as well as a series of constants: ionic valences, mobilities and the physical constants R and F.

The induced voltage difference for the standard bath and pipette solutions was calculated to be 4.88 mV and considered negligible (Selyanko *et al.*, 1995, Selyanko *et al.*, 2000), thus the measured voltages were not corrected for errors induced by junction potentials.

2.4.6. Controls

2.4.6.1. Perfusion system

A multi-barrel perfusion system was set up to deliver bath solution and drugs to the RC-26GPL bath recording chamber. Three syringe barrels (20 to 60 ml) were used as reservoirs and assembled together using three-way taps and a length of flexible thin tubing which was connected to the inflow of the chamber. The outflow was in turn

connected through tubing that ran outside the Faraday cage to a Dymax 30 pump (Charles Austen Pumps, UK).

In order to be able to adjust the rates of delivery of drugs and hypoxic solution to the recording chamber, a roller clamp (max. O.D. 6 mm, Keck Ramp Clamp, Sigma Aldrich, UK) was mounted on the inflow tubing. Several fixed positions were set for the clamp that allowed delivery of the bath solution at various fixed flow rates: low (1.1 ml/min), medium (2.09 ml/min), high (3.53 ml/min) and maximum unrestricted flow (6.06 ml/min). In most experiments, solutions were delivered using either the high or maximum flow settings.

The volume of the inflow tubing between the syringe barrels and the chamber was approximately 0.6 ml, which meant that the time required for the solution to reach the chamber was ~ 33 s at the low rate of flow and ~ 6 s at the maximum rate.

2.4.6.2. O_2 saturation measurements

A series of control experiments were carried out to monitor the oxygen saturation levels during hypoxic flow in various locations and at different depths in the bath recording chamber. For this purpose, a thin flexible NTH (needle-type housing) trace oxygen microsensor connected to a Single Channel Fiber-Optic Oxygen Meter (Microx TX3-trace, Precision Sensing GmbH, Germany) was used. Experiments were carried out at the Centre for Integrative Physiology, University of Edinburgh, with the help of Dr. Iain Rowe. Data readings were acquired using the OxyView software at the sampling rate of 0.1 Hz and were recorded as percentages of the oxygen concentration in air-saturated solution (100% oxygen saturation approximately equivalent to a Po_2 of 160 mm Hg).

The normoxic solutions were passively equilibrated with room air (i.e. non-aerated), while the hypoxic solutions were gassed with N_2 for at least 5 minutes prior to starting hypoxic flow (in separate control experiments, the O_2 levels in the syringe reservoir fell from 100.9% saturation to 25% in 1:35 min, 10% in 2:53 min and

stabilised at ~ 5-6% after 5 min). To account for flow rate induced variations in O_2 saturation, the hypoxic solutions were delivered at the same flow rate as normoxic solutions during experiments.

Initially, the oxygen electrode was positioned in the centre of the chamber and oxygen saturation was 102.8% during normoxic flow (marked (1) in Figure 2.6). The O_2 saturation declined very quickly after the onset of hypoxic flow, reaching values below 25% within 20 seconds and stabilising at 5.7% at the end of the 5-minute hypoxic period (Figure 2.7). When flow was switched back to the normoxic solution, the oxygen saturation returned within 20 seconds to levels above 90% and steadied at 100.7% after 1 minute.

In a second control experiment, after being placed initially in a central position (1), the electrode was moved to different locations in the chamber during steady continued hypoxic flow – positions marked (2) through to (5) in Figure 2.6. The positions were chosen based on the assumption that non-central locations might experience lower levels of hypoxia due to slower laminar flow (towards the edges of the chamber) or more time for reoxygenation (near outflow point). However, the O_2 saturations were at comparable hypoxic levels in all locations tested (Figure 2.8).

In an additional experiment, the tip of the electrode was positioned at three different depth levels: close to the bottom of the bath, near the surface and in an intermediate position between the first two. The recorded values were below 8% in all three positions (Figure 2.9).

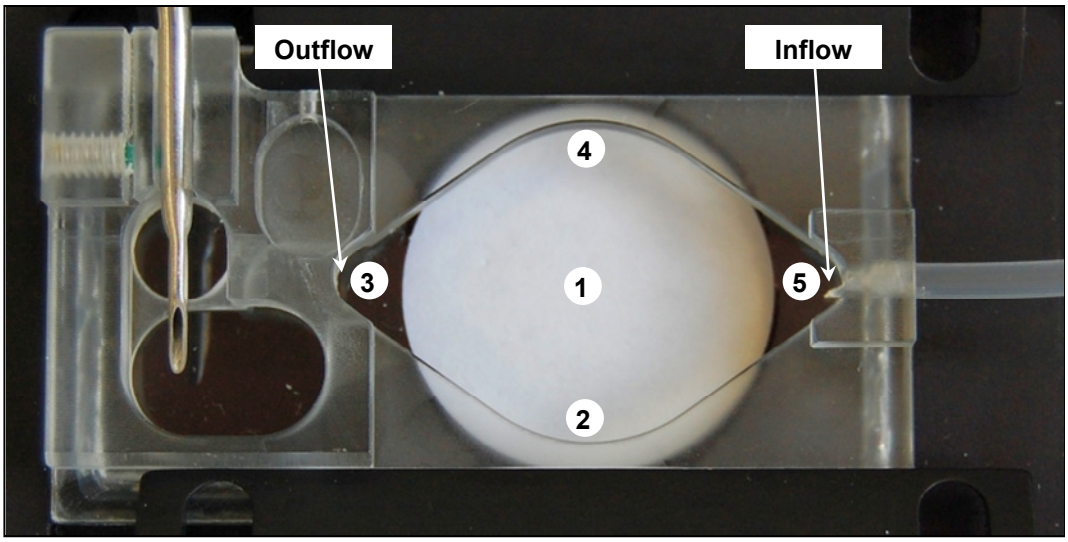

Figure 2.6. The RC-26GPL bath recording chamber. Arrows mark the inflow and outflow; numbers represent the approximate locations in the bath that were used during control O_2 saturation measurements.

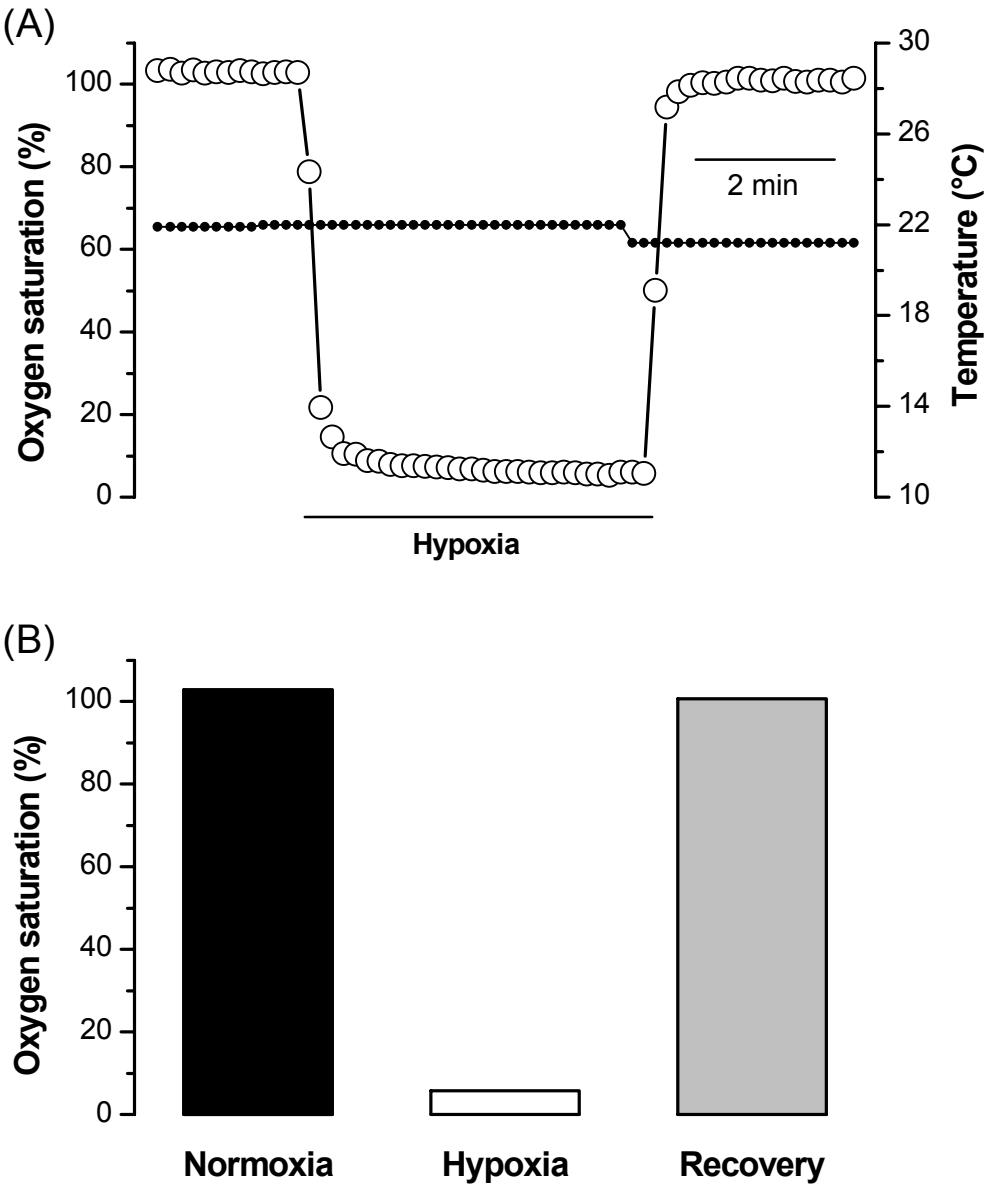

Figure 2.7. Oxygen saturation during a typical hypoxic challenge.

(A) Oxygen saturation (*empty circles*) and temperature (*small black circles*) are presented as a function of time. (B) Values recorded before, during and after a period of hypoxia.

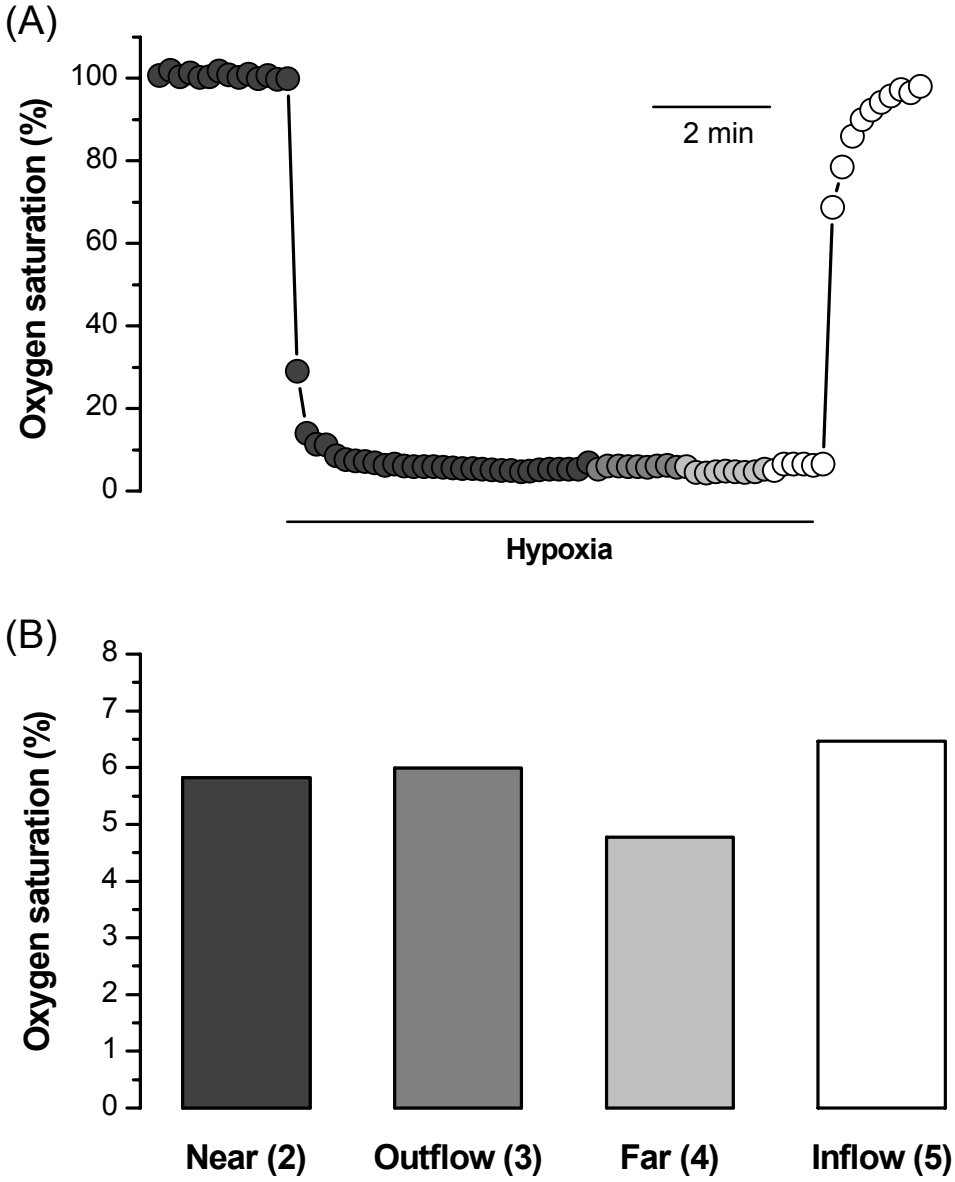

Figure 2.8. Oxygen saturation at various locations in the chamber during hypoxic flow. (A) Oxygen saturation plotted as a function of time. (B) O_2 saturation values at each of the 4 locations (as shown in Figure 2.6). Each shade of grey designates a different position of the electrode in the recording chamber in both (A) and (B).

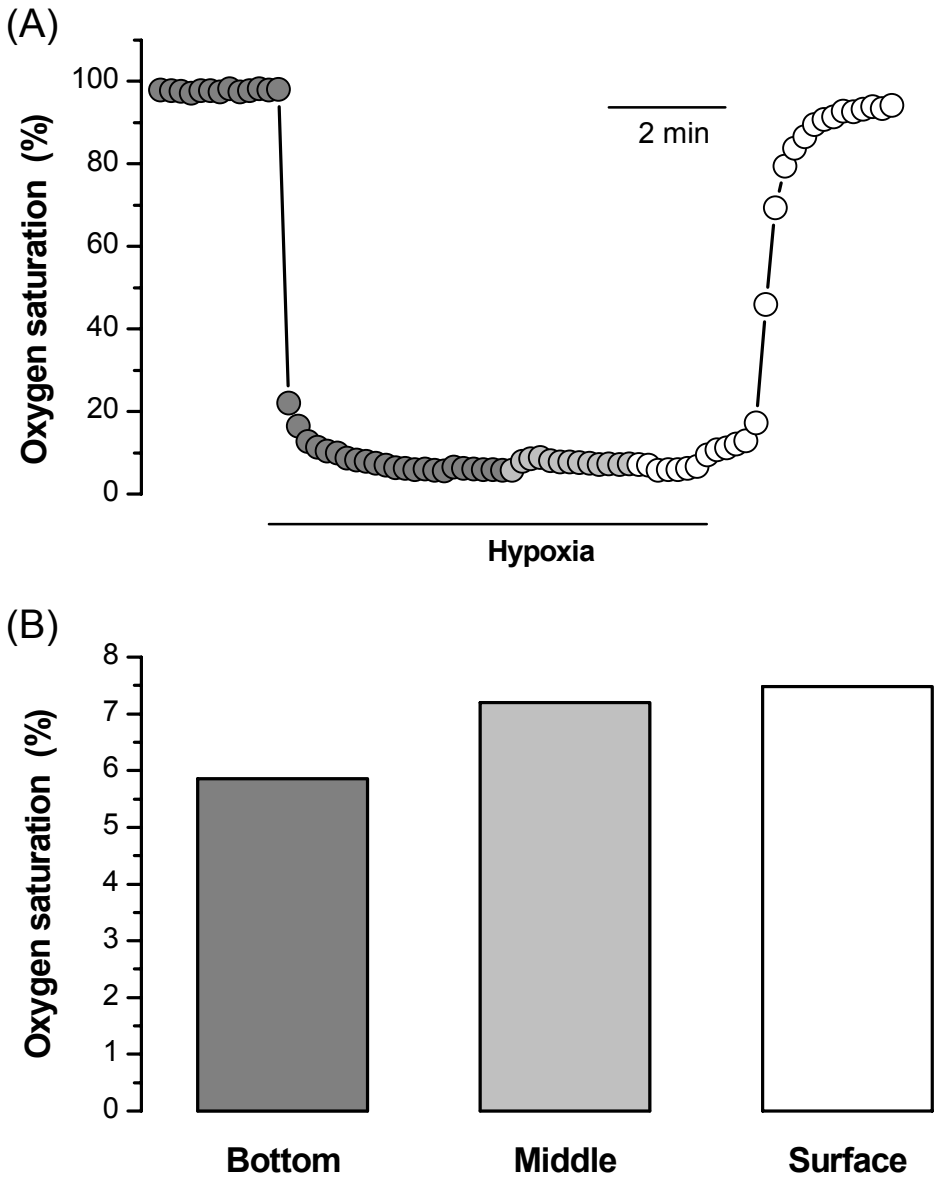

Figure 2.9. Oxygen saturation at different depths in the chamber during hypoxic flow. (A) Oxygen saturation plotted against time during hypoxic flow. (B) O_2 saturation values at various depth levels in the bath. Shades of grey represent different positions of the electrode in both (A) and (B).

2.5. Statistical analysis

Data processing and statistical analysis were performed using Microsoft Office Excel 2003 (Microsoft Corporation, USA), SPSS for Windows (Release 13.0, SPSS Inc., USA) and GraphPad Prism software (Version 4.03, GraphPad Software Inc., USA).

Where appropriate, data are presented as mean ± S.E.M. unless specified otherwise and *n* represents the number of vessels for wire myography studies and the number of cells in the case of electrophysiology experiments. Mean data were compared using either a paired or unpaired Student's *t*-test or one- or two-way ANOVA with Bonferroni post-hoc analysis, as appropriate. Differences were considered statistically significant for *P* values less than 0.05. Further details about specific data analysis are given in the respective results sections.

2.6. Materials

2.6.1. Solutions

Dissecting solution (mM): 119 NaCl, 4.7 KCl, 1.18 KH_2PO_4, 1.17 $MgSO_4$, 25 $NaHCO_3$, 10 HEPES, 5.5 Glucose (pH adjusted to 7.4 with NaOH).

HEPES-based extracellular (bath) solution (mM): 150 NaCl, 5.4 KCl, 1.2 $MgCl_2$, 1.8 $CaCl_2$, 10 HEPES, 10 Glucose (pH adjusted to 7.4 with NaOH).

Ca^{2+} free HEPES-based extracellular (bath) solution (mM): 150 NaCl, 5.4 KCl, 3 $MgCl_2$, 10 HEPES, 10 Glucose, 1 mM EGTA (pH adjusted to 7.4 with NaOH).

Low Cl^- HEPES-based extracellular (bath) solution (mM): 150 Na gluconate, 5.4 KCl, 1.2 $MgCl_2$, 1.8 $CaCl_2$, 10 HEPES, 10 Glucose (pH adjusted to 7.4 with NaOH).

Dissociation solution (mM): 128 NaCl, 5.4 KCl, 0.95 KH_2PO_4, 0.35 Na_2HPO_4, 4.16 $NaHCO_3$, 10 HEPES, 10 Glucose, 2.9 Sucrose (pH adjusted to 7.3 with NaOH).

Intracellular (pipette) solution (mM): 110 KCl, 2.5 $MgCl_2$, 10 HEPES, 3.6 ATP (pH adjusted to 7.2 with KOH) filtered through a Nalgene 0.2 µm syringe filter (25-mm surfactant free cellulose acetate membrane).

Solutions were prepared in stocks using deionised water, titrated with NaOH (10 M) to achieve the respective pH and stored at 4°C. The intracellular solution was titrated with KOH, and stored in 1.5 ml aliquots at -20°C. All pH values were measured using a digital type pH meter (SevenEasy, Mettler Toledo, Leicester, UK).

2.6.2. Drugs

KCl: 2 M stock prepared by dissolving in distilled water; final concentration of 80 mM by adding 600 µl of stock solution to 15 ml bath solution.

Prostaglandin $F_{2\alpha}$ ($PGF_{2\alpha}$): 1 mM stock prepared by dissolving in ethanol; final concentration of 2 µM by adding 30 µl of stock solution to 15 ml bath solution.

Niflumic acid (NFA): 10 mM stock prepared by dissolving in DMSO; final concentration of 50 µM by adding 75 µl of stock solution to 15 ml bath solution.

5-Nitro-2-(3-phenylpropylamino) benzoic acid (NPPB): 5 mM stock prepared by dissolving in DMSO; final concentration of 2 µM by adding 6 µl of stock solution to 15 ml bath solution.

TEA: final concentration of 5 mM; by dissolving 0.0828 g in 100 ml bath solution.

4-AP: final concentration of 5 mM, by dissolving 0.094 g in 200 ml bath solution and adjusting the pH to 7.4 with HCl.

Penitrem A: 500 µM stock prepared by dissolving in DMSO; final concentration of 100 nM, by diluting each aliquot of 40 µl in 200 ml bath solution.

Glyburide (Glibenclamide): 50 mM stock prepared by dissolving in DMSO; final concentration of 10 µM, by diluting each aliquot of 40 µl in 200 ml bath solution.

All chemicals were acquired from Sigma Aldrich, UK with the exception of Penitrem A and Glyburide (Biomol, Exeter, UK).

2.6.3. Dissociation enzymes

Papain (from Papaya latex, product no. P4762), collagenase (Type VIII, from Clostridium histolyticum, product no. C2139), DL-Dithiothreitol (product no. D0632) and bovine serum albumin (fatty acid free, product no. A6003) were all acquired from Sigma Aldrich, UK. Sigma's papain preparation has been used previously for the isolation of smooth muscle cells (Driska *et al.*, 1999, Kinoshita *et al.*, 2003). The enzymes were dissolved in dissociation medium and aliquoted as follows: 0.75 mg papain in 30 µl per aliquot; 1.5 mg collagenase in 45 µl per aliquot; 0.5 mg DTT in 40 µl per aliquot. All aliquots were stored at -20 °C.

Chapter 3.
Characterisation of the hypoxia-induced responses in isolated PV and PA

3.1. Introduction

Alveolar Po_2 regulates blood flow in the pulmonary circulation. An acute reduction in the concentration of alveolar oxygen triggers hypoxic pulmonary vasoconstriction (HPV), which causes blood flow to be diverted towards better ventilated areas of the lungs, thus optimizing the ventilation-perfusion ratio.

The pulmonary veins participate alongside arteries to the increase in vascular resistance during alveolar hypoxia (Raj and Chen, 1986). The vasoactivity of the pulmonary veins in response to several contractile stimuli has been demonstrated in numerous studies. Hypoxia (Zhao *et al.*, 1993), norepinephrine (Kadowitz *et al.*, 1975), histamine and 5-HT (Shi *et al.*, 1998), as well as thromboxane A_2 (Raj and Anderson, 1990, Ding and Murray, 2005a) and prostaglandin $F_{2\alpha}$ (Joiner *et al.*, 1975b, Walch *et al.*, 2001), all induce venoconstriction in the lungs. Furthermore, several reports indicate that the veins are more reactive than the arteries in the pulmonary circulation (Zhao *et al.*, 1993, Gao *et al.*, 1995b, Arrigoni *et al.*, 1999). Increased vascular tone in the pulmonary veins contributes to increased total pulmonary vascular resistance and postcapillary venoconstriction raises upstream microvascular hydrostatic pressures and fluid filtration during edema formation (Dauber and Weil, 1983).

HPV responses have been consistently demonstrated in intact animals and in blood- or saline-perfused isolated lungs (Madden and Gordon, 2004). However, the main disadvantage of these methods lies in the difficulty of locating the sensor and effector sites of the hypoxic pressor response. More reductionist experimental models have allowed investigators to advance the understanding of the direct effects of hypoxia on isolated pulmonary vessels and vascular smooth muscle (for discussion see section 1.2.3).

Historically, research in the field of HPV has largely focused on the pulmonary arteries. Although the temptation could be to generalise those findings to the venous side of the pulmonary circulation, the existing knowledge of the underlying mechanisms that initiate and sustain HPV is, for the most part, relevant only to the arterial segment.

The rise in $[Ca^{2+}]_i$ during vascular smooth muscle contraction is in part determined by Ca^{2+} influx through ion channels in the plasma membrane. In the pulmonary circulation, the density of L-type voltage-gated Ca^{2+} channels (VGCC) is higher in arteries than in veins (Walker, 1995, Ricci *et al.*, 2000), which could potentially underlie differences between arteries and veins in regards to contractile pathways and Ca^{2+} handling.

Vascular myocytes have a higher chloride conductance compared to skeletal and cardiac muscle cells and the intracellular concentration Cl^- is much higher in vascular smooth muscle (50 mM) compared to cardiac muscle (20 mM) (Kitamura and Yamazaki, 2001). The rise of cytosolic Ca^{2+} activates Cl^- channels in the plasma membrane of vascular myocytes. During agonist-induced contraction Ca^{2+}-activated Cl^- channels (Cl_{Ca}) provide a link between Ca^{2+} release from the intracellular stores and Ca^{2+} influx (Lamb and Barna, 1998). Once Cl_{Ca} channels are activated by the increase in $[Ca^{2+}]_i$, Cl^- ions leave the cell against their concentration gradient and driven by the electrical gradient, as the chloride equilibrium potential is more positive than the resting potential. Consequent to this efflux of negative ions the cell

depolarises, causing Ca^{2+} entry through VGCC. As such, $[Ca^{2+}]_i$ is increased even further and contraction is sustained.

The aim of this study is to verify the presence and characterise the hypoxia-induced contractile responses of isolated distal porcine intrapulmonary veins, specifically response profile, maximum elicited tension and time course; examine the HPV dependence on the presence of preconstriction; and analyse comparatively the responses elicited by hypoxia in the veins in relation to the contractions of size-matched intrapulmonary arteries, considering the characteristics listed above.

3.2. Methods and experimental protocols

The small vessel myography technique was used to study the contractility of distal porcine intrapulmonary vessels. The investigation of contractile mechanisms involved was carried out with the help of contractile agonists and antagonists, as well as by manipulating the extracellular environment, in particular ionic concentrations and oxygen tension.

Intrapulmonary veins and arteries of similar size and order were dissected from fresh porcine lungs (as described in Chapter 2).

In most experiments, one venous and one arterial segment were mounted in a single chamber, dual wire myograph (410A System, Danish Myo Technology, Aarhus, Denmark) to enable comparisons between the two types of vessel under the same conditions. In other experiments, two segments of pulmonary veins dissected from different animals were used instead.

The outer diameter and length of vessel segments used in each experiment were measured using a micrometer scale fitted in the eyepiece of a dissecting microscope, respective measurements for veins and arteries are shown in Table 3.1.

Table 3.1. Morphometric measurements of pulmonary vessels. For vessels used in wire myography experiments, outer diameter and segment length were measured directly using a dissecting microscope and branching order was recorded during dissection. The coefficient of variation (CV) was calculated as the ratio of the standard deviation to the mean.

Vessel measurement	Mean value ± SD	Minimum value	Maximum value	CV
Pulmonary vein segments (n = 77)				
Outer diameter, µm	598.7 ± 147.3	300	1000	0.25
Segment length, mm	1.52 ± 0.32	0.9	2	0.21
Branch order	5/6	4	7	-
Pulmonary artery segments (n = 57)				
Outer diameter, µm	626.3 ± 135.7	300	900	0.22
Segment length, mm	1.48 ± 0.39	0.5	2	0.26
Branch order	5/6	4	7	-

3.2.1. Equilibration and normalisation

After the segments of vessels were mounted into the temperature-controlled myograph chamber, the vessels were left to equilibrate for approximately 30 minutes to 1 hour.

At the beginning of each experiment, resting tension was normalised. The rationale behind the normalisation procedure is to find the level of passive stretch for each vessel segment equivalent to a set fraction (90%) of the internal circumference of a fully relaxed vessel at a specified transmural pressure (Danish Myo Technology, 2003).

This was completed using the Normalisation module of the Chart software (AD Instruments, UK). The target pressure chosen was the minimal value allowed by the Normalisation module, which was 5 kPa. The procedure involved measuring the length of the mounted vessel segments and performing a series of stepped passive stretches of the vessel by increasing the distance between the jaws of the myograph (see example of recording during normalisation in Figure 3.1). The last step of normalisation was to set the mobile micrometer-controlled jaw of the myograph to the calculated position for each vessel.

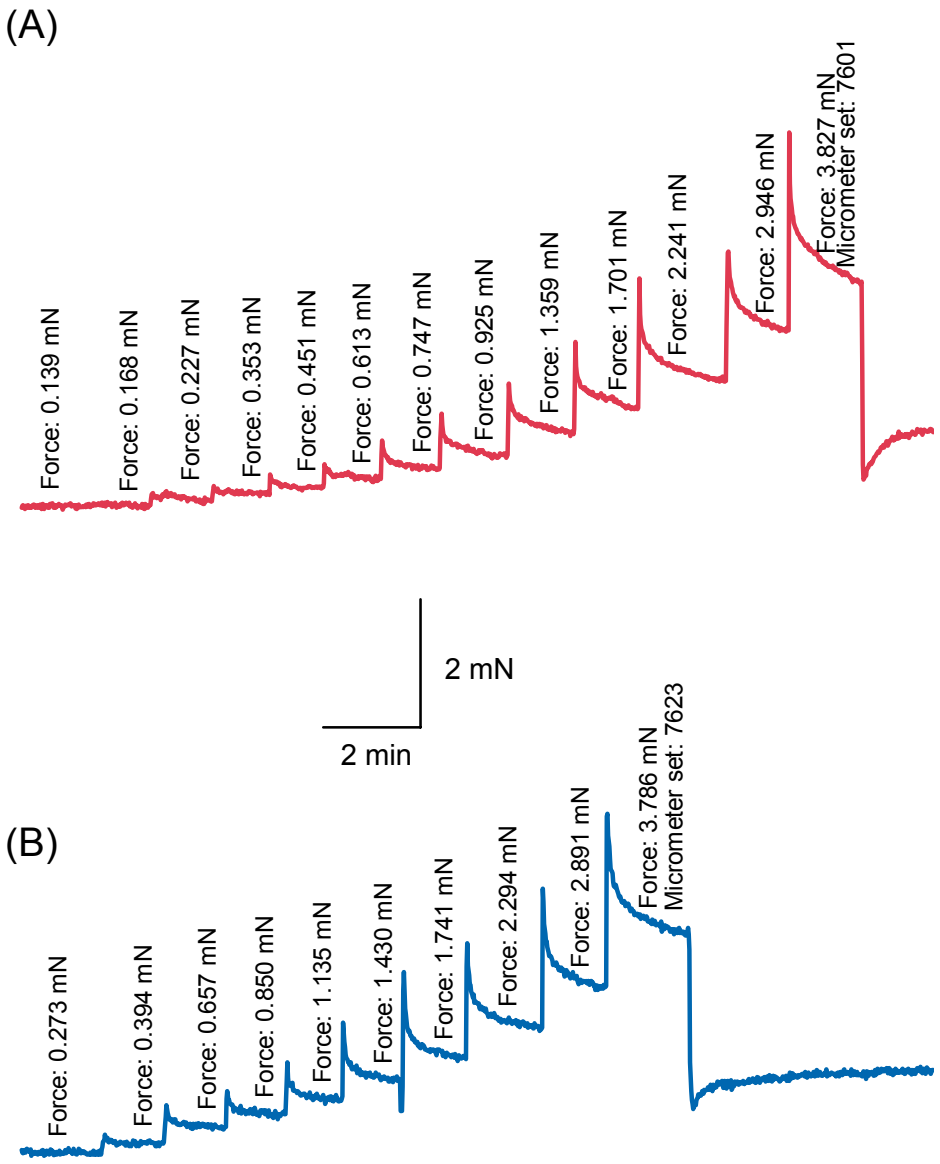

Figure 3.1. Normalisation procedure. Example of normalisation carried out with intrapulmonary veins (A) and arteries (B). At the beginning of each experiment, vessel segments were subjected to several passive stretches to achieve a normalised resting tone.

3.2.2. Control responses

Before starting experimental protocols, the viability of vessels was checked and control responses recorded. For this purpose, KCl was added directly to the myograph bath to achieve a final bath concentration of 80 mM, to which the vessels were exposed for approximately 3 to 5 minutes. The content of the myograph chamber was then replaced with fresh bath solution and the application of KCl repeated another two times for sensitisation of the contractile apparatus. Vessels that did not contract in response to 80 mM KCl were not included in the study.

Experimental protocols ran for approximately 6 to 8 hours. At the end of each experiment, the contractile function of vessels was tested using the same concentration of agonist KCl (80 mM).

3.2.3. Preconstriction

In order to obtain vigorous hypoxic pressor responses in isolated rings of pulmonary vessels, usually a small amount of agonist induced pretone is applied before the hypoxic challenge (Aaronson *et al.*, 2002). Depending on the species of animal used and experimental conditions, HPV responses in isolated pulmonary arteries may or may not be obtained without inducing pretone (see discussion in section 1.2.3); however, the presence of pretone universally augments the contraction caused by hypoxia. In the veins, robust HPV responses have been obtained without pretone even when arteries did not respond under the same conditions (Miller *et al.*, 1989), but precontraction has also been commonly used with veins (Zhao *et al.*, 1993, Feletou *et al.*, 1995).

The underlying mechanism of HPV enhancement by pretone is not entirely clear (Aaronson *et al.*, 2006), but its purpose is thought to be the priming of vessels for contraction and mimicking the physiological baseline tone present under *in vivo* conditions.

Examples of contractile agonists used to induce preconstriction include adrenergic, thromboxane and 5-HT receptor agonists or high K^+ depolarisation (Rodman *et al.*, 1989, Bennie *et al.*, 1991), but $PGF_{2\alpha}$ is one of the most commonly used preconstrictors (Thompson *et al.*, 1998, Dipp *et al.*, 2001, Robertson *et al.*, 2001) and has previously been shown to induce contractions in pulmonary veins (Gao *et al.*, 1995b, Boels *et al.*, 1997).

When preconstriction was used, it was induced with $PGF_{2\alpha}$ (2 μM), concentration chosen in preliminary experiments to elicit responses in both arteries and veins. 30 μl of the stock solution (1 mM) was added directly to the myograph chamber to achieve the desired final bath concentration. 5 minutes were allowed before starting the hypoxic challenge, as the $PGF_{2\alpha}$ contraction usually peaked during the first 5 minutes.

3.2.4. Concentration-dependent responses to $PGF_{2\alpha}$

The responses of small intrapulmonary veins to increasing concentrations of $PGF_{2\alpha}$ (0.01 μM, 0.1 μM, 1 μM, 2 μM, 5 μM and 10 μM) were elicited to assess the sensitivity of the veins to the contractile agonist $PGF_{2\alpha}$.

Cumulative volumes of stock $PGF_{2\alpha}$ solution were added directly to the myograph chamber in order to achieve the respective final bath concentrations. Approximately 5 minutes were allowed after each addition for expression of maximal responses.

3.2.5. Hypoxia-induced responses

Vessels were exposed to hypoxia by gassing with N_2 directly into the myograph chamber to achieve a Po_2 below 25 mm Hg. The hypoxic period normally lasted for 30 minutes. Po_2 was monitored continuously using an oxygen electrode (1302 Microcathode Oxygen Electrode and 782 Oxygen Meter, Strathkelvin Instruments, Glasgow, UK).

When vessels were preconstricted (as described above in section 3.2.3), N_2 gassing was commenced approximately 5 minutes after the addition of $PGF_{2\alpha}$.

At the end of the hypoxic challenge, the solution was replaced with fresh normoxic bath solution. At least 30 minutes were allowed for the vessels to recover after each of the hypoxic episodes.

3.2.6. The effect of altering extracellular ion concentrations

To investigate the role of Ca^{2+} and Cl^- ions in the development of agonist and hypoxia-induced responses in pulmonary vessels, the concentrations of these ions in the extracellular solution were decreased. Low-Cl^- HEPES-based bath solution ($HBS_{Low\text{-}Cl}$) was prepared by replacing NaCl with equimolar Na-gluconate. In Ca^{2+}-free HEPES-based bath solution ($HBS_{Ca\text{-}free}$), $CaCl_2$ was replaced with equimolar $MgCl_2$ and Ca^{2+} chelator EGTA (1 mM) was added.

3.2.7. The effect of Cl^- channel blockers

To examine further the role of Cl^-, and more specifically the involvement of the Ca^{2+}-activated Cl^- channels (Cl_{Ca}), the effect of Cl^- channel blockers niflumic acid (NFA) and 5-Nitro-2-(3-phenylpropylamino) benzoic acid (NPPB) (Cruickshank *et al.*, 2003) on agonists and hypoxia-induced contractions was assessed. Final concentrations of NFA and NPPB were achieved by direct addition of stock solution to the myograph chamber, approximately 5 minutes prior to recording agonist responses.

3.2.8. Data analysis

Isometric tension values were recorded with the Chart software (version 5, ADInstruments, UK). O_2 concentration values were acquired separately with the 782 Oxygen Meter System's software (version 3.0, Strathkelvin Instruments, Glasgow,

UK) and, at the end of experiments, were merged offline as an individual channel into the Chart file.

Data are expressed in mN or as a percentage of the control response to 80 mM KCl and are presented as mean ± SEM. Statistical difference between groups was calculated using paired or unpaired *t*-tests or analysis of variance (ANOVA) followed by Bonferroni's post-hoc test, as appropriate and significance was determined by *P* values of less than 0.05.

3.3. Results

3.3.1. Control responses

Control contractions were induced with high extracellular K^+ concentration (80 mM KCl) and were repeated three times (representative traces in Figure 3.2). The tension developed by vessels increased immediately following the application of KCl and reached a plateau after approximately 3 to 4 minutes.

The responses usually increased with each application and the last contraction was measured and used as a control to express the tension increase induced by other agonists and hypoxia.

The initial application of 80 mM KCl induced a contraction of 5.76 ± 0.62 mN/mm (n = 17) in veins and 3.22 ± 0.45 mN (n = 17) in arteries. Subsequent responses were significantly greater with each application in both types of vessel increasing to 7.4 ± 0.89 mN (n = 17, $P < 0.05$) and 5.21 ± 0.58 mN/mm (n = 17, $P < 0.05$) in veins and arteries, respectively (see Figure 3.3). At each application of KCl, veins contracted significantly more than the arteries (n = 17, $P < 0.05$).

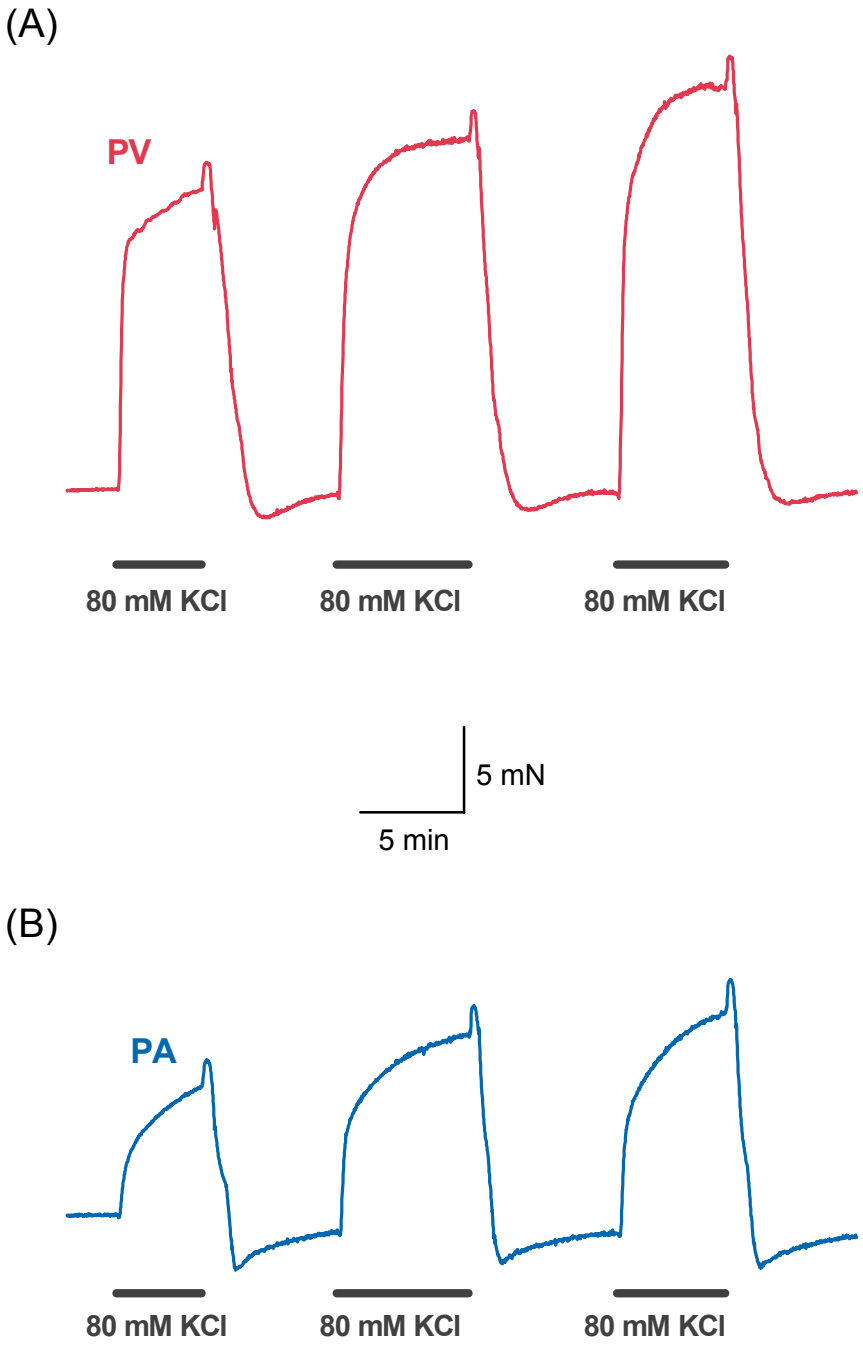

Figure 3.2. Representative control contractions of small pulmonary vessels. Intrapulmonary veins (A) and arteries (B) were stimulated with KCl (80 mM) three times at the beginning of each experiment to sensitise the contractile apparatus and elicit control responses.

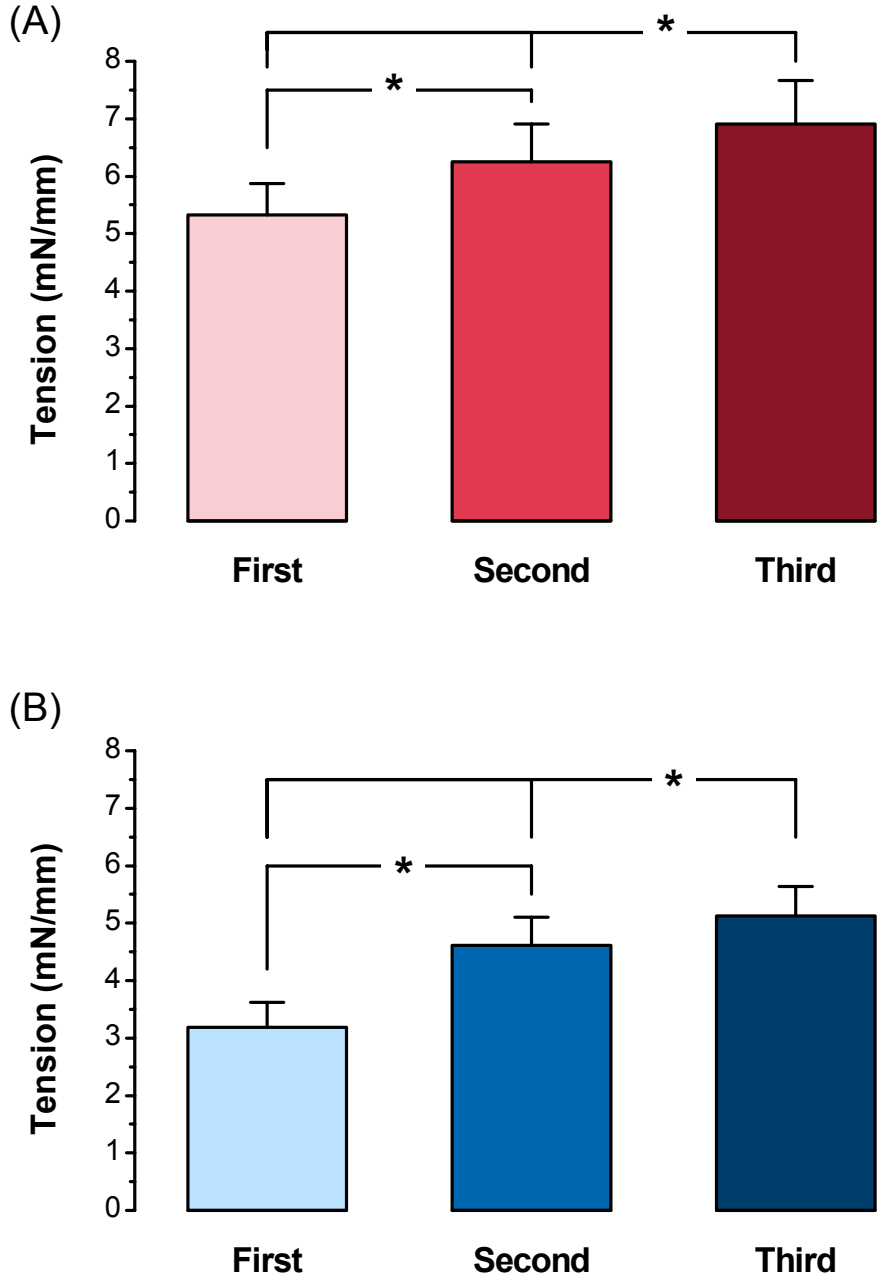

Figure 3.3. Average control contractions of small pulmonary vessels.
Mean ± SEM responses of intrapulmonary veins (n = 23) (A) and arteries (n = 21) (B) to KCl (80 mM). The third KCl contraction was used as a control to normalise the responses to other agonists and hypoxia.

3.3.2. Effect of $PGF_{2\alpha}$

The effect of $PGF_{2\alpha}$ on venous tone was examined by constructing a concentration-response curve using cumulative additions of the agonist (0.01 μM to 10 μM) (representative trace in Figure 3.4A). Responses to $PGF_{2\alpha}$ were averaged and values were fitted with a Hill slope (see Figure 3.5). The effective concentration of $PGF_{2\alpha}$ inducing half of the maximal response (EC_{50}) in pulmonary veins was calculated to be 4.53 μM, while EC_{25} was 1.65 μM.

Preconstriction of veins was made with $PGF_{2\alpha}$ at a final bath concentration of 2 μM, which was deemed appropriate as it has been shown previously that the largest hypoxic responses are obtained when $PGF_{2\alpha}$ preconstriction is made using EC_{25} and EC_{50} concentrations (Ozaki *et al.*, 1998). As vessels were in the same chamber, the same amount of agonist was used to preconstrict arteries. A concentration-response curve was not completed for $PGF_{2\alpha}$ in pulmonary arteries, but the concentration used is in the range used effectively in previous studies to induce pretone in pulmonary arteries (Robertson *et al.*, 1995, Robertson *et al.*, 2001, Dipp *et al.*, 2001). The responses to 2 μM $PGF_{2\alpha}$ were significantly greater in the veins compared to the arteries (36.5 ± 5.5% of control, n = 19 compared to 12 ± 3.3% of control, n = 18, $P < 0.05$).

During concentration-dependent responses of veins to $PGF_{2\alpha}$, contractile oscillations were observed in 6 out of 7 pulmonary venous segments (85.7%). These were continuous oscillations around a steady baseline, which appeared usually after 2 or 5 μM $PGF_{2\alpha}$, and increased in frequency and amplitude with higher concentrations of $PGF_{2\alpha}$ (see representative trace in Figure 3.4B). When the concentration-dependent contractions were repeated after a period of relaxation, the oscillations appeared at lower concentrations of $PGF_{2\alpha}$ and had higher amplitudes.

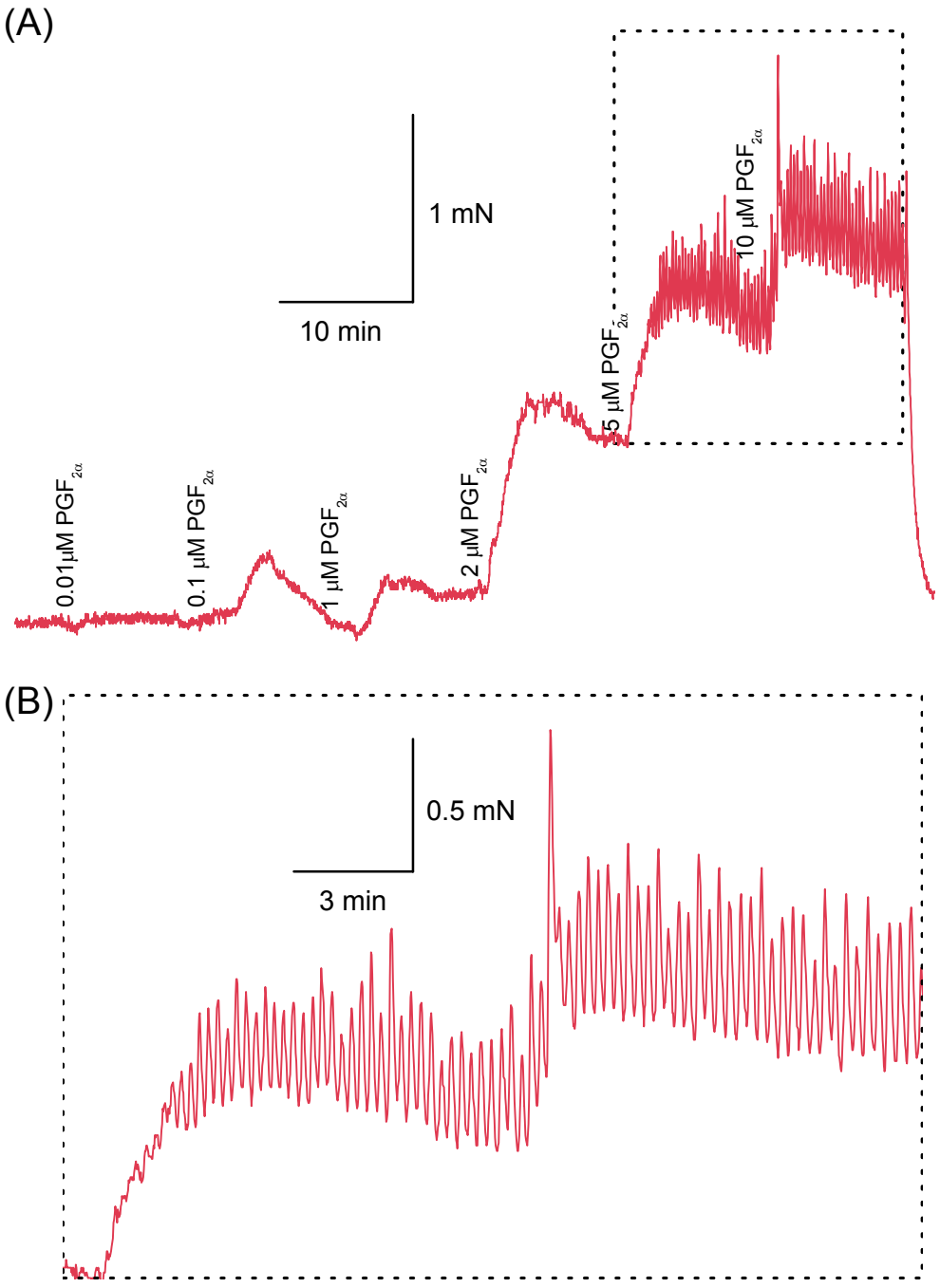

Figure 3.4. $PGF_{2\alpha}$-induced contractions of intrapulmonary veins.

(A) Intrapulmonary veins contracted in response to cumulative concentrations $PGF_{2\alpha}$, ranging from 0.01 µM to 10 µM. (B) The higher concentrations of $PGF_{2\alpha}$ induced contractile oscillations in the veins; trace represents enlarged view of marked area from (A).

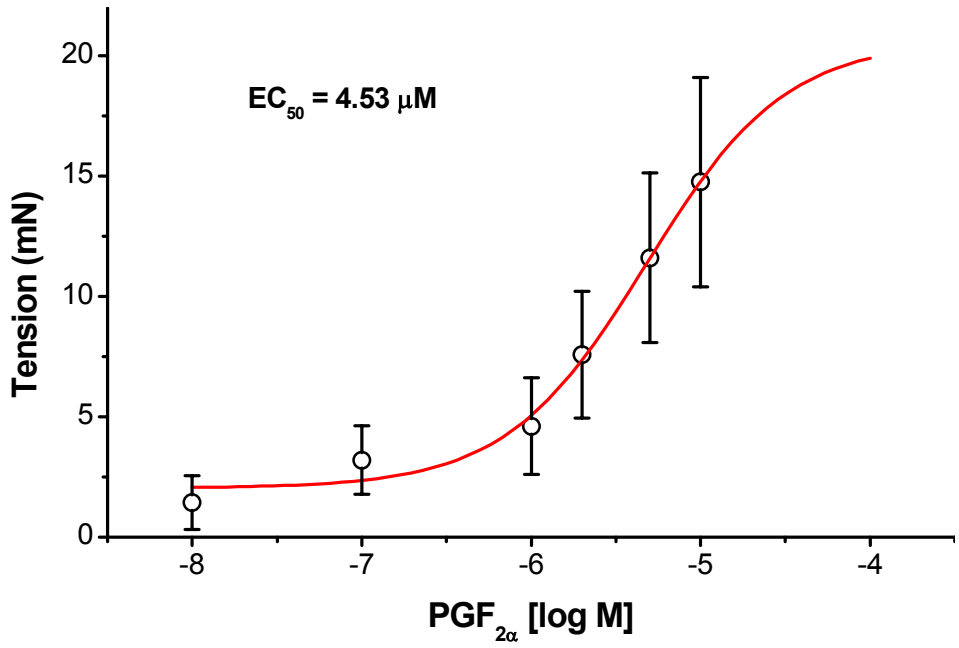

Figure 3.5. Concentration-response curve to $PGF_{2\alpha}$. Average contractile responses of intrapulmonary veins to various concentrations of $PGF_{2\alpha}$ (values represent mean ± SEM of 7 vessels from 6 animals). Red line represents non-linear curve fit using a variable Hill slope (EC_{50} = 4.53 µM).

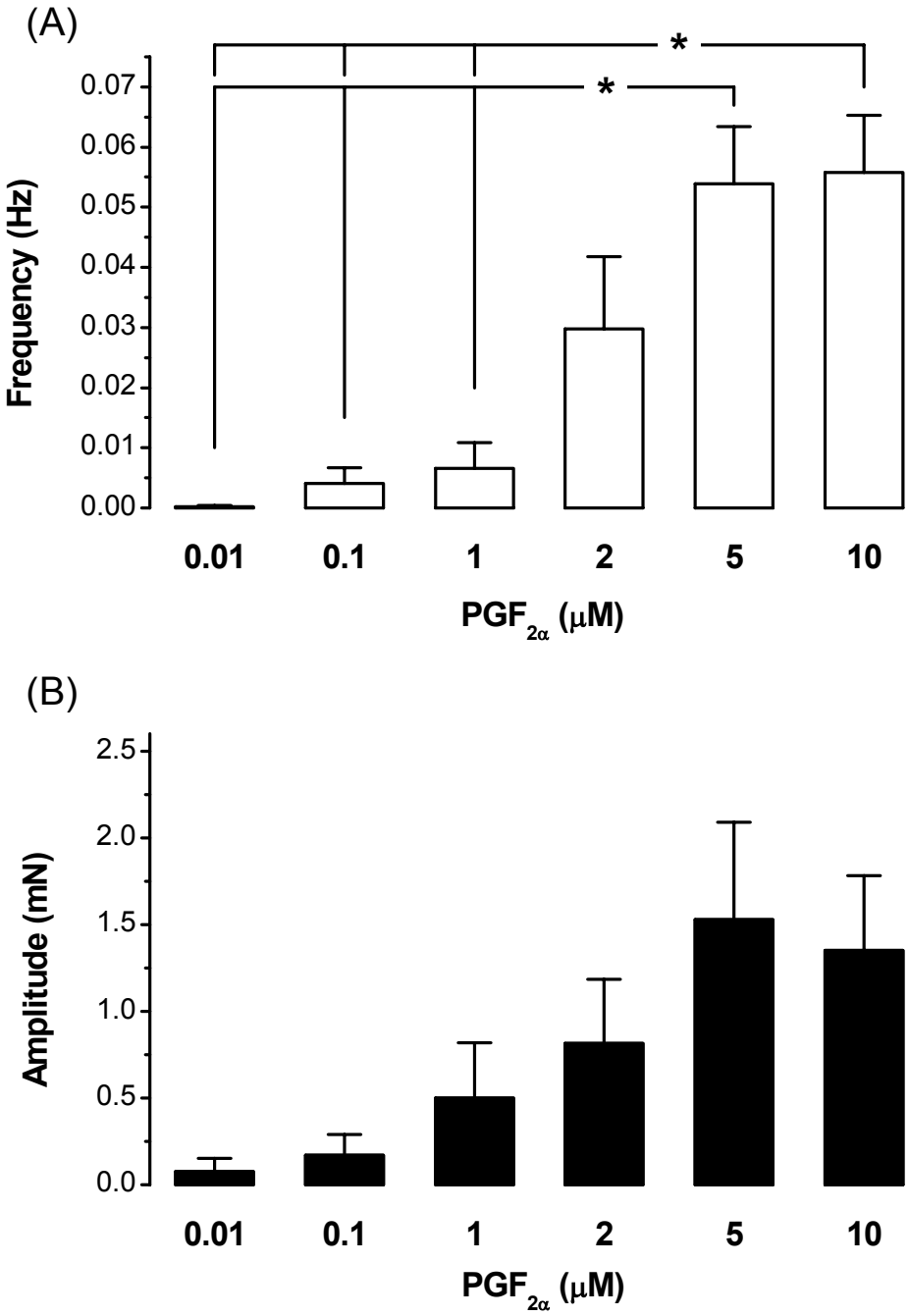

Figure 3.6. $PGF_{2\alpha}$ induced oscillations in the PV. The average frequency (A) and amplitude (B) of contractile oscillations induced in intrapulmonary veins by various concentrations of $PGF_{2\alpha}$. There was a significant difference between mean frequency and amplitude of groups with one-way ANOVA; * indicates significant difference between specific groups determined with Bonferroni's post-hoc analysis.

3.3.3. Hypoxia-induced responses in the PV and PA

Hypoxic stimulation (Po_2 < 20 mm Hg) applied while vessels were at resting tone induced contractions only in the veins (representative traces in Figure 3.7A). The venous response consisted of an early increase in tension (to a maximal level of 15.6 ± 3% of the KCl control, n = 7), which was followed by a relaxation to the initial baseline although hypoxia persisted. Conversely, intrapulmonary arteries did not contract to hypoxia in the absence of preconstriction.

When vessels were primed with $PGF_{2\alpha}$ (2 μM), the magnitude of the venous hypoxia-induced contractions increased significantly to 43.5 ± 5.1% of control (n = 9, P < 0.05). The shape of the hypoxic pressor response was similar to that of non-preconstricted veins (red trace in Figure 3.7B), with a prompt contraction following the lowering of O_2 concentration and a subsequent return to the level of $PGF_{2\alpha}$ induced tone.

Preconstricted intrapulmonary arteries also contracted to hypoxia, but their responses were significantly smaller than those of veins (13.4 ± 3.6% of control, n = 6, P < 0.05, see Figure 3.8B). The tension increase in arteries was considerably slower to develop, but was sustained over the entire 30 minutes period of hypoxia (blue trace, Figure 3.7B).

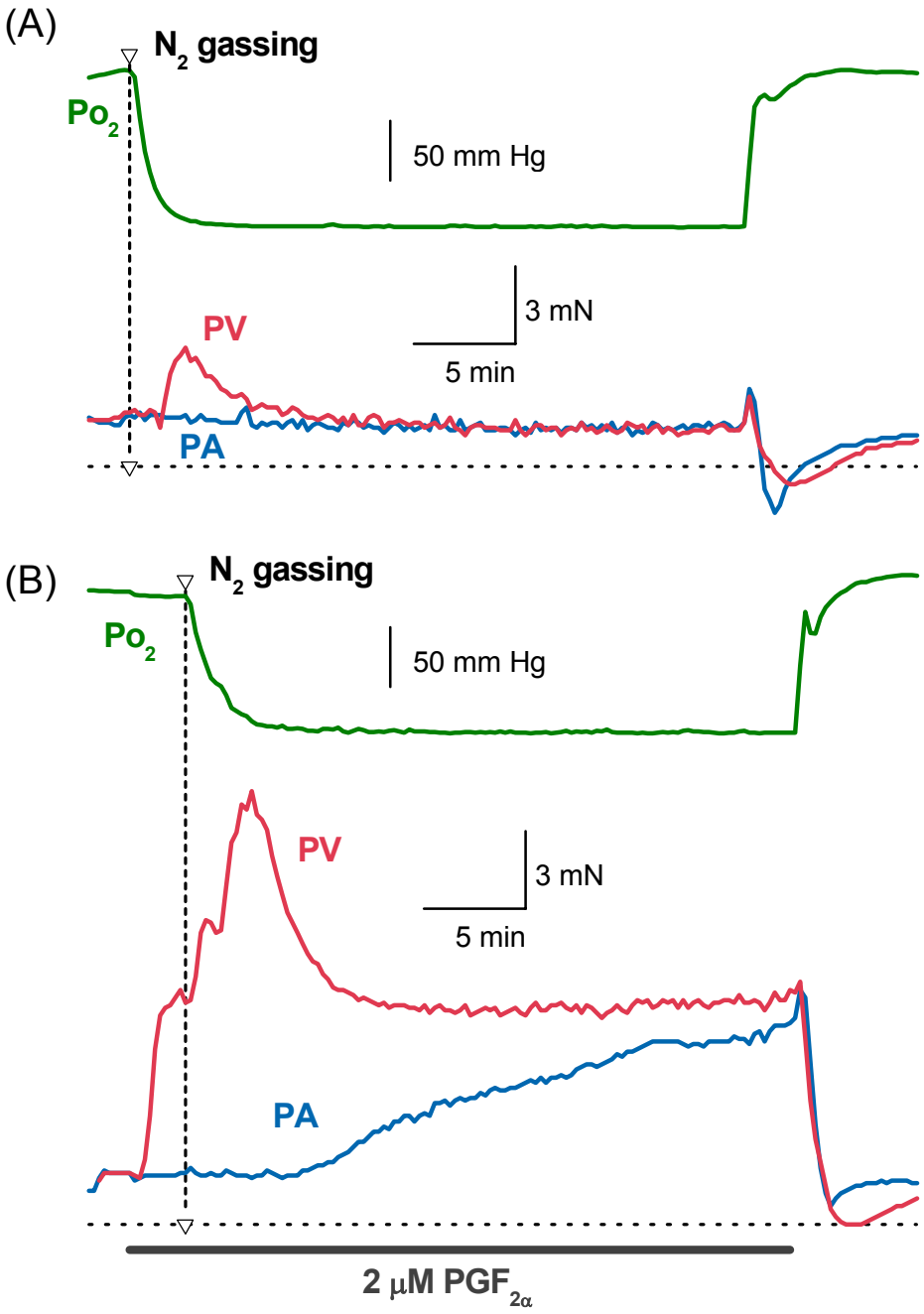

Figure 3.7. Representative responses of pulmonary veins and arteries to hypoxia. Traces represent typical hypoxia induced contractile responses in the pulmonary vein (*red*) and artery (*blue*) in the absence (A) and presence (B) of preconstriction with $PGF_{2\alpha}$; the horizontal dashed lines represent zero tension. Green traces show the corresponding Po_2 values.

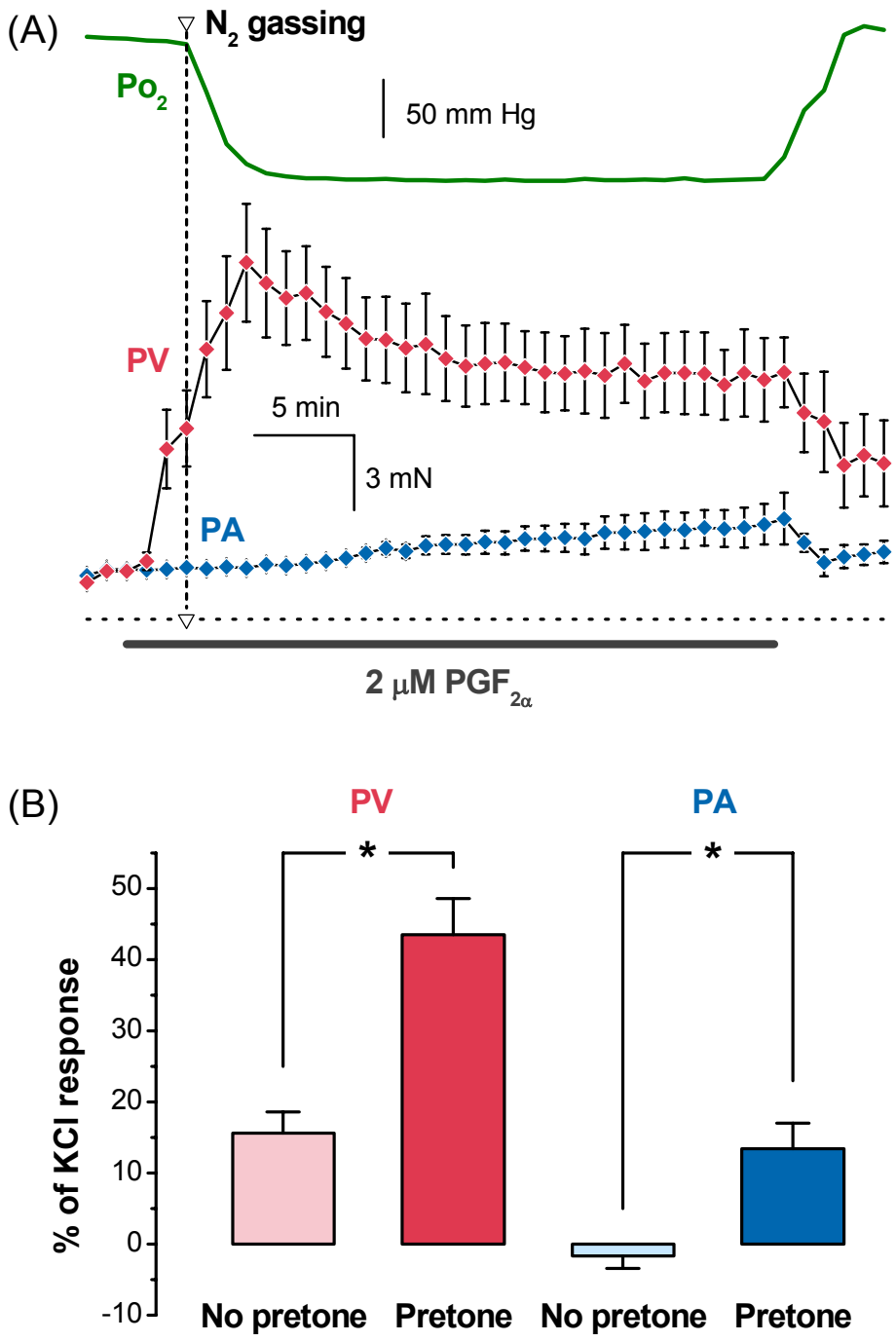

Figure 3.8. Average responses of preconstricted pulmonary arteries and veins to hypoxia. Time courses (A) and average values (B) of hypoxia-induced responses of pulmonary veins (*red*) (n = 9) and arteries (*blue*) (n = 6); data are shown as mean values ± SEM; the horizontal dashed line represents zero tension. Green trace shows an average of Po_2 values.

3.3.4. The effect of zero $[Ca^{2+}]_o$ and low $[Cl^-]_o$ and on PV and PA contractions

The effect of altering extracellular ionic concentrations on the agonist and hypoxia-induced responses was investigated by replacing standard HEPES-based bath solution (HBS) with $HBS_{Low\text{-}Cl}$ and $HBS_{Ca\text{-}free}$ extracellular media.

The response of veins to 80 mM KCl was inhibited in $HBS_{Ca\text{-}free}$ (6.1 ± 1.3 mN vs. 16 ± 2 mN, n = 7, $P < 0.05$), but was not affected in $HBS_{Low\text{-}Cl}$ (see Figure 3.9A). Similarly, in the arteries only $HBS_{Ca\text{-}free}$ significantly decreased KCl contractions (7.6 ± 1.2 mN vs. 14.4 ± 2.8 mN, n = 6, $P < 0.05$), while $HBS_{Low\text{-}Cl}$ had no effect (see Figure 3.9B).

Lowering extracellular Cl^- had opposite effects on $PGF_{2\alpha}$-induced contractions in veins and arteries. While the $PGF_{2\alpha}$ (2 μM) response was potentiated in arteries (6.4 ± 1.8 % vs. 0.9 ± 0.6, n = 7, $P < 0.05$) (see Figure 3.10B), the contraction of veins was inhibited (9.6 ± 4.8 % vs. 44.8 ± 7, n = 9, $P < 0.05$) (see Figure 3.10A). Venous contractions by $PGF_{2\alpha}$ were inhibited in $HBS_{Ca\text{-}free}$ (6 ± 6.5 %, n = 9, $P < 0.05$) (Figure 3.10A), but those of arteries were not significantly affected (4.7 ± 1.4%, n = 7, $P > 0.05$, Figure 3.10B).

The shape of the hypoxic pressor response in preconstricted veins and arteries was not fundamentally distorted by changing extracellular solutions, however its amplitude was affected (averaged time course responses in Figure 3.11).

Using $HBS_{Low\text{-}Cl}$ markedly enhanced the hypoxic response in arteries to 41.5 ± 9.8% from the control value of 13.4 ± 3.6% (n = 6, $P < 0.05$) (see Figure 3.12B), but did not significantly affect hypoxia-induced contractions of veins (38.9 ± 5.5% vs. 43.5 ± 5.1%, n= 9, p > 0.05) (see Figure 3.12A). In $HBS_{Ca\text{-}free}$, venous contractions to hypoxia were reduced (11 ± 5.1 %, n = 9, $P < 0.05$) (Figure 3.12A). In the arteries, $HBS_{Ca\text{-}free}$ did not significantly affect arterial responses to hypoxia (16 ± 5.3%, n = 6, $P > 0.05$, Figure 3.12B).

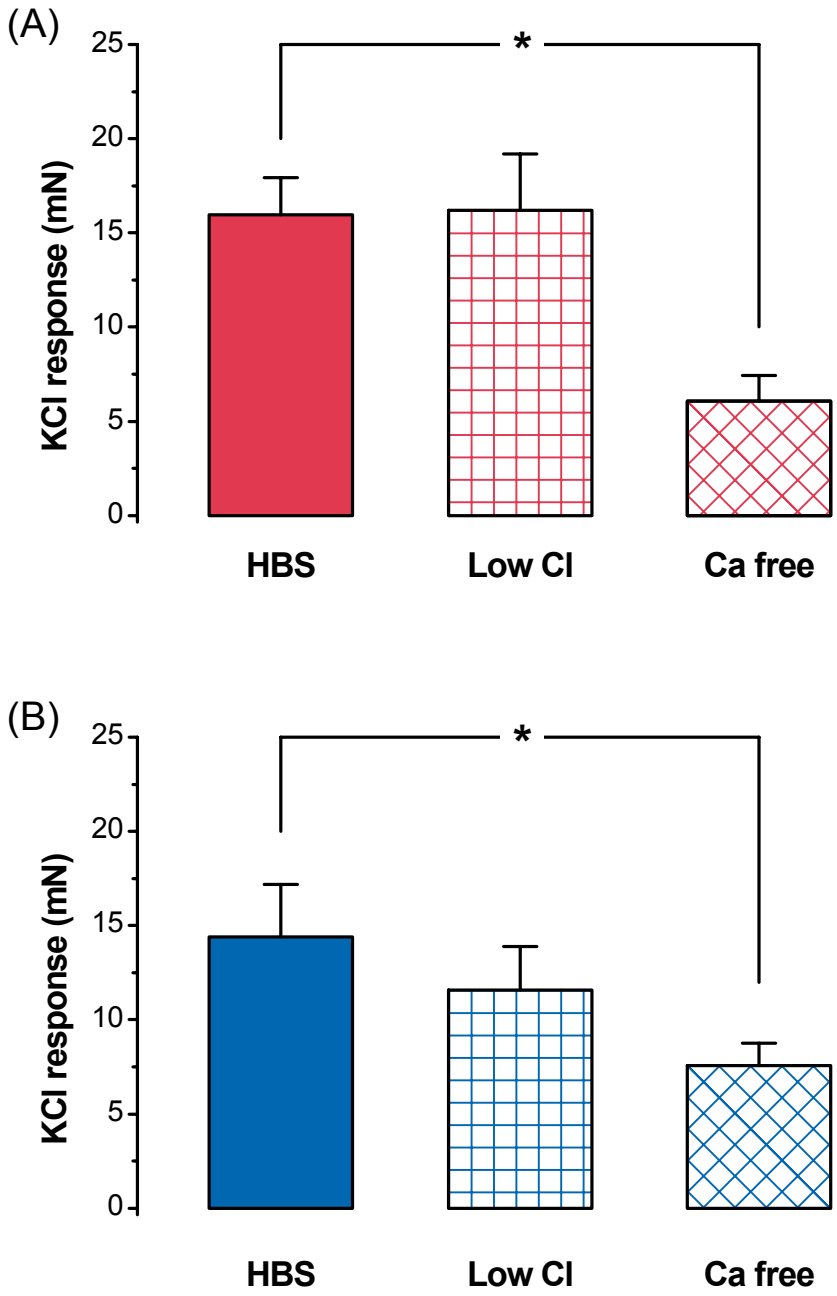

Figure 3.9. The effect of altering extracellular ionic concentrations on KCl contractions. Average KCl (80 mM) responses of intrapulmonary veins (A) (n = 7) and arteries (B) (n = 6) in different extracellular conditions (HBS, $HBS_{Low\text{-}Cl}$, $HBS_{Ca\text{-}free}$). Data are shown as mean values ± SEM; * indicates significant reduction in mean responses compared to controls in standard HBS ($P < 0.05$).

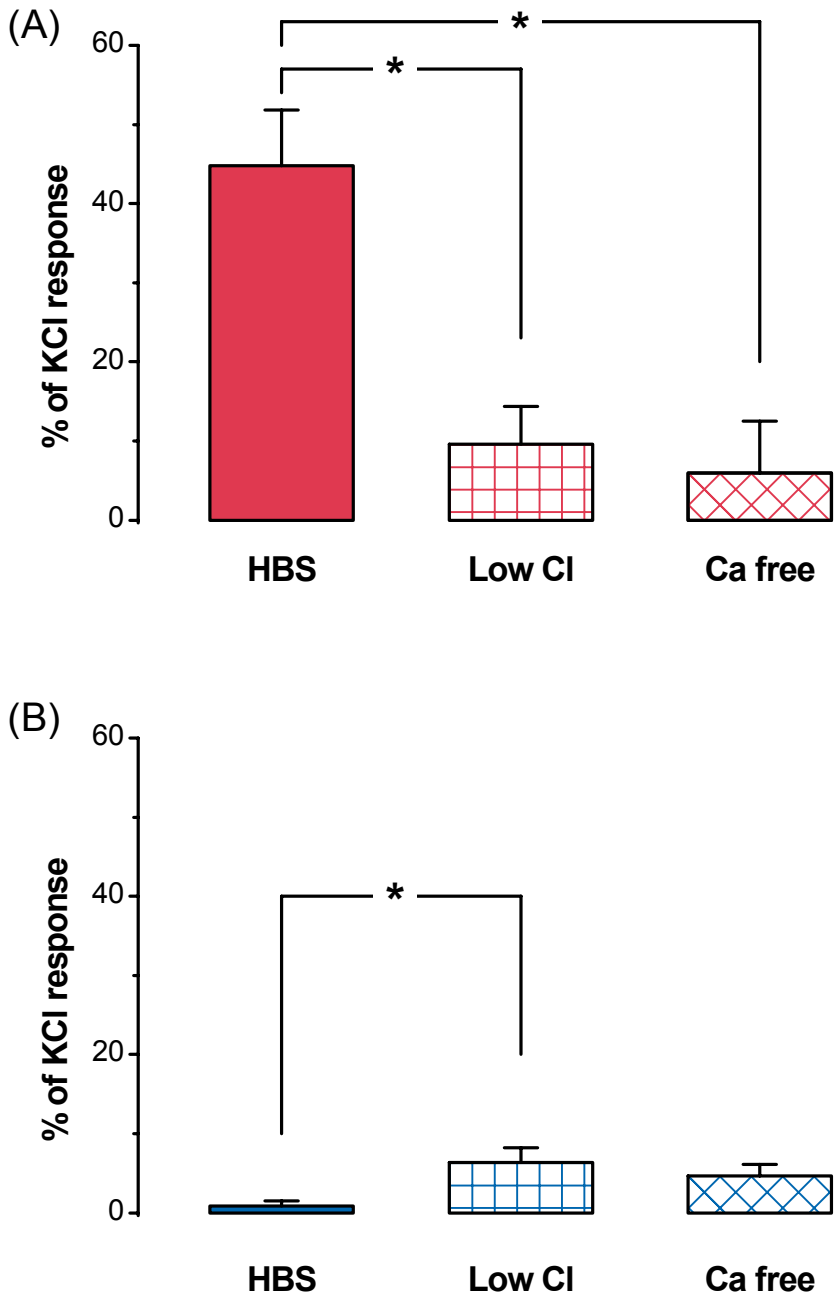

Figure 3.10. The effect of altering extracellular ionic concentrations on contractions to $PGF_{2\alpha}$. Average responses to $PGF_{2\alpha}$ (2 μM) of intrapulmonary veins (A) (n = 9) and arteries (B) (n = 7) in different extracellular conditions (HBS, $HBS_{Low\text{-}Cl}$, $HBS_{Ca\text{-}free}$). Data are shown as mean values ± SEM; * indicates significant change in mean responses compared to controls in standard HBS ($P < 0.05$).

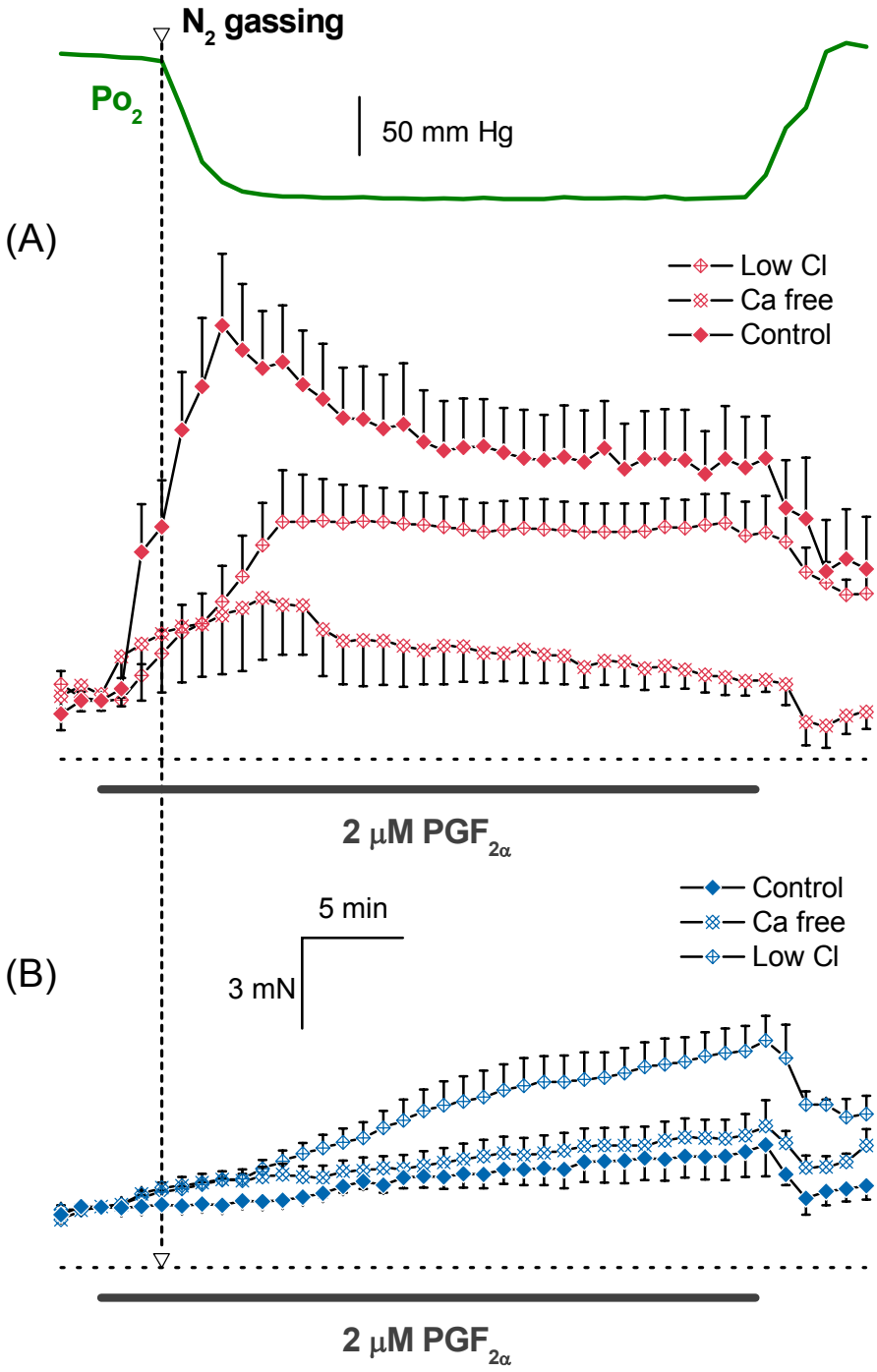

Figure 3.11. The effect of $HBS_{Low\text{-}Cl}$ and $HBS_{Ca\text{-}free}$ on hypoxic responses of preconstricted pulmonary arteries and veins. Average responses over time of preconstricted pulmonary veins (A) (n = 9) and arteries (B) (n = 6) in different extracellular conditions (HBS, $HBS_{Low\text{-}Cl}$, $HBS_{Ca\text{-}free}$); data are shown as mean values ± SEM; for clarity, not all error bars are shown. Green trace shows the average of Po_2 values.

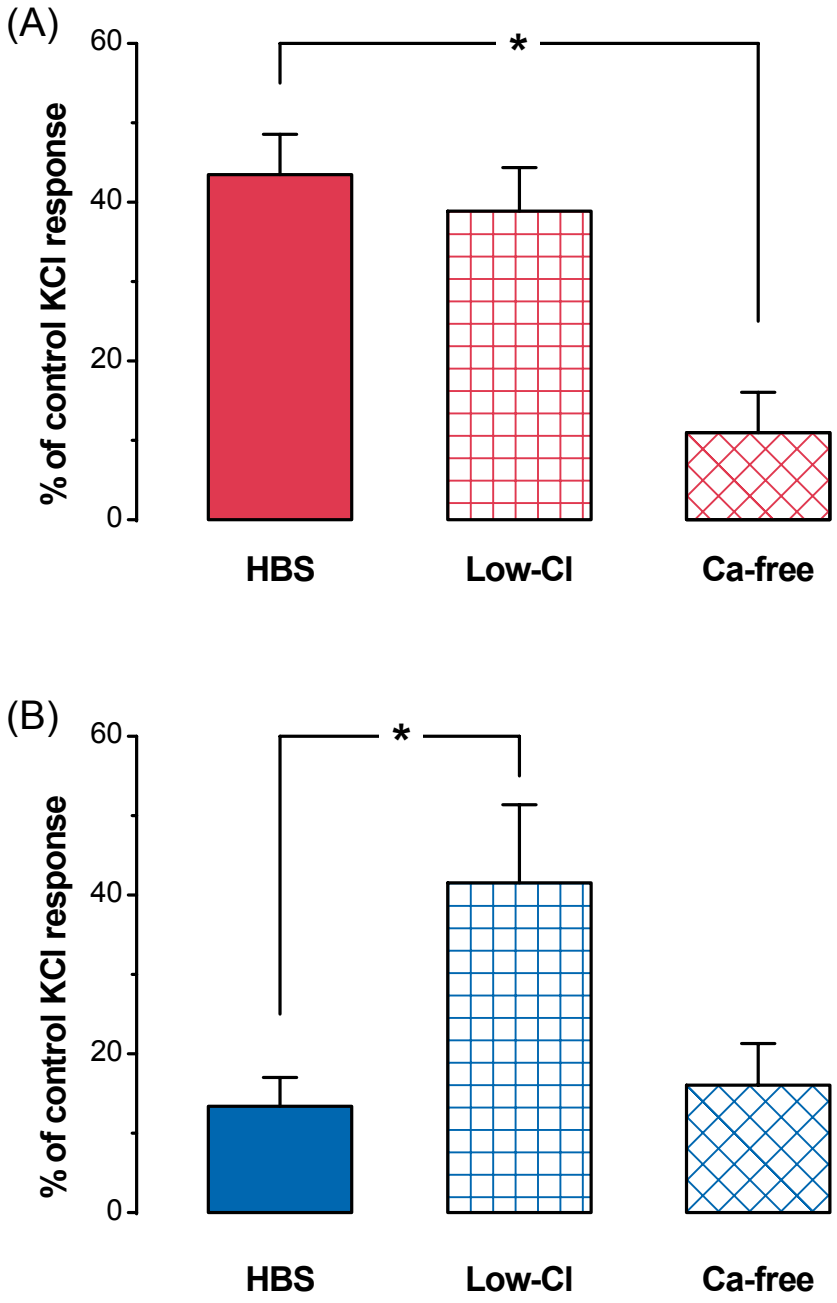

Figure 3.12. The effect of altering extracellular ionic concentrations on contractions to hypoxia. Hypoxia-induced responses of small pulmonary veins (A) (n = 9) and arteries (B) (n = 6) with pretone in different extracellular conditions (HBS, $HBS_{Low\text{-}Cl}$, $HBS_{Ca\text{-}free}$). HBS = standard HEPES-based bath solution; data are shown as mean values ± S.E.M; * indicates significant change in mean responses compared to controls in standard HBS ($P < 0.05$).

3.3.5. The effect of NFA and NPPB on the $PGF_{2\alpha}$ and hypoxia-induced vasoconstriction

In small intrapulmonary veins, NFA (50 μM) inhibited both the $PGF_{2\alpha}$ preconstriction (20.5 ± 7% compared to 43 ± 10.9%, n = 10, $P < 0.05$) (Figure 3.13A) and the hypoxic response (12 ± 4.6 % compared to 50.7 ± 10.9%, n = 10, $P < 0.05$) (Figure 3.14A), but NPPB (2 μM) had no significant effect on either response.

In the arteries, NFA (50 μM) did not significantly affect the $PGF_{2\alpha}$ or hypoxic responses (see Figure 3.13B and Figure 3.14B). However, NPPB (2 μM) potentiated the $PGF_{2\alpha}$ contractions (35.5 ± 10 % compared to 15.9 ± 5 %, n = 9, $P < 0.05$) (Figure 3.13B), but did not significantly affect the hypoxic response.

The concentration dependent effects of Cl^- channel blockers on agonist contractions were investigated further. NFA (Figure 3.15) enhanced the responses to $PGF_{2\alpha}$ in the concentration range 10^{-7} to 10^{-6} M. This effect was maximal at 0.1 μM in the veins and at 0.3 μM in the arteries. In the case of NPPB (Figure 3.16) a similar effect appeared to take place in the same concentration range, but despite the larger mean responses compared to controls, the effect was not statistically significant in either veins, or arteries.

At concentrations of approximately 10^{-5} M and higher, both antagonists increasingly inhibited the $PGF_{2\alpha}$-induced contractions. This effect was statistically significant at 30 μM in the veins and 100 μM in the arteries for NFA and at 10 μM in the veins for NPPB.

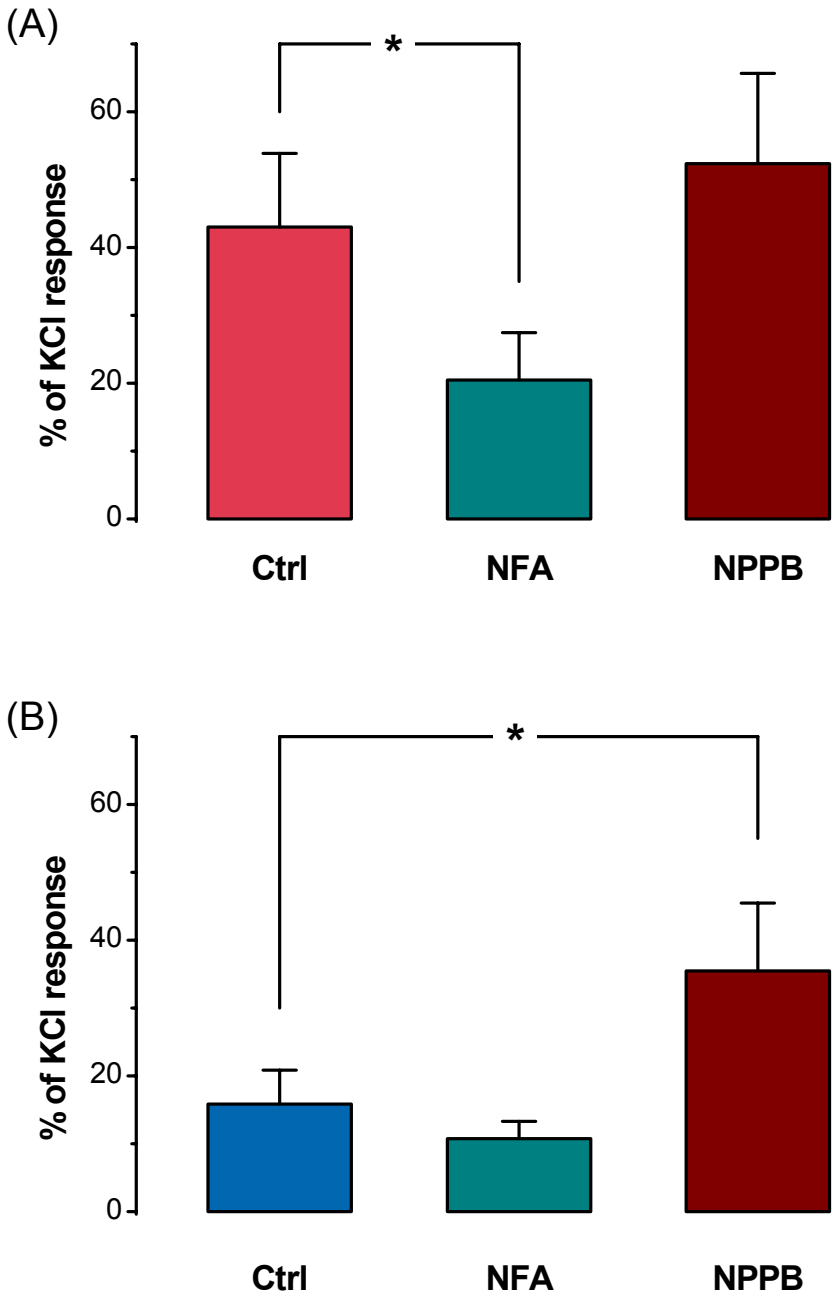

Figure 3.13. The effect of NFA and NPPB on $PGF_{2\alpha}$-induced contractions. Intrapulmonary veins (A) (n = 10) and arteries (B) (n = 9) contracted to $PGF_{2\alpha}$ (2 μM) in the presence of NFA (50 μM) and NPPB (2 μM). Data are shown as mean values ± S.E.M.; * indicates significant change in mean responses compared to controls ($P < 0.05$).

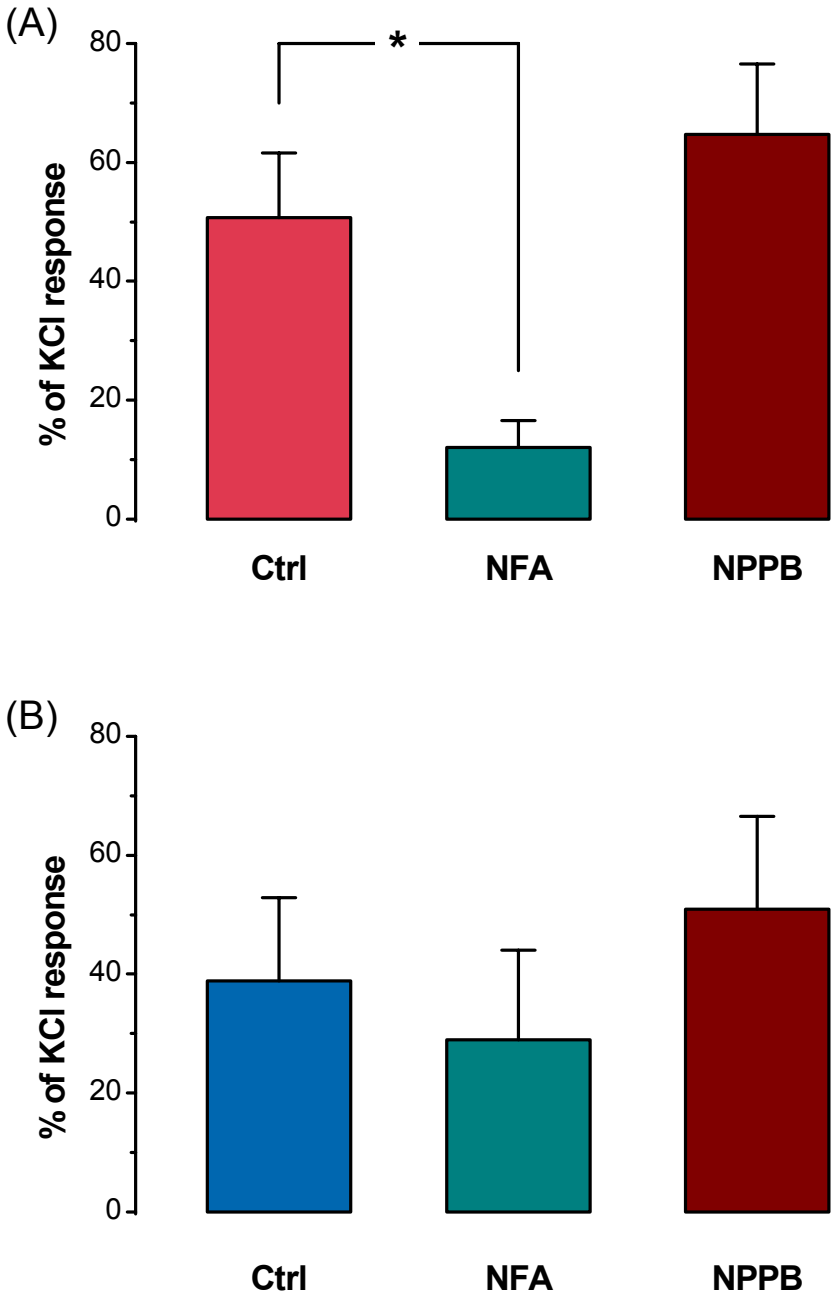

Figure 3.14. The effect of NFA and NPPB on hypoxia-induced contractions. Intrapulmonary veins (A) (n = 10) and arteries (B) (n = 9) contracted in response to hypoxia in the presence of NFA (50 μM) and NPPB (2 μM). Data are shown as mean values ± S.E.M.; * indicates significant change in mean responses compared to controls ($P < 0.05$).

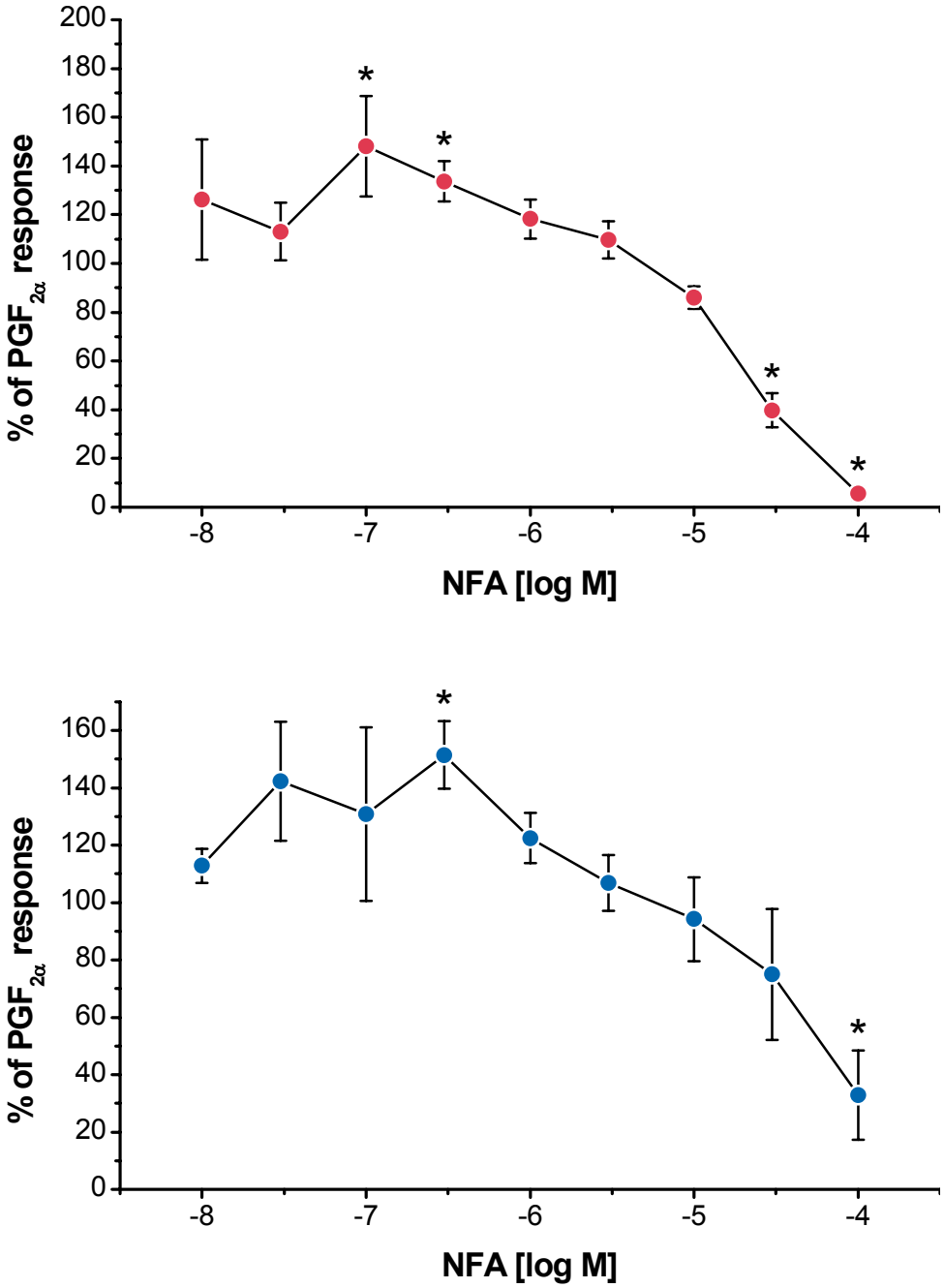

Figure 3.15. Concentration dependent effect of NFA on $PGF_{2\alpha}$-induced contractions. Responses of veins (A) (n = 5) and arteries (B) (n = 5) to $PGF_{2\alpha}$ (2 µM) in the presence of increasing concentrations of NFA (0.01 to 100 µM). Data are shown as percentages of the control $PGF_{2\alpha}$ contraction; values represent mean ± S.E.M; * indicates significant difference compared to control ($P < 0.05$).

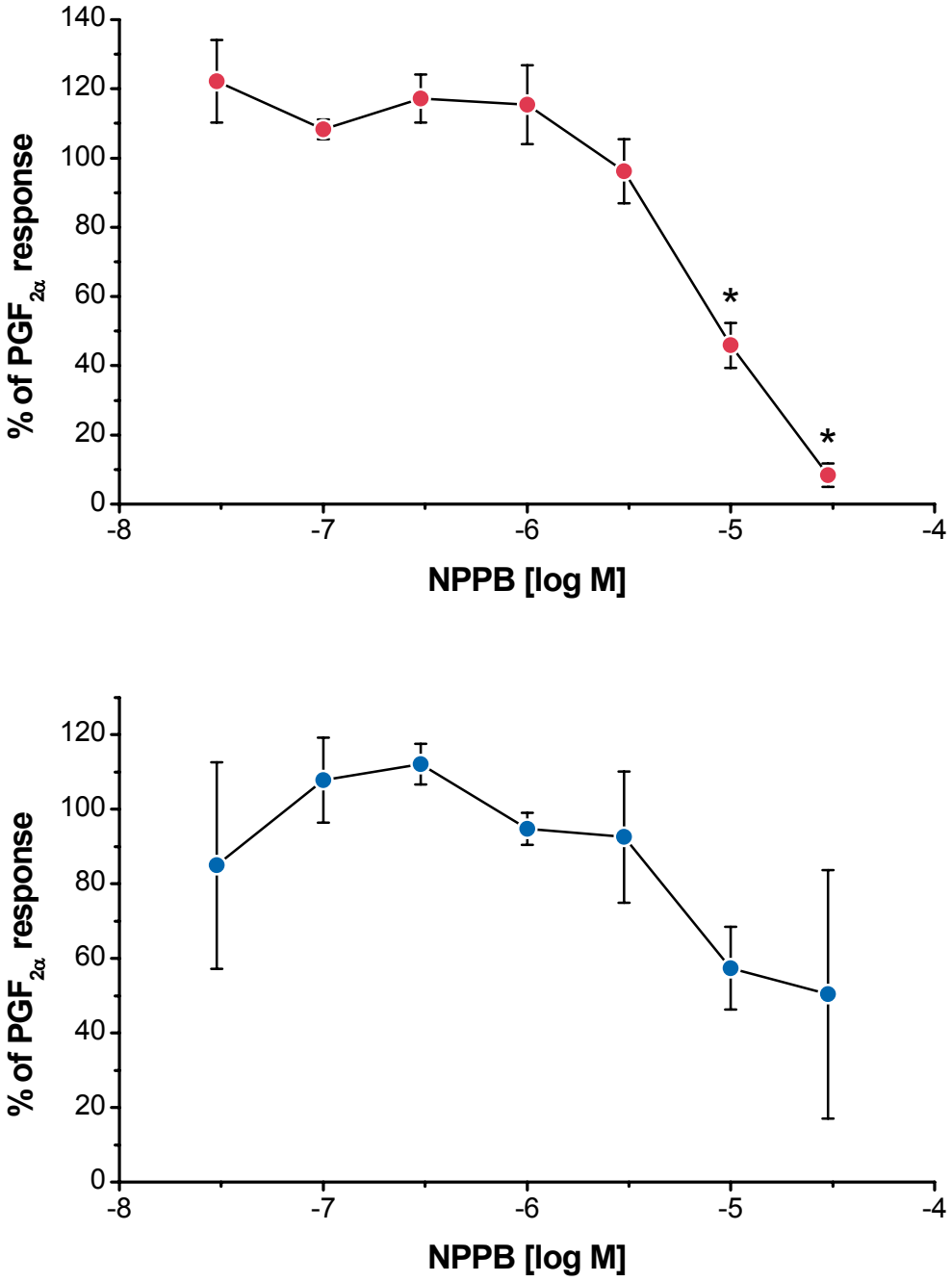

Figure 3.16. Concentration dependent effect of NPPB on $PGF_{2\alpha}$-induced contractions. Responses of veins (A) (n = 4) and arteries (B) (n = 4) to $PGF_{2\alpha}$ (2 µM) in the presence of increasing concentrations of NPPB (0.03 to 30 µM). Data are shown as percentages of the control $PGF_{2\alpha}$ contraction; values represent mean ± S.E.M; * indicates significant difference compared to control ($P < 0.05$).

3.4. Discussion

The contractile properties of isolated segments of distal intrapulmonary veins and arteries from the pig were investigated using wire myography; the main findings were the demonstration of agonist and hypoxia-induced contractions in both types of vessel, with particular differences in the role of Ca^{2+} and Cl^- conductances and the veins consistently showing more robust responses than arteries.

Small porcine intrapulmonary veins contracted more than size-matched arteries in response to both KCl (80 mM) and $PGF_{2\alpha}$ (2 μM). Greater venous contractions in the pulmonary circulation have been reported before with agonists such as histamine, 5-HT (Shi *et al.*, 1998), ET-1 (Toga *et al.*, 1992, Wang and Coceani, 1992), and thromboxane (Kemp *et al.*, 1997, Shibamoto *et al.*, 1995, Arrigoni *et al.*, 1999). However, the contrary was shown in other studies, such as with ET-1-induced contractions in guinea pig pulmonary vessels (Cardell *et al.*, 1990), 5-HT in dogs (al-Tinawi *et al.*, 1994) and noradrenaline in sheep (Kemp *et al.*, 1997). These variations are probably due to differences in the size of vessels used, as well as the diversity of experimental setups and species.

In the presence of $PGF_{2\alpha}$, spontaneous contractile oscillations became apparent in the pulmonary veins, but not in the arteries. The amplitude and frequency of these oscillations were enhanced by increasing the concentration of $PGF_{2\alpha}$. Similar $PGF_{2\alpha}$-stimulated oscillations in active tension have been reported before in vascular (Jackson, 1988), myometrial (Phillippe *et al.*, 1997) and epididymal smooth muscle (Mewe *et al.*, 2006). In the myometrium, these phasic contractions are thought to be caused by underlying oscillations of $[Ca^{2+}]_i$, which occur through the activation of the phosphatidylinositol signalling pathway (Phillippe *et al.*, 1997). No further systematic investigation on the mechanisms underlying these oscillations in porcine PV was made, but their presence suggests a predisposition of pulmonary venous smooth muscle towards phasic contractions.

When hypoxia was induced without preconstriction, only veins contracted. This is consistent with previous observations in pulmonary vessels from pigs (Miller *et al.*, 1989) and sheep (Uzun and Demiryurek, 2003). In the presence of preconstriction, the hypoxic contraction of veins was significantly increased. Preconstricted arteries also responded to hypoxia. Similarly, rat pulmonary arteries also contracted significantly to hypoxia only in the presence of agonist induced pretone (Bennie *et al.*, 1991, Leach *et al.*, 1994), but those from cats (Madden *et al.*, 1985) and rabbits (Dipp *et al.*, 2001) showed HPV responses even without preconstriction. The hypoxia-induced venous contractions were significantly larger than arterial ones, which is in agreement with previous reports in the rat (Zhao *et al.*, 1993), but contrary to findings in cat lungs (Nagasaka *et al.*, 1984).

The shape of HPV responses seen in the two types of vessel also differed. Following the onset of hypoxia, the tension in the veins rose rapidly. The contraction was maximal after approximately 5 to 10 minutes, and this was followed by partial relaxation and a steady level of tension. Similar hypoxic responses were seen in rat pulmonary veins (Zhao *et al.*, 1993).

In contrast, the hypoxic response in the arteries was slow to develop, and consisted of a monophasic sustained contraction over the entire 30 minutes of the hypoxic challenge. In some preparations of isolated pulmonary arteries, the hypoxic response is composed of two phases (Bennie *et al.*, 1991). The first, transient contraction seen in most (Robertson *et al.*, 1995, Dipp *et al.*, 2001, Leach *et al.*, 2001), but not all preparations (Talbot *et al.*, 2003), was not present in porcine intrapulmonary arteries under the conditions used in this study. However, only the sustained phase, which resembles the response seen here, is thought to be physiologically relevant, because the initial phase is transient in nature and has been reported to also occur in systemic arteries (Ward and Aaronson, 1999).

Removing extracellular Ca^{2+} produced an inhibition of venous responses to both $PGF_{2\alpha}$ and hypoxia, but had no significant effect on contractions of arteries. These

findings are consistent with reports of greater susceptibility of venous contractions to Ca^{2+}-free media compared to arteries (Mikkelsen and Pedersen, 1983). Furthermore, pulmonary arterial smooth muscle has a greater amount of SR compared to other types of smooth muscle (Devine *et al.*, 1972), which could explain its lesser reliance on extracellular Ca^{2+} influx during contraction.

Low extracellular Cl^- potentiated $PGF_{2\alpha}$-induced contraction in pulmonary arteries. Chloride currents have been shown to contribute to agonist-induced contraction of vascular smooth muscle (Lamb and Barna, 1998). Moreover, the data demonstrate that $HBS_{Low\text{-}Cl}$ increased the hypoxia-induced arterial contractions. However, $HBS_{Low\text{-}Cl}$ did not significantly affect hypoxic responses of veins, but did attenuate the $PGF_{2\alpha}$-induced contraction.

The two Cl^- channel blockers NFA and NPPB differed in their effects on $PGF_{2\alpha}$ and hypoxia-induced contractile responses. This may have been due to concentration-dependent differences in their actions, but also to non-specific effects on ion channels. NFA significantly inhibited contractions to both $PGF_{2\alpha}$ and hypoxia in the veins, but not in the arteries. These results suggest an NFA sensitive conductance is important in the hypoxic response of porcine intrapulmonary veins. This underlying pathway could involve an NFA sensitive Cl_{Ca} conductance that contributes to agonist-induced contraction (Yuan, 1997). Alternatively, NFA may reduce venous contractions through non-specific activation of BK_{Ca} channels (Ottolia and Toro, 1994, Greenwood and Large, 1995), which is known to promote vasodilation in pulmonary vessels (Barman *et al.*, 2003).

Overall, the results of the wire myography studies presented here show clear differences exist between the contractility of porcine intrapulmonary veins and arteries, in respect of the size and dynamics of responses to KCl, $PGF_{2\alpha}$ and hypoxia. These findings suggest the participation of veins to hypoxic pulmonary vasoconstriction could involve yet unknown underlying mechanisms specific to pulmonary veins.

In humans and other large mammals including pigs, vascular tone in distal intrapulmonary veins is determined exclusively by the contraction of smooth muscle cells, as cardiomyocytes only exist in the wall of extrapulmonary veins (Nathan and Gloobe, 1970, Masani, 1986). By controlling the membrane potential, ion channels in the plasma membrane of smooth muscle cells play a key role in the generation and regulation of vascular tone.

Substantial research has been carried out in the pulmonary arteries to investigate hypoxic pulmonary vasoconstriction at cellular level, including involvement of ion channels. By comparison, information on the effects of hypoxia on signal transduction pathways in pulmonary veins smooth muscle cells (PVSMC) is effectively nonexistent. Therefore, the aim of the following studies is to isolate smooth muscle cells from porcine intrapulmonary veins and investigate the effects of hypoxia on specific ion conductances (K_v, Cl_{Ca}, L-type Ca^{2+}) in single porcine PVSMC, which would provide direct insight on the contractile mechanisms of hypoxia-induced responses in the PV from pig.

Chapter 4.
Morphological and electrical membrane properties of PVSMC

4.1. Introduction

Isolated segments of porcine intrapulmonary veins exhibited significant vasoactivity in response to agonists and hypoxia, with greater contractions than in arteries of similar size. In all blood vessels, vascular smooth muscle cells are the main determinant of mechanical activity. The degree of smooth muscle contraction is modulated by factors intrinsic and extrinsic to the blood vessel, but ultimately it is the contraction of individual myocytes that leads to the development and maintenance of vascular tone.

The contractility of single smooth muscle cells is closely linked, through the second messenger Ca^{2+}, to membrane excitability and ion channel activity. Therefore, understanding the resting membrane properties of single myocytes, together with the properties of voltage-activated currents which regulate their membrane potential, is part of the process of elucidating the mechanisms underlying the control of vascular tone. Furthermore, certain features of cell shape (Tolic-Norrelykke and Wang, 2005) or size (Murphy and Khalil, 2000) may be linked with contractile force or Ca^{2+} handling in smooth muscle cells.

Owing to the development of cell isolation techniques and patch-clamping electrophysiology (Hamill *et al.*, 1981), smooth muscle cells from various vascular

beds have been extensively examined across different species. Morphological features such as shape, size and cell surface area, as well as passive electrical properties like resting membrane potential and membrane capacitance have been described in myocytes from rabbit pulmonary artery (Clapp and Gurney, 1991), dog (Wilde and Lee, 1989) and rabbit coronary artery (Matsuda *et al.*, 1990), canine renal artery (Gelband and Hume, 1992), human omental artery (Hughes *et al.*, 1994) and rabbit portal vein (Hume and Leblanc, 1989). However, smooth muscle cells from the pulmonary veins have so far not been morphologically and electrophysiologically characterised.

The aim of this study is to obtain fresh physiologically viable single smooth muscle cells through enzymatic dissociation of intrapulmonary venous smooth muscle from the pig; and, for the first time, to characterise these cells morphologically by light microscopy and analyse their membrane properties through the use of patch-clamping techniques.

4.2. Methods

4.2.1. Morphometric measurements

Following completion of the enzymatic dispersion protocol (for details, see section 2.3.2) and trituration with a wide-bore Pasteur pipette, approximately 0.5 ml of cell suspension was transferred onto a glass coverslip and the cells were left to settle for approximately 10-15 minutes.

The coverslip was mounted on the stage of a Leica DMI4000 B inverted microscope (Leica Microsystems CMS GmbH, Germany) equipped with a phase-contrast objective (magnification x20; numerical aperture 0.40). Phase-contrast photomicrographs were acquired using a Leica DFC300 FX digital colour video camera (Leica Microsystems Ltd, Heerbrugg, Switzerland) and the Leica Application Suite (LAS) software (Version 2.5.0 R1, Leica Microsystems Ltd).

Images were analysed and measurements made using the software package ImageJ, version 1.38 (US National Institutes of Health, Bethesda, Maryland, USA; available from http://rsb.info.nih.gov/ij/).

The following morphological parameters were calculated for every PVSMC:
- the *cell perimeter*, determined as the length of the outline (boundary) of the cell as measured on the photomicrograph;
- the *projected area of the cell*, defined as the total area enclosed by the cell outline;
- the *cell length and width*, calculated using the perimeter and projected area and approximating the cell with an ellipse;
- the *circularity of the cell*, which provides a measure of elongation and was calculated using the perimeter and projected area;
- the *tri-dimensional membrane surface*, calculated by approximation with a tri-dimensional ellipsoid.

Data are presented as mean ± SD and the distribution of data values is characterised by the range (minimum and maximum values) and the coefficient of variation (CV). CV is a unitless ratio of the standard deviation to the mean and is a statistical measure useful for comparing the dispersion between different groups, even if their means are significantly different from each other:

$$CV = \frac{SD}{mean} \qquad (1)$$

Histograms were plotted for each parameter and values were fitted with a Gaussian probability density function:

$$f(x) = \frac{1}{\sigma\sqrt{2\pi}} e^{-\frac{(x-\mu)^2}{2\sigma^2}} \qquad (2)$$

where σ is the standard deviation and μ is the mean.

4.2.2. Passive membrane properties

4.2.2.1. Resting membrane potential

Once the whole-cell configuration was established in patch-clamp experiments, the membrane potential was measured under resting conditions by switching to current clamp (at zero current). The data was systematically recorded for each cell in standard bath solution prior to starting experimental protocols. The values are presented as recorded, without being adjusted for differences induced by liquid junction potentials, as explained in section 2.4.5.

4.2.2.2. C_m and R_s

Membrane capacitance (C_m) is a measure of the ability of the cell membrane to store electrical charge and depends on the total surface of the membrane (Molleman, 2003). For this reason, it is regularly used to normalise whole cell currents for cell size, by converting the current values into current densities (current/membrane capacitance).

In the whole-cell patch-clamp configuration, series resistance (R_s) represents the resistance met by the current before it passes through the cell and is used to assess the quality of the patch configuration. It consists of the pipette resistance (which is normally low ~ 2-5 MΩ) and the patch resistance (which becomes very low once the patch has been ruptured to achieve the whole-cell configuration and is sometimes renamed access resistance). R_s reduces the actual voltage experienced by the patched cell, and therefore should be kept as low as possible, preferably less than 20 MΩ (Molleman, 2003). A high R_s suggests inadequate voltage clamping and affects the quality of the resulting recordings.

R_s and C_m can be calculated by analysing the capacitive current elicited in response to a depolarising step, as detailed below (Ogden and Stanfield, 1994). Following an induced change in potential (by applying a square test pulse), the voltage changes

gradually over the capacitor as the charge builds up exponentially and then reaches a steady state. This process is reflected in an initial spike in current followed by an exponential decrease (usually referred to as *the transient capacitive current*). The decay of this current is proportional to R_s and C_m and therefore the time constant of the decay of the capacitive current (τ) can be used to infer these parameters:

$$\tau = R_s C_m \tag{3}$$

A sample depolarisation-induced current is shown in Figure 4.1. The inset illustrates the capacitive portion of the current fitted with the following exponential decay function:

$$I(t) = I_{peak} e^{-t/\tau} \tag{4}$$

where I_{peak} is the initial amplitude of the capacitive current and τ is the exponential time constant of decay of the capacitance current.

R_s (in MΩ) was then calculated as the size of the applied voltage step divided by the peak capacitive current it elicits (according to Ohm's law):

$$R_s = V_{step} / I_{peak} \tag{5}$$

where V_{step} (in mV) is the size of the depolarising voltage step and I_{peak} (in nA) is the amplitude of the capacitive current.

R_s was then used for the calculation of membrane capacitance (C_m, in pF), using the following formula:

$$C_m = \tau / R_s \tag{6}$$

where τ (in ms) is the time constant of the capacitive current decay and R_s (in GΩ) is the series resistance.

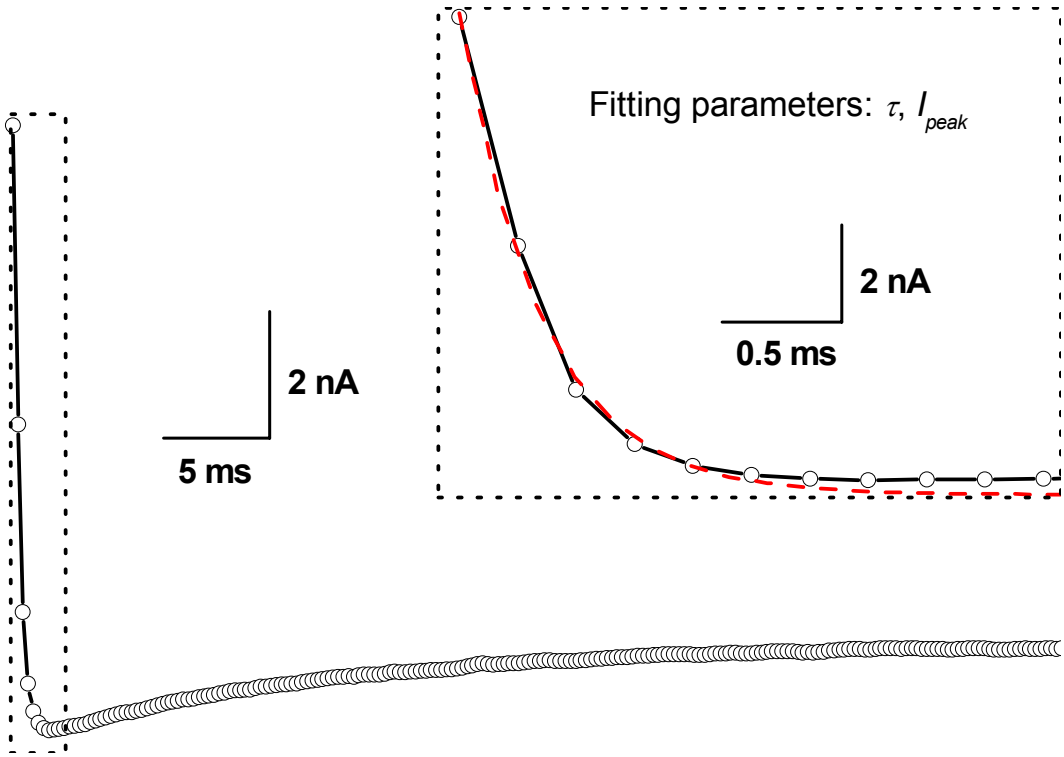

Figure 4.1. Exponential decay of the capacitive transient. Representative current trace used for calculating access resistance and membrane capacitance.
Inset: capacitive transient portion of the current; dashed red line represents the exponential decay curve fitted to the capacitive transient. The parameters that result from the fit (I_{peak} and τ) are used to calculate series resistance and membrane capacitance.

4.3. Results

4.3.1. Cell morphology

As indicated in the description of the process of developing the cell isolation protocol (section 2.3), the yield of cells and the proportion between elongated, contracted and damaged cells varied somewhat with each isolation procedure from a different animal.

However, the type of cells that were found to be viable for use in patch-clamping experiments typically appeared relaxed and elongated (as shown in Figure 4.2). These cells were spindle-shaped, without striations and with a single, centrally located nucleus, all characteristic features for smooth muscle cells.

4.3.2. Cell perimeter and projected area

Measurements were made on 258 cells from 8 intrapulmonary veins each dissected from a different animal on separate experimental days. Only viable cells were taken into consideration, where viability was indicated by a bright halo around the cell membrane (Driska and Porter, 1986). Cells that were contracted or had blebs of the membrane were non included in the analysis.

Using ImageJ, outlines were traced for each viable cell (example shown in Figure 4.4A) and measurements were obtained for the perimeter (in pixels) and area (in pixels^2) of every cell. The values were subsequently converted to μm^2 and μm respectively, using the conversion factor corresponding to x20 magnification (0.46 μm/pixel, as recorded by the Leica Application Suite software when the images were captured).

Figure 4.2. Typical examples of porcine PVSMC. Phase-contrast photomicrograph acquired at 20x magnification. The cells were elongated and had intact membranes, as indicated by the surrounding bright halo.

The cell perimeter had a minimum value of 155.2 μm and a maximum value of 712.9 μm, while the CV was 0.23. The mean perimeter was 354 ± 81.6 μm (n = 258; histogram shown in Figure 4.3B).

The projected area of intrapulmonary vein smooth muscle cells ranged from 331.5 μm^2 to 1862.8 μm^2. The distribution of values is shown in the histogram in Figure 4.3A, and was characterised by a coefficient of variation of 0.25. The average value was 1070.2 ± 267.6 μm^2 (mean ± SD; n = 258).

4.3.3. Cell length and width

In order to calculate the length and width of each cell, the shape of PVSMC was approximated to an ellipse. The corresponding ellipse was considered to have the area and perimeter of the cell as measured on the photomicrographs using the ImageJ software. Following this approximation, the length and width of PVSMC were considered to be equal to the major and minor axis of the equivalent ellipse (as shown in Figure 4.4B).

This approach was considered to be a reliable way of estimating the length and width of cells, because it excluded the error that would have been introduced through manual measurement of diameters directly on photomicrographs.

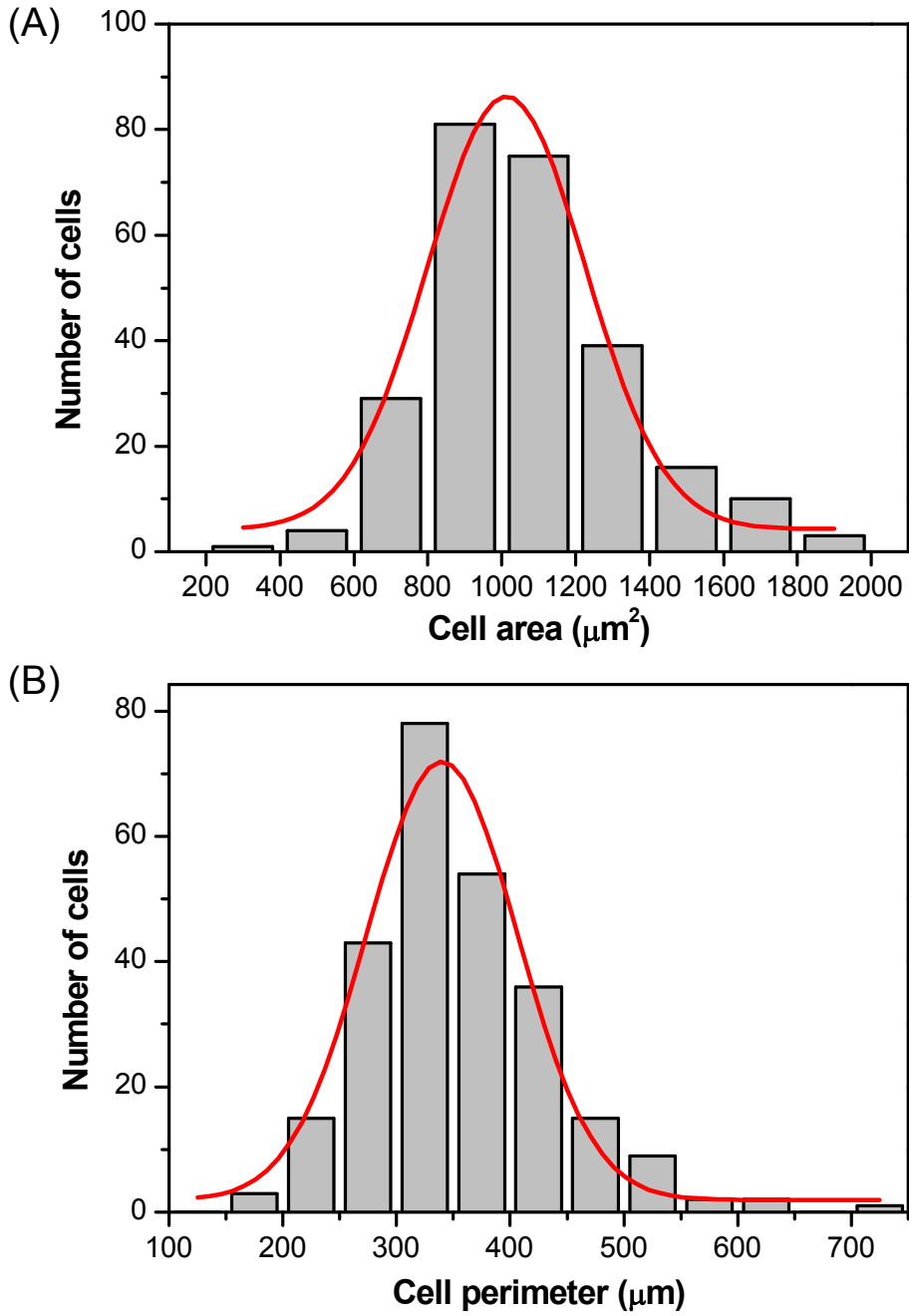

Figure 4.3. Projected area and perimeter of PVSMC. Histograms illustrate the distribution of (A) projected cell area and (B) perimeter of PVSMC, as measured on photomicrographs. Data values were fitted with Gaussian distributions (red curves).

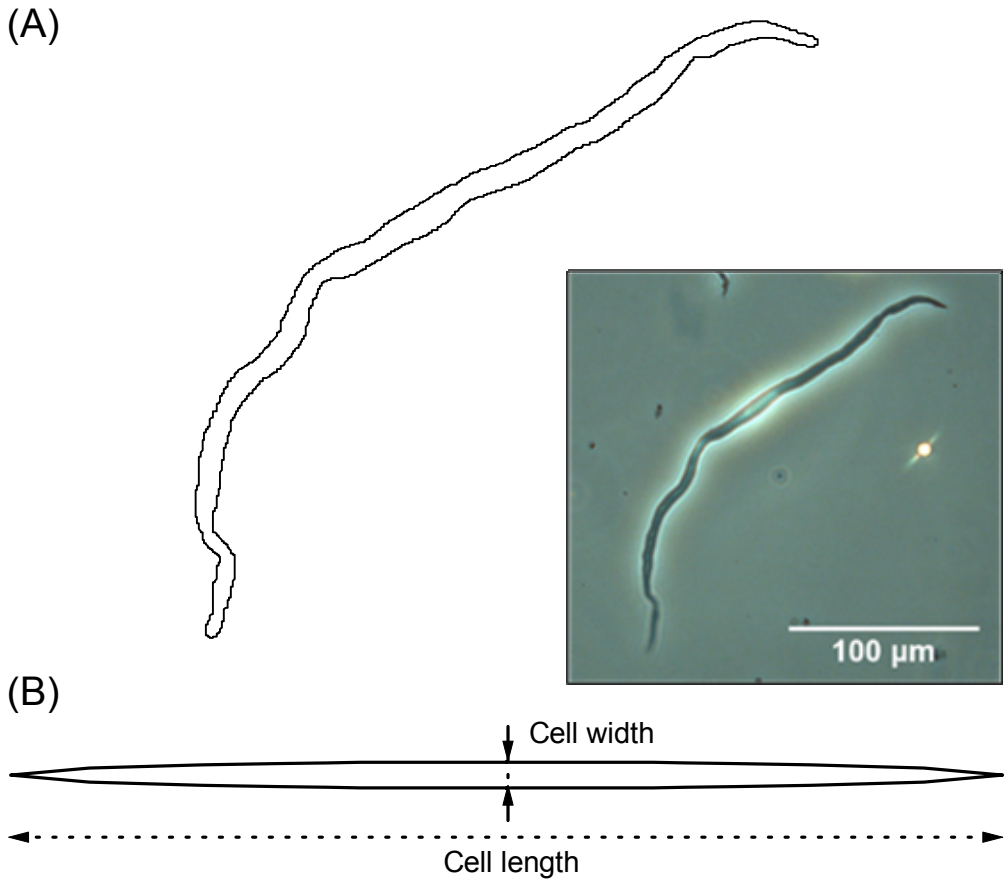

Figure 4.4. Estimation of cell shape. Shape of PVSMC was approximated to an ellipse for consistency of cell measurements. (A) Actual outline of a representative smooth muscle cell as drawn in ImageJ. *Inset*: photomicrograph of the same cell. (B) The corresponding ellipse of the same area and circumference as the cell shown in (A). The ellipse axes were used to approximate cell length and width.

The calculation of the ellipse axes was based on the following standard formula for the area of an ellipse

$$A = \pi ab \tag{7}$$

and a second formula by Euler which approximates the circumference or perimeter of an ellipse (Almkvist and Berndt, 1988):

$$P = \pi\sqrt{2(a^2 + b^2)} \tag{8}$$

where *a* and *b* are the semi-major and semi-minor axes of the ellipse, respectively.

From the two equations above and considering *A* and *P* as known parameters, the following biquadratic equation was obtained:

$$x^4 - \frac{P^2}{2\pi^2}x^2 + \frac{A^2}{\pi^2} = 0 \tag{9}$$

with the two positive solutions obtained by solving this equation being the semi-major (half length) and semi-minor axis (half width) of the ellipse, and therefore of the respective PVSMC.

According to the calculations based on these estimations, the cells had a mean length and SD of 159.1 ± 36.8 µm (n = 258; distribution shown in Figure 4.5A) with a range from 69.6 µm to 320.9 µm.

The width of PVSMC varied from 6 µm to 11.7 µm, while the mean was 8.6 ± 1.2 µm (n = 258; distribution shown in Figure 4.5B).

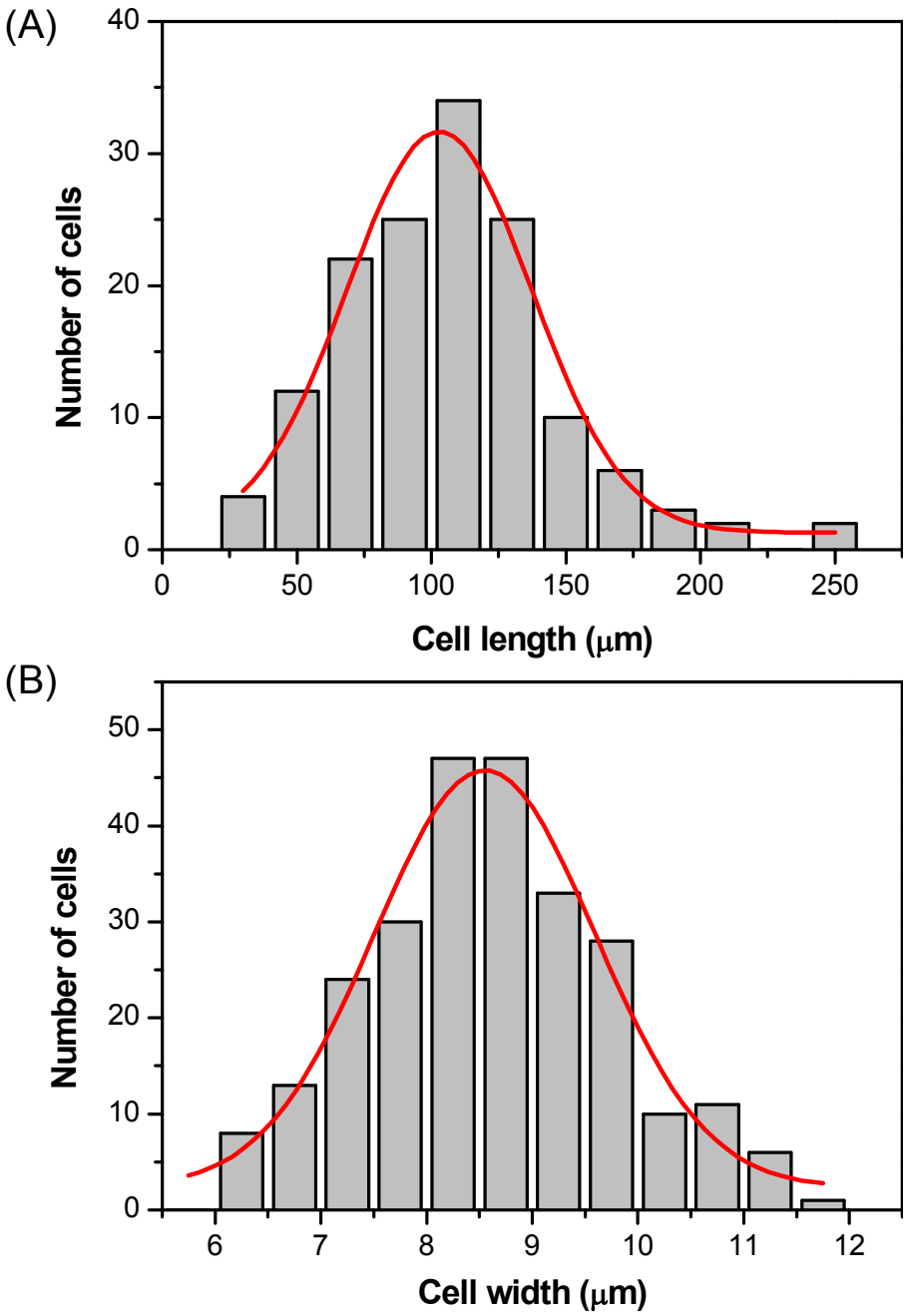

Figure 4.5. Cell length and width. Histograms illustrate the distribution of the (A) length and (B) width of PVSMC as calculated by approximating to an equivalent ellipse. Data values were fitted with Gaussian distributions (red curves).

4.3.4. Cell shape

It has been shown that cell shape can influence contractile force in smooth muscle cells (Tolic-Norrelykke and Wang, 2005) and therefore the assessment of cell shape was considered to be a relevant addition to the morphometric characterisation of PVSMC.

Further to measuring parameters of cell size, the ImageJ software was used to evaluate the shape of the pulmonary vein myocytes by calculating their circularity, which provided a quantitative measure of cell elongation (Auman *et al.*, 2007). Circularity values were obtained based on the following formula:

$$Circularity = 4\pi A / P^2 \qquad (10)$$

where A is the area and P is the perimeter of the cell as measured on the photomicrograph using the ImageJ software. Being a ratio, circularity does not have a unit of measurement and its value can range from 1 for a perfect circle, towards 0 if the shape is increasingly elongated.

Circularity of PVSMC from pig ranged from 0.04 to 0.22, with a mean ± SD value of 0.11 ± 0.03 (n = 258; histogram shown in Figure 4.6). The correlation of circularity with cell length was strongly negative (Pearson's r coefficient = -0.84, $P < 0.05$) and positive, but weaker with the width of cells (Pearson's r coefficient = 0.56, $P < 0.05$), as seen in Figure 4.7.

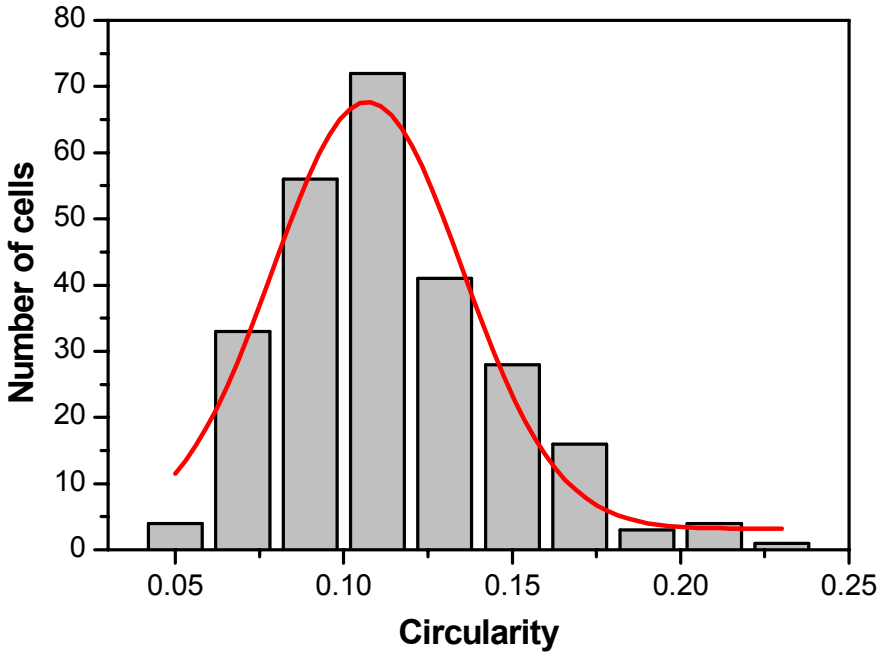

Figure 4.6. Circularity of PVSMC. Histogram illustrates the distribution of circularity, a cell shape parameter, as measured using the ImageJ software. Data values were fitted with a Gaussian distribution (red curve).

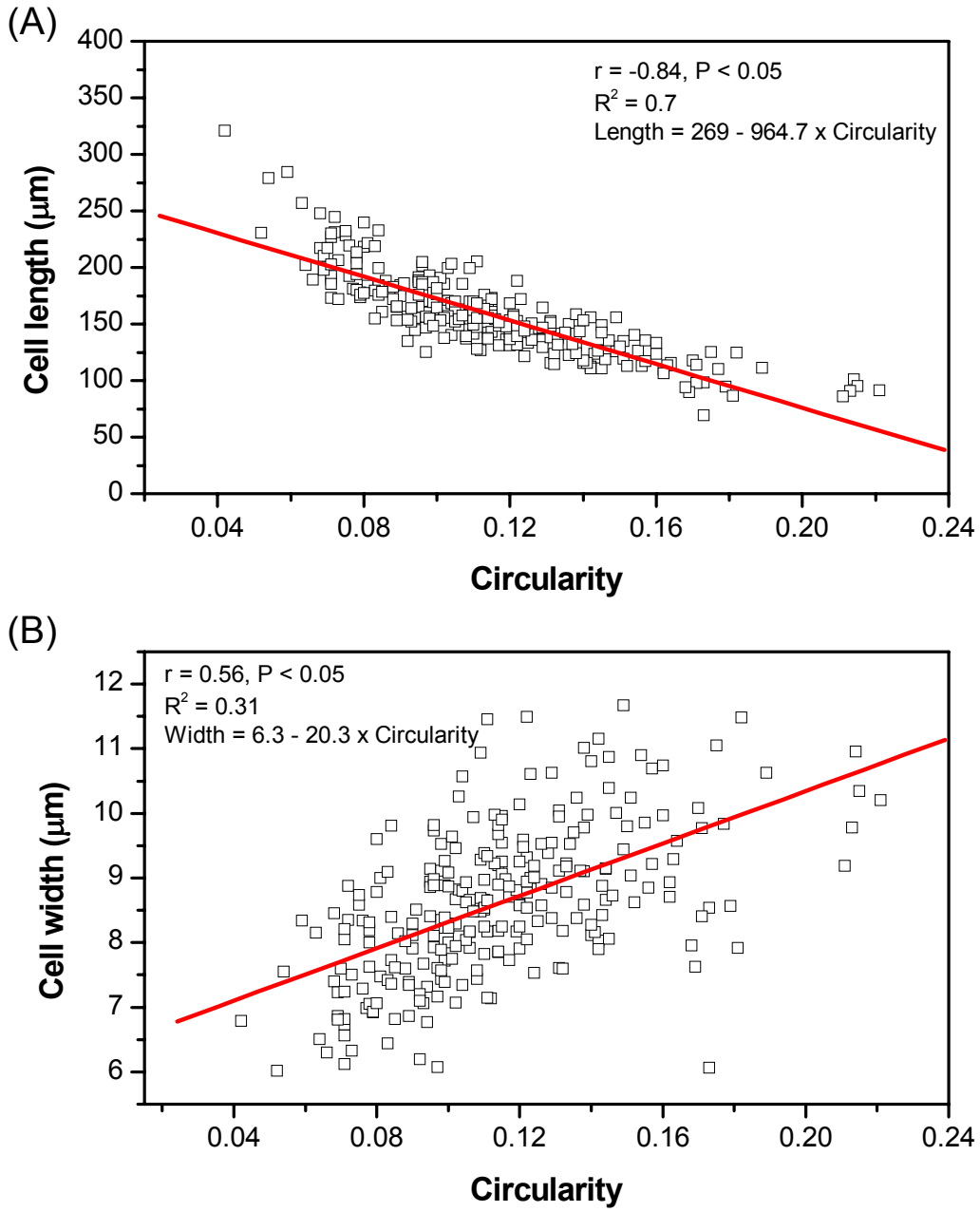

Figure 4.7. Correlation of cell length and width with circularity. Length (A) and width (B) of PVSMC were each plotted against circularity. Red lines represent the slopes calculated by linear regression analysis; r is Pearson's correlation coefficient; R^2 represents the goodness of fit.

4.3.5. Tri-dimensional cell surface

Initial measurements of the area of each cell were made on the photomicrographs using the ImageJ software (data presented above), but data obtained through this method had the disadvantage of being a bi-dimensional projection of the cell area and therefore an imprecise representation of whole membrane surface.

A more accurate, tri-dimensional, estimation of cell surface (S) was thus calculated by approximation to the surface of an ellipsoid. The particular type of ellipsoid used was spindle-shaped, namely a prolate (i.e. a spheroid with the polar axis longer than the equatorial diameter) (see Figure 4.8). The long axis was considered equivalent to the cell length (*l*) and the other two axes were both deemed equal to the width (*w*).

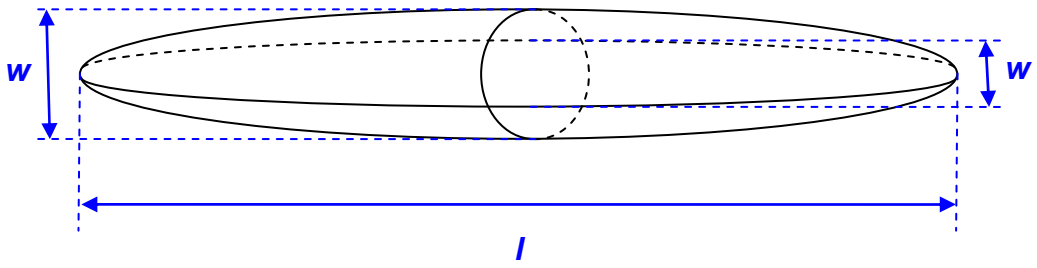

Figure 4.8. Approximation of PVSMC with a prolate spheroid. Tri-dimensional cell surface was calculated using the known cell dimensions as the prolate axes.

The surface area of the ellipsoid was calculated using a formula by Knud Thomsen (Michon, 2004, McGahon *et al.*, 2007):

$$S \approx 4\pi \left(\frac{a^p b^p + a^p c^p + b^p c^p}{3} \right)^{1/p} \qquad (11)$$

where p = lg(3) = ln(3)/ln(2) ≈ 1.6075 and a, b and c are the semiaxes of the ellipsoid; in this particular case a = *l/2* is half the length and b = c = *w/2* equal to half the width of the cells.

The tri-dimensional cell membrane surface calculated as above had a minimum value of 1036.9 μm^2 and a maximum value of 5796.1 μm^2, while the mean ± SD value was 3336.7 ± 832 μm^2 (n = 258). The coefficient of variation (CV) was 0.25 and the histogram distribution is shown in Figure 4.9.

4.3.6. Resting membrane potential

Membrane potential was recorded in 221 cells under resting conditions. The values ranged from -18 mV to -55 mV (distribution in Figure 4.10), with an average of -35.8 ± 5.9 mV (mean ± SD, n = 221).

There was a weak, but significant correlation between the resting membrane potential of PVSMC and the outer diameter of the pulmonary veins the cells were isolated from (Pearson's r coefficient = -0.16, $P < 0.05$), as shown Figure 4.11A.

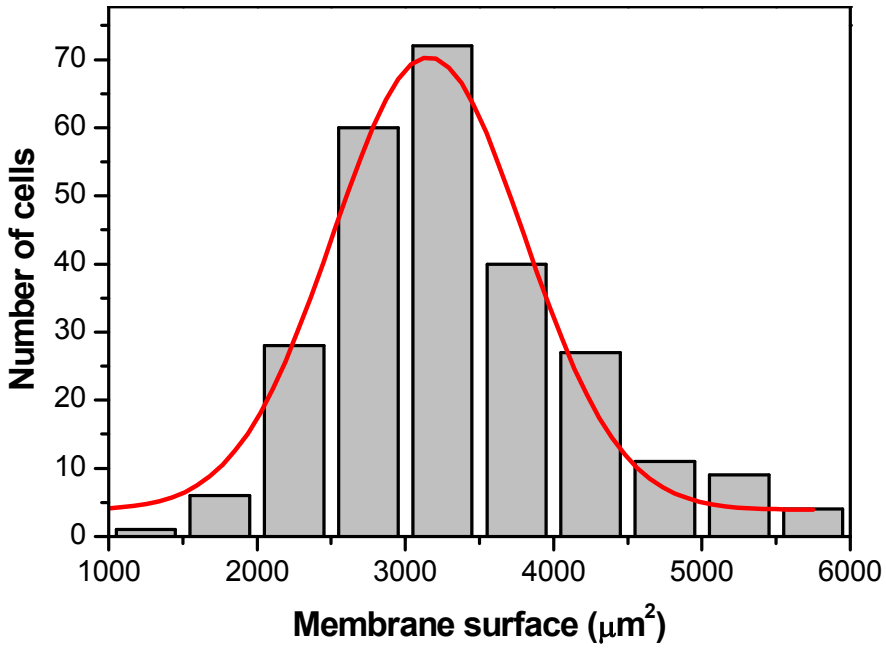

Figure 4.9. Tri-dimensional membrane surface of PVSMC. Histogram illustrates the distribution of calculated total membrane surface area. Red line represents the Gaussian fit to the distribution of values.

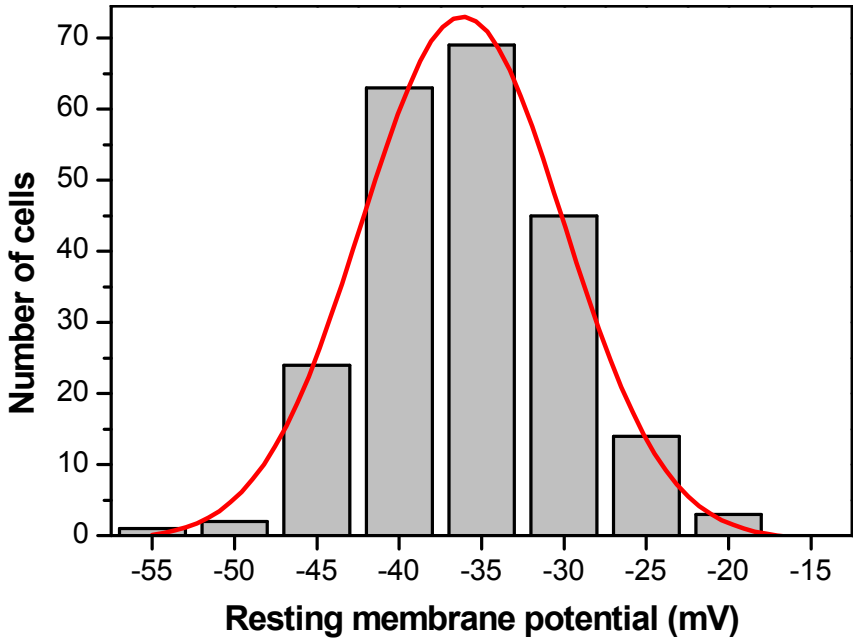

Figure 4.10. Resting membrane potential of PVSMC. Histogram illustrates the distribution of resting membrane potential measured under current clamp (I = 0). Red line represents the Gaussian fit to the distribution of values.

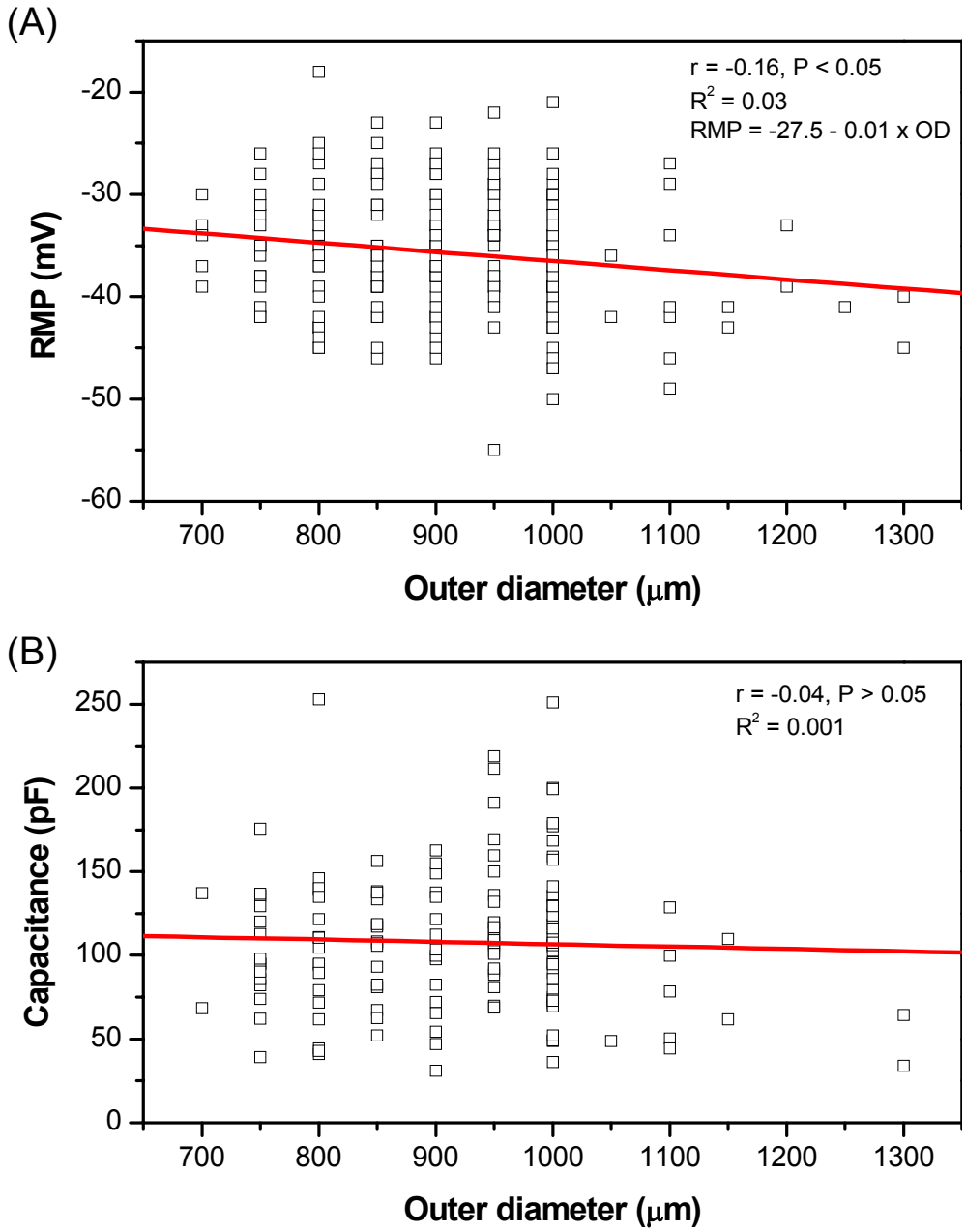

Figure 4.11. Correlation of RMP and capacitance with the outer diameter of vessels. Resting membrane potential (A) and membrane capacitance (B) of PVSMC were each plotted against the outer diameter of pulmonary veins. Red lines represent the slopes calculated by linear regression analysis; r is Pearson's correlation coefficient; R^2 represents the goodness of fit.

4.3.7. Membrane capacitance

Capacitive transient data was fitted for 145 cells. R_s had a value of 5.62 ± 0.66 MΩ (mean ± SEM). The membrane capacitance (C_m) of the PVSMC was 108 ± 42 pF (average value ± SD), with a minimum value of 31.1 pF and maximum of 252.9 pF. The distribution of values is illustrated in Figure 4.12.

There was no linear correlation between membrane capacitance and vessel outer diameter (Pearson's r coefficient = -0.04, $P > 0.05$), graphic representation shown in Figure 4.11B.

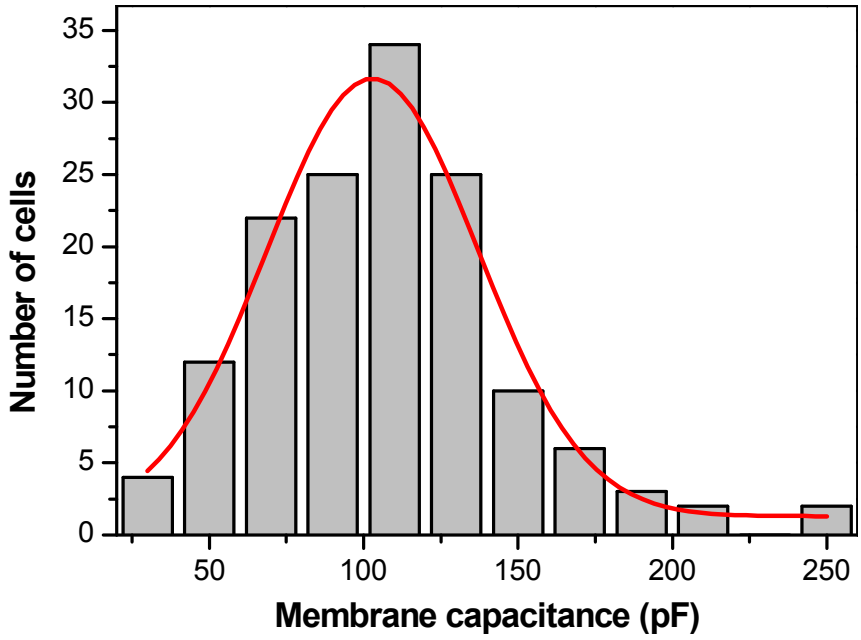

Figure 4.12. Membrane capacitance of PVSMC. Histogram illustrates the distribution of membrane capacitance. Red line represents the Gaussian fit to the distribution of values.

In excitable cells, specific membrane capacitance is defined as the value of capacitance per unit of membrane area (Gentet *et al.*, 2000) and it depends on the thickness and dielectric constant of the cellular membrane.

For porcine PVSMC, the specific membrane capacitance estimated by dividing the average cell capacitance to the average cell surface (108 pF/ 3336.7 μm^2) had a value of 3.2 $\mu F/cm^2$.

4.4. Discussion

Vascular smooth muscle cells are responsible for the development of vascular tone and thus regulation of blood flow. The shape and width of smooth muscle cells may be correlated to their ability to develop contractile force (Tolic-Norrelykke and Wang, 2005). Therefore, a quantitative morphometric characterisation of porcine PVSMC is opportune, as it adds to the little information available about this cell type.

Reports detailing the morphometric and passive membrane properties of smooth muscle cells from the pulmonary veins are not widely available in the literature. In a study focused on the contribution of potassium channels to pulmonary venous tone, Michelakis *et al*. (2001) isolated PVSMC from adult rats, but their morphometric characterisation was limited to stating the average length of cells and providing a photomicrograph of a sample cell.

The lack of PVSMC data contrasts with the substantial attention given by investigators to smooth muscle cells from the pulmonary arteries. Morphometric and/or passive electrical properties are available on freshly isolated PASMC from rabbits (Clapp and Gurney, 1991, McCulloch *et al.*, 2000), mice (Ko *et al.*, 2007) and humans (Shimoda *et al.*, 1998), as well as on cultured PASMC from human (Peng *et al.*, 1996) and rat lungs (Yuan *et al.*, 1993b).

The fresh PVSMC yielded by the optimised enzymatic dissociation protocol were normally suitable for the purpose of cell electrophysiology studies. Their morphological appearance compared favourably with previous reports of freshly dissociated PVSMC (Michelakis *et al.*, 2001) and PASMC (Clapp and Gurney, 1991, McCulloch *et al.*, 2000) (see photomicrographs in Figure 4.13). Furthermore, the features of cell viability (for details see section 2.3) were usually present in a sufficient proportion of the cells, which were used for voltage- and current-clamping experiments.

Single PVSMC had a typical appearance for smooth muscle cells. They were usually considerably elongated and thin, quite similar in those respects to single myocytes from porcine carotid arteries, which were also digested using papain (Driska and Porter, 1986). Myocytes isolated from the pulmonary artery were also elongated in the rabbit (Clapp and Gurney, 1991, McCulloch *et al.*, 2000), while those in mice were round shaped (Ko *et al.*, 2007).

The parameters of cell size are summarised in Table 4.1. In general, porcine PVSMC were larger than previously studied pulmonary smooth muscle cells. In adult rats, PVSMC were 8 ± 2 μm long (Michelakis *et al.*, 2001), the considerable difference being presumably due to the size difference between the two species. Porcine PVSMC were also significantly larger than distal porcine PASMC (77.8 ± 2 μm long, Sham *et al.*, 2000) and rabbit PASMC (60-120 μm long, Clapp and Gurney, 1991), while human cultured PASMC had a comparable average length (132.6 ± 3.5 μm long, Yuan *et al.*, 1993b).

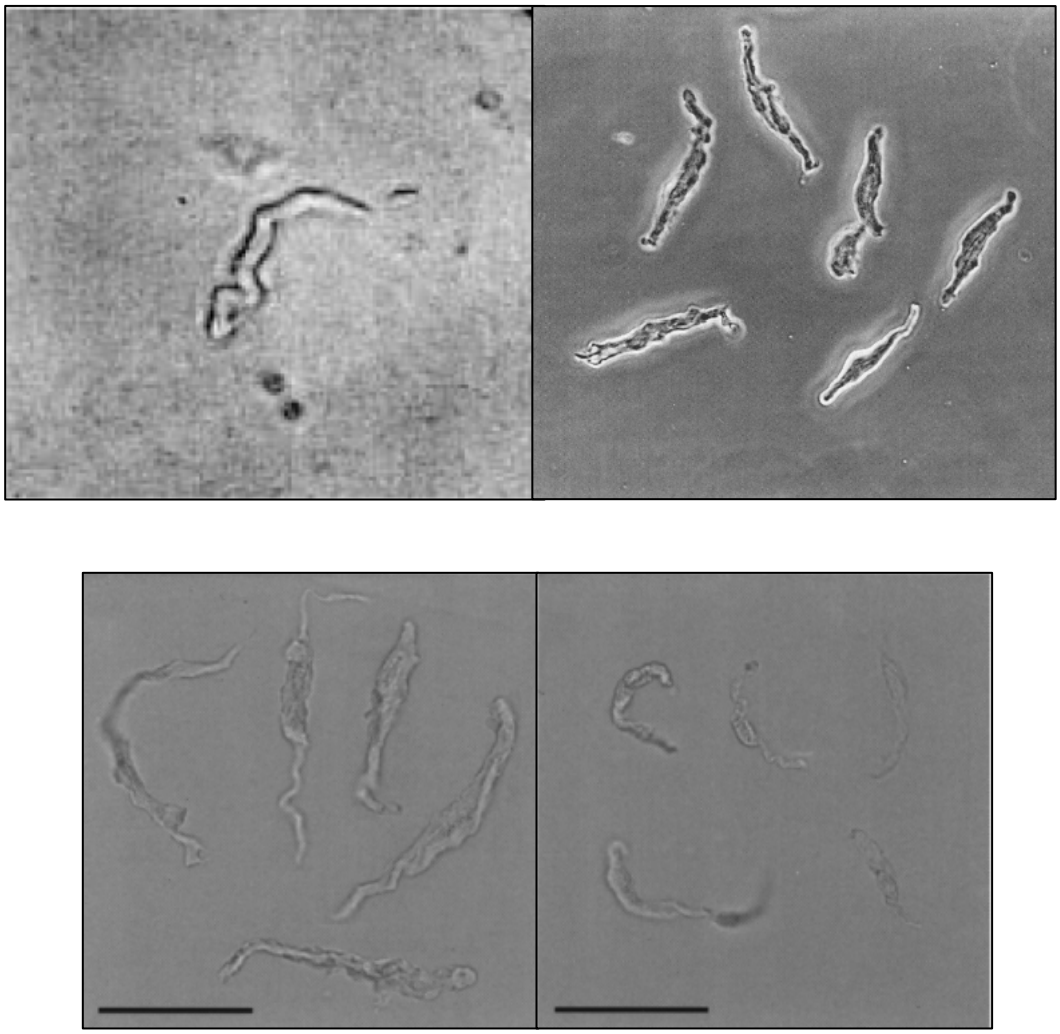

Figure 4.13. Freshly dissociated pulmonary smooth muscle cells.
Photomicrographs of isolated myocytes reported elsewhere. (*top left*) PVSMC isolated from adult rats (used with permission from Michelakis *et al.*, 2001). (*top right*) PASMC isolated from rabbit (used with permission from Clapp and Gurney, 1991). (*bottom*) PASMC isolated from large (*left*) and small (*right*) rabbit intrapulmonary arteries; bars represent 50 μm (used with permission from McCulloch *et al.*, 2000).

The size differences in these reports are most likely to be partly due to species differences. However, in the pig, the length of PVSMC (159.1 ± 36.8 μm, reported here) was twice that of PASMC (77.8 ± 2 μm long, Sham *et al.*, 2000). Differences in resting cell length could reflect an opposite difference in the basal levels of intracellular Ca^{2+} (Murphy and Khalil, 2000) and could therefore explain the difference between single arterial and venous myocytes. This theory would be consistent with previous reports that pulmonary veins depend more than arteries on influx of extracellular Ca^{2+} during contractions (Mikkelsen and Pedersen, 1983) and that pulmonary arterial smooth muscle has a higher SR content compared to other types of smooth muscle (Devine *et al.*, 1972).

Another possible contributing factor could be the variation of myocyte size along the pulmonary vascular tree, whereby cells originating in distal vessels could be larger than proximal ones. For example, the length of PASMC in the pig varied from 55.8 ± 1.2 μm in proximal arteries to 77.8 ± 2 μm in cells isolated from distal arteries (Sham *et al.*, 2000). The porcine PVSMC described here were isolated from distal 4^{th} to 7^{th} order branch intrapulmonary veins and therefore could be expected to be larger than others originating from proximal sites.

Other morphometric parameters taken into consideration included area, perimeter, width and circularity of PVSMC. The respective values for PASMC were not readily available for comparison in the literature. However, PVSMC appear considerably more elongated and proportionally thinner than PASMC (see photomicrographs in Figure 4.2 and Figure 4.13 for comparison). In cultured human airway smooth muscle, cell contractility was linked to cell shape through cell spreading and baseline contractile force did not depend on cell length, but rather on parameters of cell shape like projected area and width of cells (Tolic-Norrelykke and Wang, 2005). Moreover, wider cells were found to have a significantly greater baseline contractile force, but at the same time cells with a lower baseline tension showed a higher histamine-induced relative increase in force, which suggests that thinner cells have a superior ability to develop added force.

Table 4.1. Morphometric measurements of PVSMC. Area, perimeter and circularity were measured using ImageJ on photomicrographs; length and width were calculated by approximation of cell shape to an ellipse; tri-dimensional membrane surface was inferred by approximation to a prolate ellipsoid.

Cell measurement	Mean value ± SD	Minimum value	Maximum value	CV	N
Projected area, μm^2	1070.2 ± 267.6	331.5	1862.8	0.25	258
Perimeter, μm	354 ± 81.6	155.2	712.9	0.23	258
Length, μm	159.1 ± 36.8	69.6	320.9	0.23	258
Width, μm	8.6 ± 1.2	6	11.7	0.13	258
Circularity	0.11 ± 0.03	0.04	0.22	0.28	258
Tri-dimensional surface, μm^2	3336.7 ± 832	1036.9	5796.1	0.25	258

A summary of PVSMC electrical membrane properties is presented in Table 4.2. Resting membrane potential was measured in 221 cells. No other report for RMP of smooth muscle cells from intrapulmonary veins was available for comparison, but the average value of -35.8 mV was within the range seen in freshly isolated PASMC, such as -27.9 ± 0.9 mV in mouse (Ko *et al.*, 2007), -40 ± 1 in rat (Hogg *et al.*, 2002) and -50 ± 4 mV in rabbit (Osipenko *et al.*, 1997). When PASMC were cultured, their RMP was -55.4 ± 2 mV in human (Peng *et al.*, 1996), -41 ± 4 mV in canine (Doi *et al.*, 2000) and -39.9 ± 0.9 in rat cells (Yuan *et al.*, 1993b).

Table 4.2. Passive electrical membrane properties of PVSMC.

Cell measurement	Mean value ± SD	Minimum value	Maximum value	n
Resting membrane potential, mV	-35.8 ± 5.9	-55	-18	221
Membrane capacitance, pF	108 ± 42	31.1	252.9	145

The membrane capacitance of porcine PVSMC was 108 ± 42 pF. This value is higher than most reported for myocytes in pulmonary arteries: 25 ± 1.66 pF in freshly isolated human PASMC (Shimoda *et al.*, 1998), 35.27 ± 5.9 pF in human cultured PASMC (Peng *et al.*, 1996) and 31 ± 7 pF in freshly isolated rabbit PASMC (Franco-Obregon and Lopez-Barneo, 1996b). However, there is evidence of myocytes with comparable capacitance values. For example, Yuan *et al*. (1993b) described pulmonary artery myocytes (although not freshly dissociated) that have a membrane capacitance of 141.5 ± 14.2 pF.

The reason for the higher capacitance values in the PVSMC compared to PASMC is most probably due to differences in the size of the cells. As membrane capacitance is proportional to total membrane surface, when making comparisons it is important to take into consideration that the porcine PVSMC are relatively large cells (~160 μm long). For example, Clapp and Gurney (1991) reported a capacitance of 28 ± 1 pF in rabbit pulmonary artery myocytes that are roughly three times smaller (approximated from photomicrographs as there is no mean value provided) than those described here. Therefore, it is to be expected that much larger cells have a proportionally larger membrane capacitance.

The mean specific membrane capacitance of PVSMC was 3.2 $\mu F/cm^2$. This value is greater than the generally accepted value of 1 $\mu F/cm^2$, which is thought to be typical for smooth muscle cells (Toro *et al.*, 1986) and closer to values seen in cardiac myocytes (Powell *et al.*, 1980). However, values higher than 1 $\mu F/cm^2$ have been reported previously in smooth muscle cells: 2.3 $\mu F/cm^2$ in cultured rat myometrial cells (Mollard *et al.*, 1986) and 1.42 $\mu F/cm^2$ in freshly dissociated smooth muscle cells from the rat uterus (Yoshino *et al.*, 1997). Furthermore, a literature search revealed a relative lack of actual recorded values for specific membrane capacitance in smooth muscle cells, as many studies do not actually calculate it. This is because researchers typically measure cell capacitance and rely on the generic value of 1 $\mu F/cm^2$ for specific membrane capacitance to subsequently estimate the surface of the cells, rather than measuring the cell surface and using it to find out the specific membrane capacitance.

The difference between the values observed here and the lower typical value may be due to the intrinsic membrane properties of porcine PVSMC causing higher specific capacitance and/or an underestimation of calculated cell surface due to the presence of folds and caveolae which increase the actual membrane surface of the cell and thus leads to an overestimation of specific capacitance (Mitchell *et al.*, 1986).

The comparison between the morphometric and passive electrical properties of porcine PVSMC reported here and those of PASMC published elsewhere indicate there are significant differences between these two types of cell. These dissimilarities may have a basis in the embryological origin of the vessels. In the foetal lung, both pulmonary arteries and veins are formed by vasculogenesis, but their smooth muscle cells originate separately and have different cytoskeletal protein content (Hall *et al.*, 2002). The arteries are formed in close relation to the airways and arterial myocytes derive in part through the proliferation and migration of adjacent bronchial smooth muscle, but also through differentiation from the surrounding mesenchyme (Hall *et al.*, 2000, Fernandes *et al.*, 2004). The veins, however, develop at sites away from the bronchi and their smooth muscle cells have their embryological origin solely in undifferentiated mesenchymal cells (Hall *et al.*, 2002).

These embryological differences are likely to be reflected in the distinct structural and functional characteristics of the matured pulmonary vascular smooth muscle. For example, caldesmon – an actomyosin regulatory protein – is expressed during development in arterial smooth muscle from 56 days of gestation, but not in the veins (Hall *et al.*, 2002). Caldesmon is believed to play an inhibitory role in the regulation of smooth muscle contraction (Katsuyama *et al.*, 1992, Pronina *et al.*, 2007) and could act through tethering of actin to myosin to inhibit the actin-activated myosin ATPase (Lee *et al.*, 2000). Such structural differences may well contribute to the greater vasoactivity seen in the veins compared to the arteries (Shi *et al.*, 1998, Arrigoni *et al.*, 1999, Zhao *et al.*, 1993).

In this study, single smooth muscle cells freshly isolated from porcine distal intrapulmonary veins were obtained and characterised for the first time. The properties of PVSMC reported here revealed significant differences exist between venous and arterial smooth muscle cells. PVSMC are longer and thinner than PASMC. Furthermore, the larger size of PVSMC was also reflected in a greater membrane capacitance compared to pulmonary arterial myocytes. These results have shown viable single smooth muscle cells, which can be used successfully in cell

electrophysiology studies. The further aim of the project is to examine ion channel activity during HPV in the veins, and more specifically to investigate the effects of hypoxia on specific ion conductances in porcine PVSMC.

Chapter 5.
Effect of hypoxia and K^+ channel antagonists on whole-cell currents

5.1. Introduction

The contribution of pulmonary veins to hypoxia-induced pressor responses in the pulmonary circulation has been demonstrated under *in vivo* conditions (Shirai *et al.*, 1986), as well as in studies using the isolated, perfused whole-lung model (Hillier *et al.*, 1997). Likewise, in experiments measuring isometric tension elicited by isolated vessels, hypoxia contracts both small intrapulmonary arteries and veins (see results presented in previous chapters and reports from Raj and Chen, 1986, Zhao *et al.*, 1993, al-Tinawi *et al.*, 1994).

Early reports did not, however, clarify whether the hypoxic response is due to a direct action on vascular smooth muscle or occurs through contractile mediators released by the vascular endothelium or pulmonary parenchyma (Fishman, 1976, Heath, 1977). While current evidence supports the involvement of vasoactive substances in modulating the severity of the hypoxic response (Weir and Archer, 1995, Dumas *et al.*, 1999), it was the finding that hypoxia contracts smooth muscle cells from pulmonary arteries (Murray et al., 1990, Madden et al., 1992) which ultimately demonstrated that hypoxia sensitivity is an intrinsic feature of smooth muscle cells. In isolated pulmonary veins, hypoxic pressor responses can be elicited in vessels that have been endothelium denuded (Feletou *et al.*, 1995), suggesting the

venous response is also mediated through direct action of hypoxia on venous smooth muscle.

In pulmonary arterial smooth muscle cells (PASMC), hypoxia raises the cytosolic free Ca^{2+} concentration (Cornfield et al., 1993, Salvaterra and Goldman, 1993). This occurs at least partly as a result of membrane depolarisation caused by hypoxia-induced inhibition of whole-cell potassium currents (Post et al., 1992, Yuan et al., 1993a).

Given the involvement of K_v channels in hypoxia-induced responses in PASMC (Bonnet and Archer, 2007, Hogg *et al.*, 2002), this raises the possibility that these channels may also contribute to acute hypoxic PV constriction. As yet however, there is no available data regarding the effect of hypoxia on K^+ channels in the plasma membrane of PVSMC.

The aim of these studies was to characterise the kinetics of whole-cell voltage-activated currents in porcine PVSMC, use potassium channel antagonists to separate the components of the outward current and examine the susceptibility of these currents to hypoxic conditions.

5.2. Experimental protocols

Following the development of the isolation protocol (see section 2.3.2), freshly dispersed porcine PVSMC were used in cell electrophysiology experiments. By means of the whole-cell configuration of the patch clamp technique, various voltage clamp protocols were used to elicit whole-cell voltage activated currents under different extracellular conditions, including low O_2 and in the presence of various K^+ channel antagonists.

5.2.1. Voltage-activated whole-cell currents

A standard voltage protocol was used to elicit families of whole cell voltage activated outward currents in PVSMC. Cells were held at the resting potential of -80 mV and test voltage steps were applied for 400 ms to a range of potentials starting at -80 mV and incrementing by 10 mV up to a final voltage of +80 mV (graphic representation of voltage protocol shown in Figure 5.1).

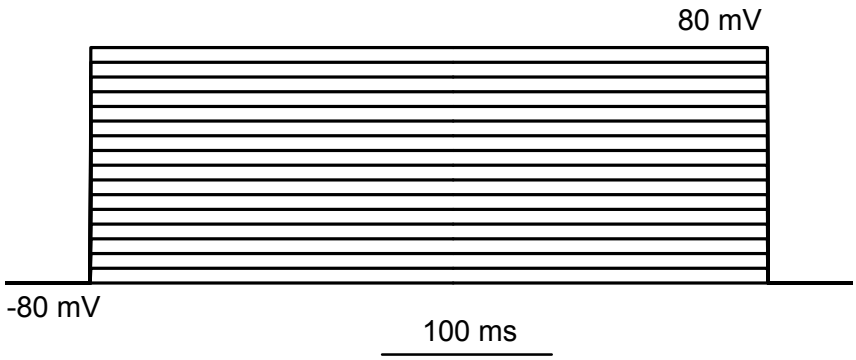

Figure 5.1. Standard voltage protocol. Voltage was stepped for 400 ms from -80 mV to +80 mV in 10 mV increments.

To describe the rate of activation of the voltage-activated outward currents, the traces were fitted with an equation following Hodgkin-Huxley kinetics (Dempster, 2006):

$$f(t) = I_{\max}\left(1 - e^{-t/\tau_{act}}\right)^{P} \qquad (12)$$

where I_{max} is the maximum level of the voltage activated current, τ_{act} is the time constant of activation and P is the power variable that best describes the channel activation.

5.2.2. Time course experiments

Time course experiments were used to investigate the dynamics of the hypoxia-induced effect on voltage-activated whole-cell currents by means of a repeated single voltage step protocol. Membrane currents were elicited by a single 400 ms voltage pulse from -80 mV to +80 mV applied repeatedly every 30 seconds for the entire duration of the recording under constant flow of bath solution (graphic representation in Figure 5.2).

Recording of membrane currents was normally started under flow of standard normoxic bath solution. Thereafter, the flow of bath solution was switched from normoxic to hypoxic for approximately 5 minutes (considered sufficient as in wire myography experiments hypoxic venoconstriction usually peaked during the first 5 minutes), followed by return to normoxic solution. In some experiments, K^+ channel antagonists were added to both normoxic and hypoxic bath solutions to observe whether they would alter the effect of hypoxia. In separate experiments designed to examine the effect of blocking K^+ channels, the flow was changed to bath solution containing K^+ channel antagonists and a few minutes were allowed for the current to achieve a steady level. The drugs were subsequently washed out with fresh standard solution.

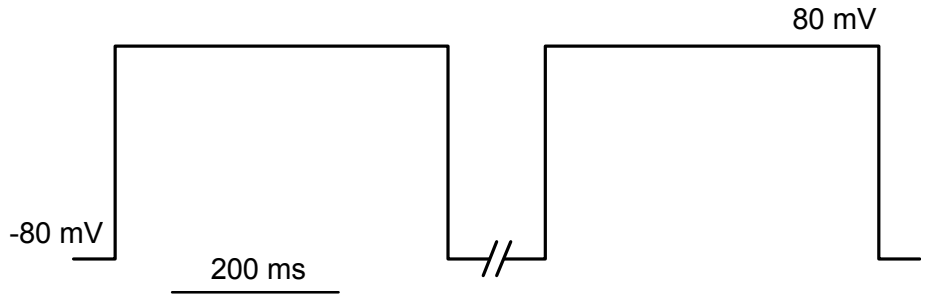

Figure 5.2. Repeated single step protocol. Single rectangular voltage pulses to +80 mV were applied repeatedly to elicit whole-cell currents. Break represents 30 seconds.

5.2.3. Data analysis

Currents were recorded using the WinWCP software and data values were exported as text files for analysis with the help of Microsoft Office Excel. Currents were measured as the average current over 50 ms during the steady state phase to minimise the influence of noise and spontaneous transient currents. Results are presented either as measured current values (in pA) or current density (in pA/pF), by dividing the measured current values by the respective cell capacitance (in pF; calculated as explained in the General Methods chapter). Differences between mean values were assessed using a paired *t*-test or one- or two-way ANOVA followed by post-hoc Bonferroni analysis as appropriate, and were considered significant for *P* values of less than 0.05.

5.3. Results

5.3.1. Voltage-activated whole-cell outward currents

In the absence of drugs and using standard normoxic bath solution, whole-cell membrane currents were elicited in pulmonary vein smooth muscle cells during 400-ms depolarising voltage steps in 10 mV increments from a holding potential of -80 mV (representative traces shown in Figure 5.3A).

The result was a family of large rapidly activating outward currents (I_{out}), which did not inactivate during the 400 ms duration of the test potential and had superimposed spontaneous transient outward currents (STOC). The STOC were more evident at more depolarised membrane potentials, suggesting a complex, multiple component current.

The steady state I_{out} current at +80 mV had an average value of 2715.9 ± 404.8 pA (n = 17). When values were converted into current density, the resulting mean was 29.2 ± 2.6 pA/pF and the current data plotted as a function of their respective voltage potential gave the current–voltage relationship for I_{out}, which is illustrated in Figure 5.3B.

To examine how current activation changed with test potential, the time constant of activation (τ_{act}) was calculated by fitting the current traces with an exponential Hodgkin-Huxley function (Figure 5.4A). As the potentials became more depolarised the currents activated faster, as τ_{act} approximately halved from 36.6 ± 7.1 at -10 mV to 18.9 ± 2.3 at +80 mV (n = 13, average values plotted against test potential shown in Figure 5.4B).

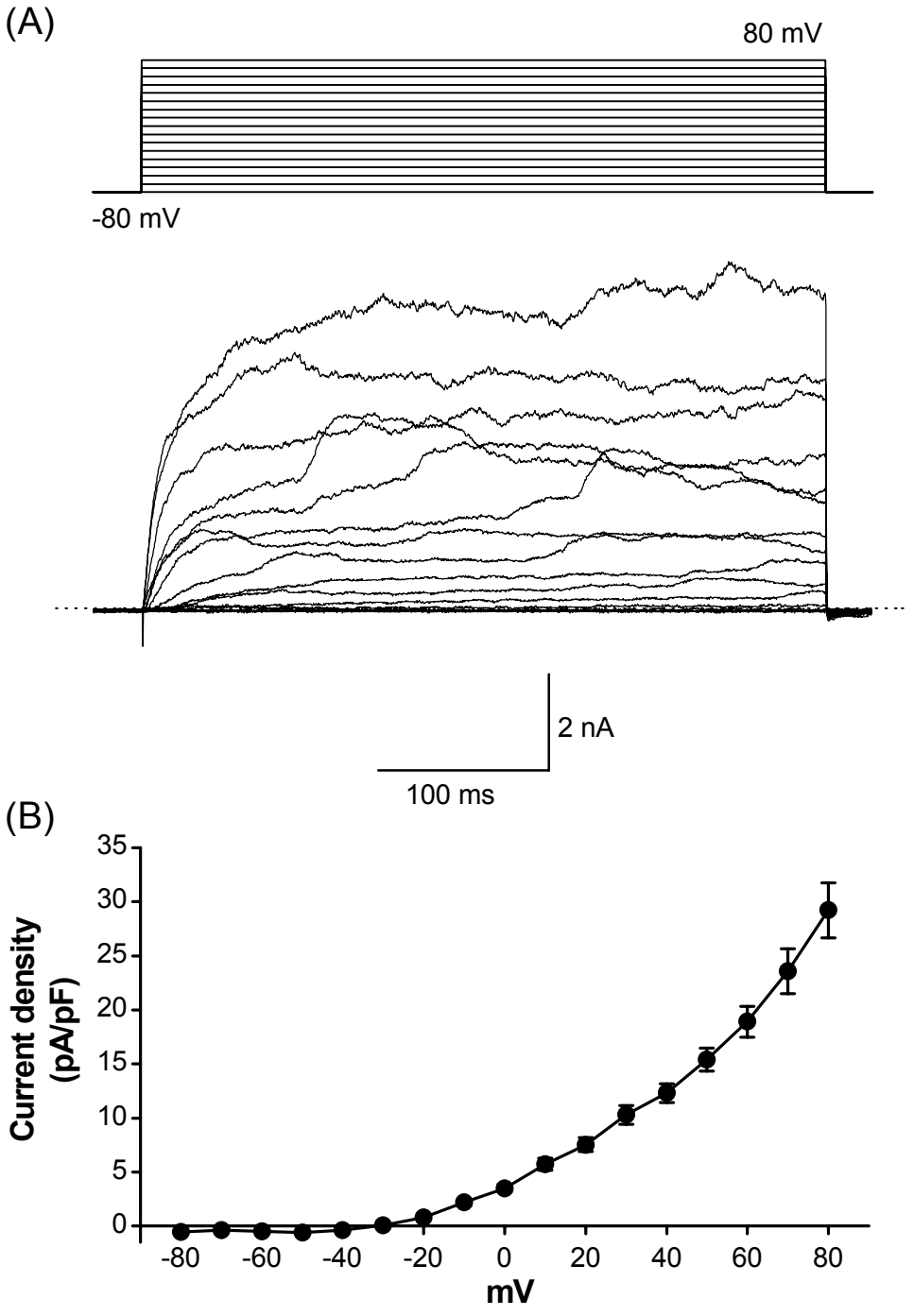

Figure 5.3. Voltage-activated outward currents in PVSMC. (A) Representative membrane currents recorded in response to the application of test pulses shown in the upper panel; dashed line marks zero current level. (B) Current density values from 17 cells were averaged and plotted (mean ± SEM) against test potential to give the current–voltage relationship.

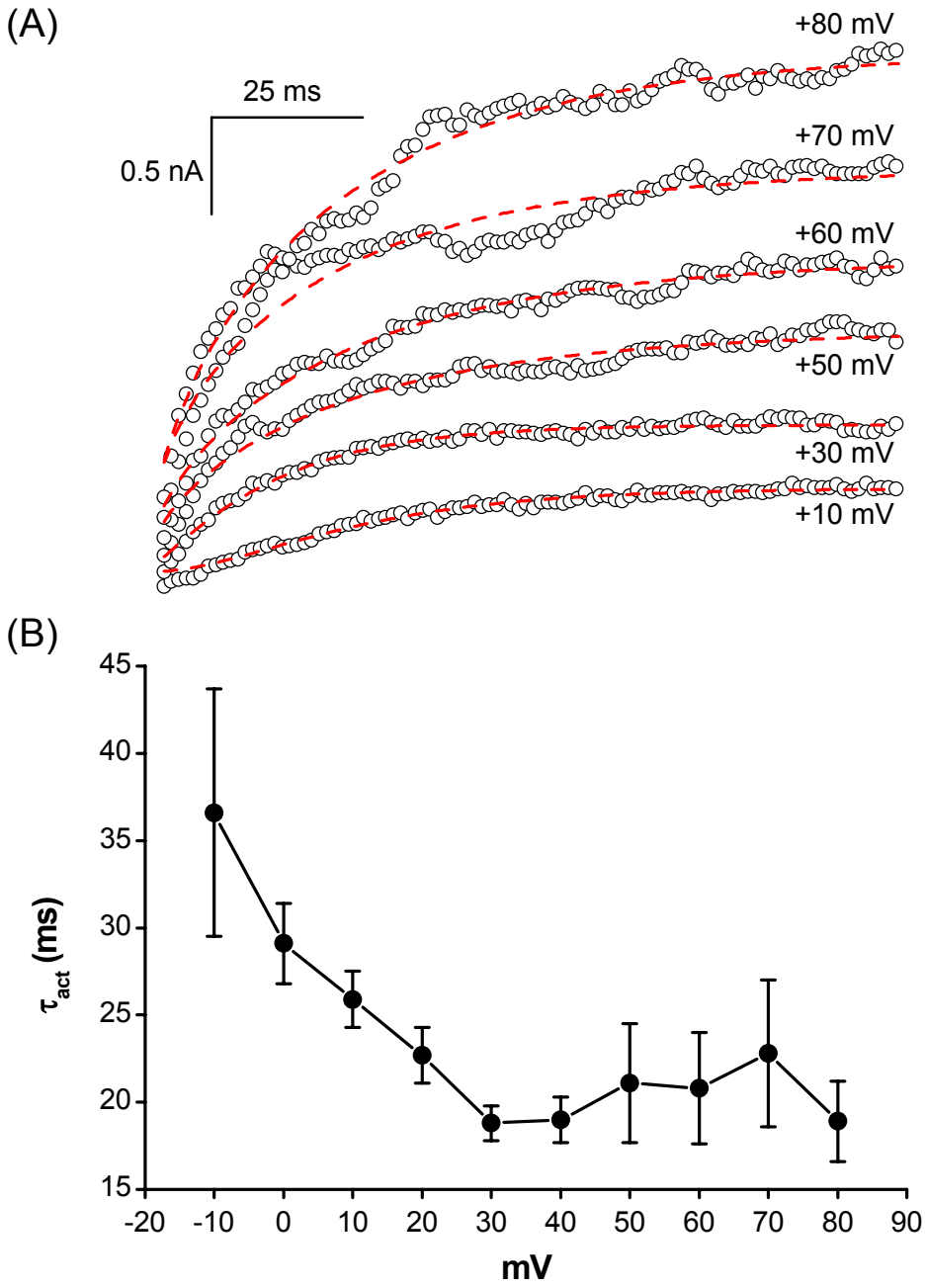

Figure 5.4. Activation of outward currents in PVSMC. (A) Activation of currents at different test potentials. Circles represent recorded current values and dashed lines are curves fitted with a Hodgkin-Huxley function. (B) The effect of voltage on the time constant of activation. Data values represent mean ± SEM from 13 cells.

5.3.2. The effect of TEA on whole-cell currents

To evaluate the effect of 5 mM tetraethylammonium chloride – a relatively non-specific blocker of K^+ channels (Michelakis *et al.*, 2001) – on the whole-cell currents, the standard bath solution was replaced with TEA-containing bath solution in the perfusion chamber, and at least 5 minutes were allowed for the drug to make its effect. TEA produced a marked inhibition of the mean steady-state current by 77.5 ± 3.8 % at +80 mV ($P < 0.05$, n = 12, representative traces in Figure 5.5A), which was reversible upon washing out with standard bath solution. Significance occurred starting with the current elicited by the +10 mV step (see Figure 5.5B). The mean value of the current activated by the last voltage step of +80 mV was 637.2 ± 121.5 pA in the presence of TEA, compared to the control value of 3118.8 ± 425.6 pA ($P < 0.05$, n = 12).

5.3.3. The effect of Penitrem A on whole-cell currents

In response to the application of 100 nM Penitrem A, a potent inhibitor of large-conductance Ca^{2+}-activated K^+ channels (BK_{Ca}) (McGahon *et al.*, 2005), the amplitude of the steady-state I_{out} current at +80 mV was irreversibly reduced to 943 ± 108.7 pA ($P < 0.05$, n = 17), corresponding to a 65% inhibition. The STOC activity observed during control recordings was abolished by Penitrem A, revealing a rapidly activating current (Figure 5.6A, lower trace). In addition to the reduction in current amplitude, the exposure of PVSMC to Penitrem A also had an effect on the activation rate of the outward currents. Mean τ_{act} for every test potential was calculated from 16 cells. After Penitrem A, the currents were more rapidly activating than controls, which was reflected in smaller time constants of activation (τ_{act}) across all test potentials (although significance was achieved only for the -10, 0 and 70 mV steps). As in the case of control currents, the relationship between mean τ_{act} and voltage showed faster currents at more depolarised potentials (τ_{act} decreased from 28.5 ± 5.1 ms at -10 mV to 10.9 ± 1.2 ms at 80 mV, see Figure 5.7).

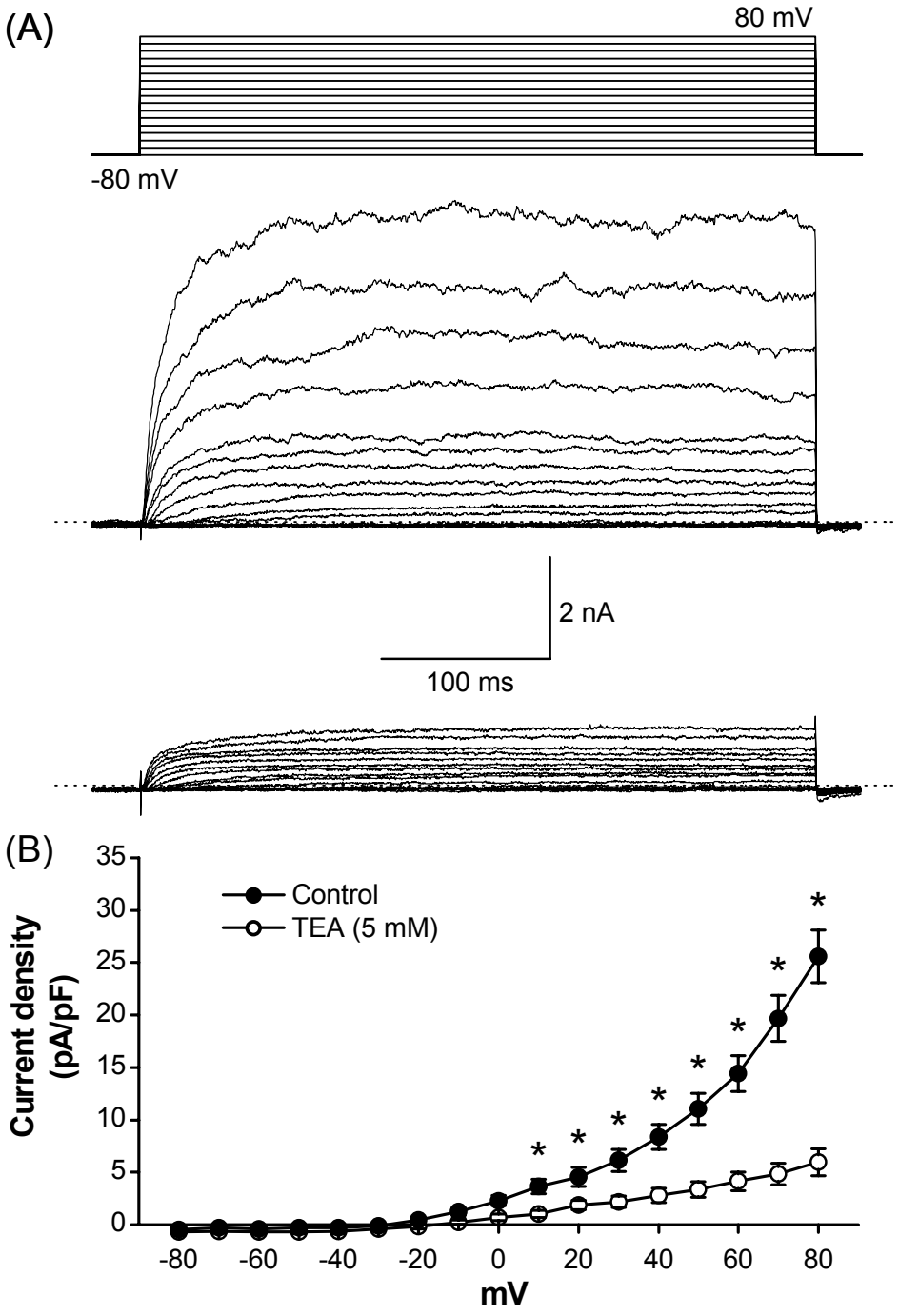

Figure 5.5. The effect of 5 mM TEA on I_{out}. (A) Representative membrane currents recorded using the standard voltage protocol in the absence (*upper panel*) and presence (*lower panel*) of TEA. (B) Mean current density–voltage relationship in the absence (*full circles*) and presence (*open circles*) of TEA containing bath solution. * indicates significant reduction in current density in the presence of TEA when compared to control ($P < 0.05$, n = 12).

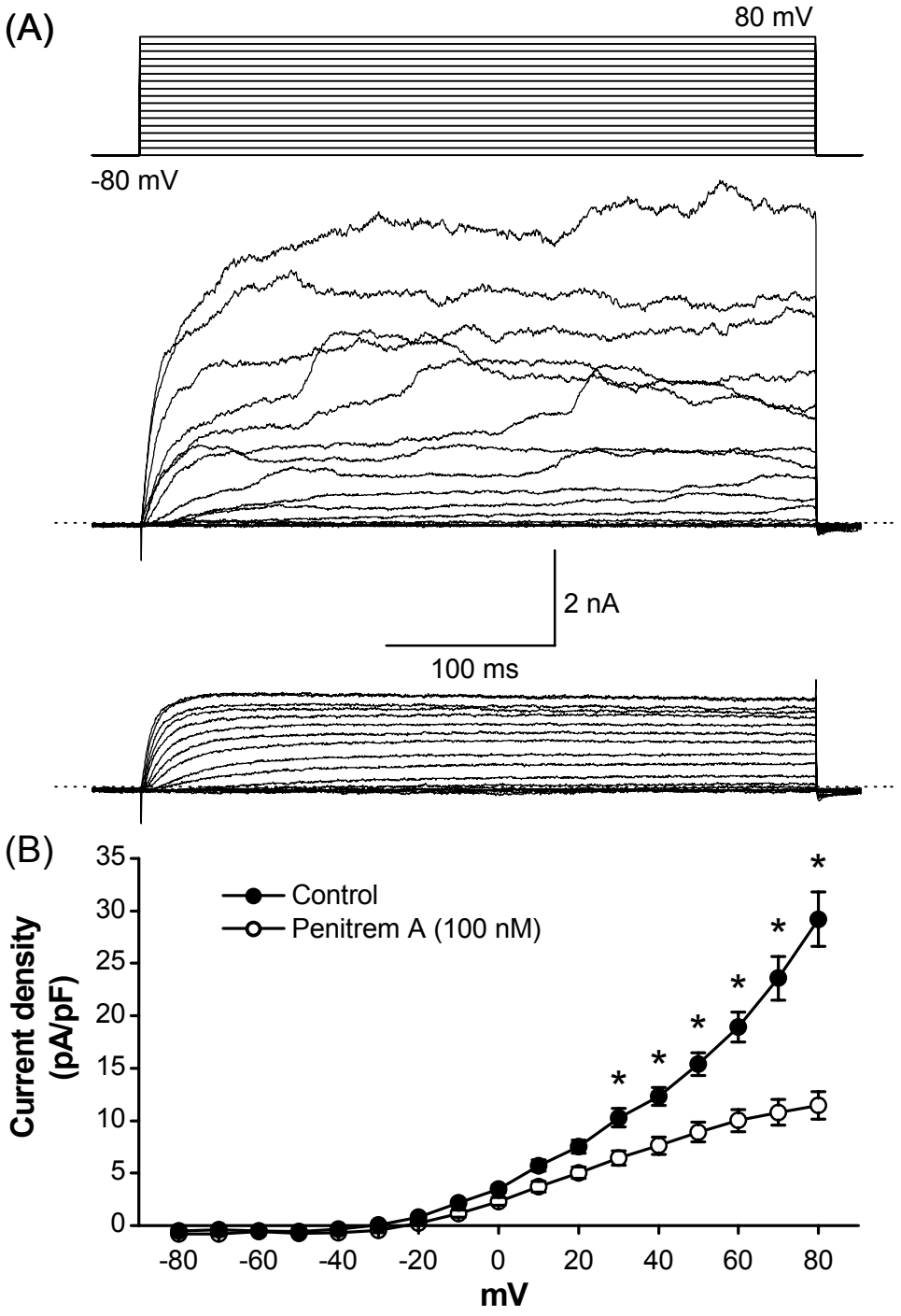

Figure 5.6. The effect of 100 nM Penitrem A on I_{out}. (A) Representative membrane currents recorded using the standard voltage protocol in the absence (*upper panel*) and presence (*lower panel*) of Penitrem A. (B) Mean current density–voltage relationship in the absence (*full circles*) and presence (*open circles*) of Penitrem A containing bath solution. * indicates significant reduction in current density in the presence of Penitrem A when compared to control ($P < 0.05$, n = 17).

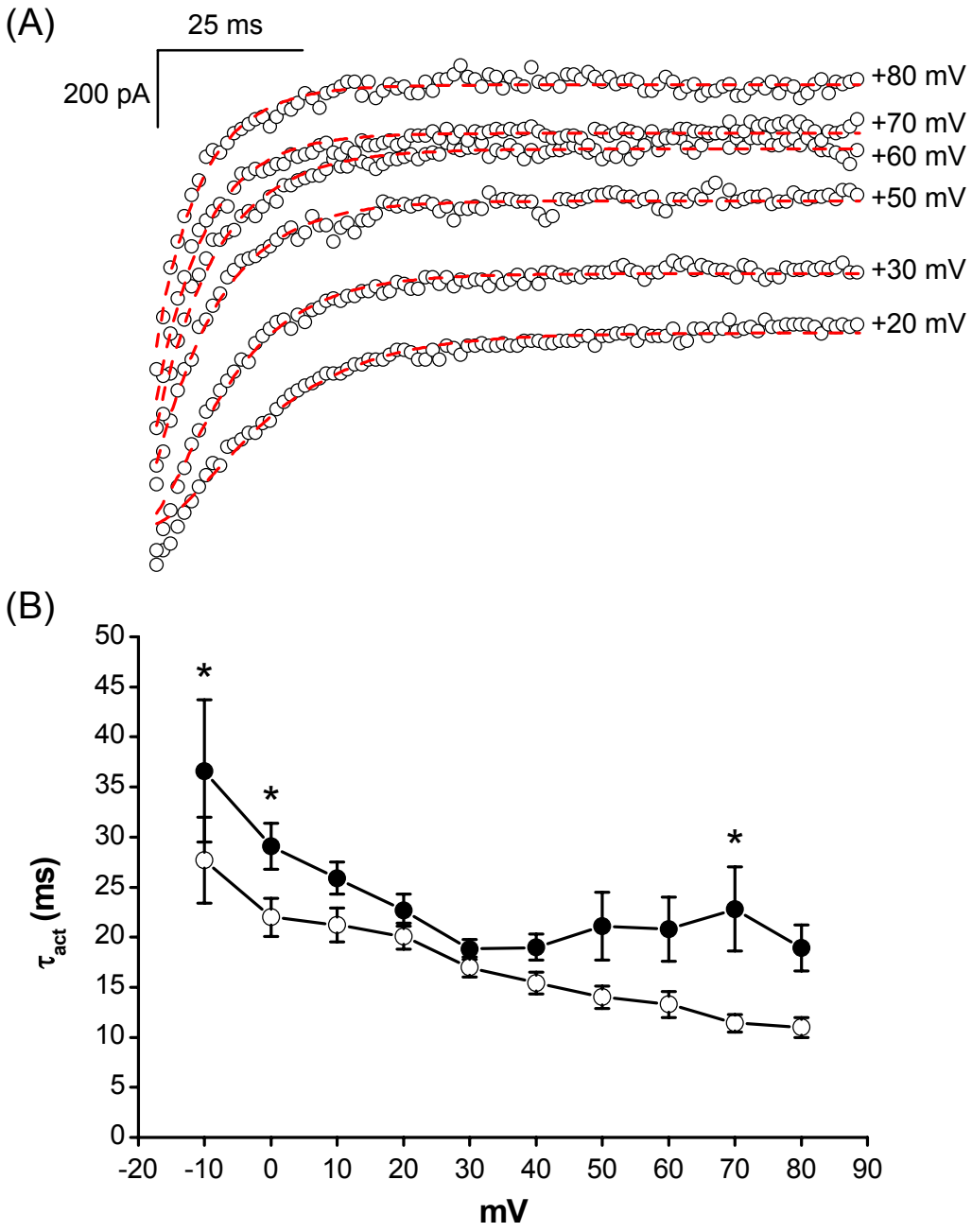

Figure 5.7. The effect of Penitrem A on activation of I_{out}. (A) Activation of currents at different test potentials in the presence of Penitrem A. Circles represent recorded current values and dashed lines are curves fitted with a Hodgkin-Huxley function; for clarity, not all traces are shown. (B) The effect of voltage on mean τ_{act} in the absence (*full circles*) and presence (*open circles*) of Penitrem A containing bath solution. * indicates significant reduction in τ_{act} in the presence of Penitrem A when compared to control ($P < 0.05$, n = 16).

5.3.4. The effect of hypoxia on the outward current

The effect of hypoxia on the family of whole-cell voltage-activated outward currents in PVSMC was examined using the standard protocol with voltage steps of 400 ms from -80 to +80 mV.

Steady state I_{out} current amplitude was not affected by perfusion with hypoxic solution (3384 ± 804.5 pA vs. 3142 ± 533.7 pA, n = 8, $P > 0.05$), representative traces and I/V curve are shown in Figure 5.8.

However, when control currents were elicited repeatedly, there was variation in the amplitude of the recorded currents, resembling a random activity with no identifiable pattern. This observation raised the possibility that a potential effect of hypoxia on a component of the whole-cell current could have been masked by the spontaneous activity.

In earlier experiments, Penitrem A inhibited both the amplitude and the spontaneous activity of I_{out} by selectively blocking BK_{Ca} channels (see Figure 5.6). This effect of Penitrem A appeared clearer in time course experiments, which involved a single voltage step from -80 mV to +80 mV repeated every 30 seconds (see Figure 5.9).

In smooth muscle cells from pulmonary arteries, hypoxia directly reduces K_V currents (Post *et al.*, 1992, Yuan *et al.*, 1993a). Therefore, blocking BK_{Ca} spontaneous activity with Penitrem A facilitated experiments designed to test whether K_V currents in PVSMC were sensitive to low O_2. Thus, further experiments examining the effect of hypoxia were performed in the presence of Penitrem A (100 nM).

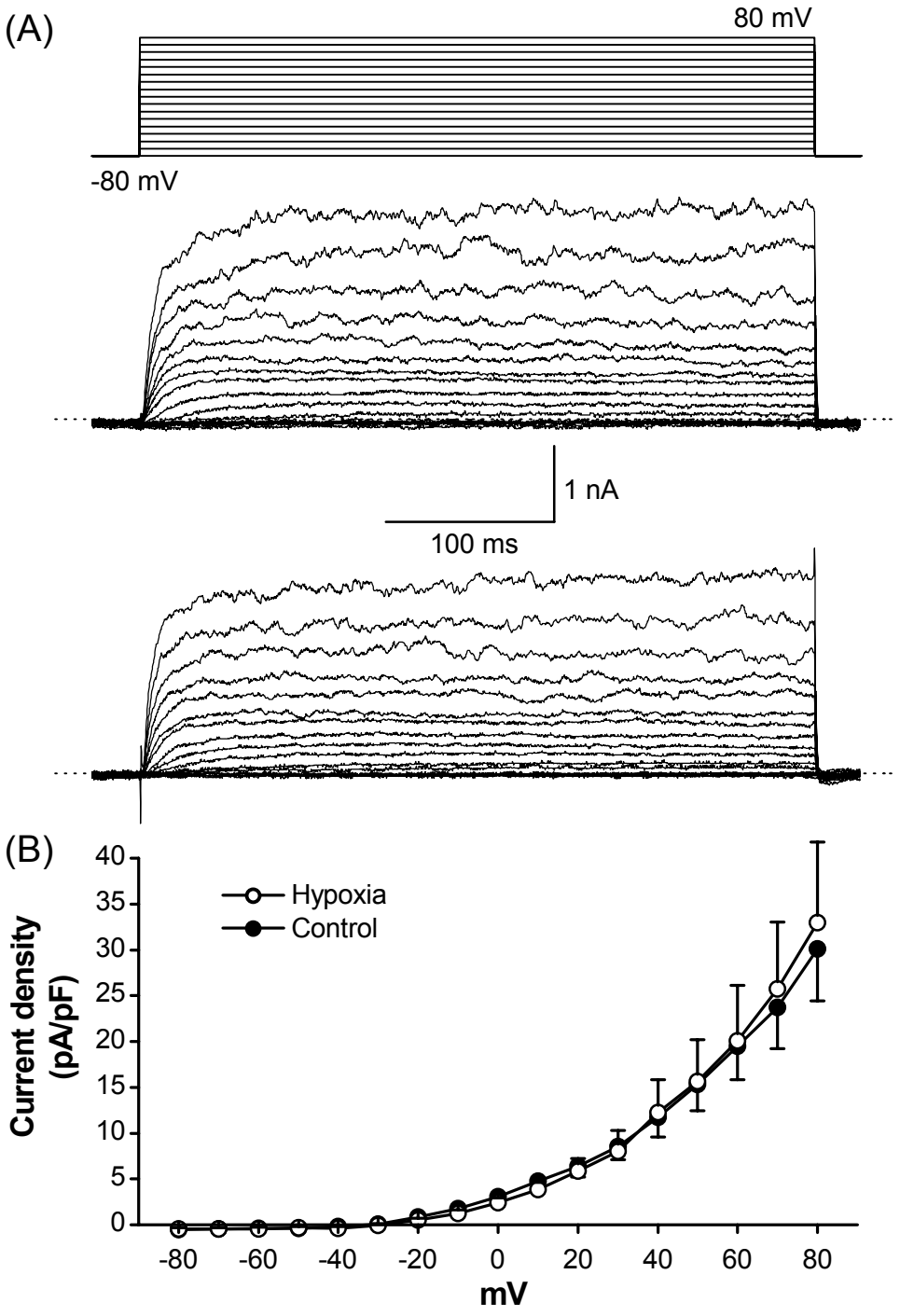

Figure 5.8. The effect of hypoxia on I_{out}. (A) Representative membrane currents recorded using the standard voltage protocol under normoxia (*upper panel*) and hypoxia (*lower panel*). (B) Mean current density–voltage relationship in normoxic (*full circles*) and hypoxic (*open circles*) bath solution; $P > 0.05$, n = 8.

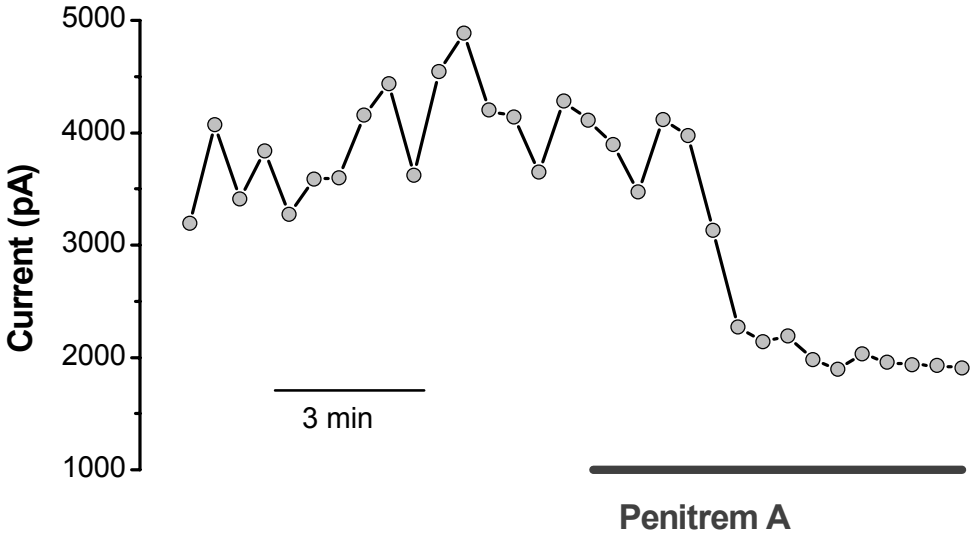

Figure 5.9. Time course effect of 100 nM Penitrem A on I_{out}. Representative whole-cell currents recorded by stepping every 30 seconds from a holding potential of -80 mV to +80 mV for 400 ms. The normoxic standard solution was replaced with Penitrem A (100 nM) containing bath solution; values represented steady-state current amplitude.

5.3.5. The effect of hypoxia on the Penitrem A insensitive current

To follow the time course of the effect of hypoxia on the outward current in the presence of Penitrem A, a repeated single step protocol was used. Hypoxic flow caused an immediate reduction in the current, which started within the first 30 seconds of the cells becoming hypoxic (see Figure 5.10A). By the end of the 5 minute period of hypoxia, the result was an inhibition of the steady-state current by 19.4 ± 2.3% to the average value of 1270.5 ± 146.5 pA ($P < 0.05$, n = 6, Figure 5.10B). Following re-oxygenation, the current returned to 1426.9 ± 192.8 pA (n = 5), which was comparable to pre-hypoxic levels (see Table 5.1), suggesting that the decrease in the current was due to channel blockade rather than channel rundown.

Hypoxic perfusion also increased the τ_{act} of the Penitrem A insensitive current ($I_{K(Pen)}$) by 81.2 ± 6.9% to 22 ± 2.6 ms ($P < 0.05$, n = 6, Figure 5.11B), suggesting hypoxia inhibited a component with fast activation kinetics. Representative activation curves fitted with a Hodgkin-Huxley model are shown in Figure 5.11A. The effect was reversible during recovery from hypoxia, as τ_{act} decreased to values which were only an average of 8.4 ± 6.4% above the normoxic levels ($P > 0.05$, n = 6, see Table 5.1).

Table 5.1. The effect of hypoxia on the steady-state current and τ_{act}. Values are means ± SEM (n). τ_{act} is the time constant of activation. Significant difference ($P < 0.05$): * between hypoxia and normoxia; § between hypoxia and recovery.

	Normoxia	Hypoxia	Recovery
Steady-state current, pA	1593 ± 207.9 (6)	1270.5 ± 146.5*§ (6)	1426.9 ± 192.8 (5)
τ_{act}, ms	12 ± 1.1 (6)	22 ± 2.6*§ (6)	13.1 ± 1.7 (6)

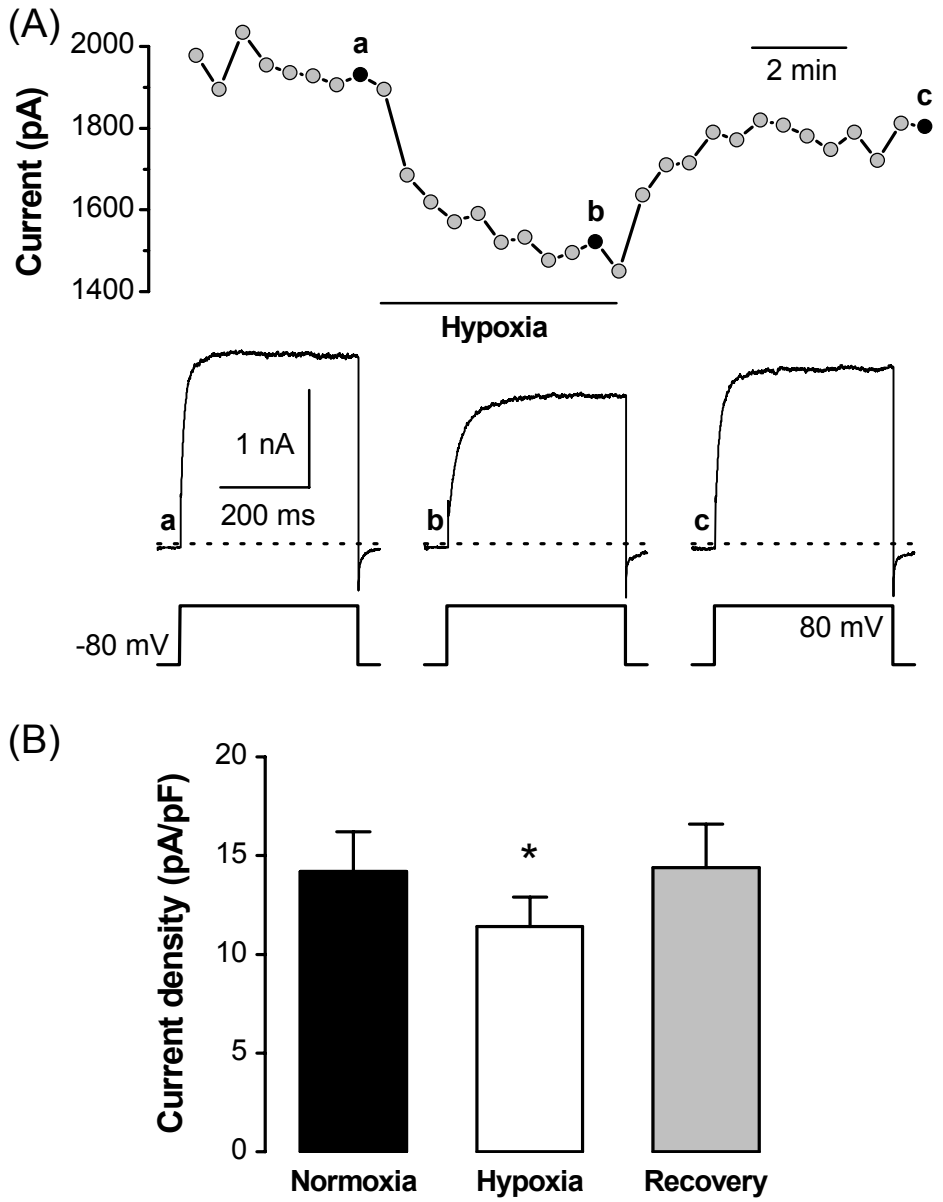

Figure 5.10. The effect of hypoxia on the Penitrem A insensitive current.
(A) Whole-cell currents were recorded by stepping every 30 seconds from a holding potential of -80 mV to +80 mV for 400 ms. The normoxic Penitrem A (100 nM) containing bath solution was made hypoxic for 5 minutes, followed by recovery to normoxia. (*Upper panel*) Representative experiment with steady state current values against time; black circles are the time points when the sample traces underneath were obtained. (*Lower panel*) Sample traces obtained before (a), during (b) and after (c) hypoxic perfusion. (B) Mean ± SEM of current densities. * indicates significant reduction in mean current density compared to normoxia ($P < 0.05$, n = 6).

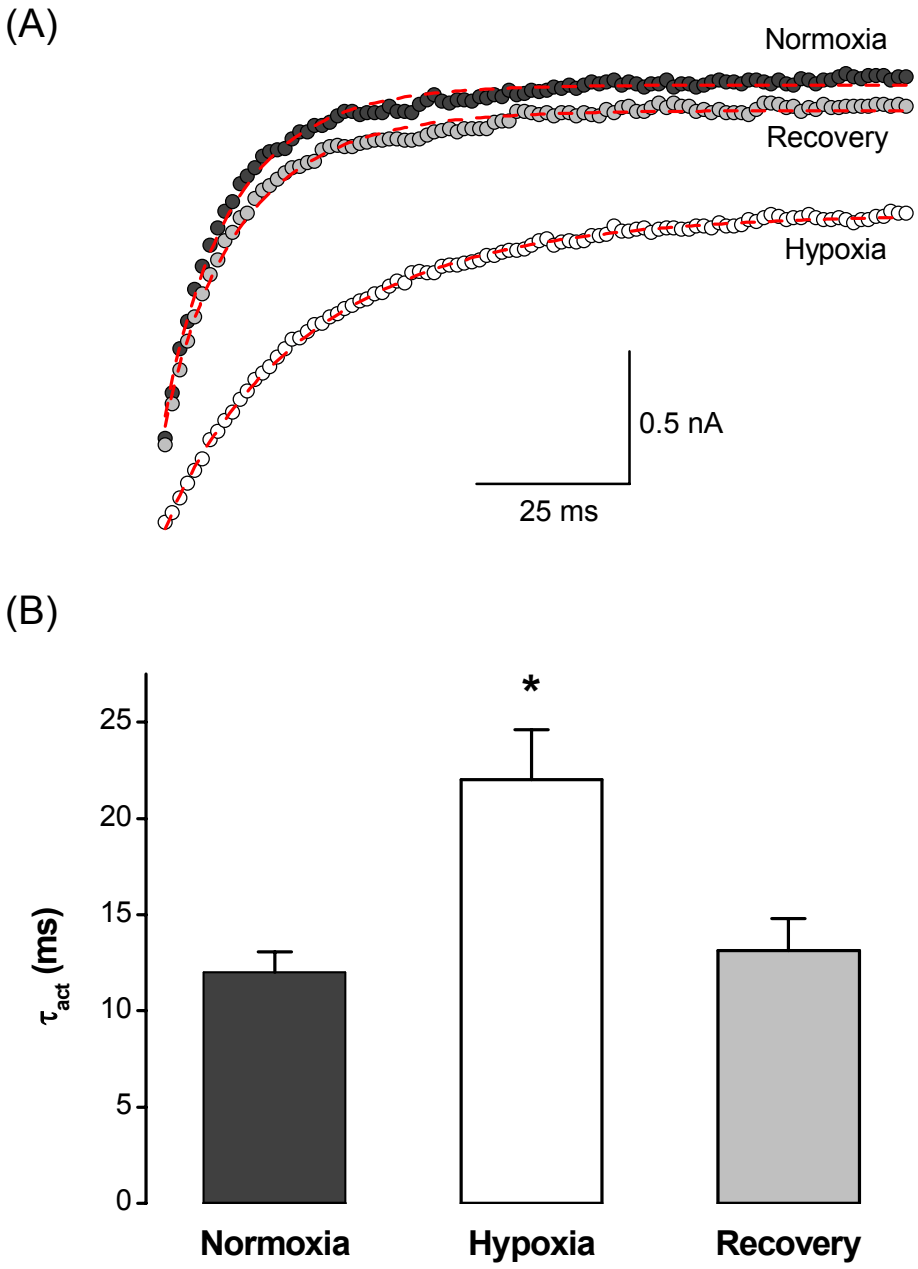

Figure 5.11. The effect of hypoxia on the activation of the Penitrem A insensitive current. (A) Activation of currents during normoxia, hypoxia and recovery. Circles represent recorded current values during the activation phase and lines are curves fitted with a Hodgkin-Huxley function. (B) The time constant of activation τ_{act} (mean ± SEM) of the outward current at +80 mV increased reversibly during hypoxia. * indicates a statistically significant difference in mean τ_{act} during hypoxia and Penitrem A vs. Penitrem A alone ($P < 0.05$, n = 6).

5.3.6. The effect of 4-AP and Glyburide on the hypoxia-induced inhibition of the Penitrem A-insensitive current

The effect of the K_v channel blocker 4-AP (5 mM) (Michelakis *et al.*, 2001) on $I_{K(Pen)}$ was assessed using the repeated single step protocol. The currents elicited by the +80 mV steps were significantly inhibited during perfusion with 4-AP containing bath solution (Figure 5.12A). The average inhibition by 4-AP had a value of 24.7 ± 4.9% ($P < 0.05$, n = 6, Figure 5.12C), with the mean steady state current at 1193.1 ± 134.1 pA compared to a control value of 1570.4 ± 120.8 pA (n = 6).

Further experiments were done to verify whether 4-AP had any influence on the hypoxic effect on $I_{K(Pen)}$. When 4-AP was present in the bath, hypoxia had no significant effect on the steady state current ($P > 0.05$, n = 6, Table 5.2), indicating that the component inhibited by hypoxia was 4-AP sensitive.

In separate experiments, the effect of Glyburide, an ATP-sensitive K^+ channel blocker, on $I_{K(Pen)}$ was tested. As shown in Figure 5.12B, the addition of 10 μM Glyburide had no significant effect ($P > 0.05$, n = 5, Table 5.2 and Figure 5.12D), thus a potential susceptibility to Glyburide of the hypoxia-sensitive current in PVSMC was ruled out.

Table 5.2. The effect of hypoxia and K^+ channel blockers on the I_{out} current. Values are means ± SEM (n). Percentage inhibition was calculated individually for every cell and subsequently averaged. * indicates significant difference ($P < 0.05$).

	Steady state current (treated vs control), pA	**Inhibition, %**
Hypoxia	1270.5 ± 146.5* vs 1593 ± 207.9 (6)	19.4 ± 2.3%
4-AP, 5 mM	1193.1 ± 134.1* vs 1570.4 ± 120.8 (6)	24.7 ± 4.9%
Hypoxia (presence of 4-AP)	1131.6 ± 125.2 vs 1193.1 ± 134.1 (6)	4.9 ± 1.8%
Glyburide, 10 μM	877 ± 203.9 vs 866.8 ± 191.5 (5)	-0.02 ± 2.8%

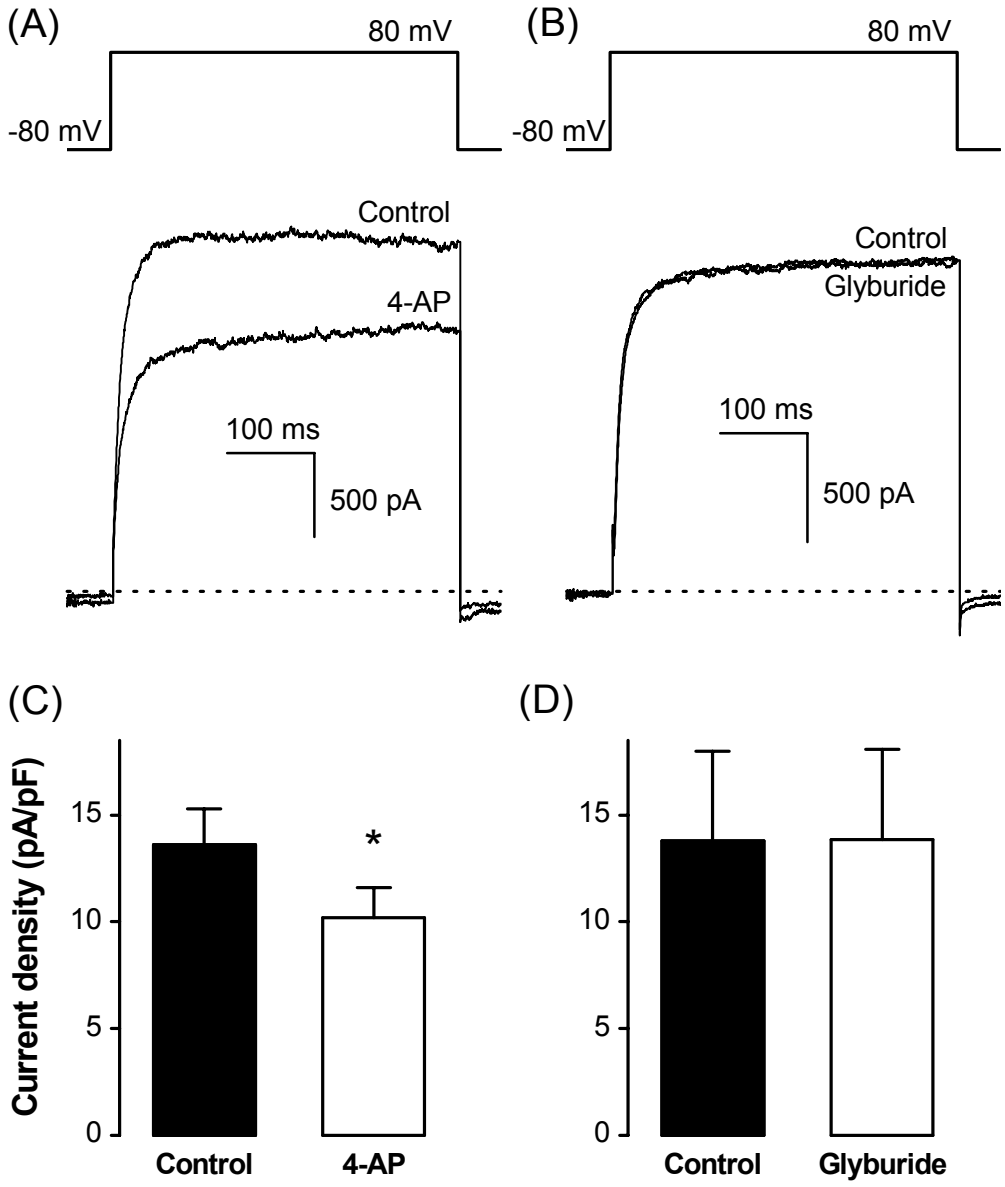

Figure 5.12. The effect of 4-AP and Glyburide on the Penitrem A insensitive current. Representative current traces illustrate the effect of 4-AP (A) and Glyburide (B) in the presence of Penitrem A; capacitive transients have been truncated offline for clarity and dashed lines mark zero current level. Comparison of mean values of the steady state current for 4-AP (C) and Glyburide (D) * indicates significant differences between amplitude of currents recorded in the presence of 4-AP and control ($P < 0.05$, n = 6).

5.3.7. The hypoxia-sensitive difference current

As shown previously, hypoxic flow reduced the amplitude of the steady state Penitrem A insensitive current and decreased its rate of activation (increased τ_{act}). These results implied that, compared to the control current, the hypoxia-inhibited component had a steady state-value of approximately 20% and was a more rapidly activating current (since its inhibition had caused a decrease in activation rate).

However, in order to further characterise the shape and kinetics of the current inhibited by hypoxia, it was necessary to isolate and illustrate this component. This was achieved by subtracting the current traces recorded before and during hypoxic perfusion (see Figure 5.13A), which revealed the hypoxia-sensitive, difference current ($I_{K(H)}$), as shown in Figure 5.13B.

$I_{K(H)}$ activated rapidly to an early peak, after which it declined, inactivating partially before reaching a steady state phase. The shape of the current revealed that previous measurements (made at the steady state phase) which estimated the amount of inhibition induced during hypoxic perfusion at ~ 19% were in fact underestimating the hypoxia sensitivity of the Penitrem A insensitive current. When the same measurements were repeated at the rise phase (at a time point equivalent to the peak of $I_{K(H)}$), it was revealed that the amplitude of $I_{K(H)}$ represented 36.3 ± 3.4% of the control current (n = 6).

5.3.8. Time course of the hypoxic inhibition of $I_{K(H)}$

To examine the time course of the hypoxic effect on $I_{K(H)}$, the hypoxia-insensitive current (i.e. the current where hypoxic inhibition was maximum) was subtracted from all other current traces recorded (Figure 5.14A). Peak $I_{K(H)}$ was attenuated by 69.5 ± 4.7% ($P < 0.05$, n = 6) after approximately 1 min from the start of the hypoxic flow (Figure 5.14B) and was, by definition, completely inhibited by the end of the hypoxic period.

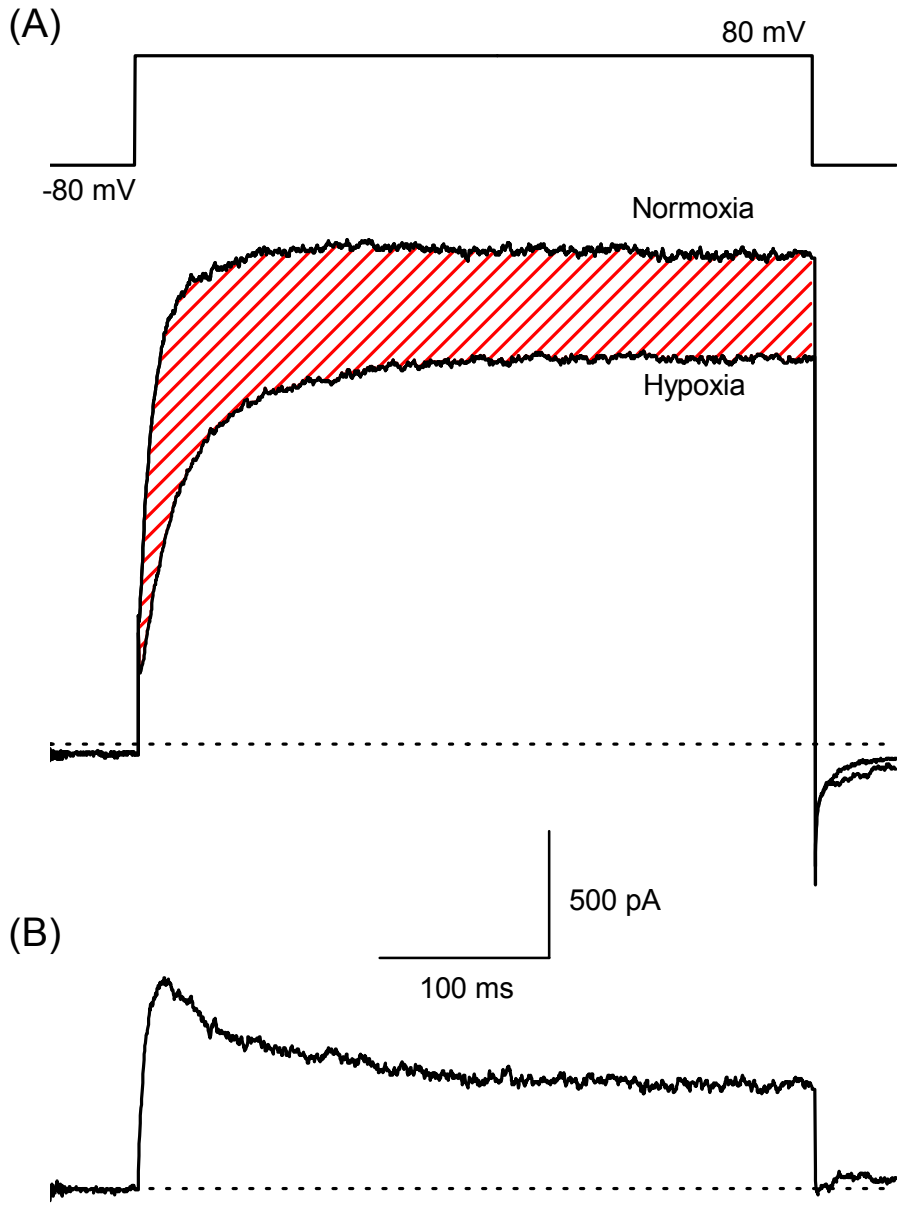

Figure 5.13. The hypoxia-sensitive difference current. (A) Representative currents elicited by depolarization from a holding potential of -80 mV to a test potential of +80 mV. Recordings made during normoxia and hypoxia are shown superimposed and the red hashed area represents the amount inhibited by hypoxia; dashed lines mark zero current level. (B) The hypoxia-sensitive, difference current ($I_{K(H)}$) shown is the difference current equivalent to the hashed area.

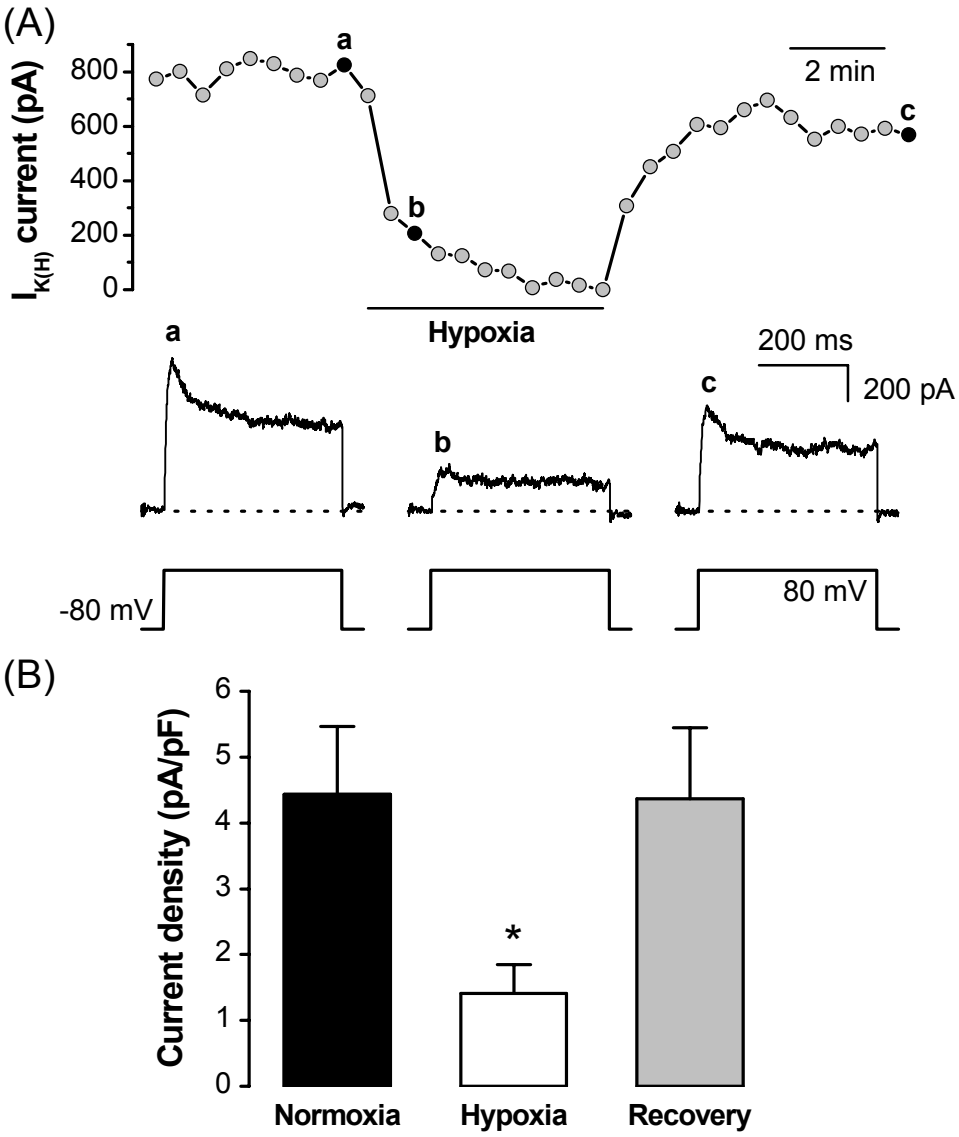

Figure 5.14. The hypoxia-sensitive $I_{K(H)}$ current during perfusion with normoxic and hypoxic solution. (A) Currents were recorded using a repeated single step protocol during perfusion with normoxic and hypoxic Penitrem A (100 nM) containing bath solution. $I_{K(H)}$ currents were obtained by subtraction. (*Upper panel*) Representative experiment with peak $I_{K(H)}$ current values plotted as a function of time; black circles represent the time points when the sample traces underneath were obtained. (*Lower panel*) Representative $I_{K(H)}$ traces obtained before (a), during (b) and after (c) perfusion with hypoxic bath solution. (B) Mean peak current density of the $I_{K(H)}$ under normoxic, hypoxic (after ~1 min) and recovery to normoxia conditions. * indicates significant reduction in mean current density in the presence of hypoxia and Penitrem A when compared to only Penitrem A ($P < 0.05$, n = 6).

5.4. Discussion

Potassium channels have a central role in maintaining the resting membrane potential in vascular smooth muscle cells (Nelson and Quayle, 1995). Consequently, vascular tone can be regulated through the activation or inhibition of different types of K^+ channels. In particular, by regulating potassium ion fluxes in response to alterations of the membrane potential, activated voltage-gated K^+ (K_V) channels act to limit further membrane depolarisation.

In pulmonary arterial smooth muscle cells, it was demonstrated that, aside from membrane potential and vascular tone regulation, K^+ currents are involved in acute O_2 sensing (Post *et al.*, 1992, Yuan *et al.*, 1993a) and also mediate the chronic effects of hypoxia (Smirnov *et al.*, 1994, Wang *et al.*, 1997). The functional and molecular features of K^+ channels from PASMC have been well described in multiple studies (see, for example: Yuan et al., 1998b, Ko et al., 2007, Bonnet and Archer, 2007). However, even though pulmonary veins also participate in acute and chronic HPV (Zhao *et al.*, 1993, Migally *et al.*, 1982), characterisations of ionic currents in PVSMC are not available in the literature, with the single exception of a brief section in a study on rat pulmonary veins (Michelakis *et al.*, 2001).

In this study, standard incremental voltage protocols activated a family of large whole-cell outward currents (I_{out}) in porcine PVSMC. I_{out} was, to a large extent, inhibited by the relatively non-selective K^+ channel blocker TEA (5 mM), which has been reported to block both K_{Ca} (Barman, 1997) and K_v channels (Ko *et al.*, 2007), suggesting it was predominantly a K^+ current.

I_{out} activated rapidly with a threshold for activation of -20 mV, became larger and noisier at more depolarised potentials and was non-inactivating. These features were consistent with those of a “spiky morphology” current in rat PVSMC (Michelakis *et al.*, 2001). In addition, the current from rat PVSMC also showed significant sensitivity to 5mM TEA. Similar rapidly-activating, non-inactivating currents were

also reported in cultured human PASMC (Peng *et al.*, 1996) and in 58% of the mouse PASMC tested (Ko *et al.*, 2007).

Following inhibition of the BK_{Ca} component of I_{out} with Penitrem A, spontaneous activity was eliminated and the remaining current had a stable steady-state amplitude. Time-course experiments revealed that this Penitrem A-insensitive current was inhibited significantly by hypoxia. In the presence of 4-AP, the hypoxia-induced inhibition of K^+ currents was abolished, implying that the hypoxia sensitive current is a 4-AP sensitive K_V current. In similar experiments, the ATP-sensitive K^+ channel antagonist Glyburide did not cause a significant effect on the Penitrem A-insensitive current.

Direct inhibition of K^+ currents by hypoxia was first observed by Post *et al*. (1992) in freshly dispersed canine PASMC. In their experiments, the effect of hypoxia was abolished by buffering intracellular Ca^{2+} or using Ca^{2+} channel blocker nisoldipine in the bath solution, therefore they suggested the hypoxic inhibition was primarily due to blocking Ca^{2+}-activated K^+ channels. Subsequently, this was disproved by Yuan *et al*. (1993a, 1995) in a study on rat PASMC. Their observations involved Ca^{2+} independent hypoxic inhibition of K^+ currents and suggested suggesting that neither K_{Ca} nor K_{ATP} were involved in the initiation of HPV. They provided evidence that hypoxia inhibits voltage-gated K^+ channels and proposed a mechanism for the initiation of hypoxic pulmonary vasoconstriction involving K_V channels. These K_V channels, with a threshold for activation more negative than the resting membrane potential, would be open at the resting state and their inhibition by hypoxia would cause membrane depolarisation, Ca^{2+} influx through voltage-gated Ca^{2+} channels and subsequent vasoconstriction.

To illustrate the hypoxia-sensitive Kv current ($I_{K(H)}$), the macroscopic currents recorded during hypoxia were subtracted from those recorded during normoxic conditions (see Figure 5.13). $I_{K(H)}$ was revealed to be a very rapidly activating,

partially inactivating current, which had its peak value reduced by ~70% during the first minute of exposure to hypoxia.

This is the first report of a hypoxia-sensitive K_V current in pulmonary vein smooth muscle cells freshly isolated from adult porcine lungs. The findings presented here suggest that this K_V current is susceptible to low O_2 within a very short exposure time and its inhibition by acute hypoxia could contribute to the initiation of hypoxic pulmonary vasoconstriction in the pulmonary veins. Its activation and inactivation characteristics, including voltage window of current availability, investigated further, should provide more information in regards to the physiological relevance of this current in porcine PVSMC.

Chapter 6.
Biophysical characterisation of the hypoxia-sensitive current in PVSMC

6.1. Introduction

According to the most widely accepted theory on HPV initiation, O_2 sensitive K^+ channels are central to the hypoxia sensitivity of smooth muscle cells from the pulmonary circulation (Mauban *et al.*, 2005, Weir and Olschewski, 2006). The inhibition of K^+ currents by hypoxia was demonstrated in PASMC from the dog (Post *et al.*, 1992) and the rat (Yuan *et al.*, 1993a). This initial event leads to membrane depolarisation, subsequent activation of VGCC and vasoconstriction induced by the rise in cytosolic Ca^{2+} (Moudgil *et al.*, 2005).

In the pulmonary artery, the channels underlying the hypoxia-sensitive current have, in turn, been suggested to belong to the families of Ca^{2+}-activated K^+ channels (K_{Ca}) (Post *et al.*, 1992, Park *et al.*, 1995) and voltage-gated K^+ channels (K_V) (Yuan *et al.*, 1995, Patel *et al.*, 1997). Most recent electrophysiological and pharmacological evidence supports the latter and indicates the O_2-sensitive current in PASMC is a slowly inactivating, voltage-dependent delayed rectifier K^+ current (Archer *et al.*, 2000). Consequently, several homo-/heteromeric subtypes from the K_V family that match that profile have been proposed as candidate channels, with Kv1.5 and Kv2.1 among the main contenders (Archer *et al.*, 1998).

For the first time, evidence of a hypoxia-sensitive K^+ current ($I_{K(H)}$) in smooth muscle cells from porcine intrapulmonary veins is presented here (see results section 5.3.7). In order to understand more about the potential physiological relevance of $I_{K(H)}$ in the response induced by hypoxia in intrapulmonary veins, the biophysical properties of the $I_{K(H)}$ current were investigated. This involved determining activation and inactivation curves, with times to half-maximal activation/inactivation and voltage window of current availability, as well as the time required for $I_{K(H)}$ to recover from inactivation induced by depolarisation.

6.2. Experimental protocols

The same approach of subtracting the currents recorded under hypoxic conditions from the normoxic currents across different voltage protocols was used to study the activation and inactivation kinetics of $I_{K(H)}$ in more detail.

6.2.1. Voltage dependence of inactivation

Steady-state inactivation of $I_{K(H)}$ was examined using a double-pulse protocol, with an initial 1-s conditioning voltage step of varying amplitude (increasing from -100 to +20 mV in 10 mV increments) followed without a delay by the application of a 500-ms common test pulse at a constant voltage (+80 mV) (see Figure 6.1).

The amount of inactivation achieved during the initial conditioning pulse was assessed through the size of the current evoked by the test step, which was proportional with the amount of channels remaining available for activation.

The inactivation curve was obtained by plotting normalized peak test currents $[(I-I_{min})/(I_{max}-I_{min})]$ as a function of the conditioning voltage and fitting the data with a Boltzmann function:

$$f(x) = \frac{A_1 - A_2}{1 + e^{(x - x_0)/dx}} + A_2 \qquad (13)$$

where A_1 is the initial amplitude, A_2 is the final amplitude, x_0 is the centre of the curve (i.e. the voltage for half-inactivation) and dx is the time constant (i.e. the slope).

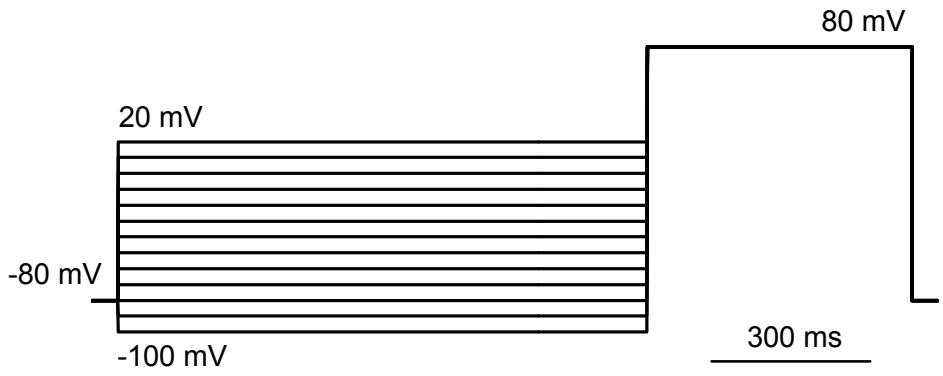

Figure 6.1. Voltage dependent inactivation protocol. Double-pulse voltage protocol consisting of an initial conditioning step of increasing amplitude (-100 mV to +20 mV) followed immediately by a constant test step at +80 mV.

6.2.2. Voltage dependence of activation

The voltage dependence of activation of $I_{K(H)}$ was also investigated. Membrane currents were elicited by stepping from the holding potential of -80 mV to potentials ranging from -50 mV to +100 mV for 500 ms. Peak currents were converted into conductance by dividing the macroscopic current by the driving force, using the following equation (McGahon *et al.*, 2005):

$$G = I(V_t - E_K) \qquad (14)$$

where G is the conductance, I is the peak current, V_t is the test potential and E_K is the potassium equilibrium potential (taken as -80 mV). Data values were subsequently normalised and fitted with a Boltzmann distribution.

6.2.3. Time of recovery from inactivation

To further characterise the hypoxia-sensitive current, the time of recovery from inactivation of $I_{K(H)}$ was investigated using a double-pulse voltage protocol. The two pulses – conditioning and test – were both depolarising steps of 200 ms duration from -80 mV to +80 mV. During the conditioning step, cells were held at +80 mV to inactivate $I_{K(H)}$ and then stepped for a variable time interval (starting from 10 ms initially and increasing by 20 ms up to 290 ms) back to -80 mV to relieve inactivation. Thereafter, a test pulse to +80 mV was applied to evaluate the degree to which inactivation had been removed (see Figure 6.2). The amount of current activation upon returning to +80 mV was dependent on time spent at -80 mV.

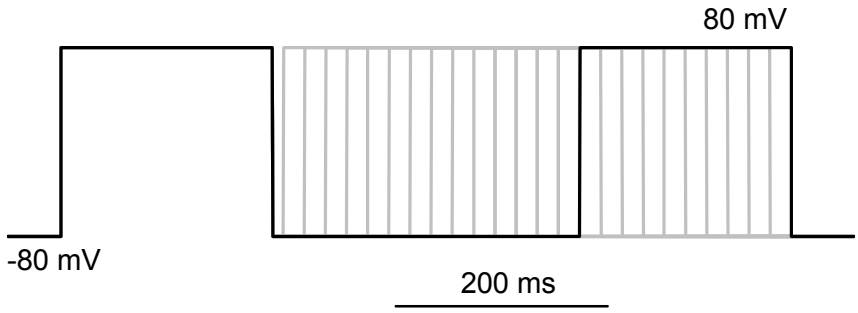

Figure 6.2. Recovery from inactivation protocol. Double-pulse voltage protocol with equal conditioning and test voltage steps from -80 mV to +80 mV, separated by a variable time interval (10 ms to 290 ms) at the holding potential of -80 mV; for clarity, all steps except the last one are shown with grey lines.

The peak currents evoked by the test pulses were measured and normalised to their respective peak conditioning currents. The normalised values were averaged and the data obtained were plotted as a function of the variable interval between the conditioning and test potentials (in ms). Thereafter, the plot was fitted with a curve using the following exponential equation:

$$f(t) = y_0 - Ae^{-t/\tau_{rec}} \qquad (15)$$

where t is the variable time interval, τ_{rec} is the time constant for recovery, y_0 is the offset (i.e. the non inactivating fraction of the current) and A is the amplitude (i.e. the inactivating component). The parameter τ_{rec} is equivalent to the time in which the current regains 63% of its inactivated fraction and describes the speed of recovery from inactivation.

6.3. Results

6.3.1. Family of $I_{K(H)}$ currents

Voltage protocols were applied to the same cells under both normoxic and hypoxic conditions, resulting in the recording of pairs of families of currents (e.g. pair of sample traces shown in Figure 6.3). The effect of hypoxia was to partially inhibit the control normoxic currents resulting in a family of smaller and slower activating currents.

In each case, the target hypoxia-sensitive currents ($I_{K(H)}$) were then obtained by subtracting the hypoxic from the normoxic currents. The result was a family of outward currents, with rapid activating and partial inactivating kinetics (representative family of $I_{K(H)}$ currents shown in Figure 6.4).

6.3.2. Current kinetics of $I_{K(H)}$

The $I_{K(H)}$ current activated rapidly to a peak current density of 4.4 ± 1 pA/pF at +80 mV (n = 6). The time to peak activation (TTP) was used to characterise the speed of activation of $I_{K(H)}$ (as illustrated in Figure 6.5).

The mean TTP value of the current activated by a +80 mV voltage pulse was 14.4 ± 3.3 ms (n = 5). Following peak activation, the current declined to a steady-state level of 53 ± 7.2% (n = 5) of peak value.

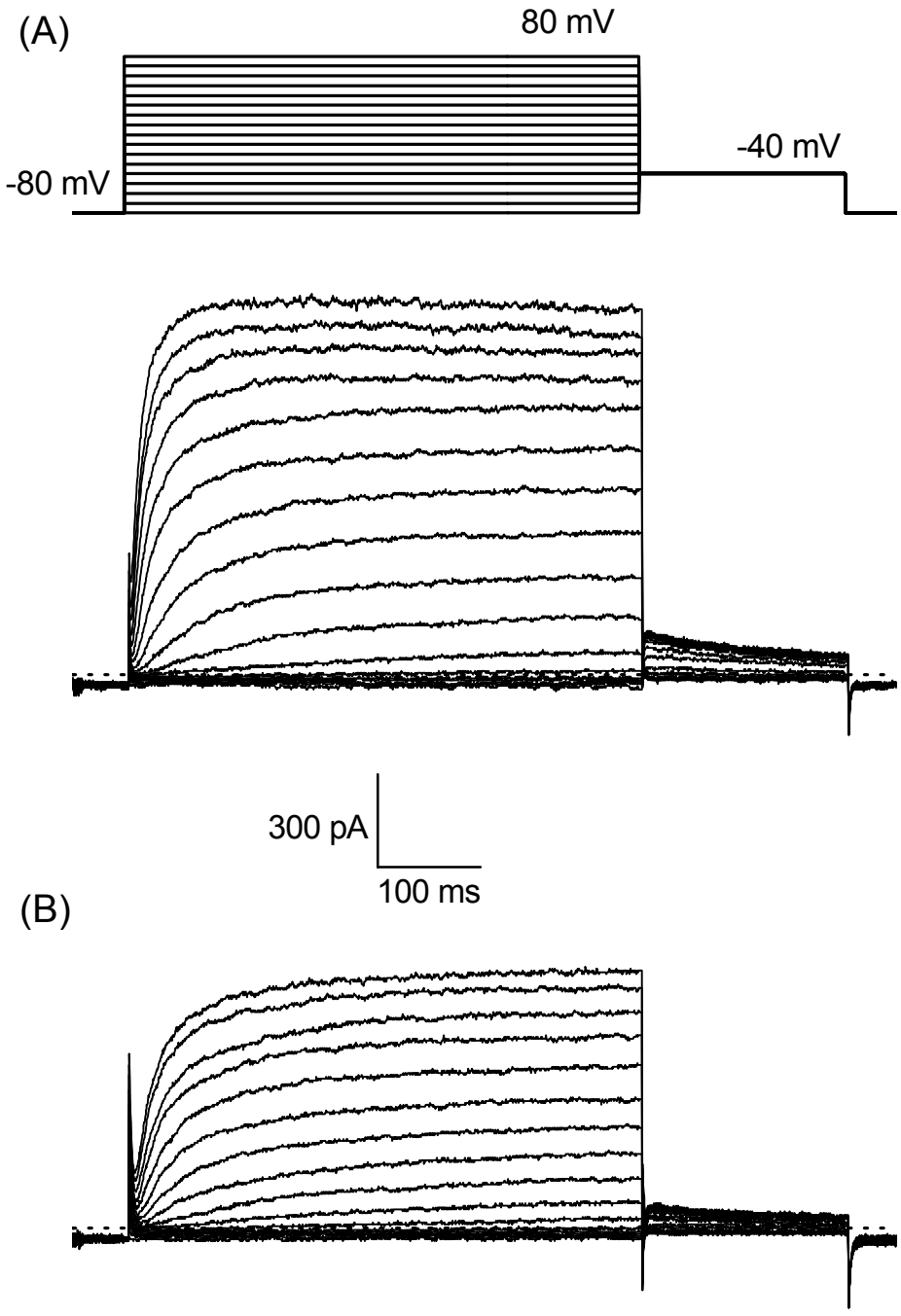

Figure 6.3. Whole-cell voltage-activated outward currents recorded under normoxia and hypoxia. Sample families of currents elicited under normoxic (A) and hypoxic (B) flow. Capacitive transients have been truncated offline for clarity; dashed lines represent zero current level.

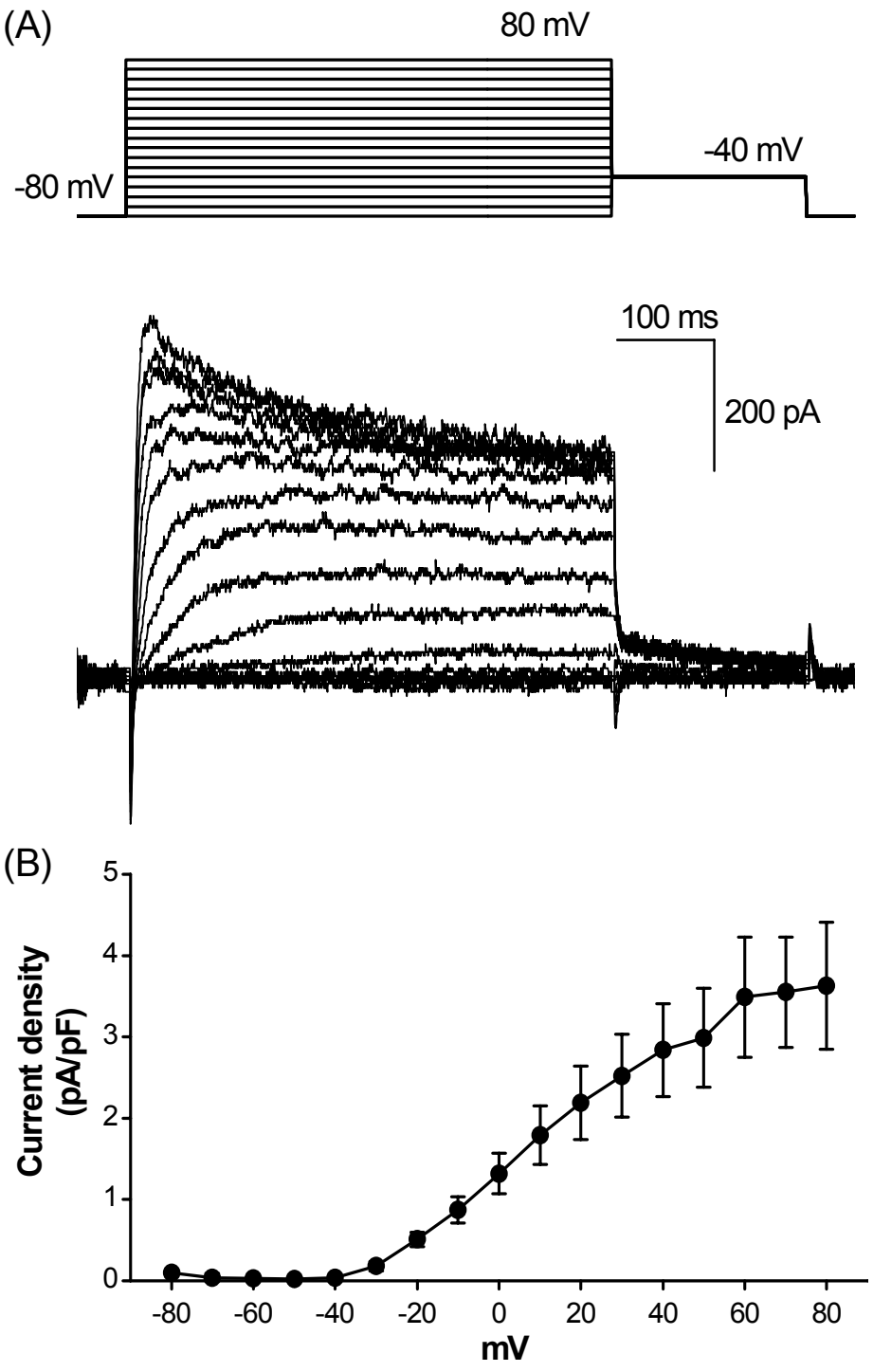

Figure 6.4. Family of $I_{K(H)}$ currents. (A) Sample families of hypoxia-sensitive currents obtained by subtraction of currents in Figure 6.3. Capacitive transients have been truncated offline for clarity; dashed line represents zero current level.
(B) Mean current density–voltage relationship for $I_{K(H)}$.

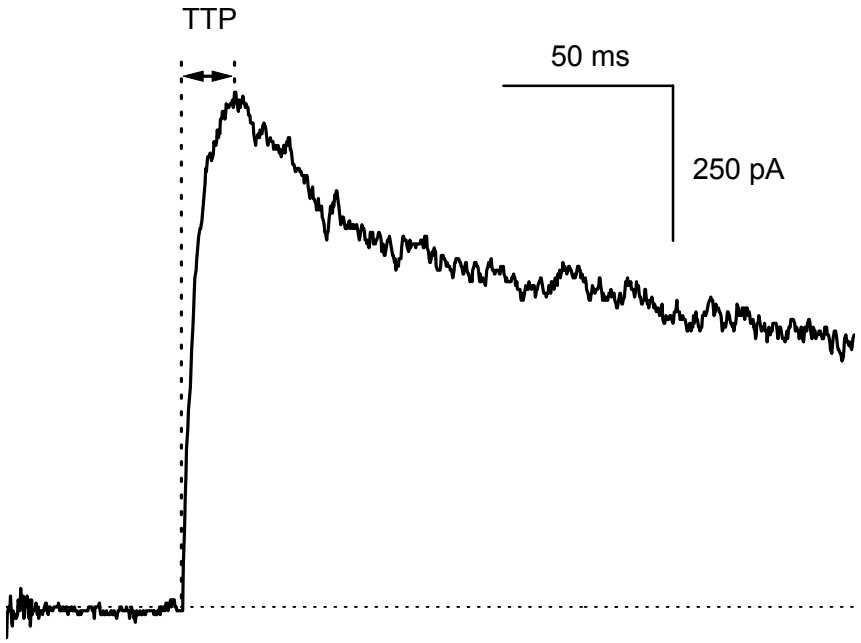

Figure 6.5. Time to peak of $I_{K(H)}$. Representative trace of $I_{K(H)}$ at + 80 mV. TTP was calculated as the time passed (in ms) between the onset of the depolarising test step and the peak of the current; dashed line marks zero current.

6.3.3. Activation and inactivation curves

The voltage dependency of activation and inactivation were used to infer the current window of availability of $I_{K(H)}$ (McGahon *et al.*, 2005), which is characterised by partial activation and incomplete inactivation of channels.

The application of the inactivation protocol evoked peak test currents that decreased as the conditioning pulse increased (representative recording in Figure 6.6A). Mean values (calculations detailed in Experimental protocols) were fitted with a Boltzmann function to give the inactivation curve (Figure 6.6B, empty circles). The voltage for half-inactivation ($V_{0.5}$) for the $I_{K(H)}$ current was derived, giving a value of -58.5 mV, while the slope was 17.6 mV. For the activation curve, mean conductance values were well fitted with a Boltzmann distribution (Figure 6.6B, full circles) with a $V_{0.5}$ activation of -13 mV and a slope of 14.9 mV.

The areas under the inactivation and activation curves overlapped to give a window of current availability between -60 mV to +20 mV, with peak window current availability at -31.86 mV (see inset in Figure 6.6B).

6.3.4. Recovery of $I_{K(H)}$ from inactivation at +80 mV

Following subtraction of the currents recorded under normoxic (Figure 6.7A) and hypoxic (Figure 6.7B) conditions, the family of $I_{K(H)}$ currents was revealed. Peak test currents were partially inactivated after the initial time interval of 10 ms, but quickly recovered as the time spent at the holding potential of -80 mV increased (Figure 6.8A). The normalised peak values of the hypoxia-sensitive currents, averaged between 4 cells, were plotted as a function of the delay time between the conditioning and the test pulse. The rate of recovery after inactivation at +80 mV was well described by a single exponential function ($R^2 = 0.96$) with a time constant (τ_{rec}) of 67 ms (shown in Figure 6.8B).

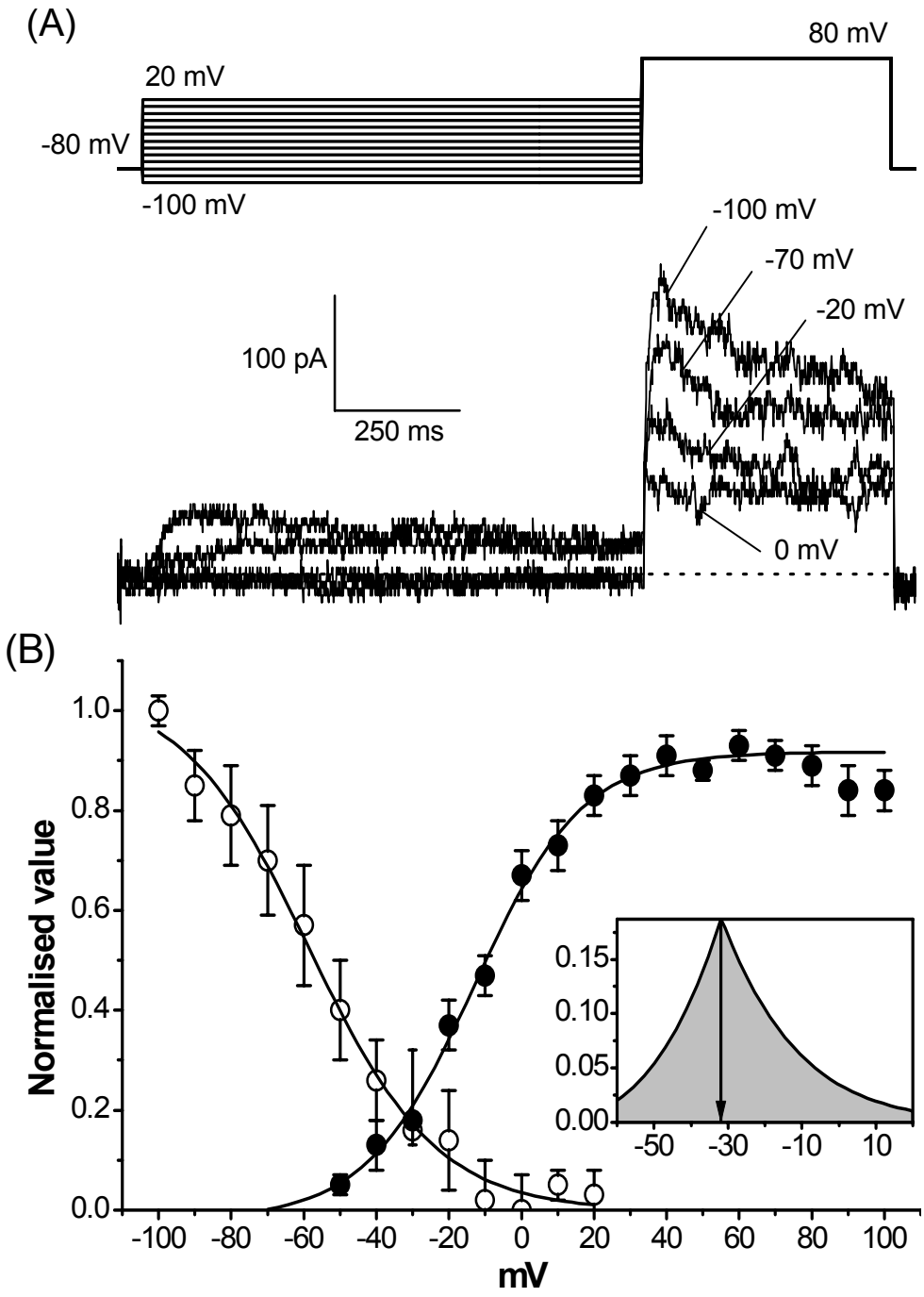

Figure 6.6. Activation and inactivation curves. (A). Representative membrane currents recorded using the voltage-dependent inactivation protocol; for clarity, not all current traces are shown. (B) Curves describing the voltage dependence of activation (*full circles*, from 7 cells) and inactivation (*open circles*, from 5 cells). Inset: the window of current availability of $I_{K(H)}$.

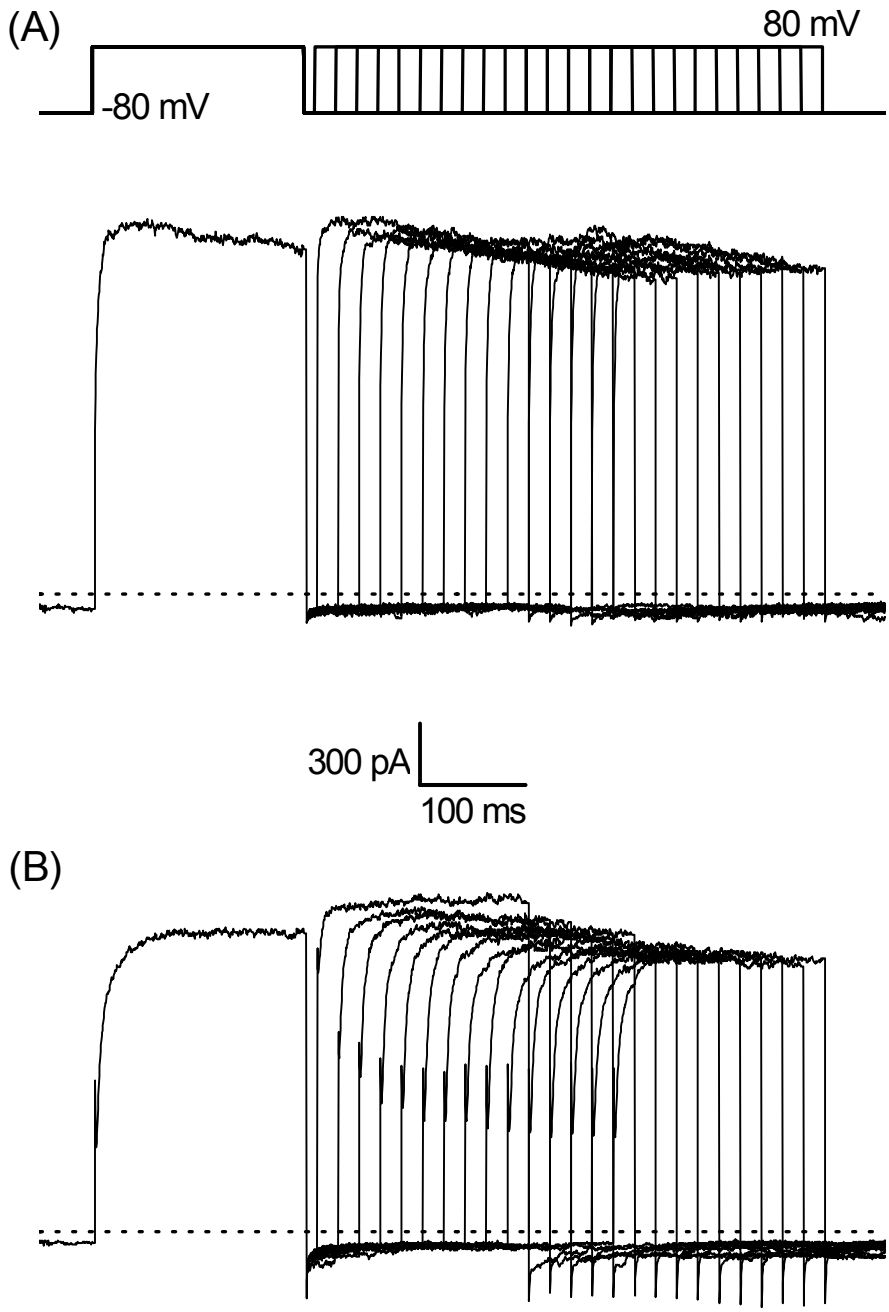

Figure 6.7. Recovery from inactivation protocol under normoxia and hypoxia. Sample families of currents elicited under normoxic (A) and hypoxic (B) flow. Capacitive transients have been truncated offline for clarity; dashed lines represent zero current level.

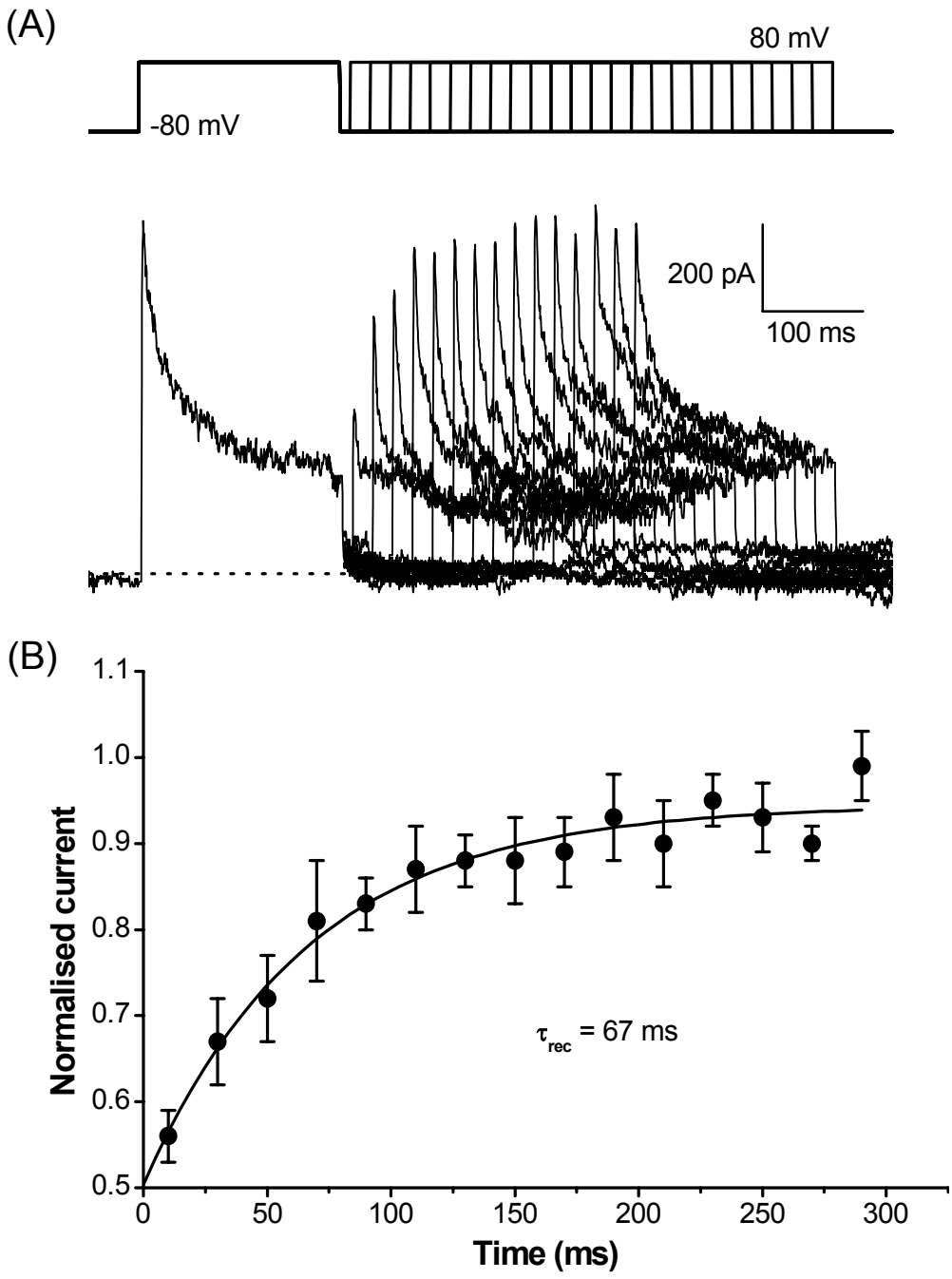

Figure 6.8. Recovery of $I_{K(H)}$ from steady-state inactivation. (A) Representative traces of hypoxia-sensitive currents obtained after subtraction; dashed lines marks zero current level; for clarity, not all current traces are shown (B) Average time course for recovery from inactivation from 4 cells. The plot was fitted with a single exponential giving a time constant for recovery of 67 ms.

6.4. Discussion

The present study reports the identification of a hypoxia-sensitive K_V current in pulmonary vein smooth muscle cells freshly isolated from the adult porcine lung. The biophysical features of the hypoxia-sensitive $I_{K(H)}$ current have similarities to the typical attributes of transient (A-type) currents, which are voltage-gated K^+ currents with rapid rates of activation and steady-state inactivation.

In previous reports, the modulation of A-type K_V currents by oxygen levels has been shown in other tissues. For example, in rabbit pulmonary neuroepithelial bodies which function as airway oxygen sensors, hypoxia sensitivity was carried by an A-type K^+ channel (Fu *et al.*, 2007) and in rodent neurons, an A-type current was regulated by the cellular redox state (Ruschenschmidt *et al.*, 2006). Also, in cultured rat pulmonary artery cells, a rapidly activating, steady-state inactivating K_v current was reversibly inhibited by hypoxia (Yuan *et al.*, 1993a).

The rapid rate of activation of $I_{K(H)}$ was comparable to observations made in rabbit portal vein (time to peak ~ 20 ms) (Beech and Bolton, 1989), but slower than an ultra-fast activating current in murine portal vein (time to peak of 4.1 ms) (Yeung *et al.*, 2006). The potential at which $I_{K(H)}$ half-inactivated was within the range seen in other vascular muscle (-78 to -38 mV), while the time of recovery from steady-state inactivation was comparable with data from gastro-intestinal smooth muscle (Amberg *et al.*, 2003), but faster than in rat retinal arterioles (118.7 ms) (McGahon *et al.*, 2005), human mesenteric arteries (254 ms) (Smirnov and Aaronson, 1992) and rabbit pulmonary artery (> 10 s) (Osipenko *et al.*, 1997).

The inactivation of the $I_{K(H)}$ current from its early peak was rapid, however it was only partial. A steady-state $I_{K(H)}$ current was present in all recordings and had a mean value of 53% of peak amplitude. This finding contrasts with the properties of A-type currents, which are usually completely inactivating (Iida *et al.*, 2005). However, this could be reconciled if, alongside a main A-type current, $I_{K(H)}$ contained a secondary non-inactivating component that was also sensitive to hypoxia and 4-AP, possibly a

delayed rectifier current such as those reported in rat PASMC (Archer *et al.*, 1996, Post *et al.*, 1995). This matter would be clarified through further research to determine the molecular identity of the channel(s) underlying $I_{K(H)}$.

Given its K_V nature, the function of the channel underlying the $I_{K(H)}$ current is intrinsically voltage dependent, therefore its functional role in vascular smooth muscle relies on the ability of the channel to maintain its activation at physiologically relevant membrane potentials. In this respect, K_V channel activity is a balance between channel activation and inactivation at any given membrane potential. In most vascular tissues, A-type currents do not contribute to the resting membrane potential (RMP) due either to their activation thresholds being more positive than RMP (Amberg *et al.*, 2003) or their voltage of complete inactivation negative to RMP (Beech and Bolton, 1989). Conversely, an A-type current has been recently identified in retinal arterioles (McGahon *et al.*, 2005) with an activation threshold that suggests it is likely to be active at RMP. Similarly, in porcine PVSMC the steady-state activation and inactivation curves for $I_{K(H)}$ revealed a voltage window of current availability that included the observed range of RMP, which suggests that $I_{K(H)}$ is likely to be active under resting conditions. Moreover, the mean RMP (-35.8 mV) was near the peak of this window (-31.86 mV), when the current registers its highest point of availability. This is consistent with observations made in PASMC, where the voltage window was narrower, between -40 and -10 mV, but the peak availability of -31.5 mV was similarly close to the RMP value of -27.9 mV (Ko *et al.*, 2007).

In smooth muscle from retinal arterioles, McGahon et al. (2005) have suggested that the A-type current is active at RMP and its hyperpolarizing effect on the RMP suppresses membrane excitability. A similar role for K_v in PVSMC is supported by the observation that application of 4-AP results in contraction of rat pulmonary veins (Michelakis *et al.*, 2001). The studies presented here provide further evidence for this role and suggest that, in common with reports for the pulmonary artery, hypoxic

inhibition of K_v channels contributes to the development of hypoxic pulmonary venous contraction.

In PASMC, existing evidence suggests that the O_2-sensitive K^+ channels with roles in acute and chronic HPV are the delayed rectifier channels Kv1.5 and Kv2.1 (Moudgil *et al.*, 2006), and that transient currents are not involved in HPV sensing (Archer and Michelakis, 2002).

However, given the biophysical properties of $I_{K(H)}$ described here, the possible candidates for O_2-sensitive K^+ channels in PVSMC have to include K_V subtypes known to generate A-type currents (e.g. Kv1.4 and Kv4.3) (Archer and Michelakis, 2002).

Regrettably, there are no studies available in the literature reporting K_V channel subtype expression in PVSMC, but Kv1.4 and Kv4.3 were found among the K_V α-subunits expressed in distal pulmonary arteries of the rat (Wang *et al.*, 2005b). Moreover, the latter has been identified in human cultured PASMC (Iida *et al.*, 2005). A comparison of the biophysical properties of $I_{K(H)}$ with those of the TEA-sensitive component of the Kv4.3 current in human PASMC shows some similarities: mean voltage at half inactivation (-54 mV vs. $I_{K(H)}$: -58.5 mV) and activation (-2.4 mV vs. $I_{K(H)}$: -13 mV) and time of recovery from inactivation (τ_{rec}) (238 ms vs. $I_{K(H)}$: 67 ms). In a different study, a Kv4.3 channel with $V_{0.5}$ of inactivation of -51.7 mV, $V_{0.5}$ of activation of -13.1 mV and τ_{rec} of 84 ms was reported in single HEK293 cells (Hatano *et al.*, 2004). Furthermore, Kv4.3 may have sensitivity to hypoxia, as its expression in pulmonary arteries of rats exposed to 3 weeks of hypoxic ventilation was decreased (Wang *et al.*, 2005b). Even if the pore forming K_V subunit is not intrinsically O_2 sensitive, this can be acquired by association with modulatory β-subunits. For example, an A-type current generating Kv4.2 α-subunit gained O_2 sensitivity by coexpression with Kvβ1.2 in transfected HEK293 cells (Perez-Garcia *et al.*, 1999).

For this same reason, the O_2 sensitive subtypes identified in PASMC (e.g. Kv1.5 and Kv.2.1) should not be ruled out in PVSMC, due to possible associations with regulatory β-subunits which are known to be able to alter the gating of the channel and change its inactivation properties. For example, a non-inactivating delayed rectifier K_V channel was shown to gain A-type properties by association with a specific Kvβ1 subunit (Rettig *et al.*, 1994).

Further work including functional studies using specific inhibitors (phrixotoxin-II for Kv4.3, 2,3 Butanedione monoxime (BDM) for Kv2.1 and DPO 1 for Kv1.5) and antibodies against specific subtypes of K_V channels and molecular studies, such as immunolocalisation, RNA isolation and RT-PCR should clarify the molecular identity of $I_{K(H)}$.

Chapter 7.
General Discussion

Hypoxic pulmonary vasoconstriction (HPV) is a unique physiological mechanism that optimises pulmonary gas exchange through a functional shunting mechanism (Traber and Traber, 2002). HPV minimises the impact of regional hypoxia (e.g. during localised lung disease) by restricting blood flow to the areas of the lungs that are poorly ventilated. Consequently, regional perfusion is matched with ventilation and the oxygen saturation of arterial blood is maintained at optimal levels. However, HPV can also have detrimental effects during acute (e.g. high-altitude pulmonary oedema) and chronic (e.g. PHT) generalised alveolar hypoxia as a result of global hypoxic vasoconstriction, which leads to raised blood pressure in the pulmonary circulation.

The main site of action of HPV is the pulmonary microcirculation, including both small pulmonary arteries and veins (Hillier *et al.*, 1997). The intrapulmonary veins participate in all manifestations of HPV, from acute hypoxic contractile responses (Zhao *et al.*, 1993), to increased reactivity during subacute hypoxia (Sheehan *et al.*, 1992) and undergo remodelling during chronic low O_2 breathing (Wagenvoort and Wagenvoort, 1976). Hypoxic contractions of the pulmonary veins have been reported in multiple species: rats (Dingemans and Wagenvoort, 1978, Zhao *et al.*, 1993), guinea pigs (Tracey *et al.*, 1989), sheep (Uzun and Demiryurek, 2003) and dogs (Hillier *et al.*, 1997).

However, despite this and other existing evidence, most investigators disregard any significant contribution of the pulmonary veins in HPV (Ward and Aaronson, 1999, Dumas *et al.*, 1999, Moudgil *et al.*, 2005, Weissmann *et al.*, 2006). Consequently, nearly all the considerable effort that has gone into researching the mechanisms involved in initiating and sustaining HPV has been focused on the pulmonary arteries, and by comparison little is known on the contractile pathways of the hypoxic responses of veins.

7.1. Main findings

The effects of hypoxia on the contractility of distal porcine intrapulmonary veins were investigated using the wire myography technique and responses elicited were compared to those of size-matched pulmonary arteries. Thereafter, single smooth muscle cells were freshly isolated from small intrapulmonary veins using a specifically developed enzymatic dissociation protocol. The PVSMC were characterised morphologically and electrophysiologically. Lastly, using whole-cell patch clamping electrophysiology, the effect of hypoxia on outward currents in PVSMC was investigated, potassium channel blockers were used to manipulate the outward currents and specific voltage protocols were applied in order to describe the biophysical properties of the hypoxia-sensitive current.

Porcine tissue was used in all experiments. The pig was considered a suitable species for investigation of HPV, as robust responses to hypoxia in porcine lungs have been previously reported (Hakim and Malik, 1988, De Canniere *et al.*, 1992, Liu *et al.*, 2001) and shown to be larger compared to responses in lungs from rabbits, cats and dogs (Peake *et al.*, 1981). Additionally, lungs from pigs have the advantage of being sufficiently large to make it practically possible to dissect and use distal intrapulmonary vessels, which are known to be the main contributors to the HPV response (Shirai *et al.*, 1986).

The effects of hypoxia at single cell level were investigated in venous smooth muscle cells. It is known that, alongside SMC, the media of pulmonary veins in all species studied contains an additional muscular layer composed of a different type of muscle cells, with morphological resemblance to the cardiomyocytes in the atrial myocardium (Nathan and Gloobe, 1970). Speculations have been made about a possible role of these cardiomyocytes in the regulation of venous tone in rats (Michelakis *et al.*, 2001). However, in large mammals including humans and pigs, the pulmonary vein's myocardial layer is restricted to extrapulmonary sites (Nathan and Gloobe, 1970, Masani, 1986), and the media of intrapulmonary veins and venules is entirely comprised of smooth muscle.

As HPV occurs predominantly in small calibre vessels (Shirai *et al.*, 1986, Hillier *et al.*, 1997), it was plausible to assume that, if hypoxia acts directly on smooth muscle in the pulmonary veins as it does in the arteries (Post *et al.*, 1992), the hypoxia sensitivity would lie within PVSMC.

7.1.1. Hypoxia constricts isolated PV

Segments of 4th to 7th order intrapulmonary veins responded with large contractions to hypoxia. The venous contractions were greater than those seen in size-matched arteries. In previous reports, when contractile responses induced by hypoxia were compared in arteries and veins, results differed with the veins exhibiting greater responses in pigs (Feletou *et al.*, 1995) and rats (Zhao *et al.*, 1993), whilst arteries contracted more in cats (Shirai *et al.*, 1986) and lambs (Wang *et al.*, 1995).

Intrapulmonary veins also contracted more than arteries in response to high K^+ and $PGF_{2\alpha}$. Similar observations were made for contractions to histamine and 5-HT in guinea-pigs (Shi *et al.*, 1998), prostaglandins in dogs (Altura and Chand, 1981), ET-1 in sheep (Toga *et al.*, 1992) and U46619 in piglets (Arrigoni *et al.*, 1999), but the opposite was found with responses to ET-1 in guinea-pigs (Cardell *et al.*, 1990), noradrenaline in sheep (Kemp *et al.*, 1997) and 5-HT in dogs (al-Tinawi *et al.*,

1994). In some cases, even when veins contracted less than arteries, they were more sensitive to the respective agonist (Joiner *et al.*, 1975a).

There were also differences in the way the hypoxic responses in veins and arteries were affected by the presence of agonist-induced pretone. A hypoxic response, albeit smaller, was present in the veins even without $PGF_{2\alpha}$-induced preconstriction, but the arteries failed to contract under the same conditions. These findings were consistent with observations made in pigs by Miller *et al.* (1989) and in sheep by Uzun and Demiryurek (2003).

The profiles of the hypoxic responses were fundamentally different in veins and arteries. Intrapulmonary veins contracted rapidly to hypoxia, reaching maximum elicited tension in the first 5-10 minutes followed by relaxation, which was similar to responses seen previously in rat pulmonary veins (Zhao *et al.*, 1993). In the arteries, however, the constriction was slow and developed over the entire hypoxic time interval. In other preparations of isolated pulmonary arteries, two contractile phases have been frequently observed (e.g. Bennie *et al.*, 1991). However, in these cases, only the second phase which develops very slowly over 40 minutes to 1 hour, resembling the arterial responses reported here, is considered physiologically relevant (Ward and Aaronson, 1999).

These differences may reflect in different contributions of veins and arteries to HPV in whole lungs. Most studies reporting *in vivo* measurements of blood pressure in the pulmonary circulation (e.g. humans Motley *et al.*, 1947, calves, Kuida *et al.*, 1962) found that the hypoxia-induced increase in pulmonary blood pressure occurs immediately following the start of low O_2 ventilation. Thereafter, maximum values are normally reached in approximately 5 minutes and the pressure plateaues at this level for the remaining period of hypoxic ventilation. Similar observations were made in preparations of isolated blood- and buffer-perfused lungs (Duke, 1954, Weissmann *et al.*, 1995).

In other words, the hypoxic pressor response develops significantly faster in whole lungs and intact animals compared to isolated pulmonary arteries, which are the site of HPV according to accepted dogma. This discrepancy could be explained by the early contribution of raised microvascular pressure due to downstream venoconstriction. In the same way, during prolonged hypoxia (> 15 minutes), the pressure in isolated veins decreases, but remains at a raised level in whole lungs, which may be due to increased contribution of arterial contraction.

The venous contractions were significantly affected when extracellular Ca^{2+} was removed from the bath solution, while arterial responses were not. This finding is consistent with work by Tracey *et al.* (1989) who reported that hypoxic venoconstriction in pigs was Ca^{2+} dependent and by Mikkelsen and Pedersen (1983) who observed that contractions of human veins were more susceptible to Ca^{2+} removal than those of arteries. Furthermore, Devine *et al.* (1972) compared the amount of SR from various types of vascular smooth muscle and then studied the contractions of the same types of smooth muscle under Ca^{2+}-free extracellular conditions. They found that pulmonary arteries had larger amounts of SR compared to other types of smooth muscle and this was consistent with their ability to maintain significant contractions in the absence of calcium influx.

Lowering extracellular Cl^- did not significantly modify responses of veins to hypoxia, but the Cl^- channel antagonist NFA inhibited venous responses. While these findings suggest an NFA-sensitive conductance is involved in promoting contraction to hypoxia in porcine intrapulmonary veins, they are difficult to interpret further due to the possible non-specific actions of Cl^- channel blockers on K_{Ca} channels (Ottolia and Toro, 1994, Greenwood and Large, 1995). Further work at cellular level using newer, more specific channel blockers would help clarify the role of the Cl^- conductance in HPV.

Overall, the differences in the contractile responses observed in wire myography studies between small veins and arteries strongly suggest specific mechanisms of

venous contraction exist and should therefore be thoroughly investigated, as have been those in the arteries.

7.1.2. Characterisation of PVSMC

Single, freshly isolated, porcine PVSMC have not been described before in the available literature. In the present study, a specific cell isolation protocol was developed and optimised for the isolation of porcine venous smooth muscle cells. Enzymatic dissociation of small segments of distal PV yielded sufficient relaxed and physiologically viable PVSMC, which have been morphometrically and electrophysiologically characterised here for the first time.

The PVSMC were found to be considerably longer and thinner than smooth muscle cells from arteries. As discussed previously (see section 4.4), the difference between the length of PVSMC and PASMC at rest could reflect an inversely proportional relationship with the resting level of cytosolic Ca^{2+} (Murphy and Khalil, 2000), which may help explain the greater reliance of venous contractions on extracellular sources of Ca^{2+} (Mikkelsen and Pedersen, 1983).

Given the normal low pulmonary venous pressure, it is intuitive that even a small contractile force could reduce the venous lumen relatively easily (Rivera-Estrada *et al.*, 1958). Since myocytes in the walls of small veins have a greater resting length, this may potentially imply a larger intrinsic ability to shorten (Tolic-Norrelykke and Wang, 2005), which would impact venous resistance to a greater extent. As vascular resistance is inversely proportional to the radius of the vessel to the fourth power (Levitzky, 2002a), a very small reduction in vessel diameter would bring about a significant rise in resistance to blood flow.

7.1.3. Hypoxia inhibits a K^+ current in PVSMC

In single smooth muscle cells from small porcine intrapulmonary veins, voltage-clamp protocols activated a family of large outward currents which were predominantly carried through K^+ channels and showed significant spontaneous transient activation. Perfusion with hypoxic solution did not inhibit the outward current, but the spontaneous activity under control conditions made the results difficult to interpret.

However, in the presence of BK_{Ca} channel antagonist Penitrem A, a stable outward current was obtained and a reversible inhibitory effect of hypoxia of the Penitrem A-insensitive whole-cell current was apparent. Using subtraction to obtain the difference current, the hypoxia-sensitive current ($I_{K(H)}$) was revealed in PVSMC. $I_{K(H)}$ is a rapidly activating, partially inactivating current with a fast time of recovery from steady-state inactivation.

In the presence of K_V channel blocker 4-AP, the effect of hypoxia on the Penitrem A-insensitive current was abolished, suggesting $I_{K(H)}$ is a 4-AP-sensitive current.

The biophysical properties of this current include a voltage window of current availability (i.e. interval in which modulation by voltage permits channel activity) described by thresholds of activation and inactivation of -60 mV and +20 mV respectively, with peak availability at -31.86 mV. The resting membrane potential of PVSMC measured under zero current clamp (-35.8 mV) falls between these thresholds suggesting $I_{K(H)}$ is active under resting conditions.

The rapid inactivation of $I_{K(H)}$ was only partial, with a steady-state sustained current present in all recordings, while A-type currents are known to inactivate almost entirely (Iida *et al.*, 2005). This observation could be explained if alongside the main A-type current that inactivates completely, $I_{K(H)}$ contained a secondary component, a slower or non-inactivating current, possibly a delayed rectifier that also possesses

hypoxia sensitivity. Such currents were observed in pulmonary arteries from rat (Archer *et al.*, 1996, Post *et al.*, 1995).

In PASMC, the main candidate channel subtypes are Kv1.2 and Kv1.5. Rapidly inactivating currents (e.g. Kv1.4 and Kv4.3) are not believed to be involved in HPV (Archer and Michelakis, 2002). However, the properties of $I_{K(H)}$ described here suggest that transient A-type currents such as Kv1.4 and Kv4.3 may play a role in HPV in porcine PVSMC. Alternatively, the association of non-inactivating pore-forming α-subunits with the regulatory β-subunits could change the gating of the channel pore and confer inactivation properties to these channels (Rettig *et al.*, 1994). Further work to determine the molecular identity of $I_{K(H)}$ would help clarify these aspects.

In conclusion, in view of the available literature, this is the first study to identify and functionally characterise a hypoxia-sensitive K^+ current in PVSMC. These results have shown that this current possesses rapid activation and inactivation kinetics suggestive of an A-type K^+ current (McGahon *et al.*, 2005). Furthermore, the voltage dependence of channel availability suggests $I_{K(H)}$ is likely to be involved in the maintenance of resting membrane potential. Thus, these findings indicate that inhibition of $I_{K(H)}$ by hypoxia is physiologically relevant and any subsequent membrane depolarisation may initiate the HPV response in porcine intrapulmonary veins.

7.2. Perspectives

The studies presented here bring evidence in support of the participation of pulmonary veins to HPV and highlight fundamental distinctions in how veins and arteries respond to low O_2. These findings suggest that existing knowledge on the mechanisms of HPV in the arteries should not automatically be presumed to apply to the venous side. Therefore, further research is required to advance the understanding

of individual mechanisms underlying pulmonary venous contraction and bridge the gap with the knowledge of arterial contractile mechanisms.

The description of the hypoxia-sensitive current and its biophysical characteristics reported here provides the basis for establishing its physiological significance, but further studies are required to determine the molecular identity of the underlying channel(s) and its(their) potential role in regulating venous return within the pulmonary circulation.

This would include functional studies into the susceptibility of $I_{K(H)}$ to specific inhibitors of candidate K_V subtypes channels, such as phrixotoxin-II for Kv4.3, BDM for Kv2.1 and DPO-1 for Kv1.5 or targeted antibodies for Kv1.4, as well as examining the effect of these functional antagonists on resting membrane potential in PVSMC. Secondly, the confirmation of the presence of specific K_V subtypes in PV smooth muscle should be sought by molecular biology techniques, such as immunolocalisation, RNA isolation and RT-PCR to establish the functional expression of channels.

In addition, further contractile studies should investigate the effect of generic K^+ channel blockers as well as specific inhibitors of K_V subtypes on hypoxic responses of isolated porcine intrapulmonary veins. This would establish whether antagonism of K_V channels mimics the HPV response in veins, as was previously shown in arteries (Post et al., 1992).

In the pulmonary artery, the functional expression of K_V channels is essential to the regulation of pulmonary arterial tone and the downregulation or dysfunction of K_V channels plays a part in the development of pulmonary hypertension and vascular remodelling (Stenmark and Mecham, 1997, Yuan *et al.*, 1998a). A better understanding of K_V channel function in the pulmonary vein may point to their potential as therapeutically relevant targets in preventing or limiting high-altitude oedema formation and/or reducing venous remodelling in chronic pulmonary respiratory disease.

Finally, additional mechanisms previously shown to contribute to HPV in pulmonary arteries could be involved in the veins. In rabbit PASMC, Franco-Obregon and Lopez-Barneo (1996a) reported modulation of L-type Ca^{2+} channel activity by O_2 levels. They observed that Ca^{2+} currents in PASMC from resistance arteries were reversibly increased in response to hypoxia, which would contribute to hypoxic vasoconstriction. Otherwise, Cl_{Ca} are present in rat PASMC and their activation by depolarisation-induced Ca^{2+} influx is functionally important during agonist-induced contractions (Yuan, 1997). Moreover, Cl_{Ca} have also been implicated in promoting increased $[Ca^{2+}]_i$ in rat PASMC during chronic hypoxia (Yang *et al.*, 2006). Therefore, the contributions of Cl_{Ca} and L-type Ca^{2+} channels to membrane potential in PVSMC should be examined under normoxic and hypoxic conditions using patch-clamping studies.

7.3. Conclusions

While the distal arteries are probably the main site of HPV in terms of contribution to the increase in vascular resistance during hypoxia (see discussion in section 1.2.2), small veins have the ability to sense alveolar hypoxia (Raj and Chen, 1986) and have been repeatedly shown to play a significant part in HPV (reviewed in Gao and Raj, 2005b). Therefore, their role should not be disregarded, particularly as they may be increasingly important during pathological states, such as pulmonary oedema and PHT.

Arteries have received much attention from investigators, but pulmonary veins are still being largely overlooked in recent reviews (Ward and Aaronson, 1999, Dumas *et al.*, 1999, Sylvester, 2001, Moudgil *et al.*, 2005, Weissmann *et al.*, 2006) despite compelling evidence that active venous constriction takes place in response to hypoxia in many species (e.g. lamb, Raj and Chen, 1986, guinea pig, Tracey *et al.*, 1989, ferret, Raj *et al.*, 1990, rat, Zhao *et al.*, 1993, pig, Feletou *et al.*, 1995, sheep, Uzun and Demiryurek, 2003).

This trend is unfortunate, in that it has led to most new investigation techniques introduced in the field of HPV research being applied exclusively with pulmonary arterial smooth muscle, whilst leaving a considerable gap in the understanding of cellular processes in the PVSMC during HPV.

All the findings reported here support the hypothesis that small porcine intrapulmonary veins are capable of considerable vasomotion and actively participate in HPV through different mechanisms than arteries. Moreover, smooth muscle cells from pulmonary veins showed intrinsic hypoxia sensitivity. For these reasons, and bearing in mind the fact that the relative importance of the veins is significantly higher in the pulmonary than in the systemic circulation (Levitzky, 2002a), more research should be done to uncover the specific mechanisms underlying pulmonary venous contraction. To conclude, the words of two among the few investigators recognising the importance of pulmonary veins seem appropriate (Fung and Huang, 2004 p. 39):

> *"In the future, we should pay as much attention to the pulmonary venous smooth muscle as to the pulmonary arterial smooth muscle."*

Chapter 8.

References

AARONSON, P. I., ROBERTSON, T. P., KNOCK, G. A., BECKER, S., LEWIS, T. H., SNETKOV, V. & WARD, J. P. (2006) Hypoxic pulmonary vasoconstriction: mechanisms and controversies. *J Physiol,* 570**,** 53-8.

AARONSON, P. I., ROBERTSON, T. P. & WARD, J. P. (2002) Endothelium-derived mediators and hypoxic pulmonary vasoconstriction. *Respir Physiol Neurobiol,* 132**,** 107-20.

AL-TINAWI, A., KRENZ, G. S., RICKABY, D. A., LINEHAN, J. H. & DAWSON, C. A. (1994) Influence of hypoxia and serotonin on small pulmonary vessels. *J Appl Physiol,* 76**,** 56-64.

ALMKVIST, G. & BERNDT, B. C. (1988) Gauss, Landen, Ramanujan, the Arithmetic-Geometric Mean, Ellipses, π, and the Ladies Diary. *Am Math Mon,* 95**,** 585-608.

ALTURA, B. M. & CHAND, N. (1981) Differential effects of prostaglandins on canine intrapulmonary arteries and veins. *Br J Pharmacol,* 73**,** 819-27.

AMBERG, G. C., KOH, S. D., IMAIZUMI, Y., OHYA, S. & SANDERS, K. M. (2003) A-type potassium currents in smooth muscle. *Am J Physiol Cell Physiol,* 284**,** C583-95.

ARCHER, S. & MICHELAKIS, E. (2002) The mechanism(s) of hypoxic pulmonary vasoconstriction: potassium channels, redox O(2) sensors, and controversies. *News Physiol Sci,* 17**,** 131-7.

ARCHER, S. L., HUANG, J., HENRY, T., PETERSON, D. & WEIR, E. K. (1993) A redox-based O2 sensor in rat pulmonary vasculature. *Circ Res,* 73**,** 1100-12.

ARCHER, S. L., HUANG, J. M., REEVE, H. L., HAMPL, V., TOLAROVA, S., MICHELAKIS, E. & WEIR, E. K. (1996) Differential distribution of electrophysiologically distinct myocytes in conduit and resistance arteries determines their response to nitric oxide and hypoxia. *Circ Res,* 78**,** 431-42.

ARCHER, S. L., LONDON, B., HAMPL, V., WU, X., NSAIR, A., PUTTAGUNTA, L., HASHIMOTO, K., WAITE, R. E. & MICHELAKIS, E. D. (2001) Impairment of hypoxic pulmonary vasoconstriction in mice lacking the voltage-gated potassium channel Kv1.5. *Faseb J,* 15**,** 1801-3.

ARCHER, S. L., SOUIL, E., DINH-XUAN, A. T., SCHREMMER, B., MERCIER, J. C., EL YAAGOUBI, A., NGUYEN-HUU, L., REEVE, H. L. & HAMPL, V. I. C. (1998) Molecular identification of the role of voltage-gated K+ channels, Kv1.5 and Kv2.1, in hypoxic pulmonary vasoconstriction and control of resting membrane potential in rat pulmonary artery myocytes. *J Clin Invest,* 101**,** 2319-30.

ARCHER, S. L., WEIR, E. K., REEVE, H. L. & MICHELAKIS, E. (2000) Molecular identification of O2 sensors and O2-sensitive potassium channels in the pulmonary circulation. *Adv Exp Med Biol,* 475**,** 219-40.

ARRIGONI, F. I., HISLOP, A. A., HAWORTH, S. G. & MITCHELL, J. A. (1999) Newborn intrapulmonary veins are more reactive than arteries in normal and hypertensive piglets. *Am J Physiol,* 277**,** L887-92.

AUMAN, H. J., COLEMAN, H., RILEY, H. E., OLALE, F., TSAI, H. J. & YELON, D. (2007) Functional modulation of cardiac form through regionally confined cell shape changes. *PLoS Biol,* 5**,** e53.

AVIADO, D. M. (1960) Pulmonary venular responses to anoxia, 5-hydroxytryptamine and histamine. *Am J Physiol,* 198**,** 1032-6.

BARMAN, S. A. (2001) Effect of protein kinase C inhibition on hypoxic pulmonary vasoconstriction. *Am J Physiol Lung Cell Mol Physiol,* 280**,** L888-95.

BARMAN, S. A., ZHU, S., HAN, G. & WHITE, R. E. (2003) cAMP activates BKCa channels in pulmonary arterial smooth muscle via cGMP-dependent protein kinase. *Am J Physiol Lung Cell Mol Physiol,* 284**,** L1004-11.

BARMAN, S. A. I. C. (1997) Role of calcium-activated potassium channels and cyclic nucleotides on pulmonary vasoreactivity to serotonin. *Am J Physiol,* 273**,** L142-7.

BARNES, P. J. & LIU, S. F. (1995) Regulation of pulmonary vascular tone. *Pharmacol Rev,* 47**,** 87-131.

BARTSCH, P., MAIRBAURL, H., MAGGIORINI, M. & SWENSON, E. R. (2005) Physiological aspects of high-altitude pulmonary edema. *J Appl Physiol,* 98**,** 1101-10.

BEECH, D. J. & BOLTON, T. B. (1989) A voltage-dependent outward current with fast kinetics in single smooth muscle cells isolated from rabbit portal vein. *J Physiol,* 412**,** 397-414.

BENNIE, R. E., PACKER, C. S., POWELL, D. R., JIN, N. & RHOADES, R. A. (1991) Biphasic contractile response of pulmonary artery to hypoxia. *Am J Physiol,* 261**,** L156-63.

BERKOV, S. (1974) Hypoxic Pulmonary Vasoconstriction in the Rat: The Necessary Role of Angiotensin II. *Circ Res,* 35**,** 256-261.

BIXBY, C. E., IBE, B. O., ABDALLAH, M. F., ZHOU, W., HISLOP, A. A., LONGO, L. D. & RAJ, J. U. (2007) Role of platelet-activating factor in pulmonary vascular remodeling associated with chronic high altitude hypoxia in ovine fetal lambs. *Am J Physiol Lung Cell Mol Physiol,* 293**,** L1475-82.

BLYTHE, D., VAN HEERDEN, P. V. & POWER, B. M. (1998) Pulmonary hypertension and selective pulmonary vasodilators in acute lung injury. *Anaesth Intensive Care,* 26**,** 26-39.

BOELS, P. J., GAO, B., DEUTSCH, J. & HAWORTH, S. G. I. C. (1997) ATP-dependent K+ channel activation in isolated normal and hypertensive newborn and adult porcine pulmonary vessels. *Pediatr Res,* 42**,** 317-26.

BONNET, S. & ARCHER, S. L. (2007) Potassium channel diversity in the pulmonary arteries and pulmonary veins: implications for regulation of the pulmonary vasculature in health and during pulmonary hypertension. *Pharmacol Ther,* 115**,** 56-69.

BRADFORD, J. R. & DEAN, H. P. (1894) The Pulmonary Circulation. *J Physiol,* 16**,** 34-158 25.

BRUNTON, T. L. & FAYRER, J. (1876) Note on Independent Pulsation of the Pulmonary Veins and Vena Cava. *Proceedings of the Royal Society of London,* 25**,** 174-176.

BURCH, G. E. & ROMNEY, R. B. (1954) Functional anatomy and throttle valve action on the pulmonary veins. *Am Heart J,* 47**,** 58-66.

BURKHOFF, D. & TYBERG, J. V. (1993) Why does pulmonary venous pressure rise after onset of LV dysfunction: a theoretical analysis. *Am J Physiol,* 265**,** H1819-28.

CARDELL, L. O., UDDMAN, R. & EDVINSSON, L. (1990) Analysis of endothelin-1-induced contractions of guinea-pig trachea, pulmonary veins and different types of pulmonary arteries. *Acta Physiol Scand,* 139**,** 103-11.

CHAMLEY-CAMPBELL, J., CAMPBELL, G. R. & ROSS, R. (1979) The smooth muscle cell in culture. *Physiol Rev,* 59**,** 1-61.

CHAZOVA, I., LOYD, J. E., ZHDANOV, V. S., NEWMAN, J. H., BELENKOV, Y. & MEYRICK, B. (1995) Pulmonary artery adventitial changes and venous involvement in primary pulmonary hypertension. *Am J Pathol,* 146**,** 389-97.

CHEN, C. R., VOELKEL, N. F. & CHANG, S. W. (1990) PAF potentiates protamine-induced lung edema: role of pulmonary venoconstriction. *J Appl Physiol,* 68**,** 1059-68.

CHEN, S. A., HSIEH, M. H., TAI, C. T., TSAI, C. F., PRAKASH, V. S., YU, W. C., HSU, T. L., DING, Y. A. & CHANG, M. S. (1999) Initiation of atrial fibrillation by ectopic beats originating from the pulmonary veins: electrophysiological characteristics, pharmacological responses, and effects of radiofrequency ablation. *Circulation,* 100**,** 1879-86.

CHEN, Y. J., CHEN, S. A., CHANG, M. S. & LIN, C. I. (2000) Arrhythmogenic activity of cardiac muscle in pulmonary veins of the dog: implication for the genesis of atrial fibrillation. *Cardiovasc Res,* 48**,** 265-73.

CHEUNG, D. W. (1981a) Electrical activity of the pulmonary vein and its interaction with the right atrium in the guinea-pig. *J Physiol,* 314**,** 445-56.

CHEUNG, D. W. (1981b) Pulmonary vein as an ectopic focus in digitalis-induced arrhythmia. *Nature,* 294**,** 582-4.

CLAPP, L. H. & GURNEY, A. M. (1991) Outward currents in rabbit pulmonary artery cells dissociated with a new technique. *Exp Physiol,* 76**,** 677-93.

CORNFIELD, D. N., STEVENS, T., MCMURTRY, I. F., ABMAN, S. H. & RODMAN, D. M. (1993) Acute hypoxia increases cytosolic calcium in fetal pulmonary artery smooth muscle cells. *Am J Physiol,* 265**,** L53-6.

CORNFIELD, D. N., STEVENS, T., MCMURTRY, I. F., ABMAN, S. H. & RODMAN, D. M. (1994) Acute hypoxia causes membrane depolarization and calcium influx in fetal pulmonary artery smooth muscle cells. *Am J Physiol,* 266**,** L469-75.

COURNAND, A. (1950) Some aspects of the pulmonary circulation in normal man and in chronic cardiopulmonary diseases. *Circulation,* 2**,** 641-57.

CRUICKSHANK, S. F., BAXTER, L. M. & DRUMMOND, R. M. (2003) The Cl(-) channel blocker niflumic acid releases Ca(2+) from an intracellular store in rat pulmonary artery smooth muscle cells. *Br J Pharmacol,* 140**,** 1442-50.

CRUICKSHANK, S. F. & DRUMMOND, R. M. (2003) The effects of hypoxia on [Ca2+]i signalling in phenotypically distinct myocytes from the rat pulmonary vein. *J Physiol,* 548P**,** P68.

DANISH MYO TECHNOLOGY (2003) Dual Wire Myograph System Model 410A - User Manual Version 2.00. Aarhus, Denmark.

DAUBER, I. M. & WEIL, J. V. (1983) Lung injury edema in dogs. Influence of sympathetic ablation. *J Clin Invest,* 72**,** 1977-86.

DAVIDSON, D., SINGH, M. & WALLACE, G. F. (1990) Role of leukotriene C4 in pulmonary hypertension: platelet-activating factor vs. hypoxia. *J Appl Physiol,* 68**,** 1628-33.

DAVIES, S. P., REDDY, H., CAIVANO, M. & COHEN, P. (2000) Specificity and mechanism of action of some commonly used protein kinase inhibitors. *Biochem J,* 351**,** 95-105.

DE CANNIERE, D., STEFANIDIS, C., HALLEMANS, R., DELCROIX, M., BRIMIOULLE, S. & NAEIJE, R. (1992) Stimulus-response curves for hypoxic pulmonary vasoconstriction in piglets. *Cardiovasc Res,* 26**,** 944-9.

DEMBINSKI, R., HENZLER, D. & ROSSAINT, R. (2004) Modulating the pulmonary circulation: an update. *Minerva Anestesiol,* 70**,** 239-43.

DEMIRYUREK, A. T., WADSWORTH, R. M. & KANE, K. A. (1991a) Effects of hypoxia on isolated intrapulmonary arteries from the sheep. *Pulm Pharmacol,* 4**,** 158-64.

DEMIRYUREK, A. T., WADSWORTH, R. M. & KANE, K. A. (1991b) Pharmacological evidence for the role of mediators in hypoxia-induced vasoconstriction in sheep isolated intrapulmonary artery rings. *Eur J Pharmacol,* 203**,** 1-8.

DEMIRYUREK, A. T., WADSWORTH, R. M., KANE, K. A. & PEACOCK, A. J. (1993) The role of endothelium in hypoxic constriction of human pulmonary artery rings. *Am Rev Respir Dis,* 147**,** 283-90.

DEMPSTER, J. (2006) Strathclyde Electrophysiology Software. Whole Cell Program. WCP for Windows V3.7. User Guide. Glasgow, Scotland.

DETAR, R. & GELLAI, M. (1971) Oxygen and isolated vascular smooth muscle from the main pulmonary artery of the rabbit. *Am J Physiol,* 221**,** 1791-4.

DEVINE, C. E., SOMLYO, A. V. & SOMLYO, A. P. (1972) Sarcoplasmic reticulum and excitation-contraction coupling in mammalian smooth muscles. *J Cell Biol,* 52**,** 690-718.

DING, X. & MURRAY, P. A. (2005a) Cellular mechanisms of thromboxane A2-mediated contraction in pulmonary veins. *Am J Physiol Lung Cell Mol Physiol*.

DING, X. & MURRAY, P. A. (2005b) Regulation of pulmonary venous tone in response to muscarinic receptor activation. *Am J Physiol Lung Cell Mol Physiol,* 288**,** L131-40.

DINGEMANS, K. P. & WAGENVOORT, C. A. (1978) Pulmonary arteries and veins in experimental hypoxia. An ultrastructural study. *Am J Pathol,* 93**,** 353-68.

DIPP, M. & EVANS, A. M. (2001) Cyclic ADP-ribose is the primary trigger for hypoxic pulmonary vasoconstriction in the rat lung in situ. *Circ Res,* 89**,** 77-83.

DIPP, M., NYE, P. C. & EVANS, A. M. (2001) Hypoxic release of calcium from the sarcoplasmic reticulum of pulmonary artery smooth muscle. *Am J Physiol Lung Cell Mol Physiol,* 281**,** L318-25.

DOI, S., DAMRON, D. S., OGAWA, K., TANAKA, S., HORIBE, M. & MURRAY, P. A. (2000) K(+) channel inhibition, calcium signaling, and vasomotor tone in canine pulmonary artery smooth muscle. *Am J Physiol Lung Cell Mol Physiol,* 279**,** L242-51.

DOUGLAS, S. A., VICKERY-CLARK, L. M. & OHLSTEIN, E. H. (1993) Endothelin-1 does not mediate hypoxic vasoconstriction in canine isolated blood vessels: effect of BQ-123. *Br J Pharmacol,* 108**,** 418-21.

DRISKA, S. P., LAUDADIO, R. E., WOLFSON, M. R. & SHAFFER, T. H. (1999) A method for isolating adult and neonatal airway smooth muscle cells and measuring shortening velocity. *J Appl Physiol,* 86**,** 427-35.

DRISKA, S. P. & PORTER, R. (1986) Isolation of smooth muscle cells from swine carotid artery by digestion with papain. *Am J Physiol,* 251**,** C474-81.

DU, W., FRAZIER, M., MCMAHON, T. J. & EU, J. P. (2005) Redox activation of intracellular calcium release channels (ryanodine receptors) in the sustained phase of hypoxia-induced pulmonary vasoconstriction. *Chest,* 128**,** 556S-558S.

DUKE, H. N. (1954) The site of action of anoxia on the pulmonary blood vessels of the cat. *J Physiol,* 125**,** 373-82.

DUKE, H. N. & KILLICK, E. M. (1952) Pulmonary vasomotor responses of isolated perfused cat lungs to anoxia. *J Physiol,* 117**,** 303-16.

DUMAS, J. P., BARDOU, M., GOIRAND, F. & DUMAS, M. (1999) Hypoxic pulmonary vasoconstriction. *Gen Pharmacol,* 33**,** 289-97.

EHRLICH, J. R., CHA, T. J., ZHANG, L., CHARTIER, D., MELNYK, P., HOHNLOSER, S. H. & NATTEL, S. (2003) Cellular electrophysiology of canine pulmonary vein cardiomyocytes: action potential and ionic current properties. *J Physiol,* 551**,** 801-13.

FELETOU, M., GIRARD, V. & CANET, E. (1995) Different involvement of nitric oxide in endothelium-dependent relaxation of porcine pulmonary artery and vein: influence of hypoxia. *J Cardiovasc Pharmacol,* 25**,** 665-73.

FERNANDES, D. J., MCCONVILLE, J. F., STEWART, A. G., KALINICHENKO, V. & SOLWAY, J. (2004) Can we differentiate between airway and vascular smooth muscle? *Clin Exp Pharmacol Physiol,* 31**,** 805-10.

FESLER, P., PAGNAMENTA, A., VACHIERY, J. L., BRIMIOULLE, S., ABDEL KAFI, S., BOONSTRA, A., DELCROIX, M., CHANNICK, R. N., RUBIN, L. J. & NAEIJE, R. (2003) Single arterial occlusion to locate resistance in patients with pulmonary hypertension. *Eur Respir J,* 21**,** 31-6.

FIKE, C. D. & KAPLOWITZ, M. R. (1992) Pulmonary venous pressure increases during alveolar hypoxia in isolated lungs of newborn pigs. *J Appl Physiol,* 73**,** 552-6.

FISHMAN, A. P. (1961) Respiratory gases in the regulation of the pulmonary circulation. *Physiol Rev,* 41**,** 214-80.

FISHMAN, A. P. (1976) Hypoxia on the pulmonary circulation. How and where it acts. *Circ Res,* 38**,** 221-31.

FORREST, J. B. & FARGAS-BABJAK, A. (1978) Variability of the pulmonary vascular response to hypoxia and relation to gas exchange in dogs. *Can Anaesth Soc J,* 25**,** 479-87.

FRANCO-OBREGON, A. & LOPEZ-BARNEO, J. (1996a) Differential oxygen sensitivity of calcium channels in rabbit smooth muscle cells of conduit and resistance pulmonary arteries. *J Physiol,* 491 (Pt 2)**,** 511-8.

FRANCO-OBREGON, A. & LOPEZ-BARNEO, J. (1996b) Low PO2 inhibits calcium channel activity in arterial smooth muscle cells. *Am J Physiol,* 271**,** H2290-9.

FRED, H. L., SCHMIDT, A. M., BATES, T. & HECHT, H. H. (1962) Acute Pulmonary Edema of Altitude: Clinical and Physiologic Observations. *Circulation,* 25**,** 929-937.

FROSTELL, C., FRATACCI, M. D., WAIN, J. C., JONES, R. & ZAPOL, W. M. (1991) Inhaled nitric oxide. A selective pulmonary vasodilator reversing hypoxic pulmonary vasoconstriction. *Circulation,* 83**,** 2038-47.

FU, X. W., NURSE, C. & CUTZ, E. (2007) Characterization of slowly inactivating KV{alpha} current in rabbit pulmonary neuroepithelial bodies: effects of hypoxia and nicotine. *Am J Physiol Lung Cell Mol Physiol,* 293**,** L892-902.

FUNG, Y. C. & HUANG, W. (2004) The Physics of Hypoxic Pulmonary Hypertension and its Connection with Gene Actions. IN YUAN, X. J. (Ed.) *Hypoxic Pulmonary Vasoconstriction: Cellular and Molecular Mechanisms.* Springer.

FYNN, S. P. & KALMAN, J. M. (2004) Pulmonary veins: anatomy, electrophysiology, tachycardia, and fibrillation. *Pacing Clin Electrophysiol,* 27**,** 1547-59.

GAO, Y. & RAJ, J. U. (2005a) Parathyroid hormone-related protein-mediated responses in pulmonary arteries and veins of newborn lambs. *Am J Physiol Lung Cell Mol Physiol,* 289**,** L60-6.

GAO, Y. & RAJ, J. U. (2005b) Role of veins in regulation of pulmonary circulation. *Am J Physiol Lung Cell Mol Physiol,* 288**,** L213-26.

GAO, Y., ZHOU, H. & RAJ, J. U. (1995a) Endothelium-derived nitric oxide plays a larger role in pulmonary veins than in arteries of newborn lambs. *Circ Res,* 76**,** 559-65.

GAO, Y., ZHOU, H. & RAJ, J. U. (1995b) PAF induces relaxation of pulmonary arteries but contraction of pulmonary veins in the ferret. *Am J Physiol,* 269**,** H704-9.

GELBAND, C. H. & GELBAND, H. (1997) Ca2+ release from intracellular stores is an initial step in hypoxic pulmonary vasoconstriction of rat pulmonary artery resistance vessels. *Circulation,* 96**,** 3647-54.

GELBAND, C. H. & HUME, J. R. (1992) Ionic currents in single smooth muscle cells of the canine renal artery. *Circ Res,* 71**,** 745-58.

GENTET, L. J., STUART, G. J. & CLEMENTS, J. D. (2000) Direct measurement of specific membrane capacitance in neurons. *Biophys J,* 79**,** 314-20.

GLAZIER, J. B. & MURRAY, J. F. (1971) Sites of pulmonary vasomotor reactivity in the dog during alveolar hypoxia and serotonin and histamine infusion. *J Clin Invest,* 50**,** 2550-8.

GRAY, H. (1918) *Anatomy of the Human Body,* Philadelphia, Lea & Febiger. Available from: Bartleby.com, 2000. www.bartleby.com/107/ [Accessed 1 October 2008].

GREENWOOD, I. A. & LARGE, W. A. (1995) Comparison of the effects of fenamates on Ca-activated chloride and potassium currents in rabbit portal vein smooth muscle cells. *Br J Pharmacol,* 116**,** 2939-48.

HAISSAGUERRE, M., JAIS, P., SHAH, D. C., TAKAHASHI, A., HOCINI, M., QUINIOU, G., GARRIGUE, S., LE MOUROUX, A., LE METAYER, P. & CLEMENTY, J. (1998) Spontaneous initiation of atrial fibrillation by ectopic beats originating in the pulmonary veins. *N Engl J Med,* 339**,** 659-66.

HAKIM, T. S. (1988) Identification of constriction in large versus small vessels using the arterial-venous and the double-occlusion techniques in isolated canine lungs. *Respiration,* 54**,** 61-9.

HAKIM, T. S., GRUNSTEIN, M. M. & MICHEL, R. P. (1992) Opiate action in the pulmonary circulation. *Pulm Pharmacol,* 5**,** 159-65.

HAKIM, T. S. & MALIK, A. B. (1988) Hypoxic vasoconstriction in blood and plasma perfused lungs. *Respir Physiol,* 72**,** 109-21.

HALES, C. A. (2004) Physiological Function of Hypoxic Pulmonary Vasoconstriction. IN YUAN, X. J. (Ed.) *Hypoxic Pulmonary Vasoconstriction: Cellular and Molecular Mechanisms.* Springer.

HALL, P. W., JR. & HALL, P. W., 3RD (1953) Effects of anoxia on postarteriolar pulmonary vascular resistance. *Circ Res,* 1**,** 238-41.

HALL, S. M., HISLOP, A. A. & HAWORTH, S. G. (2002) Origin, differentiation, and maturation of human pulmonary veins. *Am J Respir Cell Mol Biol,* 26**,** 333-40.

HALL, S. M., HISLOP, A. A., PIERCE, C. M. & HAWORTH, S. G. (2000) Prenatal origins of human intrapulmonary arteries: formation and smooth muscle maturation. *Am J Respir Cell Mol Biol,* 23**,** 194-203.

HAMILL, O. P., MARTY, A., NEHER, E., SAKMANN, B. & SIGWORTH, F. J. (1981) Improved patch-clamp techniques for high-resolution current recording from cells and cell-free membrane patches. *Pflugers Arch,* 391**,** 85-100.

HARDER, D. R., MADDEN, J. A. & DAWSON, C. (1985a) Hypoxic induction of Ca2+-dependent action potentials in small pulmonary arteries of the cat. *J Appl Physiol,* 59**,** 1389-93.

HARDER, D. R., MADDEN, J. A. & DAWSON, C. (1985b) A membrane electrical mechanism for hypoxic vasoconstriction of small pulmonary arteries from cat. *Chest,* 88**,** 233S-235S.

HASEBE, N., ONODERA, S., YAMASHITA, H., KAWAMURA, Y., HANEDA, T. & TOBISE, K. (1992) Site of hypoxic pulmonary vasoconstriction in pulsatile perfused canine lung lobes. *Jpn Circ J,* 56**,** 837-46.

HASUNUMA, K., YAMAGUCHI, T., RODMAN, D. M., O'BRIEN, R. F. & MCMURTRY, I. F. (1991) Effects of inhibitors of EDRF and EDHF on vasoreactivity of perfused rat lungs. *Am J Physiol,* 260**,** L97-104.

HATANO, N., OHYA, S., MURAKI, K., CLARK, R. B., GILES, W. R. & IMAIZUMI, Y. (2004) Two arginines in the cytoplasmic C-terminal domain are essential for voltage-dependent regulation of A-type K+ current in the Kv4 channel subfamily. *J Biol Chem,* 279**,** 5450-9.

HEATH, D. (1977) Hypoxia and the pulmonary circulation. *J Clin Pathol Suppl (R Coll Pathol),* 11**,** 21-9.

HILLIER, S. C., GRAHAM, J. A., HANGER, C. C., GODBEY, P. S., GLENNY, R. W. & WAGNER, W. W., JR. (1997) Hypoxic vasoconstriction in pulmonary arterioles and venules. *J Appl Physiol,* 82**,** 1084-90.

HIMPENS, B., MATTHIJS, G., SOMLYO, A. V., BUTLER, T. M. & SOMLYO, A. P. (1988) Cytoplasmic free calcium, myosin light chain phosphorylation, and force in phasic and tonic smooth muscle. *J Gen Physiol,* 92**,** 713-29.

HIRSCHMAN, J. C. & BOUCEK, R. J. (1963) Angiographic evidence of pulmonary vasomotion in the dog. *Br Heart J,* 25**,** 375-81.

HISLOP, A. & REID, L. (1973) Fetal and childhood development of the intrapulmonary veins in man--branching pattern and structure. *Thorax,* 28**,** 313-9.

HO, S. Y., CABRERA, J. A., TRAN, V. H., FARRE, J., ANDERSON, R. H. & SANCHEZ-QUINTANA, D. (2001) Architecture of the pulmonary veins: relevance to radiofrequency ablation. *Heart,* 86**,** 265-70.

HOGG, D. S., DAVIES, A. R., MCMURRAY, G. & KOZLOWSKI, R. Z. (2002) K(V)2.1 channels mediate hypoxic inhibition of I(KV) in native pulmonary arterial smooth muscle cells of the rat. *Cardiovasc Res,* 55**,** 349-60.

HOLDEN, W. E. & MCCALL, E. (1984) Hypoxia-induced contractions of porcine pulmonary artery strips depend on intact endothelium. *Exp Lung Res,* 7**,** 101-12.

HONJO, H., BOYETT, M. R., NIWA, R., INADA, S., YAMAMOTO, M., MITSUI, K., HORIUCHI, T., SHIBATA, N., KAMIYA, K. & KODAMA, I. (2003) Pacing-induced spontaneous activity in myocardial sleeves of pulmonary veins after treatment with ryanodine. *Circulation,* 107**,** 1937-43.

HOSHINO, Y., MORRISON, K. J. & VANHOUTTE, P. M. (1994) Mechanisms of hypoxic vasoconstriction in the canine isolated pulmonary artery: role of endothelium and sodium pump. *Am J Physiol,* 267**,** L120-7.

HOSHINO, Y., OBARA, H., KUSUNOKI, M., FUJII, Y. & IWAI, S. (1988) Hypoxic contractile response in isolated human pulmonary artery: role of calcium ion. *J Appl Physiol,* 65**,** 2468-74.

HUGHES, A. D., WIJETUNGE, S. & PARKINSON, N. A. (1994) Isolation of single vascular smooth muscle cells from human omental resistance arteries. *J Hum Hypertens,* 8**,** 615-8.

HUGHES, J. M. B. & MORRELL, N. W. (2001) Vascular Structure and Function. *Pulmonary Circulation: From Basic Mechanisms to Clinical Practice.* London, Imperial College Press.

HULME, J. T., COPPOCK, E. A., FELIPE, A., MARTENS, J. R. & TAMKUN, M. M. (1999) Oxygen sensitivity of cloned voltage-gated K(+) channels expressed in the pulmonary vasculature. *Circ Res,* 85**,** 489-97.

HULTGREN, H. N., GROVER, R. F. & HARTLEY, L. H. (1971) Abnormal circulatory responses to high altitude in subjects with a previous history of high-altitude pulmonary edema. *Circulation,* 44**,** 759-70.

HULTGREN, H. N., LOPEZ, C. E., LUNDBERG, E. & MILLER, H. (1964) Physiologic Studies of Pulmonary Edema at High Altitude. *Circulation,* 29**,** 393-408.

HUME, J. R. & LEBLANC, N. (1989) Macroscopic K+ currents in single smooth muscle cells of the rabbit portal vein. *J Physiol,* 413**,** 49-73.

IBE, B. O., ABDALLAH, M. F., PORTUGAL, A. M. & RAJ, J. U. (2008) Platelet-activating factor stimulates ovine foetal pulmonary vascular smooth muscle cell proliferation: role of nuclear factor-kappa B and cyclin-dependent kinases. *Cell Prolif,* 41**,** 208-29.

IIDA, H., JO, T., IWASAWA, K., MORITA, T., HIKIJI, H., TAKATO, T., TOYO-OKA, T., NAGAI, R. & NAKAJIMA, T. (2005) Molecular and pharmacological characteristics of transient voltage-dependent K+ currents in cultured human pulmonary arterial smooth muscle cells. *Br J Pharmacol,* 146**,** 49-59.

JABR, R. I., TOLAND, H., GELBAND, C. H., WANG, X. X. & HUME, J. R. (1997) Prominent role of intracellular Ca2+ release in hypoxic vasoconstriction of canine pulmonary artery. *Br J Pharmacol,* 122**,** 21-30.

JACKSON, W. F. (1988) Oscillations in active tension in hamster aortas: role of the endothelium. *Blood Vessels,* 25**,** 144-56.

JAMESON, A. G. (1964) Gaseous Diffusion From Alveoli Into Pulmonary Arteries. *J Appl Physiol,* 19**,** 448-56.

JIN, N., PACKER, C. S., ENGLISH, D. & RHOADES, R. A. (1993) Inositol trisphosphate is involved in norepinephrine- but not in hypoxia-induced pulmonary arterial contraction. *Am J Physiol,* 264**,** L160-4.

JIN, N., PACKER, C. S. & RHOADES, R. A. (1992) Pulmonary arterial hypoxic contraction: signal transduction. *Am J Physiol,* 263**,** L73-8.

JOINER, P. D., KADOWITZ, P. J., DAVIS, L. B. & HYMAN, A. L. (1975a) Contractile responses of canine isolated pulmonary lobar arteries and veins to norepinephrine, serotonin, and tyramine. *Can J Physiol Pharmacol,* 53**,** 830-8.

JOINER, P. D., KADOWITZ, P. J., HUGHES, J. P. & HYMAN, A. L. (1975b) Actions of prostaglandins E1 and F2alpha on isolated intrapulmonary vascular smooth muscle. *Proc Soc Exp Biol Med,* 150**,** 414-21.

KADOWITZ, P. J., JOINER, P. D. & HYMAN, A. L. (1975) Influence of sympathetic stimulation and vasoactive substances on the canine pulmonary veins. *J Clin Invest,* 56**,** 354-65.

KARAKI, H., OZAKI, H., HORI, M., MITSUI-SAITO, M., AMANO, K., HARADA, K., MIYAMOTO, S., NAKAZAWA, H., WON, K. J. & SATO, K. (1997) Calcium movements, distribution, and functions in smooth muscle. *Pharmacol Rev,* 49**,** 157-230.

KARAMSETTY, M. R., KLINGER, J. R. & HILL, N. S. (2002) Evidence for the role of p38 MAP kinase in hypoxia-induced pulmonary vasoconstriction. *Am J Physiol Lung Cell Mol Physiol,* 283**,** L859-66.

KATO, M. & STAUB, N. C. (1966) Response of small pulmonary arteries to unilobar hypoxia and hypercapnia. *Circ Res,* 19**,** 426-40.

KATSUYAMA, H., WANG, C. L. & MORGAN, K. G. (1992) Regulation of vascular smooth muscle tone by caldesmon. *J Biol Chem,* 267**,** 14555-8.

KAY, J. M. (1983) Comparative morphologic features of the pulmonary vasculature in mammals. *Am Rev Respir Dis,* 128**,** S53-7.

KEMP, B. K., SMOLICH, J. J. & COCKS, T. M. (1997) Evidence for specific regional patterns of responses to different vasoconstrictors and vasodilators in sheep isolated pulmonary arteries and veins. *Br J Pharmacol,* 121**,** 441-50.

KENYON, J. L. (2002) Primer on Junction Potentials. [online] 3rd ed., Available from: http://www.physio.unr.edu/Faculty/kenyon/Junction_Potentials/Revised_Primer_on_Junction_Potentials_3e.pdf [Accessed 26 January 2007].

KHAN, R. (2004) Identifying and understanding the role of pulmonary vein activity in atrial fibrillation. *Cardiovasc Res,* 64**,** 387-94.

KINOSHITA, K., SATO, K., HORI, M., OZAKI, H. & KARAKI, H. (2003) Decrease in activity of smooth muscle L-type Ca2+ channels and its reversal by NF-kappaB inhibitors in Crohn's colitis model. *Am J Physiol Gastrointest Liver Physiol,* 285**,** G483-93.

KITAMURA, K. & YAMAZAKI, J. (2001) Chloride channels and their functional roles in smooth muscle tone in the vasculature. *Jpn J Pharmacol,* 85**,** 351-7.

KLEGER, G. R., BARTSCH, P., VOCK, P., HEILIG, B., ROBERTS, L. J., 2ND & BALLMER, P. E. (1996) Evidence against an increase in capillary permeability in subjects exposed to high altitude. *J Appl Physiol,* 81**,** 1917-23.

KO, E. A., BURG, E. D., PLATOSHYN, O., MSEFYA, J., FIRTH, A. L. & YUAN, J. X. (2007) Functional characterization of voltage-gated K+ channels in mouse pulmonary artery smooth muscle cells. *Am J Physiol Cell Physiol,* 293**,** C928-37.

KOVITZ, K. L., ALESKOWITCH, T. D., SYLVESTER, J. T. & FLAVAHAN, N. A. (1993) Endothelium-derived contracting and relaxing factors contribute to hypoxic responses of pulmonary arteries. *Am J Physiol,* 265**,** H1139-48.

KUIDA, H., BROWN, A. M., THORNE, J. L., LANGE, R. L. & HECHT, H. H. (1962) Pulmonary vascular response to acute hypoxia in normal, unanesthetized calves. *Am J Physiol,* 203**,** 391-6.

KUIDA, H., HINSHAW, L. B., GILBERT, R. P. & VISSCHER, M. B. (1958) Effect of gram-negative endotoxin on pulmonary circulation. *Am J Physiol,* 192**,** 335-44.

LAMB, F. S. & BARNA, T. J. (1998) Chloride ion currents contribute functionally to norepinephrine-induced vascular contraction. *Am J Physiol,* 275**,** H151-60.

LARGE, W. A. & WANG, Q. (1996) Characteristics and physiological role of the Ca(2+)-activated Cl- conductance in smooth muscle. *Am J Physiol,* 271**,** C435-54.

LE CRAS, T. D. & MCMURTRY, I. F. (2001) Nitric oxide production in the hypoxic lung. *Am J Physiol Lung Cell Mol Physiol,* 280**,** L575-82.

LEACH, R. M., HILL, H. M., SNETKOV, V. A., ROBERTSON, T. P. & WARD, J. P. (2001) Divergent roles of glycolysis and the mitochondrial electron transport chain in hypoxic pulmonary vasoconstriction of the rat: identity of the hypoxic sensor. *J Physiol,* 536**,** 211-24.

LEACH, R. M., ROBERTSON, T. P., TWORT, C. H. & WARD, J. P. (1994) Hypoxic vasoconstriction in rat pulmonary and mesenteric arteries. *Am J Physiol,* 266**,** L223-31.

LEE, S.-J. & KIM, K. W. (1999) Characteristics of Hypoxic Pulmonary Vasoconstriction of the Rat: Study by the Vessels Size and Location in the Lung. *Korean J Physiol Pharmacol,* 3**,** 321-328.

LEE, Y. H., GALLANT, C., GUO, H., LI, Y., WANG, C. A. & MORGAN, K. G. (2000) Regulation of vascular smooth muscle tone by N-terminal region of caldesmon. Possible role of tethering actin to myosin. *J Biol Chem,* 275**,** 3213-20.

LEVICK, J. R. (2003) Specialization in individual circulations. *An introduction to cardiovascular physiology.* 4th ed. London, Hodder Arnold.

LEVITZKY, M. G. (2002a) Blood Flow to the Lung. *Pulmonary Physiology.* 6th ed., McGraw-Hill Professional.

LEVITZKY, M. G. (2002b) Function & Structure of the Respiratory System. *Pulmonary Physiology.* 6th ed., McGraw-Hill Professional.

LITTLER, C. M., MORRIS, K. G., JR., FAGAN, K. A., MCMURTRY, I. F., MESSING, R. O. & DEMPSEY, E. C. (2003) Protein kinase C-epsilon-null mice have decreased hypoxic pulmonary vasoconstriction. *Am J Physiol Heart Circ Physiol,* 284**,** H1321-31.

LIU, Q., SHAM, J. S., SHIMODA, L. A. & SYLVESTER, J. T. (2001) Hypoxic constriction of porcine distal pulmonary arteries: endothelium and endothelin dependence. *Am J Physiol Lung Cell Mol Physiol,* 280**,** L856-65.

LLOYD, T. C., JR. (1964) Effect Of Alveolar Hypoxia On Pulmonary Vascular Resistance. *J Appl Physiol,* 19**,** 1086-94.

LLOYD, T. C., JR. (1968) Hypoxic pulmonary vasoconstriction: role of perivascular tissue. *J Appl Physiol,* 25**,** 560-5.

LUDATSCHER, R. M. (1968) Fine structure of the muscular wall of rat pulmonary veins. *J Anat,* 103**,** 345-57.

MADDEN, J. A., DAWSON, C. A. & HARDER, D. R. (1985) Hypoxia-induced activation in small isolated pulmonary arteries from the cat. *J Appl Physiol,* 59**,** 113-8.

MADDEN, J. A. & GORDON, J. B. (2004) Animal and In Vitro Models for Studying Hypoxic Pulmonary Vasoconstriction. IN YUAN, X. J. (Ed.) *Hypoxic Pulmonary Vasoconstriction: Cellular and Molecular Mechanisms.* Springer.

MADDEN, J. A., VADULA, M. S. & KURUP, V. P. (1992) Effects of hypoxia and other vasoactive agents on pulmonary and cerebral artery smooth muscle cells. *Am J Physiol,* 263**,** L384-93.

MAGGIORINI, M., MELOT, C., PIERRE, S., PFEIFFER, F., GREVE, I., SARTORI, C., LEPORI, M., HAUSER, M., SCHERRER, U. & NAEIJE, R. (2001) High-altitude pulmonary edema is initially caused by an increase in capillary pressure. *Circulation,* 103**,** 2078-83.

MALIK, A. B. & KIDD, B. S. (1973) Time course of pulmonary vascular response to hypoxia in dogs. *Am J Physiol,* 224**,** 1-6.

MANDEL, J., MARK, E. J. & HALES, C. A. (2000) Pulmonary veno-occlusive disease. *Am J Respir Crit Care Med,* 162**,** 1964-73.

MARSHALL, B. E., MARSHALL, C., BENUMOF, J. & SAIDMAN, L. J. (1981) Hypoxic pulmonary vasoconstriction in dogs: effects of lung segment size and oxygen tension. *J Appl Physiol,* 51**,** 1543-51.

MARSHALL, C. & MARSHALL, B. E. (1992) Hypoxic pulmonary vasoconstriction is not endothelium dependent. *Proc Soc Exp Biol Med,* 201**,** 267-70.

MASANI, F. (1986) Node-like cells in the myocardial layer of the pulmonary vein of rats: an ultrastructural study. *J Anat,* 145**,** 133-42.

MATSUDA, J. J., VOLK, K. A. & SHIBATA, E. F. (1990) Calcium currents in isolated rabbit coronary arterial smooth muscle myocytes. *J Physiol,* 427**,** 657-80.

MATTHAY, M. A. & ZIMMERMAN, G. A. (2005) Acute lung injury and the acute respiratory distress syndrome: four decades of inquiry into pathogenesis and rational management. *Am J Respir Cell Mol Biol,* 33**,** 319-27.

MAUBAN, J. R., REMILLARD, C. V. & YUAN, J. X. I. C. (2005) Hypoxic pulmonary vasoconstriction: role of ion channels. *J Appl Physiol,* 98**,** 415-20.

MCCULLOCH, K. M., KEMPSILL, F. E., BUCHANAN, K. J. & GURNEY, A. M. (2000) Regional distribution of potassium currents in the rabbit pulmonary arterial circulation. *Exp Physiol,* 85**,** 487-96.

MCGAHON, M. K., DAWICKI, J. M., ARORA, A., SIMPSON, D. A., GARDINER, T. A., STITT, A. W., SCHOLFIELD, C. N., MCGEOWN, J. G. & CURTIS, T. M. (2007) Kv1.5 is a major component underlying the A-

type potassium current in retinal arteriolar smooth muscle. *Am J Physiol Heart Circ Physiol,* 292**,** H1001-8.

MCGAHON, M. K., DAWICKI, J. M., SCHOLFIELD, C. N., MCGEOWN, J. G. & CURTIS, T. M. (2005) A-type potassium current in retinal arteriolar smooth muscle cells. *Invest Ophthalmol Vis Sci,* 46**,** 3281-7.

MCMURTRY, I. F. (1985) BAY K 8644 potentiates and A23187 inhibits hypoxic vasoconstriction in rat lungs. *Am J Physiol,* 249**,** H741-6.

MCMURTRY, I. F., DAVIDSON, A. B., REEVES, J. T. & GROVER, R. F. (1976) Inhibition of hypoxic pulmonary vasoconstriction by calcium antagonists in isolated rat lungs. *Circ Res,* 38**,** 99-104.

MEDBO, S., YU, X. Q., ASBERG, A. & SAUGSTAD, O. D. (1998) Pulmonary hemodynamics and plasma endothelin-1 during hypoxemia and reoxygenation with room air or 100% oxygen in a piglet model. *Pediatr Res,* 44**,** 843-9.

MELNYK, P., EHRLICH, J. R., POURRIER, M., VILLENEUVE, L., CHA, T. J. & NATTEL, S. (2005) Comparison of ion channel distribution and expression in cardiomyocytes of canine pulmonary veins versus left atrium. *Cardiovasc Res,* 65**,** 104-16.

MEWE, M., BAUER, C. K., SCHWARZ, J. R. & MIDDENDORFF, R. (2006) Mechanisms regulating spontaneous contractions in the bovine epididymal duct. *Biol Reprod,* 75**,** 651-9.

MICHELAKIS, E. D., WEIR, E. K., WU, X., NSAIR, A., WAITE, R., HASHIMOTO, K., PUTTAGUNTA, L., KNAUS, H. G. & ARCHER, S. L. I. C. (2001) Potassium channels regulate tone in rat pulmonary veins. *Am J Physiol Lung Cell Mol Physiol,* 280**,** L1138-47.

MICHON, G. P. (2004) Surface Area of an Ellipsoid. Numericana.com. Available from: http://home.att.net/~numericana/answer/ellipsoid.htm#thomsen [Accessed 15 November 2008].

MIGALLY, N., TUCKER, A. & ZAMBERNARD, J. (1982) Fine structural changes in pulmonary veins of chronically hypoxic mice. *J Submicrosc Cytol,* 14**,** 239-46.

MIKKELSEN, E. & PEDERSEN, O. L. (1983) Regional differences in the response of isolated human vessels to vasoactive substances. *Gen Pharmacol,* 14**,** 89-90.

MILLER, D. S., YAGHI, A., HAMILTON, J. T. & PATERSON, N. A. (1989) Role of arachidonic acid metabolites in hypoxic contractions of isolated porcine pulmonary artery and vein. *Exp Lung Res,* 15**,** 213-22.

MITCHELL, M. R., POWELL, T., STURRIDGE, M. F., TERRAR, D. A. & TWIST, V. W. (1986) Electrical properties and response to noradrenaline of individual heart cells isolated from human ventricular tissue. *Cardiovasc Res,* 20**,** 869-76.

MITZNER, W. & SYLVESTER, J. T. (1981) Hypoxic vasoconstriction and fluid filtration in pig lungs. *J Appl Physiol,* 51**,** 1065-71.

MOLLARD, P., MIRONNEAU, J., AMEDEE, T. & MIRONNEAU, C. (1986) Electrophysiological characterization of single pregnant rat myometrial cells in short-term primary culture. *Am J Physiol,* 250**,** C47-54.

MOLLEMAN, A. (2003) *Patch clamping: an introductory guide to patch clamp electrophysiology*, John Wiley & Sons Ltd.

MORGANROTH, M. L., REEVES, J. T., MURPHY, R. C. & VOELKEL, N. F. (1984) Leukotriene synthesis and receptor blockers block hypoxic pulmonary vasoconstriction. *J Appl Physiol,* 56**,** 1340-6.

MORIO, Y. & MCMURTRY, I. F. (2002) Ca(2+) release from ryanodine-sensitive store contributes to mechanism of hypoxic vasoconstriction in rat lungs. *J Appl Physiol,* 92**,** 527-34.

MOTLEY, H. L., COURNAND, A., WERKO, L., HIMMELSTEIN, A. & DRESDALE, D. (1947) The influence of short periods of induced acute anoxia upon pulmonary artery pressures in man. *Am J Physiol,* 150**,** 315-320.

MOUDGIL, R., MICHELAKIS, E. D. & ARCHER, S. L. (2005) Hypoxic pulmonary vasoconstriction. *J Appl Physiol,* 98**,** 390-403.

MOUDGIL, R., MICHELAKIS, E. D. & ARCHER, S. L. (2006) The role of k+ channels in determining pulmonary vascular tone, oxygen sensing, cell

proliferation, and apoptosis: implications in hypoxic pulmonary vasoconstriction and pulmonary arterial hypertension. *Microcirculation,* 13**,** 615-32.

MULVANY, M. J. & HALPERN, W. (1977) Contractile properties of small arterial resistance vessels in spontaneously hypertensive and normotensive rats. *Circ Res,* 41**,** 19-26.

MURPHY, J. G. & KHALIL, R. A. (2000) Gender-specific reduction in contractility and [Ca(2+)](i) in vascular smooth muscle cells of female rat. *Am J Physiol Cell Physiol,* 278**,** C834-44.

MURRAY, T. R., CHEN, L., MARSHALL, B. E. & MACARAK, E. J. (1990) Hypoxic contraction of cultured pulmonary vascular smooth muscle cells. *Am J Respir Cell Mol Biol,* 3**,** 457-65.

NAGASAKA, Y., BHATTACHARYA, J., NANJO, S., GROPPER, M. A. & STAUB, N. C. (1984) Micropuncture measurement of lung microvascular pressure profile during hypoxia in cats. *Circ Res,* 54**,** 90-5.

NATHAN, H. & GLOOBE, H. (1970) Myocardial atrio-venous junctions and extensions (sleeves) over the pulmonary and caval veins. Anatomical observations in various mammals. *Thorax,* 25**,** 317-24.

NELSON, M. T. & QUAYLE, J. M. (1995) Physiological roles and properties of potassium channels in arterial smooth muscle. *Am J Physiol,* 268**,** C799-822.

NG, L. C., KYLE, B. D., LENNOX, A. R., SHEN, X. M., HATTON, W. J. & HUME, J. R. (2008) Cell culture alters Ca2+ entry pathways activated by store-depletion or hypoxia in canine pulmonary arterial smooth muscle cells. *Am J Physiol Cell Physiol,* 294**,** C313-23.

NG, L. C., WILSON, S. M. & HUME, J. R. (2005) Mobilization of sarcoplasmic reticulum stores by hypoxia leads to consequent activation of capacitative Ca2+ entry in isolated canine pulmonary arterial smooth muscle cells. *J Physiol,* 563**,** 409-419.

NISELL, O. (1951) The influence of blood gases on the pulmonary vessels of the cat. *Acta Physiol Scand,* 23**,** 85-90.

O'RIORDAN, M. (2005) Experts say time has come for AF ablation RCTs: "Only thing missing is the data". theheart.org. [HeartWire > Features] Avaliable from: http://www.theheart.org/article/546039.do [Accessed 9 September 2008].

OGDEN, D. & STANFIELD, P. (1994) Patch clamp techniques for single channel and whole-cell recording. IN OGDEN, D. (Ed.) *Microelectrode techniques. The Plymouth Workshop Handbook.* 2nd ed. Cambridge, The Company of Biologists Limited.

OHE, M., OGATA, M., KATAYOSE, D. & TAKISHIMA, T. (1992) Hypoxic contraction of pre-stretched human pulmonary artery. *Respir Physiol,* 87**,** 105-14.

OHLSTEIN, E. H., HOROHONICH, S., SHEBUSKI, R. J. & RUFFOLO, R. R., JR. (1989) Localization and characterization of alpha-2 adrenoceptors in the isolated canine pulmonary vein. *J Pharmacol Exp Ther,* 248**,** 233-9.

OPARIL, S., CHEN, S. J., MENG, Q. C., ELTON, T. S., YANO, M. & CHEN, Y. F. (1995) Endothelin-A receptor antagonist prevents acute hypoxia-induced pulmonary hypertension in the rat. *Am J Physiol,* 268**,** L95-100.

ORTON, E. C., RAFFESTIN, B. & MCMURTRY, I. F. (1990) Protein kinase C influences rat pulmonary vascular reactivity. *Am Rev Respir Dis,* 141**,** 654-8.

OSIPENKO, O. N., EVANS, A. M. & GURNEY, A. M. (1997) Regulation of the resting potential of rabbit pulmonary artery myocytes by a low threshold, O2-sensing potassium current. *Br J Pharmacol,* 120**,** 1461-70.

OTTOLIA, M. & TORO, L. (1994) Potentiation of large conductance KCa channels by niflumic, flufenamic, and mefenamic acids. *Biophys J,* 67**,** 2272-9.

OWEN-THOMAS, J. B. & REEVES, J. T. (1969) Hypoxia and pulmonary arterial pressure in the rabbit. *J Physiol,* 201**,** 665-72.

OZAKI, M., MARSHALL, C., AMAKI, Y. & MARSHALL, B. E. (1998) Role of wall tension in hypoxic responses of isolated rat pulmonary arteries. *Am J Physiol,* 275**,** L1069-77.

PARK, M. K., LEE, S. H., HO, W. K. & EARM, Y. E. (1995) Redox agents as a link between hypoxia and the responses of ionic channels in rabbit pulmonary vascular smooth muscle. *Exp Physiol,* 80**,** 835-42.

PATEL, A. J., LAZDUNSKI, M. & HONORE, E. (1997) Kv2.1/Kv9.3, a novel ATP-dependent delayed-rectifier K+ channel in oxygen-sensitive pulmonary artery myocytes. *Embo J,* 16**,** 6615-25.

PEAKE, M. D., HARABIN, A. L., BRENNAN, N. J. & SYLVESTER, J. T. (1981) Steady-state vascular responses to graded hypoxia in isolated lungs of five species. *J Appl Physiol,* 51**,** 1214-9.

PEARL, R. G., BAER, E. R., SIEGEL, L. C., BENSON, G. V. & RICE, S. A. (1992) Longitudinal distribution of pulmonary vascular resistance after endotoxin administration in sheep. *Crit Care Med,* 20**,** 119-25.

PENG, W., KARWANDE, S. V., HOIDAL, J. R. & FARRUKH, I. S. (1996) Potassium currents in cultured human pulmonary arterial smooth muscle cells. *J Appl Physiol,* 80**,** 1187-96.

PEREZ-GARCIA, M. T., LOPEZ-LOPEZ, J. R. & GONZALEZ, C. (1999) Kvbeta1.2 subunit coexpression in HEK293 cells confers O2 sensitivity to kv4.2 but not to Shaker channels. *J Gen Physiol,* 113**,** 897-907.

PETERS, R. M. & ROOS, A. (1952) Effect of unilateral nitrogen breathing upon pulmonary blood flow. *Am J Physiol,* 171**,** 250-5.

PHILLIPPE, M., SAUNDERS, T. & BASA, A. (1997) Intracellular mechanisms underlying prostaglandin F2alpha-stimulated phasic myometrial contractions. *Am J Physiol,* 273**,** E665-73.

PIPER, A. S. & LARGE, W. A. (2003) Multiple conductance states of single Ca2+-activated Cl- channels in rabbit pulmonary artery smooth muscle cells. *J Physiol,* 547**,** 181-96.

PLATOSHYN, O., GOLOVINA, V. A., BAILEY, C. L., LIMSUWAN, A., KRICK, S., JUHASZOVA, M., SEIDEN, J. E., RUBIN, L. J. & YUAN, J. X. (2000) Sustained membrane depolarization and pulmonary artery smooth muscle cell proliferation. *Am J Physiol Cell Physiol,* 279**,** C1540-9.

PLATOSHYN, O., YU, Y., GOLOVINA, V. A., MCDANIEL, S. S., KRICK, S., LI, L., WANG, J. Y., RUBIN, L. J. & YUAN, J. X. (2001) Chronic hypoxia decreases K(V) channel expression and function in pulmonary artery myocytes. *Am J Physiol Lung Cell Mol Physiol,* 280**,** L801-12.

PLATOSHYN, O., YU, Y., KO, E. A., REMILLARD, C. V. & YUAN, J. X. (2007) Heterogeneity of hypoxia-mediated decrease in IK(V) and increase in [Ca2+]cyt in pulmonary artery smooth muscle cells. *Am J Physiol Lung Cell Mol Physiol*.

POST, J. M., GELBAND, C. H. & HUME, J. R. (1995) [Ca2+]i inhibition of K+ channels in canine pulmonary artery. Novel mechanism for hypoxia-induced membrane depolarization. *Circ Res,* 77**,** 131-9.

POST, J. M., HUME, J. R., ARCHER, S. L. & WEIR, E. K. (1992) Direct role for potassium channel inhibition in hypoxic pulmonary vasoconstriction. *Am J Physiol,* 262**,** C882-90.

POWELL, T., TERRAR, D. A. & TWIST, V. W. (1980) Electrical properties of individual cells isolated from adult rat ventricular myocardium. *J Physiol,* 302**,** 131-53.

PRONINA, O. E., MAKUCH, R., WRZOSEK, A., DABROWSKA, R. & BOROVIKOV, Y. S. (2007) Caldesmon inhibits both force development and transition of actin monomers from "OFF" to "ON" conformational state by changing its position in thin filaments. *Cell Biol Int,* 31**,** 394-404.

PUTNEY, J. W., JR., BROAD, L. M., BRAUN, F. J., LIEVREMONT, J. P. & BIRD, G. S. (2001) Mechanisms of capacitative calcium entry. *J Cell Sci,* 114**,** 2223-9.

RAJ, J. U. & ANDERSON, J. (1990) Pulmonary venous responses to thromboxane A2 analogue and atrial natriuretic peptide in lambs. *Circ Res,* 66**,** 496-502.

RAJ, J. U. & CHEN, P. (1986) Micropuncture measurement of microvascular pressures in isolated lamb lungs during hypoxia. *Circ Res,* 59**,** 398-404.

RAJ, J. U., HILLYARD, R., KAAPA, P., GROPPER, M. & ANDERSON, J. (1990) Pulmonary arterial and venous constriction during hypoxia in 3- to 5-wk-old and adult ferrets. *J Appl Physiol,* 69**,** 2183-9.

RATHORE, R., ZHENG, Y. M., LI, X. Q., WANG, Q. S., LIU, Q. H., GINNAN, R., SINGER, H. A., HO, Y. S. & WANG, Y. X. (2006) Mitochondrial ROS-PKCepsilon signaling axis is uniquely involved in hypoxic increase in [Ca2+]i in pulmonary artery smooth muscle cells. *Biochem Biophys Res Commun,* 351**,** 784-90.

RATHORE, R., ZHENG, Y. M., NIU, C. F., LIU, Q. H., KORDE, A., HO, Y. S. & WANG, Y. X. (2008) Hypoxia activates NADPH oxidase to increase [ROS]i and [Ca2+]i through the mitochondrial ROS-PKCepsilon signaling axis in pulmonary artery smooth muscle cells. *Free Radic Biol Med,* 45**,** 1223-31.

RETTIG, J., HEINEMANN, S. H., WUNDER, F., LORRA, C., PARCEJ, D. N., DOLLY, J. O. & PONGS, O. (1994) Inactivation properties of voltage-gated K+ channels altered by presence of beta-subunit. *Nature,* 369**,** 289-94.

RICCI, A., BRONZETTI, E., EL-ASSOUAD, D., FELICI, L., GRECO, S., MARIOTTA, S., SABBATINI, M. & AMENTA, F. (2000) Influence of age on L-type Ca2+ channels in the pulmonary artery and vein of spontaneously hypertensive rats. *Mech Ageing Dev,* 120**,** 33-44.

RIVERA-ESTRADA, C., SALTZMAN, P. W., SINGER, D. & KATZ, L. N. (1958) Action of hypoxia on the pulmonary vasculature. *Circ Res,* 6**,** 10-4.

ROBERTSON, T. P., AARONSON, P. I. & WARD, J. P. (1995) Hypoxic vasoconstriction and intracellular Ca2+ in pulmonary arteries: evidence for PKC-independent Ca2+ sensitization. *Am J Physiol,* 268**,** H301-7.

ROBERTSON, T. P., AARONSON, P. I. & WARD, J. P. (2003) Ca2+ sensitization during sustained hypoxic pulmonary vasoconstriction is endothelium dependent. *Am J Physiol Lung Cell Mol Physiol,* 284**,** L1121-6.

ROBERTSON, T. P., DIPP, M., WARD, J. P., AARONSON, P. I. & EVANS, A. M. (2000a) Inhibition of sustained hypoxic vasoconstriction by Y-27632 in isolated intrapulmonary arteries and perfused lung of the rat. *Br J Pharmacol,* 131**,** 5-9.

ROBERTSON, T. P., HAGUE, D., AARONSON, P. I. & WARD, J. P. (2000b) Voltage-independent calcium entry in hypoxic pulmonary vasoconstriction of intrapulmonary arteries of the rat. *J Physiol,* 525 Pt 3**,** 669-80.

ROBERTSON, T. P. & MCMURTRY, I. F. (2004) Critical Role of Ca2+ Sensitization in Acute Hypoxic Pulmonary Vasoconstriction. IN YUAN, X. J. (Ed.) *Hypoxic Pulmonary Vasoconstriction: Cellular and Molecular Mechanisms.* Springer.

ROBERTSON, T. P., WARD, J. P. & AARONSON, P. I. (2001) Hypoxia induces the release of a pulmonary-selective, Ca(2+)-sensitising, vasoconstrictor from the perfused rat lung. *Cardiovasc Res,* 50**,** 145-50.

RODMAN, D. M., STELZNER, T. J., ZAMORA, M. R., BONVALLET, S. T., OKA, M., SATO, K., O'BRIEN, R. F. & MCMURTRY, I. F. (1992) Endothelin-1 increases the pulmonary microvascular pressure and causes pulmonary edema in salt solution but not blood-perfused rat lungs. *J Cardiovasc Pharmacol,* 20**,** 658-63.

RODMAN, D. M., YAMAGUCHI, T., HASUNUMA, K., O'BRIEN, R. F. & MCMURTRY, I. F. (1990) Effects of hypoxia on endothelium-dependent relaxation of rat pulmonary artery. *Am J Physiol,* 258**,** L207-14.

RODMAN, D. M., YAMAGUCHI, T., O'BRIEN, R. F. & MCMURTRY, I. F. (1989) Hypoxic contraction of isolated rat pulmonary artery. *J Pharmacol Exp Ther,* 248**,** 952-9.

ROGERS, T. K., THOMPSON, J. S. & MORICE, A. H. (1997) Inhibition of hypoxic pulmonary vasoconstriction in isolated rat resistance arteries by atrial natriuretic peptide. *Eur Respir J,* 10**,** 2061-5.

ROSSI, P., PERSSON, B., BOELS, P. J., ARNER, A., WEITZBERG, E. & OLDNER, A. (2008) Endotoxemic pulmonary hypertension is largely mediated by endothelin-induced venous constriction. *Intensive Care Med*.

ROUX, N., HAVET, E. & MERTL, P. (2004) The myocardial sleeves of the pulmonary veins: potential implications for atrial fibrillation. *Surg Radiol Anat,* 26**,** 285-9.

RUSCHENSCHMIDT, C., CHEN, J., BECKER, A., RIAZANSKI, V. & BECK, H. (2006) Functional properties and oxidative modulation of A-type K currents in hippocampal granule cells of control and chronically epileptic rats. *Eur J Neurosci,* 23**,** 675-85.

SACKNER, M. A., WILL, D. H. & DUBOIS, A. B. (1966) The site of pulmonary vasomotor activity during hypoxia or serotonin administration. *J Clin Invest,* 45**,** 112-21.

SALVATERRA, C. G. & GOLDMAN, W. F. (1993) Acute hypoxia increases cytosolic calcium in cultured pulmonary arterial myocytes. *Am J Physiol,* 264**,** L323-8.

SATO, K., MORIO, Y., MORRIS, K. G., RODMAN, D. M. & MCMURTRY, I. F. (2000) Mechanism of hypoxic pulmonary vasoconstriction involves ET(A) receptor-mediated inhibition of K(ATP) channel. *Am J Physiol Lung Cell Mol Physiol,* 278**,** L434-42.

SELYANKO, A. A., HADLEY, J. K., WOOD, I. C., ABOGADIE, F. C., JENTSCH, T. J. & BROWN, D. A. (2000) Inhibition of KCNQ1-4 potassium channels expressed in mammalian cells via M1 muscarinic acetylcholine receptors. *J Physiol,* 522 Pt 3**,** 349-55.

SELYANKO, A. A., ROBBINS, J. & BROWN, D. A. (1995) Putative M-type potassium channels in neuroblastoma-glioma hybrid cells: inhibition by muscarine and bradykinin. *Receptors Channels,* 3**,** 147-59.

SHAM, J. S., CRENSHAW, B. R., JR., DENG, L. H., SHIMODA, L. A. & SYLVESTER, J. T. (2000) Effects of hypoxia in porcine pulmonary arterial myocytes: roles of K(V) channel and endothelin-1. *Am J Physiol Lung Cell Mol Physiol,* 279**,** L262-72.

SHEEHAN, D. W., FARHI, L. E. & RUSSELL, J. A. (1992) Prolonged lobar hypoxia in vivo enhances the responsivity of isolated pulmonary veins to hypoxia. *Am Rev Respir Dis,* 145**,** 640-5.

SHELTON, D. M., KEAL, E. & REID, L. (1977) The pulmonary circulation in chronic bronchitis and emphysema. *Chest,* 71**,** 303-6.

SHI, W., WANG, C. G., DANDURAND, R. J., EIDELMAN, D. H. & MICHEL, R. P. (1998) Differential responses of pulmonary arteries and veins to histamine and 5-HT in lung explants of guinea-pigs. *Br J Pharmacol,* 123**,** 1525-32.

SHIBAMOTO, T., HAYASHI, T., JR., SAWANO, F., SAEKI, Y., MATSUDA, Y., KAWAMOTO, M. & KOYAMA, S. (1992) Pulmonary vascular response to anaphylaxis in isolated canine lungs. *Am J Physiol,* 263**,** R1024-9.

SHIBAMOTO, T., WANG, H. G., YAMAGUCHI, Y., HAYASHI, T., SAEKI, Y., TANAKA, S. & KOYAMA, S. (1995) Effects of thromboxane A2 analogue on vascular resistance distribution and permeability in isolated blood-perfused dog lungs. *Lung,* 173**,** 209-21.

SHIMIZU, S., DING, X. & MURRAY, P. A. (2006) Intravenous anesthetics inhibit capacitative calcium entry in pulmonary venous smooth muscle cells. *Anesthesiology,* 104**,** 791-7.

SHIMODA, L. A., SYLVESTER, J. T. & SHAM, J. S. (1998) Inhibition of voltage-gated K+ current in rat intrapulmonary arterial myocytes by endothelin-1. *Am J Physiol,* 274**,** L842-53.

SHIMODA, L. A., SYLVESTER, J. T. & SHAM, J. S. (1999) Chronic hypoxia alters effects of endothelin and angiotensin on K+ currents in pulmonary arterial myocytes. *Am J Physiol,* 277**,** L431-9.

SHIRAI, M., SADA, K. & NINOMIYA, I. (1986) Effects of regional alveolar hypoxia and hypercapnia on small pulmonary vessels in cats. *J Appl Physiol,* 61**,** 440-8.

SHIRAI, M., SHIMOUCHI, A., KAWAGUCHI, A. T., IKEDA, S., SUNAGAWA, K. & NINOMIYA, I. (1997) Endogenous nitric oxide attenuates hypoxic vasoconstriction of small pulmonary arteries and veins in anaesthetized cats. *Acta Physiol Scand,* 159**,** 263-4.

SMIRNOV, S. V. & AARONSON, P. I. (1992) Ca(2+)-activated and voltage-gated K+ currents in smooth muscle cells isolated from human mesenteric arteries. *J Physiol,* 457**,** 431-54.

SMIRNOV, S. V., ROBERTSON, T. P., WARD, J. P. & AARONSON, P. I. (1994) Chronic hypoxia is associated with reduced delayed rectifier K+ current in rat pulmonary artery muscle cells. *Am J Physiol,* 266**,** H365-70.

SMITH, D. J. & COXE, J. W. (1951) Reactions of isolated pulmonary blood vessels to anoxia, epinephrine, acetylcholine and histamine. *Am J Physiol,* 167**,** 732-7.

SMITH, P. & HEATH, D. (1977) Ultrastructure of hypoxic hypertensive pulmonary vascular disease. *J Pathol,* 121**,** 93-100.

SMITH, W. S. & MATTHAY, M. A. (1997) Evidence for a Hydrostatic Mechanism in Human Neurogenic Pulmonary Edema. *Chest,* 111**,** 1326-1333.

SOBOL, B. J., BOTTEX, G., EMIRGIL, C. & GISSEN, H. (1963) Gaseous Diffusion From Alveoli To Pulmonary Vessels Of Considerable Size. *Circ Res,* 13**,** 71-9.

SOMLYO, A. P. & SOMLYO, A. V. (2000) Signal transduction by G-proteins, rho-kinase and protein phosphatase to smooth muscle and non-muscle myosin II. *J Physiol,* 522 Pt 2**,** 177-85.

SOMLYO, A. V. & SOMLYO, A. P. (1993) Intracellular signaling in vascular smooth muscle. *Adv Exp Med Biol,* 346**,** 31-8.

SOVARI, A. A. (2008) Pulmonary Edema, Cardiogenic. *eMedicine.*

STENMARK, K. R. & MECHAM, R. P. (1997) Cellular and molecular mechanisms of pulmonary vascular remodeling. *Annu Rev Physiol,* 59**,** 89-144.

STEUSLOFF, A., PAUL, E., SEMENCHUK, L. A., DI SALVO, J. & PFITZER, G. (1995) Modulation of Ca2+ sensitivity in smooth muscle by genistein and protein tyrosine phosphorylation. *Arch Biochem Biophys,* 320**,** 236-42.

SWENSON, E. R., MAGGIORINI, M., MONGOVIN, S., GIBBS, J. S., GREVE, I., MAIRBAURL, H. & BARTSCH, P. (2002) Pathogenesis of high-altitude pulmonary edema: inflammation is not an etiologic factor. *Jama,* 287**,** 2228-35.

SYLVESTER, J. T. (2001) Hypoxic pulmonary vasoconstriction: a radical view. *Circ Res,* 88**,** 1228-30.

SYLVESTER, J. T., MITZNER, W., NGEOW, Y. & PERMUTT, S. (1983) Hypoxic constriction of alveolar and extra-alveolar vessels in isolated pig lungs. *J Appl Physiol,* 54**,** 1660-6.

TAKAHASHI, H., SOMA, S., MURAMATSU, M., OKA, M. & FUKUCHI, Y. (2001) Upregulation of ET-1 and its receptors and remodeling in small pulmonary veins under hypoxic conditions. *Am J Physiol Lung Cell Mol Physiol,* 280**,** L1104-14.

TAKEDA, S., NAKANISHI, K., INOUE, T. & OGAWA, R. (1997) Delayed elevation of plasma endothelin-1 during unilateral alveolar hypoxia without systemic hypoxemia in humans. *Acta Anaesthesiol Scand,* 41**,** 274-80.

TALBOT, N. P., ROBBINS, P. A. & DORRINGTON, K. L. (2003) Release by hypoxia of a soluble vasoconstrictor from rabbit small pulmonary arteries. *Br J Anaesth,* 91**,** 592-4.

THILENIUS, O. G., HOFFER, P. B., FITZGERALD, R. S. & PERKINS, J. F., JR. (1964) Response Of Pulmonary Circulation Of Resting, Unanesthetized Dogs To Acute Hypoxia. *Am J Physiol,* 206**,** 867-74.

THOMAS, T. & MARSHALL, J. M. (1993) The role of adenosine in hypoxic pulmonary vasoconstriction in the anaesthetized rat. *Exp Physiol,* 78**,** 541-3.

THOMPSON, J. S., JONES, R. D., ROGERS, T. K., HANCOCK, J. & MORICE, A. H. (1998) Inhibition of hypoxic pulmonary vasoconstriction in isolated rat pulmonary arteries by diphenyleneiodonium (DPI). *Pulm Pharmacol Ther,* 11**,** 71-5.

THYBERG, J. (1996) Differentiated properties and proliferation of arterial smooth muscle cells in culture. *Int Rev Cytol,* 169**,** 183-265.

TOGA, H., IBE, B. O. & RAJ, J. U. (1992) In vitro responses of ovine intrapulmonary arteries and veins to endothelin-1. *Am J Physiol,* 263**,** L15-21.

TOLIC-NORRELYKKE, I. M. & WANG, N. (2005) Traction in smooth muscle cells varies with cell spreading. *J Biomech,* 38**,** 1405-12.

TORO, L., GONZALEZ-ROBLES, A. & STEFANI, E. (1986) Electrical properties and morphology of single vascular smooth muscle cells in culture. *Am J Physiol,* 251**,** C763-73.

TRABER, D. L. & TRABER, L. D. (2002) Hypoxic Pulmonary Vasoconstriction and the Pulmonary Microcirculation. IN VINCENT, J.-L. (Ed.) *Intensive Care Medicine.* Springer.

TRACEY, W. R., HAMILTON, J. T., CRAIG, I. D. & PATERSON, N. A. (1989) Responses of isolated guinea pig pulmonary venules to hypoxia and anoxia. *J Appl Physiol,* 67**,** 2147-53.

TSAI, B. M., PATEL, K., WANG, M., MORRELL, E. D., CRISOSTOMO, P. R. & MELDRUM, D. R. (2007) Selective protein kinase C inhibition attenuates pulmonary artery cytokine expression without affecting hypoxic pulmonary vasoconstriction. *Shock,* 27**,** 36-9.

TSENG, C. M., MCGEADY, M., PRIVETT, T., DUNN, A. & SYLVESTER, J. T. (1990) Does leukotriene C4 mediate hypoxic vasoconstriction in isolated ferret lungs? *J Appl Physiol,* 68**,** 253-9.

TURNER, J. L. & KOZLOWSKI, R. Z. (1997) Relationship between membrane potential, delayed rectifier K+ currents and hypoxia in rat pulmonary arterial myocytes. *Exp Physiol,* 82**,** 629-45.

UFLACKER, R. (2006) *Atlas of Vascular Anatomy: An Angiographic Approach*, Lippincott Williams & Wilkins.

UZUN, O. & DEMIRYUREK, A. T. (2003) Involvement of tyrosine kinase pathway in acute hypoxic vasoconstriction in sheep isolated pulmonary vein. *Vascul Pharmacol,* 40**,** 175-81.

UZUN, O., DEMIRYUREK, A. T. & KANZIK, I. (1998) The role of tyrosine kinase in hypoxic constriction of sheep pulmonary artery rings. *Eur J Pharmacol,* 358**,** 41-7.

VADULA, M. S., KLEINMAN, J. G. & MADDEN, J. A. (1993) Effect of hypoxia and norepinephrine on cytoplasmic free Ca2+ in pulmonary and cerebral arterial myocytes. *Am J Physiol,* 265**,** L591-7.

VON EULER, U. S. & LILJESTRAND, G. (1946) Observations on the pulmonary arterial blood pressure in the cat. *Acta Physiol Scand,* 12**,** 301.

WADSWORTH, R. M. (1994) Vasoconstrictor and vasodilator effects of hypoxia. *Trends Pharmacol Sci,* 15**,** 47-53.

WAGENVOORT, C. A. & WAGENVOORT, N. (1976) Pulmonary venous changes in chronic hypoxia. *Virchows Arch A Pathol Anat Histol,* 372**,** 51-6.

WAGENVOORT, C. A. & WAGENVOORT, N. (1982) Pulmonary veins in high-altitude residents: a morphometric study. *Thorax,* 37**,** 931-5.

WALCH, L., DE MONTPREVILLE, V., BRINK, C. & NOREL, X. (2001) Prostanoid EP(1)- and TP-receptors involved in the contraction of human pulmonary veins. *Br J Pharmacol,* 134**,** 1671-8.

WALCH, L., LABAT, C., GASCARD, J. P., DE MONTPREVILLE, V., BRINK, C. & NOREL, X. (1999) Prostanoid receptors involved in the relaxation of human pulmonary vessels. *Br J Pharmacol,* 126**,** 859-66.

WALKER, B. R. (1995) Evidence for uneven distribution of L-type calcium channels in rat pulmonary circulation. *Am J Physiol,* 269**,** H2051-6.

WANG, J., JUHASZOVA, M., RUBIN, L. J. & YUAN, X. J. (1997) Hypoxia inhibits gene expression of voltage-gated K+ channel alpha subunits in pulmonary artery smooth muscle cells. *J Clin Invest,* 100**,** 2347-53.

WANG, J., SHIMODA, L. A., WEIGAND, L., WANG, W., SUN, D. & SYLVESTER, J. T. (2005a) Acute hypoxia increases intracellular [Ca2+] in pulmonary arterial smooth muscle by enhancing capacitative Ca2+ entry. *Am J Physiol Lung Cell Mol Physiol,* 288**,** L1059-69.

WANG, J., WEIGAND, L., WANG, W., SYLVESTER, J. T. & SHIMODA, L. A. (2005b) Chronic hypoxia inhibits Kv channel gene expression in rat distal pulmonary artery. *Am J Physiol Lung Cell Mol Physiol,* 288**,** L1049-58.

WANG, Y. & COCEANI, F. (1992) Isolated pulmonary resistance vessels from fetal lambs. Contractile behavior and responses to indomethacin and endothelin-1. *Circ Res,* 71**,** 320-30.

WANG, Y., COE, Y., TOYODA, O. & COCEANI, F. (1995) Involvement of endothelin-1 in hypoxic pulmonary vasoconstriction in the lamb. *J Physiol,* 482 (Pt 2)**,** 421-34.

WANG, Z., JIN, N., GANGULI, S., SWARTZ, D. R., LI, L. & RHOADES, R. A. (2001) Rho-kinase activation is involved in hypoxia-induced pulmonary vasoconstriction. *Am J Respir Cell Mol Biol,* 25**,** 628-35.

WARD, J. P. & AARONSON, P. I. (1999) Mechanisms of hypoxic pulmonary vasoconstriction: can anyone be right? *Respir Physiol,* 115**,** 261-71.

WARD, J. P., KNOCK, G. A., SNETKOV, V. A. & AARONSON, P. I. (2004) Protein kinases in vascular smooth muscle tone--role in the pulmonary vasculature and hypoxic pulmonary vasoconstriction. *Pharmacol Ther,* 104**,** 207-31.

WEIR, E. K. & ARCHER, S. L. I. C. (1995) The mechanism of acute hypoxic pulmonary vasoconstriction: the tale of two channels. *Faseb J,* 9**,** 183-9.

WEIR, E. K. & OLSCHEWSKI, A. (2006) Role of ion channels in acute and chronic responses of the pulmonary vasculature to hypoxia. *Cardiovasc Res,* 71**,** 630-41.

WEISSMANN, N., GRIMMINGER, F., WALMRATH, D. & SEEGER, W. (1995) Hypoxic vasoconstriction in buffer-perfused rabbit lungs. *Respir Physiol,* 100**,** 159-69.

WEISSMANN, N., SEEGER, W., CONZEN, J., KISS, L. & GRIMMINGER, F. (1998) Effects of arachidonic acid metabolism on hypoxic vasoconstriction in rabbit lungs. *Eur J Pharmacol,* 356**,** 231-7.

WEISSMANN, N., SOMMER, N., SCHERMULY, R. T., GHOFRANI, H. A., SEEGER, W. & GRIMMINGER, F. (2006) Oxygen sensors in hypoxic pulmonary vasoconstriction. *Cardiovasc Res,* 71**,** 620-9.

WEISSMANN, N., VOSWINCKEL, R., HARDEBUSCH, T., ROSSEAU, S., GHOFRANI, H. A., SCHERMULY, R., SEEGER, W. & GRIMMINGER, F. (1999) Evidence for a role of protein kinase C in hypoxic pulmonary vasoconstriction. *Am J Physiol,* 276**,** L90-5.

WEITZENBLUM, E. & CHAOUAT, A. (2001) Hypoxic pulmonary hypertension in man: what minimum daily duration of hypoxaemia is required? *Eur Respir J,* 18**,** 251-3.

WETZEL, R. C. & SYLVESTER, J. T. (1983) Gender differences in hypoxic vascular response of isolated sheep lungs. *J Appl Physiol,* 55**,** 100-4.

WILDE, D. W. & LEE, K. S. (1989) Outward potassium currents in freshly isolated smooth muscle cell of dog coronary arteries. *Circ Res,* 65**,** 1718-34.

WILLETTE, R. N., OHLSTEIN, E. H., MITCHELL, M. P., SAUERMELCH, C. F., BECK, G. R., LUTTMANN, M. A. & HAY, D. W. (1997) Nonpeptide endothelin receptor antagonists. VIII: attenuation of acute hypoxia-induced pulmonary hypertension in the dog. *J Pharmacol Exp Ther,* 280**,** 695-701.

WITTKAMPF, F. H., VONKEN, E. J., DERKSEN, R., LOH, P., VELTHUIS, B., WEVER, E. F., BOERSMA, L. V., RENSING, B. J. & CRAMER, M. J. (2003) Pulmonary vein ostium geometry: analysis by magnetic resonance angiography. *Circulation,* 107**,** 21-3.

WU, T. J., ONG, J. J., CHANG, C. M., DOSHI, R. N., YASHIMA, M., HUANG, H. L., FISHBEIN, M. C., TING, C. T., KARAGUEUZIAN, H. S. & CHEN, P. S. (2001) Pulmonary veins and ligament of marshall as sources of rapid activations in a canine model of sustained atrial fibrillation. *Circulation,* 103**,** 1157-63.

YAMAGUCHI, K., SUZUKI, K., NAOKI, K., NISHIO, K., SATO, N., TAKESHITA, K., KUDO, H., AOKI, T., SUZUKI, Y., MIYATA, A. & TSUMURA, H. (1998) Response of intra-acinar pulmonary microvessels to hypoxia, hypercapnic acidosis, and isocapnic acidosis. *Circ Res,* 82**,** 722-8.

YANG, Z., ZHANG, Z., XU, Y., LI, Y. & YE, T. (2006) Relationship of intracellular free Ca2+ concentration and calcium-activated chloride channels of pulmonary artery smooth muscle cells in rats under hypoxic conditions. *J Huazhong Univ Sci Technolog Med Sci,* 26**,** 172-4, 191.

YANG, Z., ZHANG, Z., XU, Y., WANG, T., MA, D. & YE, T. (2008) Effects of calcium-activated chloride channels on proliferation of pulmonary artery

smooth muscle cells in rats under chronic hypoxic condition. *Journal of Nanjing Medical University,* 22**,** 39-43.

YEUNG, S. Y., OHYA, S., SERGEANT, G. P., PUCOVSKY, V. & GREENWOOD, I. A. (2006) Pharmacological and molecular evidence for the involvement of Kv4.3 in ultra-fast activating K+ currents in murine portal vein myocytes. *Br J Pharmacol,* 149**,** 676-86.

YOSHIMURA, K., TOD, M. L., PIER, K. G. & RUBIN, L. J. (1989) Role of venoconstriction in thromboxane-induced pulmonary hypertension and edema in lambs. *J Appl Physiol,* 66**,** 929-35.

YOSHINO, M., WANG, S. Y. & KAO, C. Y. (1997) Sodium and calcium inward currents in freshly dissociated smooth myocytes of rat uterus. *J Gen Physiol,* 110**,** 565-77.

YUAN, J. X., ALDINGER, A. M., JUHASZOVA, M., WANG, J., CONTE, J. V., JR., GAINE, S. P., ORENS, J. B. & RUBIN, L. J. (1998a) Dysfunctional voltage-gated K+ channels in pulmonary artery smooth muscle cells of patients with primary pulmonary hypertension. *Circulation,* 98**,** 1400-6.

YUAN, X. J., GOLDMAN, W. F., TOD, M. L., RUBIN, L. J. & BLAUSTEIN, M. P. (1993a) Hypoxia reduces potassium currents in cultured rat pulmonary but not mesenteric arterial myocytes. *Am J Physiol,* 264**,** L116-23.

YUAN, X. J., GOLDMAN, W. F., TOD, M. L., RUBIN, L. J. & BLAUSTEIN, M. P. (1993b) Ionic currents in rat pulmonary and mesenteric arterial myocytes in primary culture and subculture. *Am J Physiol,* 264**,** L107-15.

YUAN, X. J., TOD, M. L., RUBIN, L. J. & BLAUSTEIN, M. P. (1995) Hypoxic and metabolic regulation of voltage-gated K+ channels in rat pulmonary artery smooth muscle cells. *Exp Physiol,* 80**,** 803-13.

YUAN, X. J., WANG, J., JUHASZOVA, M., GOLOVINA, V. A. & RUBIN, L. J. (1998b) Molecular basis and function of voltage-gated K+ channels in pulmonary arterial smooth muscle cells. *Am J Physiol,* 274**,** L621-35.

YUAN, X. J. I. C. (1997) Role of calcium-activated chloride current in regulating pulmonary vasomotor tone. *Am J Physiol,* 272**,** L959-68.

ZELLERS, T. M., MCCORMICK, J. & WU, Y. (1994) Interaction among ET-1, endothelium-derived nitric oxide, and prostacyclin in pulmonary arteries and veins. *Am J Physiol,* 267**,** H139-47.

ZHAO, Y., PACKER, C. S. & RHOADES, R. A. (1993) Pulmonary vein contracts in response to hypoxia. *Am J Physiol,* 265**,** L87-92.

ZHUANG, F. Y., FUNG, Y. C. & YEN, R. T. (1983) Analysis of blood flow in cat's lung with detailed anatomical and elasticity data. *J Appl Physiol,* 55**,** 1341-8.